Westinghouse Non-Proprietary Class 3

WCAP-14777

WCOBRA/TRAC OSU Long-Term Cooling Final Validation Report

Westinghouse Energy Systems

Westinghouse Non-Proprietary Class 3

WCAP-14777

WCOBRA/TRAC OSU Long-Term Cooling Final Validation Report

Westinghouse Energy Systems

AP600 DOCUMENT COVER SHEET

Form 58202G(5/94)

0058.FRM

AP600 CENTRAL FILE USE ONLY:

TDC: _____ IDS: I _____ S _____

RFS#: RFS ITEM #:

AP600 DOCUMENT NO.	REVISION NO.		ASSIGNED TO
LTCT-GSR-003	1	Page 1 of {XXX}	D. C. Garner

ALTERNATE DOCUMENT NUMBER: WCAP-14776

WORK BREAKDOWN #: 3.1.1.91

DESIGN AGENT ORGANIZATION: WESTINGHOUSE

TITLE: WCOBRA/TRAC OSU Long-Term Cooling Final Validation Report (Non-Proprietary)
WCAP-14776 is the Proprietary version of this document.

ATTACHMENTS: N/A

DCP #/REV. INCORPORATED IN THIS DOCUMENT
REVISION: N/A

CALCULATION/ANALYSIS REFERENCE:

ELECTRONIC FILENAME	ELECTRONIC FILE FORMAT	ELECTRONIC FILE DESCRIPTION
m:\3358w.wpf	WordPerfect 5.2 WINDOWS	DOCUMENT TEXT AND FIGURES

COMPLETE 1 IF WORK PERFORMED UNDER DESIGN CERTIFICATION OR COMPLETE 2 IF WORK PERFORMED UNDER FOAKE.

1 ☒ **DOE DESIGN CERTIFICATION PROGRAM** – GOVERNMENT LIMITED RIGHTS STATEMENT [See page 2]

Copyright statement: A license is reserved to the U.S. Government under contract DE-AC03-90SF18495.

☐ DOE CONTRACT DELIVERABLES (DELIVERED DATA)
Subject to specified exceptions, disclosure of this data is restricted until September 30, 1995 or Design Certification under DOE contract DE-AC03-90SF18495, whichever is later.

EPRI CONFIDENTIAL: NOTICE: 1 ☐ 2 ☐ 3 ☒ 4 ☐ 5 ☐ CATEGORY: A ☒ B ☐ C ☐ D ☐ E ☐ F ☐

2 ☐ **ARC FOAKE PROGRAM** – ARC LIMITED RIGHTS STATEMENT [See page 2]

Copyright statement: A license is reserved to the U.S. Government under contract DE-FC02-NE34267 and subcontract ARC-93-3-SC-001.

☐ ARC CONTRACT DELIVERABLES (CONTRACT DATA)
Subject to specified exceptions, disclosure of this data is restricted under ARC Subcontract ARC-93-3-SC-001.

ORIGINATOR	SIGNATURE/DATE	
D. C. Garner		
AP600 RESPONSIBLE MANAGER	SIGNATURE*	APPROVAL DATE
E. H. Novendstern		

*Approval of the responsible manager signifies that document is complete, all required reviews are complete, electronic file is attached and document is released for use.

Form 58202G(5/94)

LIMITED RIGHTS STATEMENTS

DOE GOVERNMENT LIMITED RIGHTS STATEMENT

(A) These data are submitted with limited rights under government contract No. DE-AC03-90SF18495. These data may be reproduced and used by the government with the express limitation that they will not, without written permission of the contractor, be used for purposes of manufacturer nor disclosed outside the government; except that the government may disclose these data outside the government for the following purposes, if any, provided that the government makes such disclosure subject to prohibition against further use and disclosure:
   (I) This "Proprietary Data" may be disclosed for evaluation purposes under the restrictions above.
   (II) The "Proprietary Data" may be disclosed to the Electric Power Research Institute (EPRI), electric utility representatives and their direct consultants, excluding direct commercial competitors, and the DOE National Laboratories under the prohibitions and restrictions above.

(B) This notice shall be marked on any reproduction of these data, in whole or in part.

ARC LIMITED RIGHTS STATEMENT:

This proprietary data, furnished under Subcontract Number ARC-93-3-SC-001 with ARC may be duplicated and used by the government and ARC, subject to the limitations of Article H-17.F. of that subcontract, with the express limitations that the proprietary data may not be disclosed outside the government or ARC, or ARC's Class 1 & 3 members or EPRI or be used for purposes of manufacture without prior permission of the Subcontractor, except that further disclosure or use may be made solely for the following purposes:

This proprietary data may be disclosed to other than commercial competitors of Subcontractor for evaluation purposes of this subcontract under the restriction that the proprietary data be retained in confidence and not be further disclosed, and subject to the terms of a non-disclosure agreement between the Subcontractor and that organization, excluding DOE and its contractors.

DEFINITIONS

CONTRACT/DELIVERED DATA — Consists of documents (e.g. specifications, drawings, reports) which are generated under the DOE or ARC contracts which contain no background proprietary data.

EPRI CONFIDENTIALITY / OBLIGATION NOTICES

NOTICE 1: The data in this document is subject to no confidentiality obligations.

NOTICE 2: The data in this document is proprietary and confidential to Westinghouse Electric Corporation and/or its Contractors. It is forwarded to recipient under an obligation of Confidence and Trust for limited purposes only. Any use, disclosure to unauthorized persons, or copying of this document or parts thereof is prohibited except as agreed to in advance by the Electric Power Research Institute (EPRI) and Westinghouse Electric Corporation. Recipient of this data has a duty to inquire of EPRI and/or Westinghouse as to the uses of the information contained herein that are permitted.

NOTICE 3: The data in this document is proprietary and confidential to Westinghouse Electric Corporation and/or its Contractors. It is forwarded to recipient under an obligation of Confidence and Trust for use only in evaluation tasks specifically authorized by the Electric Power Research Institute (EPRI). Any use, disclosure to unauthorized persons, or copying this document or parts thereof is prohibited except as agreed to in advance by EPRI and Westinghouse Electric Corporation. Recipient of this data has a duty to inquire of EPRI and/or Westinghouse as to the uses of the information contained herein that are permitted. This document and any copies or excerpts thereof that may have been generated are to be returned to Westinghouse, directly or through EPRI, when requested to do so.

NOTICE 4: The data in this document is proprietary and confidential to Westinghouse Electric Corporation and/or its Contractors. It is being revealed in confidence and trust only to Employees of EPRI and to certain contractors of EPRI for limited evaluation tasks authorized by EPRI. Any use, disclosure to unauthorized persons, or copying of this document or parts thereof is prohibited. This Document and any copies or excerpts thereof that may have been generated are to be returned to Westinghouse, directly or through EPRI, when requested to do so.

NOTICE 5: The data in this document is proprietary and confidential to Westinghouse Electric Corporation and/or its Contractors. Access to this data is given in Confidence and Trust only at Westinghouse facilities for limited evaluation tasks assigned by EPRI. Any use, disclosure to unauthorized persons, or copying of this document or parts thereof is prohibited. Neither this document nor any excerpts therefrom are to be removed from Westinghouse facilities.

EPRI CONFIDENTIALITY / OBLIGATION CATEGORIES

CATEGORY "A" — (See Delivered Data) Consists of CONTRACTOR Foreground Data that is contained in an issued reported.

CATEGORY "B" — (See Delivered Data) Consists of CONTRACTOR Foreground Data that is not contained in an issued report, except for computer programs.

CATEGORY "C" — Consists of CONTRACTOR Background Data except for computer programs.

CATEGORY "D" — Consists of computer programs developed in the course of performing the Work.

CATEGORY "E" — Consists of computer programs developed prior to the Effective Date or after the Effective Date but outside the scope of the Work.

CATEGORY "F" — Consists of administrative plans and administrative reports.

WCAP-14777

WCOBRA/TRAC OSU LONG-TERM COOLING FINAL VALIDATION REPORT

D. C. Garner
L. E. Hochreiter
R. M. Kemper
N. Petkov

November 1996

Westinghouse Electric Corporation
Energy System Business Unit
Advanced Technology Business Area
P.O. Box 355
Pittsburgh, PA 15230-0355

TABLE OF CONTENTS

TABLE OF CONTENTS (Cont)

LIST OF TABLES

LIST OF FIGURES

LIST OF FIGURES (Cont)

LIST OF FIGURES (Cont)

LIST OF FIGURES (Cont)

LIST OF FIGURES (Cont)

SUMMARY

WCOBRA/TRAC has been used to model selected tests conducted at the Oregon State University (OSU) integral systems test facility, which is a scaled model of the AP600 plant. The tests simulated a small-break loss-of-coolant accident (LOCA), which transitions into the long-term cooling (LTC) transient, where core cooling was accomplished using only the passive safety systems. A WCOBRA/TRAC model was developed to predict the LTC thermal-hydraulic phenomena of the OSU tests. A Phenomena Identification Ranking Table (PIRT) was developed to identify the key thermal-hydraulic phenomena for the LTC transient. The PIRT indicates the key phenomena that the WCOBRA/TRAC code must model to ensure that the code is suitable for application to the AP600 LTC analyses.

Several OSU LTC tests that encompassed the expected range of conditions for the AP600 plant were simulated. Comparisons of the test data and the WCOBRA/TRAC predictions indicate that WCOBRA/TRAC can accurately model the key PIRT phenomena and is applicable for calculating the AP600 plant LTC transient.

1.0 INTRODUCTION

1.1 Purpose of the Report

This report evaluates the performance of WCOBRA/TRAC in predicting the long-term cooling (LTC) thermal-hydraulic effects observed in the Oregon State University (OSU) integral systems test facility, a reduced-pressure, reduced-height facility. These tests have been scaled to the AP600 plant, including the passive safety systems. The OSU facility, the test data, and the analysis of data from these tests are described in References 1-1, 1-2, and 1-3.

The objective of this report is to examine the capability of WCOBRA/TRAC to predict key LTC thermal-hydraulic phenomena, as defined in the Phenomena Identification Ranking Table (PIRT), that were observed during selected transient tests.

1.2 WCOBRA/TRAC Code Role in AP600 Safety Analysis

COBRA/TRAC was originally developed for the U.S. Nuclear Regulatory Commission (NRC) at Pacific Northwest Laboratory. Westinghouse then modified the code, added specific models, and developed the basis for applying the code for safety analysis. The code name was changed to WCOBRA/TRAC to reflect the Westinghouse modifications.

COBRA/TRAC is a combination of two codes, COBRA-TF and TRAC-PD2. The COBRA-TF computer code uses a two-fluid, three-field representation of two-phase flow. Each field is treated in three dimensions and is compressible. The three fields are: a continuous vapor field, a continuous liquid field, and an entrained liquid drop field. The conservation equations for each of the three fields and for heat transfer from and within the solid structures in contact with the fluid are solved using a semi-implicit, finite-difference numerical technique on an Eulerian mesh. COBRA-TF utilizes extremely flexible noding for both the hydrodynamic mesh and the heat transfer solution. With this flexibility, the wide variety of geometries found in components of nuclear reactor primary systems can be modeled.

TRAC-PD2 is a code designed to model the behavior of the reactor primary system. It features special models for each component in the system. These include accumulators, pumps, valves, pipes, pressurizers, steam generators (SGs), and the reactor vessel. With the exception of the reactor vessel, the thermal-hydraulic response of these components to transients is treated with a five-equation drift flux representation of two-phase flow. The TRAC-PD2 vessel module has been removed, and COBRA-TF has been implemented instead as the new vessel component in TRAC-PD2. The resulting code is COBRA/TRAC. The vessel component in COBRA/TRAC has the extended capabilities of three-field representation of two-phase flow and flexible noding.

WCOBRA/TRAC has two roles in the AP600 analysis plan:

- WCOBRA/TRAC is used for the large-break loss-of-coolant accident (LOCA) with the approved best-estimate methodology.

- WCOBRA/TRAC is used in an Appendix K version for the calculation of the AP600 plant performance for the LTC portion of both small- and large-break LOCA transients.

Since WCOBRA/TRAC was originally developed as a best-estimate large-break LOCA code, use of this code for the AP600 is straight-forward and logical. The LTC transient is a quasi-steady-state situation in which the venting of the flow from the automatic depressurization system Stage 4 (ADS4) valves is the primary flow path out of the reactor coolant system (RCS). The pressure drop in the RCS as the flow is vented affects the absolute pressure within the RCS, which then affects the injection flow from the sump or in-containment refueling water storage tank (IRWST). The effective driving heads for the IRWST, and particularly for the sump injection, are measured in feet of water. Therefore, while the system is in a quasi-steady state, there is a delicate pressure balance that can significantly affect the injection flow into the RCS.

Because of the small driving heads, the importance of the pressure drops in the system, and the fact that these pressure drops are dependent on the flow regime that the code would calculate for a particular component, as well as the modeling needed for the hot legs and ADS4 piping, it was decided to use the most accurate low-pressure code to predict the AP600 LTC transient, WCOBRA/TRAC. WCOBRA/TRAC has been compared to a wide range of low-pressure gravity reflood systems tests such as the Cylindrical Core Test Facility (CCTF) and the Slab Core Test Facility (SCTF), as well as low-pressure separate effects tests such as FLECHT, FLECHT-SEASET, and FEBA, as discussed in Reference 1-4. The WCOBRA/TRAC comparisons to the low-pressure gravity reflood tests give added confidence that this code accurately represents the low-pressure gravity reflood processes expected for the AP600 LTC transient.

The objective of the AP600 LTC plant analysis is to show that the AP600 passive safety systems have the same pedigree as active systems to provide core cooling. Therefore, the AP600 SSAR plant calculations are performed in a conservative manner using the Appendix K assumptions, which maximize the decay power to be removed, and use the upper bound line resistances such that the injection and venting capability is challenged in a conservative manner. Once the pedigree of the passive systems is established, simpler methods can be used to estimate the injection flows and the system behavior

1.3 Important AP600 Long-Term Cooling Phenomena

The small-break LOCA and LTC periods are shown in Figure 1-1. LTC is defined as the time after which injection from the IRWST has become stable, until the plant is recovered. The same definition applies for the LTC period after a large-break LOCA. The AP600 passive safety systems indefinitely

provide post-accident core cooling. The cooling flow path is from the downcomer, through the core to the containment via ADS Stages 1 to 3 (ADS1–3), ADS4, and the break. Steam generated in the core is vented to containment and condensed on the containment shell. The condensate is directed into the IRWST and the sump where it can then flow into the core through the direct vessel injection (DVI) line. The core-generated energy is removed from the containment by the passive containment cooling system. The closed-circuit reflux condensation process ensures adequate cooling inventory to maintain the core in a coolable state indefinitely.

The PIRT for the LTC transient is shown in Table 1-1 and identifies the key phenomena of interest.

When the reactor system is in the LTC mode, the primary system is drained to the hot leg level, such that the primary side of the SGs, the pressurizer, and the upper head of the reactor vessel are filled with stagnant steam. The core makeup tanks (CMTs) and accumulators have already injected, and the passive residual heat removal heat exchanger (PRHR HX) is not active because either the temperature difference across the heat exchanger is small, or IRWST level will have drained and uncovered the HX. The injection flow to the vessel comes from the IRWST as long as the IRWST head is larger than the sump head. If the IRWST has drained to the sump level, there will be injection from both the sump and the IRWST. If the IRWST has drained further and the sump head is larger, vessel injection is from the sump alone. Gravity-driven flow from the sump or IRWST is directed to the reactor vessel through the DVI line into the downcomer.

The driving force for the injection flow is the head of the sump fluid as well as the absolute pressure difference between the top of the sump and the RCS pressure in the downcomer. The driving force for core cooling is the level in the reactor downcomer, which provides the elevation head to drive the flow through the core and out of the hot leg and the ADS4 valves. Inclusion of a large vent path on the top of the hot leg through the ADS4 valves provides a low-pressure drop vent path so that ample flow through the core occurs. If this is compared to operating plants, the same downcomer head must drive the core flow through the SG primary side, which superheats the primary fluid and creates a back pressure that reduces the core inlet flow (steam binding). This situation is avoided in the AP600 by using the large vent areas on the top of the hot legs so that very little flow, if any, goes through the SGs. Also, once the IRWST drains, the ADS1–3 vent path is also available to vent the core-generated steam flow to the containment.

At the start of LTC, the DVI nozzles inject the colder water at the bottom of the IRWST. Toward the end of IRWST injection, the injected water temperature increases because of the energy that has been deposited in the IRWST from the PRHR HX and ADS1–3. The increased injection temperature, combined with the reduced IRWST flow that is due to the decreasing level in the IRWST results in a net steam generation in the core. The reactor primary system accommodates the steam generation due to the venting of the ADS4 valves. After the IRWST has drained, water will be injected from the sump. As water is injected from the sump, the flow is reduced further due to the lower sump draining head, and the injection temperature increases toward saturation. This results in a higher rate of steam production in the core, and reduced mass inventory in the core. However, the reduced inventory in the

core does not imply a core uncovery; rather, the void fraction in the core increases as more boiling occurs.

Since the entire primary system is near containment pressure, the resulting core flow is determined by the gravity driving head in the downcomer, the head in the core, and the two-phase pressure drop in the core, hot legs, and ADS4. The LTC PIRT is given in Table 1-1 and contains the phenomena ranking for the IRWST injection phase as well as for the sump injection phase. Most of the highly ranked items are the same for both IRWST and sump injection. The levels in the core, upper plenum, and downcomer are all ranked high since the levels determine if the core remains covered and coolable. Most of the RCS components above the hot legs and cold legs are empty and full of stagnant steam and do not contribute to the LTC phenomena. These components are either ranked very low in the PIRT or are not applicable for this period of the transient. The decay power is ranked high since this is the source of steam generation within the vessel. Using the Appendix K assumptions for the decay heat in the AP600 plant calculations will clearly be conservative for the LTC period.

The hot leg flow pattern and the effects of the "T" connection at the top of the hot leg are ranked high since these components determine the void fraction and quality of the flow that is vented out the ADS4 valves. The venting of ADS4 valves is important since reduced ADS vent area or increased pressure drop adversely affects the flow through the core and the core steam generation rate. Higher ADS4 pressure drop reduces the core flow and increases the steam generation rate, and hence, the volume of steam that must be vented.

The IRWST flow and the sump flow are ranked high since these flows are needed to maintain core cooling. The temperature of the sump flow is also ranked high since a reduced subcooling of the sump flow results in additional steam generation in the core which then must be vented.

The DVI line resistance is ranked high. This is an important quality, because for a given head difference between the IRWST or the sump and the RCS, it is the DVI line resistance that determines the flow into the reactor vessel.

All the parameters ranked high in Table 1-1 will be evaluated in the analysis of the OSU LTC tests.

1.4 Window-Mode Analysis of Long-Term Cooling

The AP600 small-break LOCA and LTC transients can extend for very long periods (typically 5 to 24 hours), during which time there is a stable injection from the sump into the reactor vessel. While long simulations are possible, they are not practicable with WCOBRA/TRAC or any other existing systems computer code due to the extremely long computer time that is necessary.

In the WCOBRA/TRAC preliminary LTC validation report (Reference 1-5), a "window-mode" approach was used for the LTC calculations. The LTC transient is quasi-steady state, with very small changes occurring over long periods of time. The flow through the primary system is very low, but

sufficient to maintain core cooling. The pressures in the RCS, IRWST, and sump are constant with very little variation, and the core decay power decreases slowly. Since this period of the transient is nearly steady state, a window is analyzed to verify the adequacy of the WCOBRA/TRAC code for this portion of the transient. The WCOBRA/TRAC window-mode approach is also used for the final validation report as well as for the plant SSAR calculations.

The windows selected reflect the times when the core cooling has minimal margin and include the following:

- Late IRWST injection phase when the injection fluid temperature increases and the driving head is reduced

- Sump injection when the sump temperature is high

For these situations, the window-mode calculations have been made for the OSU transients to compare the WCOBRA/TRAC predictions with the OSU data. Initial conditions for the calculation were obtained from the data. However, when the WCOBRA/TRAC code initiates the calculation, the code experiences a transient as the mass distribution, which was initially assumed, is redistributed and the flows are initiated. Therefore, the WCOBRA/TRAC calculation must be performed for approximately three times the primary system time constant so that the WCOBRA/TRAC calculated flows and mass distributions reach a quasi-steady state similar to the tests. The calculational times used for the WCOBRA/TRAC window-mode calculations were approximately 1,000 seconds long for each window. At the end of the window time, the WCOBRA/TRAC calculation had reached a quasi-steady-state condition and the results could be compared to the experiments.

To validate the WCOBRA/TRAC code for the LTC transient, the following four OSU tests were examined:

- SB01 – 2-in. cold leg break test. This is the reference test. The break becomes submerged in this test as the sump fills.

- SB10 – double-ended CMT balance line break test. This simulates a complete failure of an 8-inch balance line. The break location is above the flood-up level, so that venting through the break can occur.

- SB12 – double-ended DVI line break test. This simulates the complete failure of an 8-inch injection line. Sump injection is achieved earlier in time when the core decay power is still high; hence, steaming rates are large.

- SB23 – simulated 1/2-in. break at the bottom of cold leg 3. This small-break test has the largest heatup of the IRWST due to the PRHR heat transfer and the ADS1–3. Therefore, the IRWST injection temperature is the highest.

These tests capture the thermal-hydraulic phenomena of interest for small breaks and LTC and are suitable to validate the performance of WCOBRA/TRAC.

1.5 References

1-1. WCAP-14124, Volume I and Volume II, *AP600 Low Pressure Integral Systems Test at Oregon State University, Facility Description Report*, July 1994.

1-2. Dumsday, C. L., Carter, M., Copper, M. H., Lau, L. K., Loftus, M. J., Nayyar, V. K., Tupper, R. B., and Willis, J. W., WCAP-14252, Volumes 1-4, *AP600 Low Pressure Integral Systems Test at Oregon State University, Final Data Report*, May 1995.

1-3. Andreychek, T. S., Chismar, S. A., Delose, F., Fanto, S. V., Fittante, R. L., Frepoli, C., Friend, M. T., Haberstroh, R. C., Hochreiter, L. E., Morrison, W. R., Ogrinsh, M., Peters, F. E., Wright, R. F., and Yeh, H. C., WCAP-14292, Rev. 1, *AP600 Low Pressure Integral Systems Tests at Oregon State University, Test Analysis Report*, September 1995.

1-4. Bajorek, S. M., Hochreiter, L. E., Young, M. Y., Dederer, S. I., Nissley, M. E., Tsai, C. K., Yeh, H. C., Chow, S. K., Takeuchi, K., Cunningham, J. P., and Stucker, D. L., WCAP-12945P, Vols. 1-5, *Code Qualification Document for Best Estimate LOCA Analysis*, June 1992.

1-5. Chow, S. K., Grela, I., Ward, P., Frepoli, C., Petkov, N., and Hochreiter, L. E., *WCOBRA/TRAC OSU Long-Term Cooling Preliminary Validation Report*, LTCT-GSR-003, August 1995.

TABLE 1-1
PHENOMENA IDENTIFICATION RANKING TABLE
FOR AP600 LOCA LTC TRANSIENT (Rev. 1)

Component Phenomenon	IRWST Injection[1]	Sump Injection[1]
Break		
Critical flow	M	N/A
Subsonic flow	M	L
ADS Stages 1 to 3		
Critical flow	M	N/A
Subsonic flow	M	L
Two-phase pressure drop	L	L
Valve loss coefficients	M/L	L
Single-phase pressure drop	L	L
Vessel/Core		
Decay heat	H	H
Flow resistance	L	L
Flashing	N/A	N/A
Wall-stored energy	M	M
Natural circulation flow and heat transfer	M	M
Mixture level mass inventory	H	H
Pressurizer		
Pressurizer fluid level	L	N/A
Wall-stored heat	L	N/A
Pressurizer Surge Line		
Pressure drop/flow regime	L	L
Downcomer/Lower Plenum		
Pressure	H	H
Liquid level	H	H
Condensation	M	M
Upper Head		
Liquid level	N/A	N/A
Flow through downcomer top nozzles	M	M

TABLE 1-1 (Cont)
PHENOMENA IDENTIFICATION RANKING TABLE
FOR AP600 LOCA LTC TRANSIENT (Rev. 1)

Component Phenomenon	IRWST Injection[1]	Sump Injection[1]
Upper Plenum		
Liquid level	H	H
Entrainment/deentrainment	M	M
Cold Legs		
Condensation	L	L
Separation at balance line tee	L	L
Steam Generator		
2φ - natural circulation	N/A	N/A
Steam generator heat transfer	L/NA[2]	N/A
Secondary conditions	L/NA[2]	N/A
Hot Leg		
Flow pattern transition	H/M	H/M
Separation at ADS4 tee	H/M	H/M
ADS4		
Critical flow	H	N/A
Subsonic flow	H	H
CMT		
Recirculation injection	N/A	N/A
Gravity draining injection	L	L
Vapor condensation rate	L	L
CMT Balance Lines		
Pressure drop	N/A	N/A
Flow composition	L	L
Accumulators		
Noncondensible gas entrainment	N/A	N/A
IRWST		
Gravity draining injection	H	M
Vapor condensation rate	L	L
Temperature distribution	M	M

TABLE 1-1 (Cont)
PHENOMENA IDENTIFICATION RANKING TABLE
FOR AP600 LOCA LTC TRANSIENT (Rev. 1)

Component Phenomenon	IRWST Injection[1]	Sump Injection[1]
DVI Line		
Pressure drop	H	H
PRHR		
Liquid natural circulation flow and heat transfer	N/A	N/A
Sump		
Gravity draining injection	N/A	H
Level	N/A	H
Temperature	N/A	H

Note:
1. H = High
   M = Medium
   L = Low
   N/A = Not Applicable

2. The rankings for steam generator heat transfer and secondary conditions are Low for IRWST injection after a large break and Not Applicable for IRWST injection after a small break.

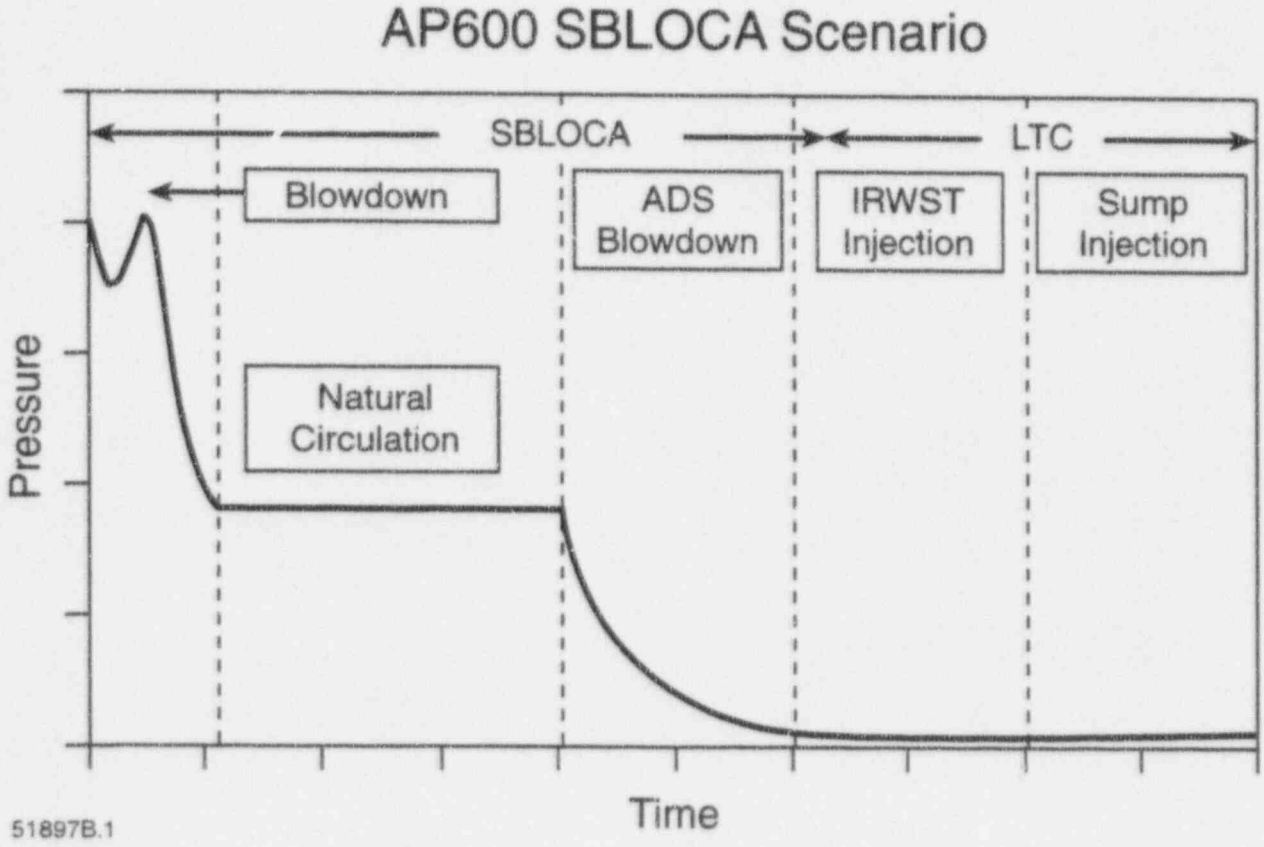

Figure 1-1 AP600 Small-Break LOCA and LTC Scenario

2.0 WCOBRA/TRAC OSU LONG-TERM COOLING MODEL

The Oregon State University (OSU) test facility is a quarter-scale model of the Westinghouse AP600 systems. It is a low-pressure, integral systems facility designed for test conditions up to 400 psig and 450°F. The facility consists of the following AP600 systems:

- Reactor coolant system (RCS)
- Steam generator (SG) system – primary side
- Passive core cooling system (PXS)
- Partial chemical and volume control system (CVS)
- Partial nonsafety-related normal residual heat removal system (RNS)
- Automatic depressurization system (ADS)

Detailed descriptions of these systems are given in References 2-1 and 2-2.

The WCOBRA/TRAC long-term cooling (LTC) model has the same components as the OSU test facility. Figure 2-1 shows the components simulated by the model. The following subsections describe the main components.

2.1 Vessel Component

The WCOBRA/TRAC VESSEL components are shown in Figures 2-2 through 2-9. These components simulate the OSU test vessel that contains electrical heater rods as the energy source. As shown, seven sections with 15 levels are used to model the vessel. Because the downcomer has four main loop connections, the model downcomer is divided into four sectors, one section for each leg.

Section 1, shown in Figure 2-3, represents the lower plenum; it has one level and five flow channels.

Section 2, shown in Figure 2-4, represents the downcomer and the heater rod core; it has two levels and one channel modeling the core. The total height of Section 2 is 39.62 in. This height is the sum of the heater rod active length (36 in.) and the space between the top rod grid and the upper core plate (3.62 in.). Although the model provides a two-rod option, the simulation calculations use a constant power level for both rods because the OSU tests used a uniform radial power distribution.

Sections 3 through 5, shown in Figures 2-5 to 2-7, represent the upper plenum region. Section 3 models the downcomer and the region above the upper core plate and below the bottom of the hot leg nozzle; it has one level and six channels. Sections 4 and 5 model the upper-plenum region, hot legs, downcomer, and cold legs. The cold legs and horizontal portions of the hot legs are modeled as part of the vessel. This noding approach is used because countercurrent flow and flow stratification may occur in the hot legs and cold legs during LTC simulations. These phenomena could not be accurately simulated if the hot legs and cold legs were modeled as one-dimensional pipes using the drift-flux approach. The upper plenum is represented by one channel for each section; two channels represent

each hot leg, and three channels represent each cold leg. Using on this noding approach, Section 4 has nine channels, and Section 5 has 17 channels.

Sections 6 and 7, shown in Figures 2-8 and 2-9, represent the upper-head region. Section 6 has five levels and three channels, and Section 7 has one level and two channels.

The code's unheated conductors model the vessel metal structure. The surface boundaries of the unheated conductors connect to the fluid channels.

Vertical flow channels simulate the axial flow paths, and the code's gaps represent lateral flow paths. There are 47 channels, 43 gaps, and 99 computational cells in the OSU vessel model.

2.2 Primary Loop

The primary loop includes the following major components: a pressurizer, two SGs with four reactor coolant pumps (RCPs), valves, hot legs and cold legs, and a surge line. These components are shown in Figure 2-1 and described in the following subsections.

2.2.1 Pressurizer

The pressurizer vent line connects to the ADS Stages 1 to 3 (ADS1–3) valves. Because the code's standard PRIZER component does not have a vent line connection option, a PIPE component with five cells simulates the pressurizer (component 50). The top of the pressurizer connects to the ADS1–3 valves, and the bottom connects to the surge line (component 49). The surge line connects to hot leg 2 (HL-2).

2.2.2 Steam Generators

The code's STGEN component models the SGs (components 75 and 76) with 10 cells for the primary side, and five cells for the secondary side. VALVE components simulate the main feedwater and steam line isolation valves.

2.2.3 Reactor Coolant Pumps

The RCPs are part of the SG lower plenum. The code's PIPE component models the pumps adjacent to the STGEN outlets. TEE components connect the SGs and pumps. Components 59 through 62 represent these pumps. PIPE components are used because the RCPs have coasted down completely before the start of the LTC phase, when the RCPs represent a simple flow resistance.

2.2.4 Loop Lines

The code's PIPE, TEE, and VALVE components model the primary loop piping. Components 49 and 63 represent the sloping portions of the hot legs. The horizontal portions of the hot legs are modeled as part of the reactor vessel. The simulation preserves key elevations, fluid volumes, pipe lengths, and pipe inside diameters.

2.3 Accumulators

The two accumulators are not modeled because they are empty before the LTC phase begins.

2.4 Core Makeup Tanks

PIPE components model the core makeup tanks (CMTs) (components 6 and 25). Balance lines connect the top of the CMTs to the cold legs. The bottom of the CMTs connect to the direct vessel injection (DVI) lines through the CMT discharge lines. Each CMT has six cells. VALVE components model the flow control valves and check valves in the connecting lines. The CMTs are simulated, since the OSU CMTs refilled due to heat losses and condensation during the LTC period of the tests.

2.5 Passive Residual Heat Removal Heat Exchanger/In-Containment Refueling Water Storage Tank

Test data indicate that the passive residual heat removal heat exchanger (PRHR HX) is inactive in the LTC phase because of open ADS Stage 4 (ADS4) valves and reduced IRWST water level. Therefore, the PRHR HX is not modeled in WCOBRA/TRAC. PIPE component 93 models the IRWST tank.

2.6 In-Containment Refueling Water Storage Tank Injection Lines

Components 13 through 15, 32 through 34, and 48 model the two IRWST injection pipe lines and associated valves. These pipe lines, simulated by the code's PIPE, TEE, and VALVE components, connect the IRWST and two DVI lines.

2.7 Automatic Depressurization System Stage 1 to 3 Valves

Component 46 models the ADS1–3 valves. In the AP600 plant, each set of valves has two flow paths. The OSU test facility uses a one-flow-path, two-flow-path, or combination-simulation option depending on the matrix test specification. In WCOBRA/TRAC, the ADS1–3 valves are modeled as a single VALVE component. The VALVE component is open during LTC phase.

The sparger line is not modeled in the WCOBRA/TRAC LTC simulations. In the LTC mode, the IRWST is draining and the sparger line is empty. Consequently, sparger line simulation is unnecessary.

2.8 Automatic Depressurization System Stage 4 Valves

Components 64 and 67 represent ADS Stage 4-1 and 4-2 valves, respectively. These valves reduce RCS pressure through HL-1 and HL-2. In the AP600 plant, each fourth stage has two flow paths. In the OSU test facility, a single flow path is available with optional orifices to model either a single valve (50-percent valve opening area) or two valves (100-percent valve opening area) to simulate the various matrix test specifications.

2.9 Primary Sump Tanks

The head of sump water is represented by four BREAK components (components 518, 519, 536, 537). These components connect to the IRWST injection lines by flow control valves (components 18 and 36) and check valves (components 19 and 37).

2.10 Break Component

The code's BREAK component represents various breaks in the specified OSU test cases. BREAK components also simulate conditions at the ADS1–3, and ADS Stages 4-1 and 4-2 outlets.

2.11 Normal Residual Heat Removal System

This system is not represented in any tests in this report.

2.12 References

2-1. WCAP-14124, Volume I and Volume II, *AP600 Low Pressure Integral Systems Test at Oregon State University, Facility Description Report*, July 1994.

2-2. Dumsday, C. L., Carter, M., Copper, M. H., Lau, L. K., Loftus, M. J., Nayyar, V. K., Tupper, R. B., and Willis, J. W., WCAP-14252, Volumes 1-4, *AP600 Low Pressure Integral Systems Test at Oregon State University, Final Data Report*, May 1995.

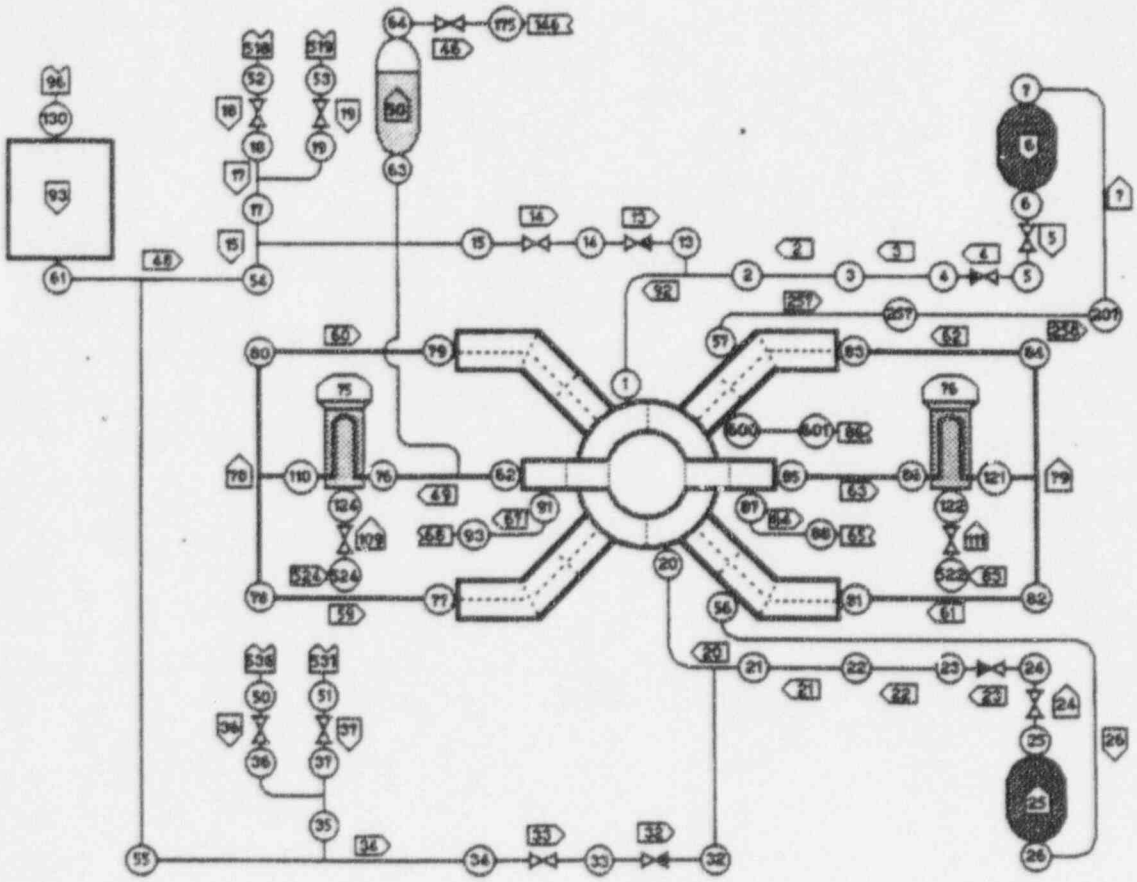

Figure 2-1 OSU WCOBRA/TRAC Schematic Diagram

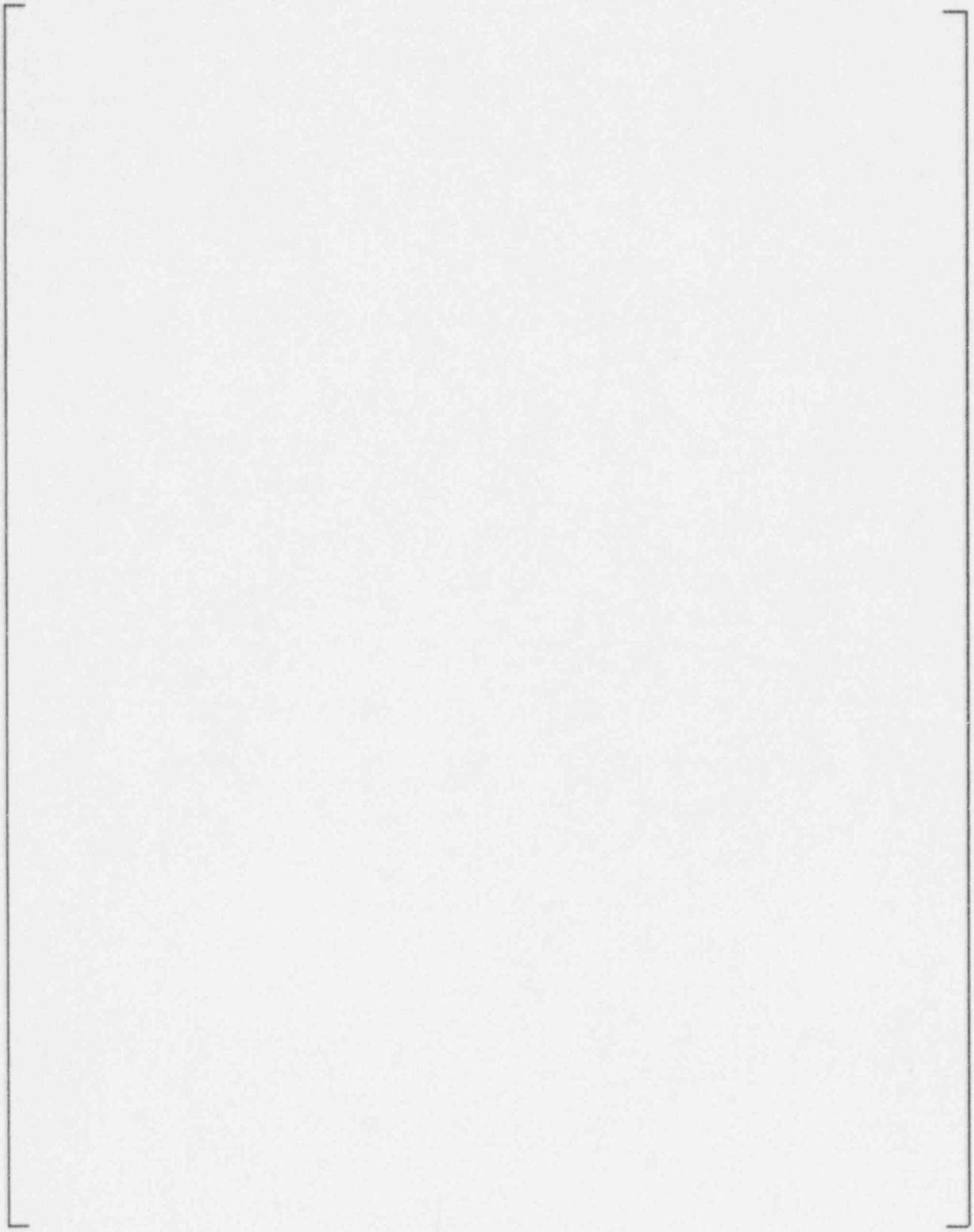

a,c

Figure 2-2 OSU WCOBRA/TRAC Vessel Model (Front View)

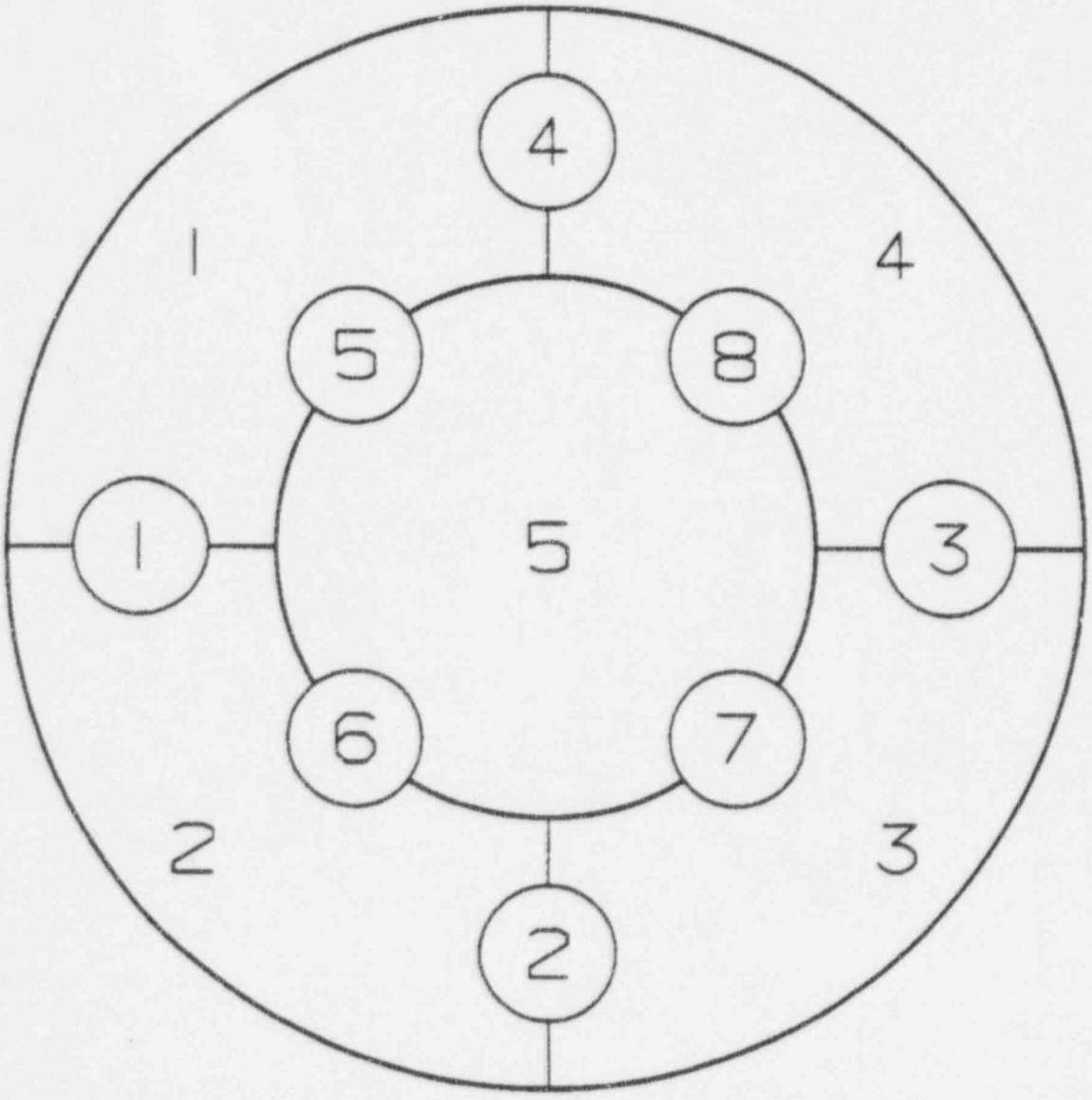

Figure 2-3 OSU Vessel Model – Section 1

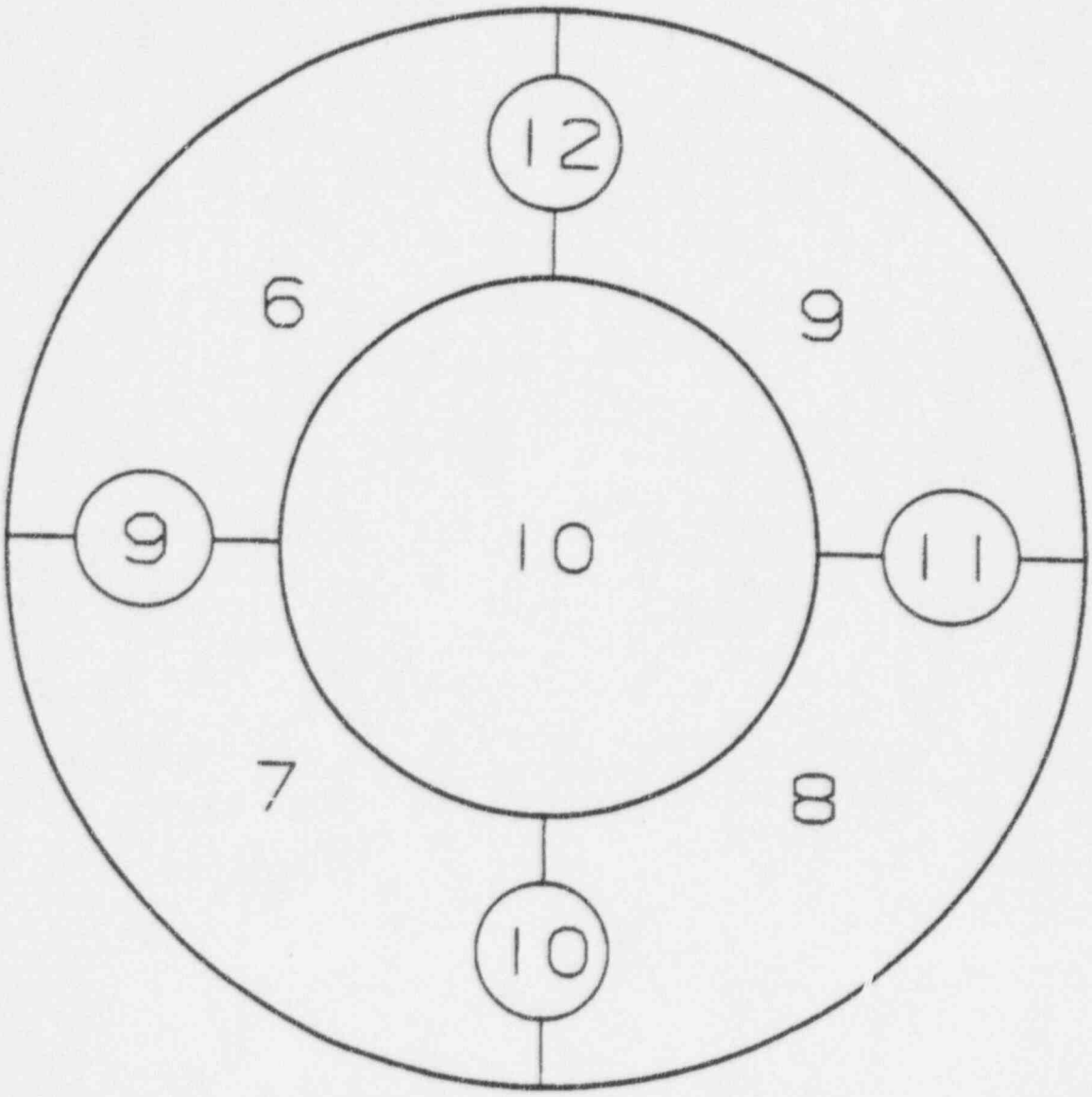

Figure 2-4 OSU Vessel Model – Section 2

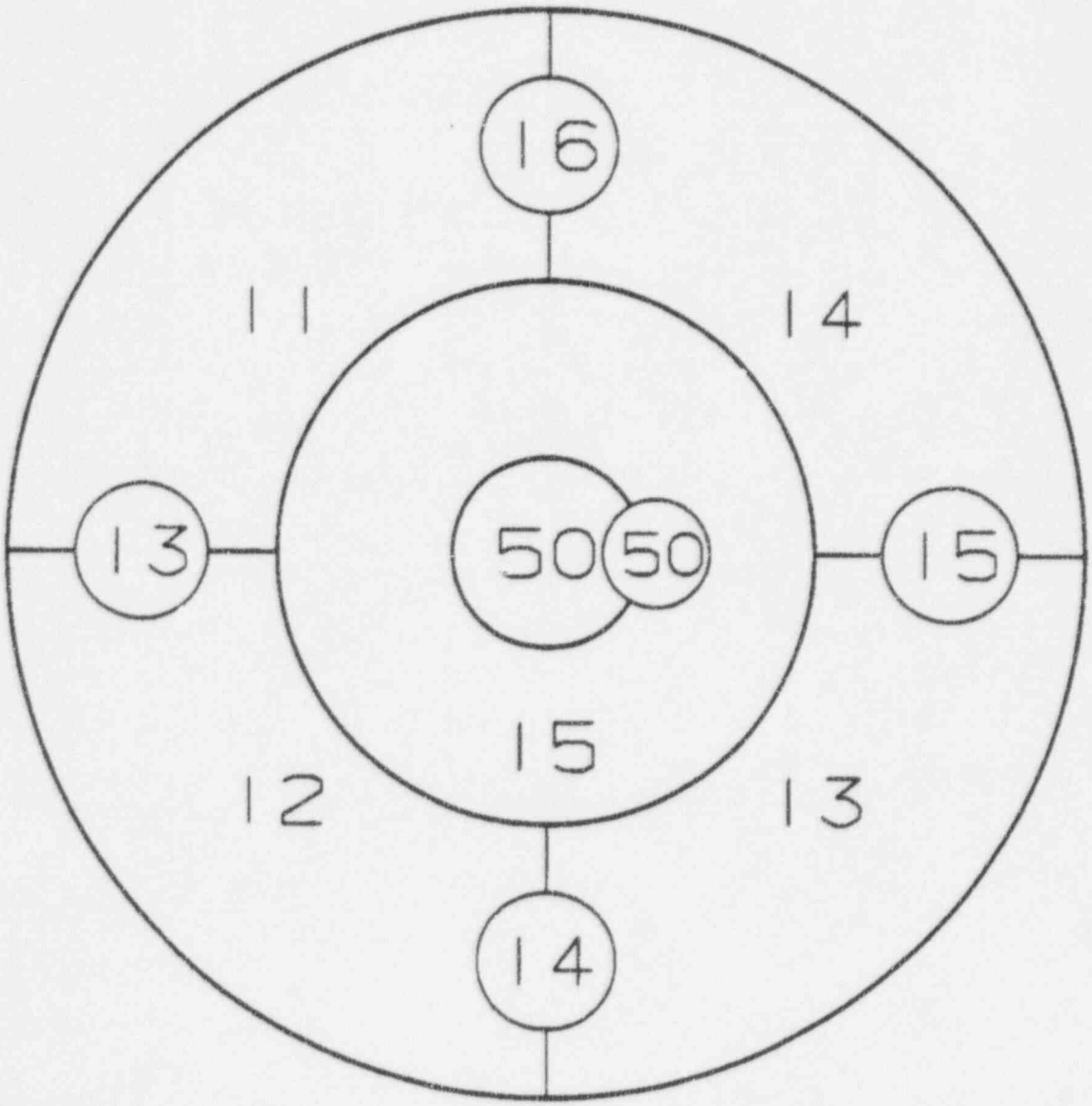

Figure 2-5 OSU Vessel Model – Section 3

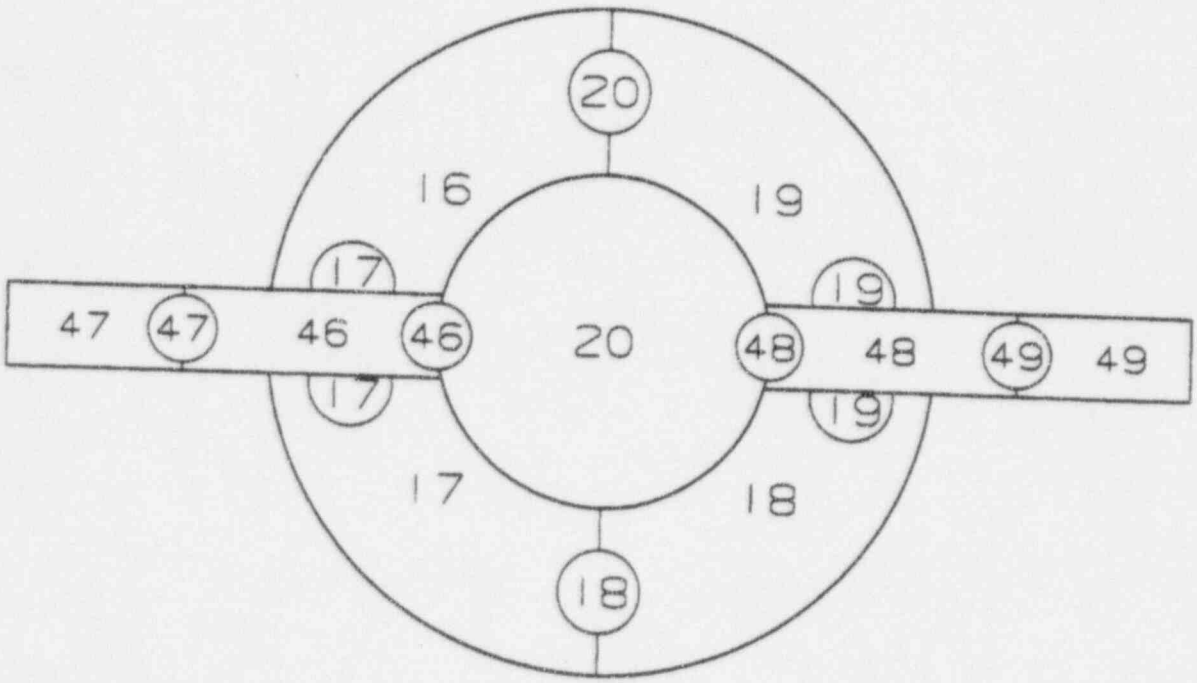

Figure 2-6 OSU Vessel Model – Section 4

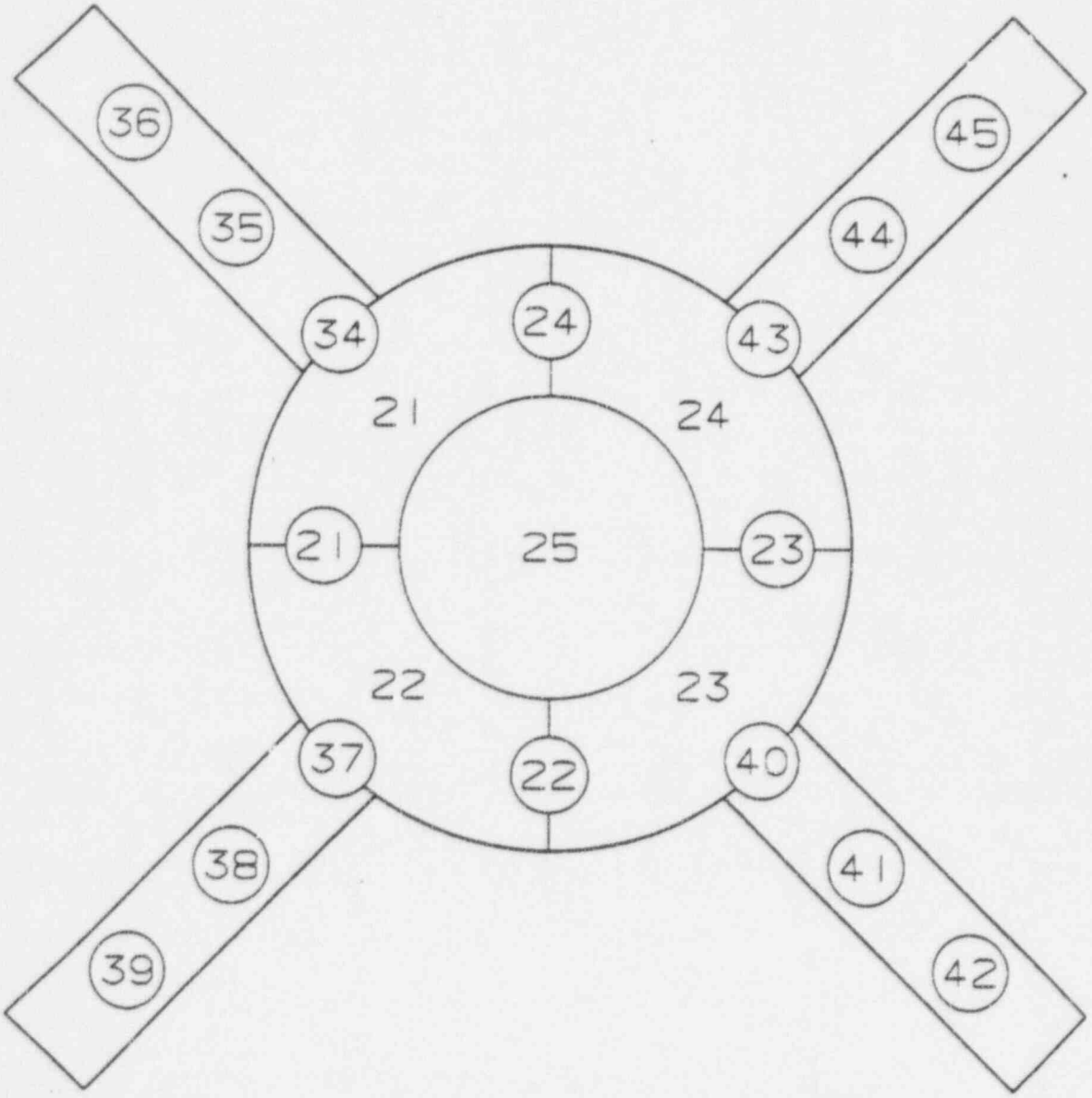

Figure 2-7 OSU Vessel Model – Section 5

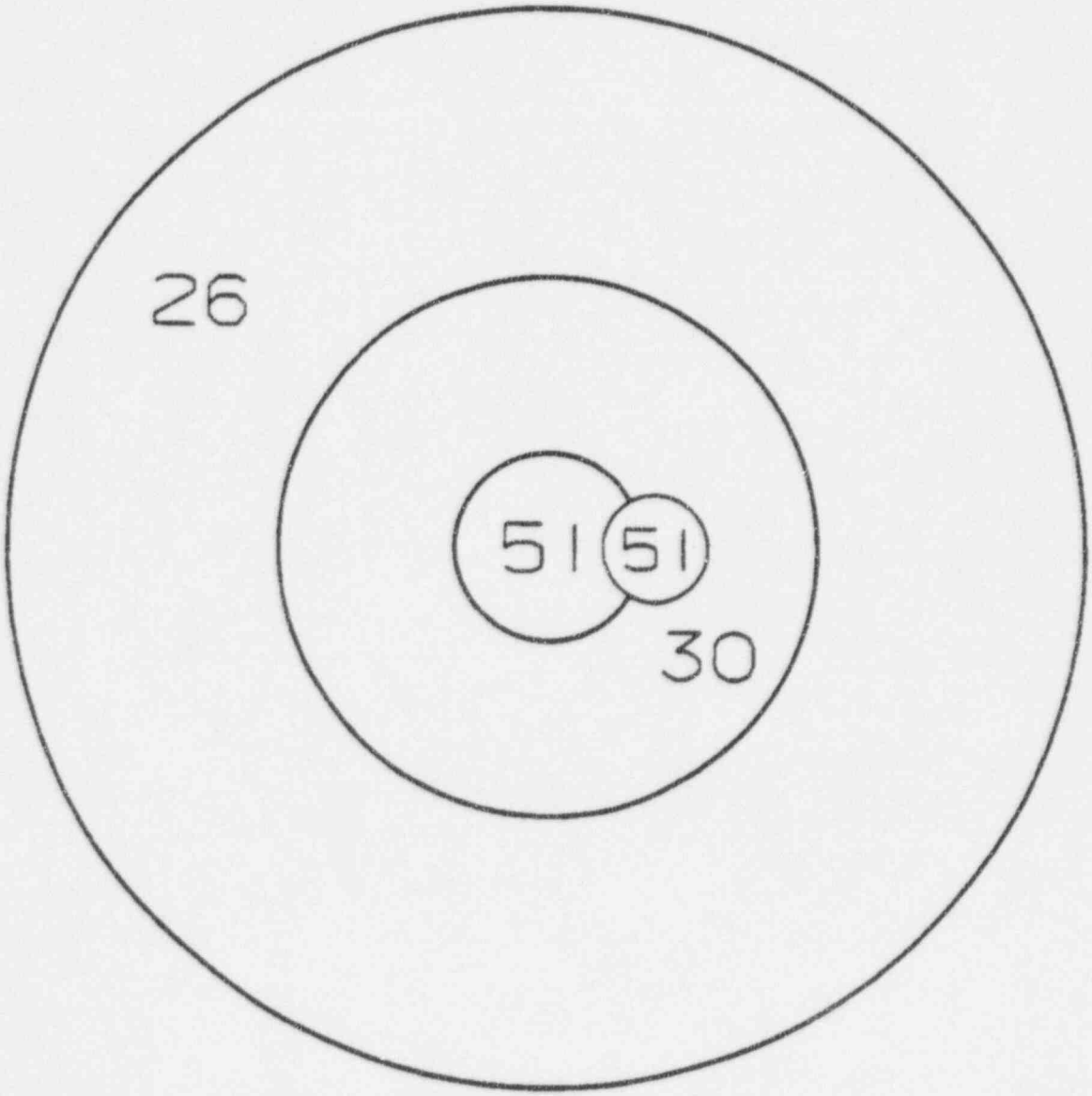

Figure 2-8 OSU Vessel Model – Section 6

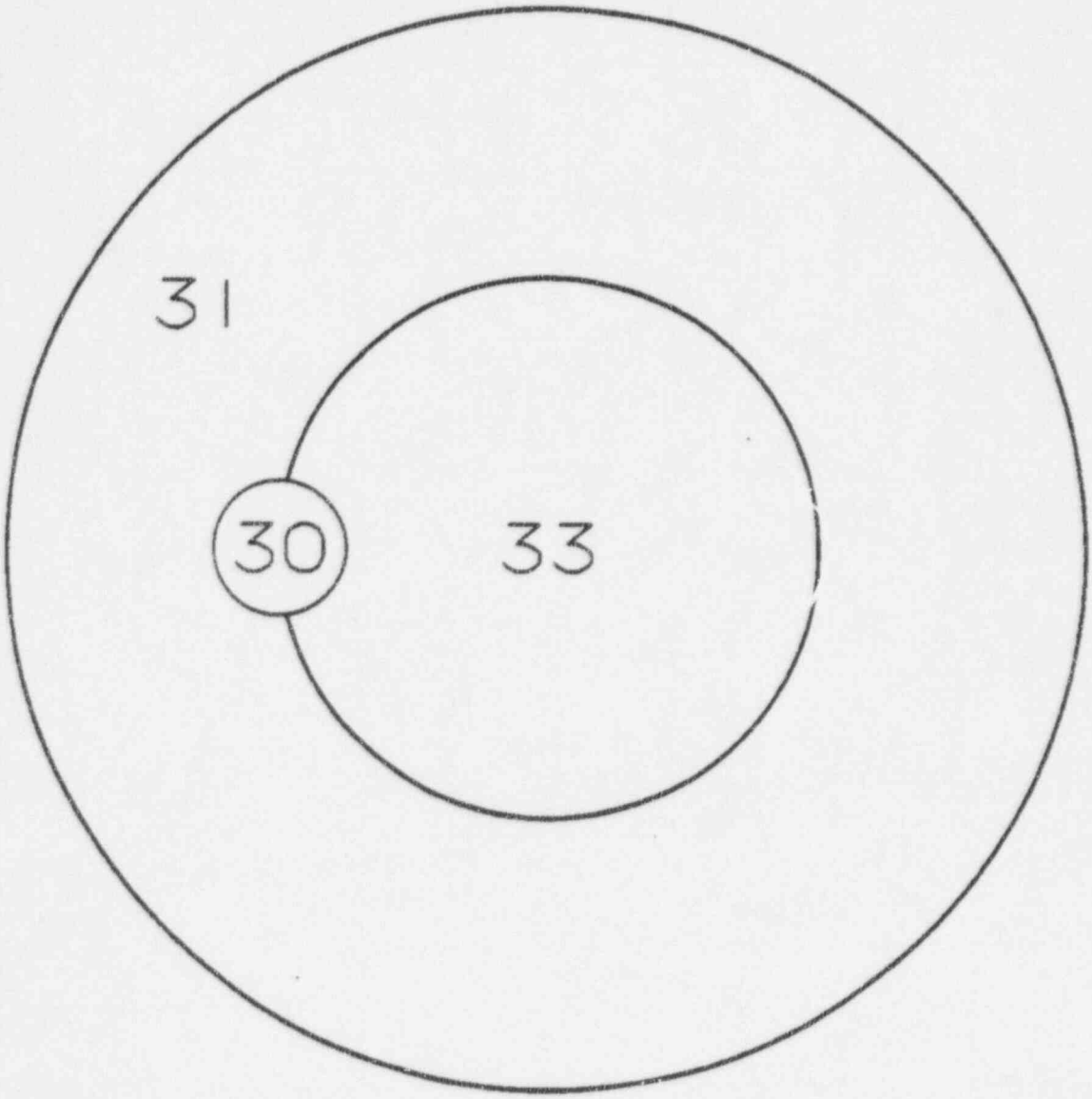

Figure 2-9 OSU Vessel Model – Section 7

3.0 WCOBRA/TRAC OSU MODEL VERIFICATION APPROACH

Section 2 describes the WCOBRA/TRAC modeling of the Oregon State University (OSU) test facility components. This section discusses the WCOBRA/TRAC features that model the OSU boundary conditions and control processes, and describes the window-mode approach.

3.1 Reactor Vessel/Loop Connections

In conventional pressurized water reactor (PWR) modeling, the cold leg and hot leg pipes are modeled as one-dimensional components. As described in Section 2.1, the WCOBRA/TRAC model for the AP600 incorporates the cold leg and a portion of the hot leg into the COBRA reactor vessel model to allow detailed modeling of countercurrent flow and flow stratification.

The hot leg horizontal sections are modeled as part of the VESSEL component. The remaining vertical portion of the hot legs are modeled as pipes connecting the reactor vessel and steam generators. The four cold legs are also incorporated in the COBRA reactor vessel model and they connect to the TRAC reactor coolant pump (RCP) components. Because there are two levels in the cold legs and three levels in the hot legs, with each level connected to the same one-dimensional component cell, the code was revised to provide multi-connection capability between a TRAC one-dimensional cell and several COBRA reactor vessel cells. Section 4.2 describes this code revision in detail.

3.2 Power Shape and Decay Heat Curve

Figure 3-1 shows the OSU normalized axial power profile. A power shape with the step variation simulating this profile was used as the power shape input for the WCOBRA/TRAC OSU model.

Figure 3-2 shows the decay power after the simulated reactor trip. This power time history was used during transient simulations. The total initial core power during steady-state operation is 600 kW. The OSU bundle has 48 rods with the average power of 4.167 kW/ft. Each rod has an active length of 3 feet.

3.3 Pressurizer and Core Makeup Tanks

PIPE components model both the pressurizer and core makeup tanks (CMTs). Each of these components is initialized with saturated steam.

3.4 Automatic Depressurization System Stage 1 to 3 Valves

The ADS Stages 1 to 3 (ADS1-3) valves are three parallel sets of valves controlling flow between the pressurizer and the sparger lines. In the AP600, each set of valves has two flow paths; however, in the OSU facility only one flow path is provided for each set of valves. To simulate various valve

failures, different sized orifices are inserted into each valve's flow path to represent valve failure conditions.

In the WCOBRA/TRAC simulation, the three valve sets combine into one equivalent valve since the ADS1–3 valves are fully open at the start of the long-term cooling (LTC) transient.

3.5 Passive Residual Heat Removal System Heat Exchanger/In-Containment Refueling Water Storage Tank

The in-containment refueling water refueling storage tank (IRWST) is simulated as a pipe component and break in order to apply a pressure boundary condition to the tank. The passive residual heat removal heat exchanger (PRHR HX) is not modeled for the LTC transient because this system is not effective during this period. It is conservative to ignore the PRHR HX since it condenses steam that otherwise would have to be vented out the ADS4 valves. The ADS1–3 system is modeled assuming the sparger is uncovered.

3.6 Line Pressure Loss

WCOBRA/TRAC calculates nonrecoverable pressure loss due to wall friction using specific models. Additional form loss can be implemented by specifying the form loss coefficient for the reactor channels. OSU pressure loss measurement test results (Reference 3-1) were converted into nondimensional form loss coefficients. These pressure losses are compared to those obtained from WCOBRA/TRAC model simulations. Stand-alone WCOBRA/TRAC modules were established to verify that the calculated pressure drops agree with the test data. Table 3-1 shows the form loss coefficient comparison between the test data and the calculated values.

3.7 Initial Conditions

Four cases are investigated in this report: SB01, SB10, SB12, and SB23. The OSU Final Data Report provides the LTC initial conditions for these cases (Reference 3-2). The transient calculation is initiated using the test conditions as a guide. The WCOBRA/TRAC calculation is initially a transient until the mass redistributions occur and the flow stabilizes. Once steady, the calculation is compared to the test data.

3.8 In-Containment Refueling Water Storage Tank/Direct Vessel Injection

Two injection lines connect the IRWST to the two direct vessel injection (DVI) lines. Two types of valves are used on each line: a flow control valve and a check valve, with the check valve on the downstream side. The flow control valve is normally closed; it opens when the pressure at the top of the reactor vessel is equal to or less than 57.4 psia. Each line resistance is different such that each line is individually recorded.

3.9 Long-Term Cooling Analysis Approach

The OSU test results have IRWST injection for periods greater than 10,000 seconds. Sump injection begins when the IRWST level falls to the low-low level (15 percent full) or when the DVI line pressure falls sufficiently to open the sump check valves. In tests SB01, SB10, and SB23, sump injection continued for longer than 10,000 seconds, until these tests ended. In test SB12, the data acquisition system failed after the start of sump injection and the test was terminated; however, sufficient data were collected for comparison with the simulation.

Even using the relatively coarse noding model for this analysis, modeling an entire test is not feasible because of the computer analysis time required. Instead, the tests are modeled using the window-mode approach, which examines a portion of the LTC transient since the OSU facility reaches a quasi-equilibrium state during the long periods of IRWST and sump injection. The calculation starts during sump or IRWST injection with appropriate initial conditions, and the solution converges to the quasi-equilibrium condition observed in the test. The initial conditions for the window-mode simulations are taken from the test data at or near the time period of interest. The changing conditions during the long period of IRWST injection are sufficiently small and the window-mode calculations are sufficiently long such that the solution obtained is independent of the assumed initial conditions. The initial and boundary conditions required for the window-mode simulations, which are taken from the tests, include the temperatures and water levels of the sump and IRWST, and the decay power.

For each of the four test simulations, the selected window includes the start of sump injection. This period has a low flow rate and a high temperature in the DVI lines and the highest core power of the sump injection period. The window-mode simulations for test SB01, SB10, and SB23 begin approximately 200 to 400 seconds before the start of sump injection and typically run for 1,000 seconds. In the case of test SB12, the window selected is the final 1,000 seconds of IRWST injection. During the initial approximately 400 seconds of each simulation, the solution approaches a quasi-equilibrium state. Average values compared to the test data are taken during the 400 seconds after the start of the window until the end of the window simulation.

3.10 Window Mode Sensitivity Study Calculations

A series of window-mode sensitivity calculations were performed to show the convergence of the WCOBRA/TRAC calculation for a given test. Two tests were examined: SB01 and SB10. Two different types of sensitivity studies were performed. The initial level in the core and the initial temperature in the downcomer were varied. The objective of these sensitivity studies was to show that the WCOBRA/TRAC calculation reaches the same quasi-steady-state conditions regardless of the initial conditions assumed. The window-mode calculations are a boundary value problem in which the final solution is determined by the imposed boundary conditions, not the assumed initial conditions. In the WCOBRA/TRAC window-mode calculations, the IRWST conditions, pressure, and heater rod power are the boundary conditions, while the fluid temperature and levels in the simulated vessel are the initial conditions. As the calculation proceeds, the flow and the liquid temperature from the

IRWST will replace the initial fluid conditions in the vessel and the calculation will converge to the same quasi-steady-state end point.

In the SB01 simulations, the initial collapsed level in the calculation was varied from the reference condition. The reference collapsed level was at the top of the heated length of the simulated core. The two sensitivity calculations varied the initial level from the top of the hot leg (overfilling the vessel), to 75 percent of the initial core level (underfilling the vessel). The calculations had the same imposed boundary conditions of pressure, power, and IRWST conditions, and began at 14,000 seconds into the transient.

The upper plenum pressure is shown in Figure 3-3 for all three calculations. As the figure indicates, variation occurs at the beginning of the calculation; however by 14,320 seconds, or 320 seconds of calculation time, the pressures converge. This behavior is seen in Figure 3-4 for the downcomer levels. Figure 3-4 shows that the system adjusts for the difference in the initial collapsed level in the vessel. The initial low level increases and reaches the reference level case by approximately 14,380 seconds. Similarly, the initial high level decreases and reaches the reference level at the same time. This behavior is also observed in the core levels in Figure 3-5 and in the upper plenum levels in Figure 3-6. The upper plenum levels are the clearest indication of the system readjustment from the initial conditions to the final quasi-steady-state conditions as imposed by the system boundary conditions. Plots of the calculated void fraction at the top of the core and in the upper plenum in Figures 3-7 and 3-8 also show the convergence to quasi-steady-state values.

The calculated IRWST DVI-1 flow rates are shown in Figure 3-9, and the integral of these flow rates is given in Figure 3-10. These valves for DVI-2 are given in Figures 3-11 and 3-12. Comparison of DVI flow rates with the level plots in Figure 3-3 clearly shows that the case with the initial low level has higher DVI line flows due to a greater initial driving head for the IRWST; whereas, the case with the higher initial level has lower DVI flows due to the lower initial IRWST driving head. As the figures indicate, all the flows become the same, the vessel levels stabilize, and the flows are identical after 14,480 seconds. This flow behavior is confirmed by examining the DVI integral flow figures, which show that the integral values become parallel after 14,480 seconds.

The core steam generation for the three cases is shown in Figure 3-13. As with the DVI injection flows, some initial variation in the calculated steam flows from the IRWST occur in response to the different initial level conditions in the vessel. However, after the flows stabilize, the steam generation calculated in the rod bundle becomes the same. This is also confirmed by the integrated core exit steam flow shown in Figure 3-14.

The flow out of the primary system moves through the ADS4 valves located on each hot leg. Figure 3-15 shows the ADS Stage 4-1 flow rate for the three cases, and indicates that after the levels and the IRWST flows stabilize, the flow through the ADS4 valves also stabilizes. The assumed single failure simulated in ADS Stage 4-1 has one-half the flow area of ADS Stage 4-2. Figure 3-15 and the integral of the ADS Stage 4-1 flows in Figure 3-16 show that when the initial level is low, the ADS

flow is nearly zero, because the IRWST flow is refilling the vessel. The ADS4 flow for the lower initial level is nearly zero on Figure 3-15 until 14,160 seconds. When the vessel fills to its quasi-steady-state level, the ADS Stage 4-1 flow increases and is equal to the reference level case. The converse is true of the higher initial level case. In this case, the ADS Stage 4-1 flows are larger because the vessel is initially overfilled and additional mass must be vented for the vessel to reach its quasi-steady-state value. The same behavior is shown in Figures 3-17 and 3-18 for ADS Stage 4-2.

The same initial level sensitivity study was also performed using test SB10, which is a double-ended cold leg balance line break. This break is elevated and is not submerged as the sump fills to its maximum elevation. Figures 3-19 through 3-34 show the same set of plots for the SB10 initial level sensitivity study. Figures 3-19 through 3-22 show that the different initial levels quickly converge to the reference case and become quasi-steady-state. The IRWST injection flows and their integrated values are shown in Figures 3-25 to 3-28. Figures 3-25 through 3-28 also show that the system quickly converges to quasi-steady-state injection (typically within 300 seconds). The steady injection flow is also reflected in the steady calculated steam generation within the heater rod bundle and the integrated steam flow, shown in Figures 3-29 and 3-30, respectively. The ADS Stages 4-1 and 4-2 flows and their integrated values are shown in Figures 3-31 through 3-34. The ADS4 flows show the same behavior as observed in test SB01, and the ADS flow quickly stabilizes and reaches the quasi-steady-state value. The steady values are confirmed by the slope of the integral flow figures.

In addition to the initial level sensitivity calculations, sensitivity calculations were performed for tests SB01 and SB10 with different initial downcomer fluid temperatures. These sensitivity calculations had the initial collapsed level at the top of the heated core region.

The results of the SB10 initial temperature sensitivity calculations are shown in Figures 3-35 through 3-50. The reference calculation used a downcomer fluid temperature of 150°F, while the sensitivity calculation used an initial downcomer fluid temperature of 212°F. Figure 3-35 shows the pressure quickly stabilizes approximately 300 to 400 seconds into the transient calculation time. The levels in the downcomer, core, and upper plenum are shown in Figures 3-36 through 3-38. These levels also quickly come to a quasi-steady-state value in 300 to 400 seconds of calculational time (13,900 seconds). A similar behavior is observed in the core top and upper plenum void fraction, as shown in Figures 3-39 and 3-40. The IRWST injection flows and their integrated values are shown in Figures 3-41 through 3-44. The figures show initial differences occur when the hotter downcomer flow is lower than the reference case. However, as time progresses, the flows become equal, as indicated from the flow plots and the parallel slope of the integrated flow values. The difference in the IRWST flows is caused by the initial increase in the core steam generation rate due to the initially hotter downcomer fluid temperature. The core steam flow is shown in Figure 3-45 and the integrated value is given in Figure 3-46. The steam flow is initially higher for the hotter downcomer fluid case, since the liquid flowing into the core boils more easily. There is a feedback effect of the higher steaming rate that increases the pressure drop in the core, hot leg, and ADS4 valves when the steam is vented. As the flow proceeds down the downcomer, heat is transferred to the metal walls in the downcomer which lowers the temperature of the liquid flowing into the heater bundle and reduces the

steam generation rate. Figures 3-47 through 3-50 show the ADS4 flow rates and the integrated flow values. The ADS flows are initially higher for the hotter downcomer fluid case because more steam initially vents out through the ADS4 valves. However, after the initial surge of hot liquid into the core, the ADS flows quickly become stable and the slopes of the integral curves are identical.

A similar downcomer temperature study was also performed for test SB01. The analysis results are given in Figures 3-51 through 3-66. The observed behavior for this test was the same as test SB10. More initial level variation of the two cases occurs at the beginning of the window calculation as shown in Figures 3-52 through 3-54. However, the levels quickly stabilize and reach a quasi-steady-state value for the majority of the transient time of the window calculation. The remainder of the calculated values in Figures 3-55 through 3-66 show a similar behavior and the results reach quasi-steady-state values for the majority of the transient window time.

3.11 References

3-1. *Westinghouse AP600 Long-Term Cooling Quick Look Report for the Flow Resistance Determination*, LTCT-T2R,-002, July 1994.

3-2. Dumsday, C. L., Carter, M., Copper, M. H., Lau, L. K., Loftus, M. J., Nayyar, V. K., Tupper, R. B., and Willis, J. W., WCAP-14252, Volumes 1-4, *AP600 Low Pressure Integral Systems Test at Oregon State University, Final Data Report*, May 1995.

TABLE 3-1
OSU TEST AND CALCULATED PRESSURE LOSS COEFFICIENT COMPARISON

Pipe Section	Total Line Resistance (fL/D+K)	
	OSU Test Facility	WCOBRA/TRAC Model
CMT-1 Balance Line	[ ]a,b,c	11.81
CMT-2 Balance Line		10.48
CMT-1 to DVI-1		65.10
CMT-2 to DVI-2		60.65
IRWST to DVI-1		37.33
IRWST to DVI-2		36.24
SUMP to DVI-1		162.43
SUMP to DVI-2		190.00

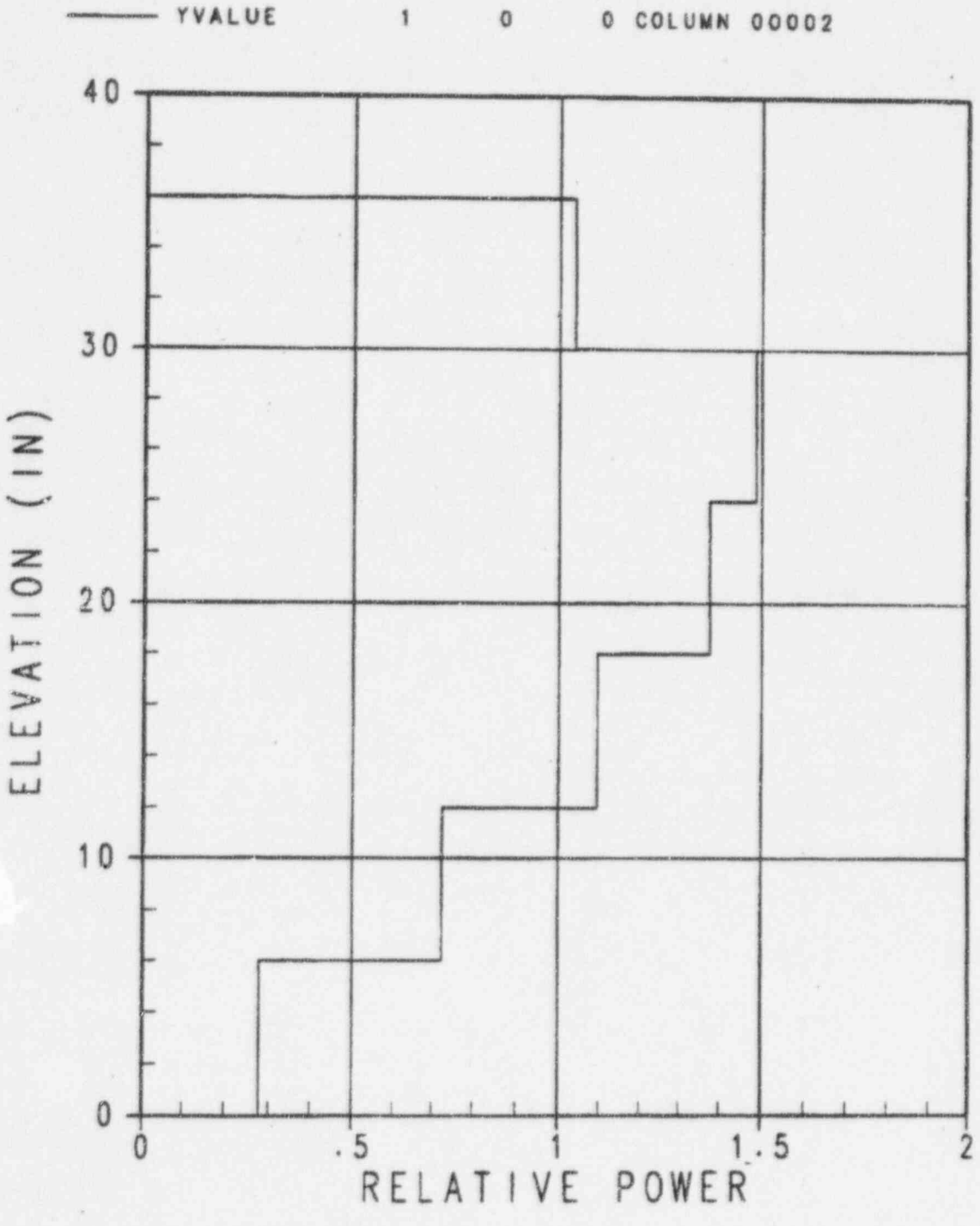

Figure 3-1 Axial Power Shape for OSU (Normalized) – Step Variation

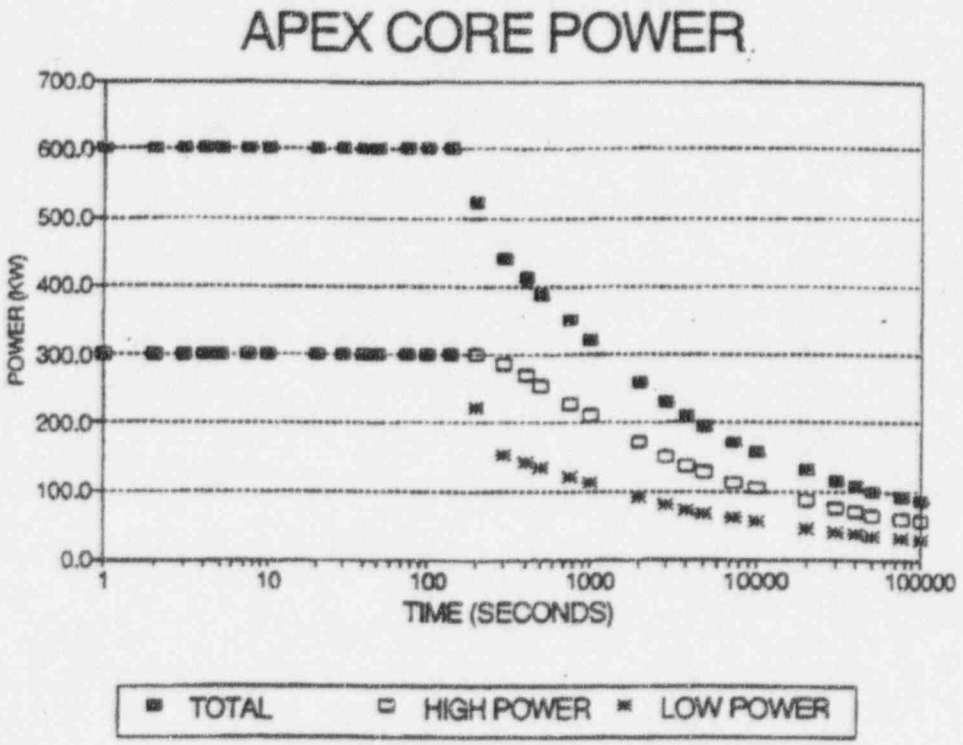

Figure 3-2 Decay Power

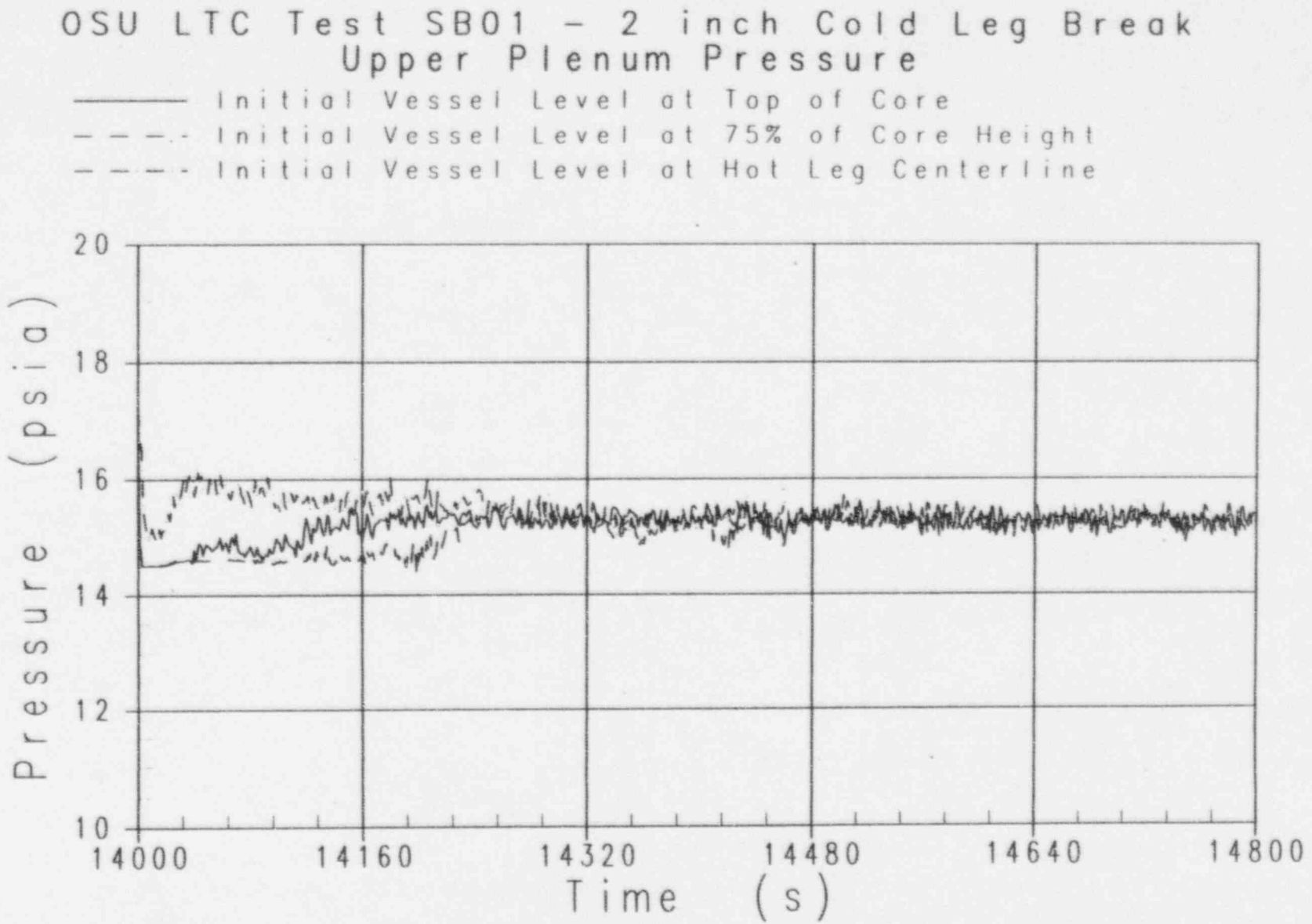
OSU LTC Test SB01 - 2 inch Cold Leg Break
Upper Plenum Pressure
Initial Vessel Level at Top of Core
Initial Vessel Level at 75% of Core Height
Initial Vessel Level at Hot Leg Centerline
Pressure (psia)
20
18
16
14
12
10
14000
14160
14320
14480
14640
14800
Time (s)

Figure 3 - 3

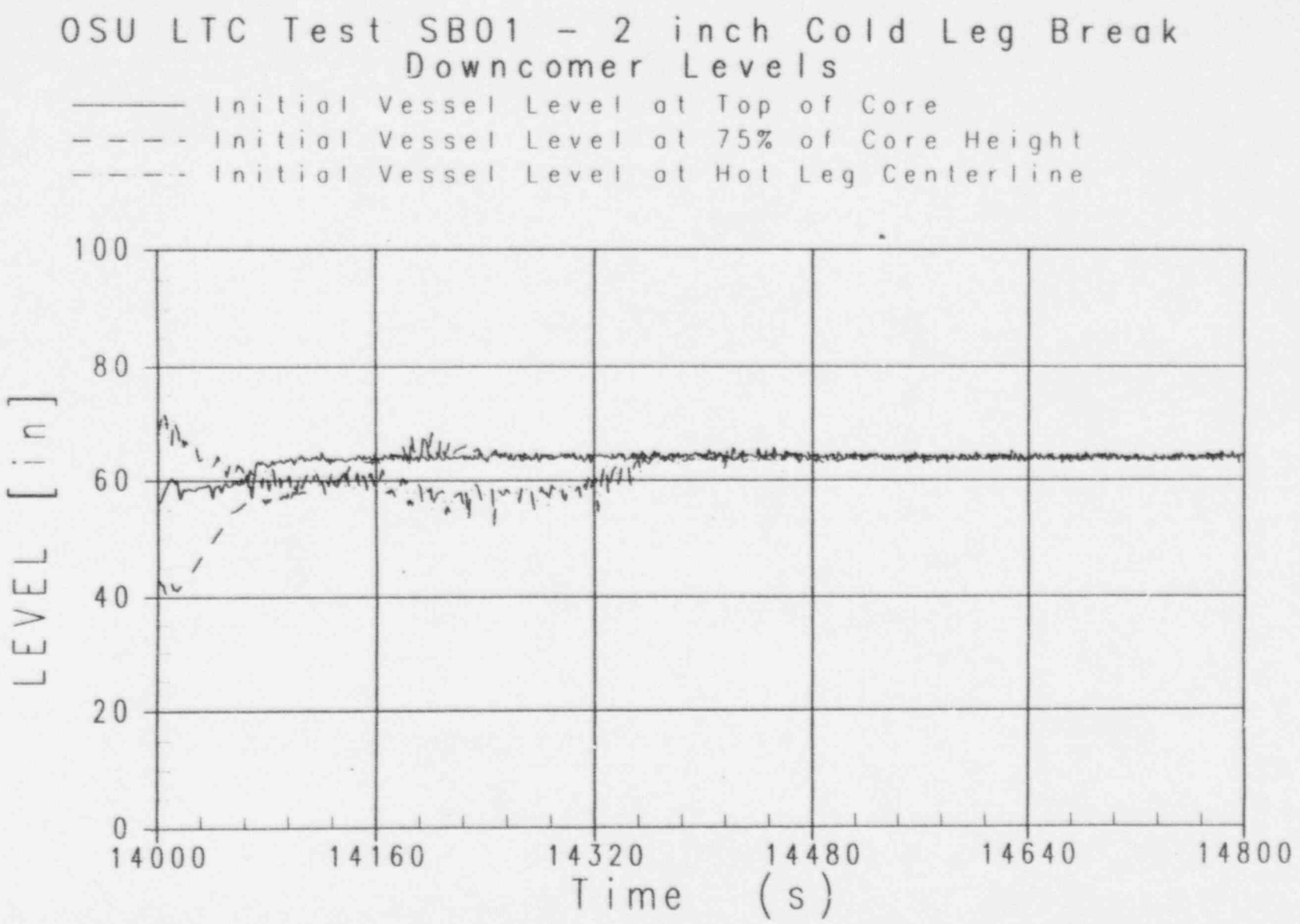
OSU LTC Test SB01 - 2 inch Cold Leg Break
Downcomer Levels
Initial Vessel Level at Top of Core
Initial Vessel Level at 75% of Core Height
Initial Vessel Level at Hot Leg Centerline
LEVEL [in]
100
80
60
40
20
0
14000
14160
14320
14480
14640
14800
Time (s)

Figure 3 - 4

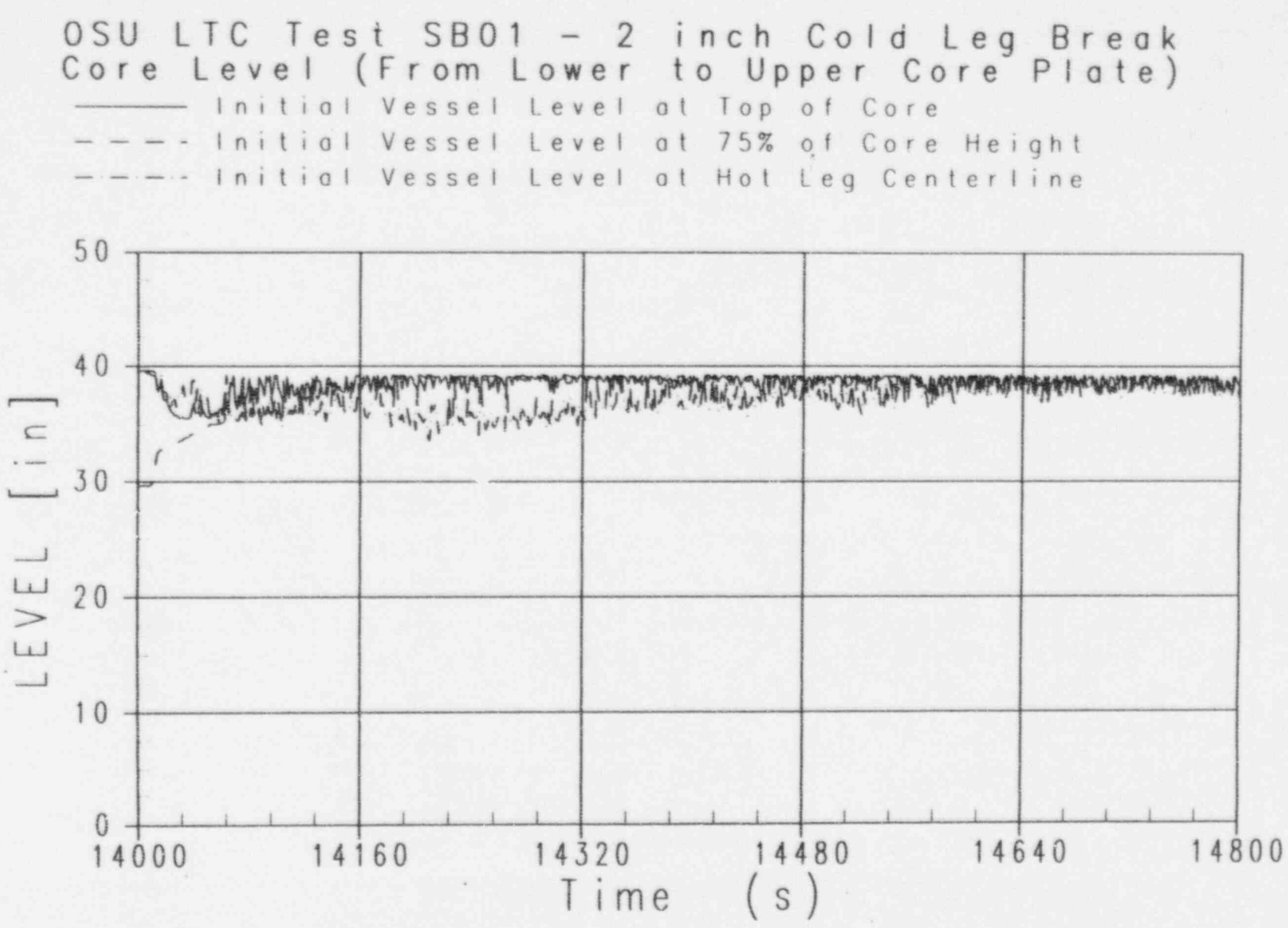
OSU LTC Test SB01 - 2 inch Cold Leg Break
Core Level (From Lower to Upper Core Plate)
Initial Vessel Level at Top of Core
Initial Vessel Level at 75% of Core Height
Initial Vessel Level at Hot Leg Centerline
LEVEL [in]
50
40
30
20
10
0
14000
14160
14320
14480
14640
14800
Time (s)

Figure 3 - 5

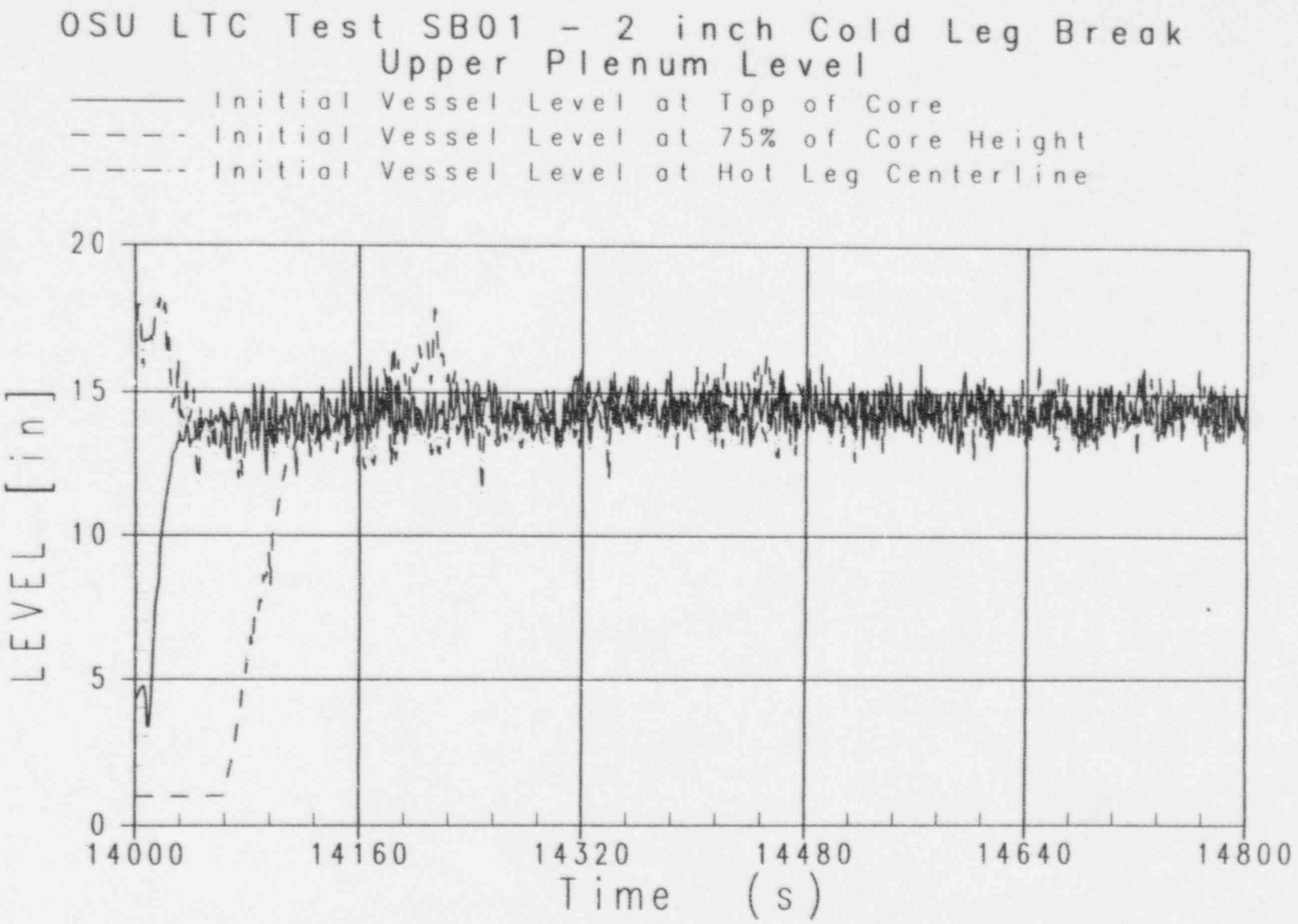
OSU LTC Test SB01 - 2 inch Cold Leg Break
Upper Plenum Level
Initial Vessel Level at Top of Core
Initial Vessel Level at 75% of Core Height
Initial Vessel Level at Hot Leg Centerline
LEVEL [in]
20
15
10
5
0
14000
14160
14320
14480
14640
14800
Time (s)

Figure 3 - 6

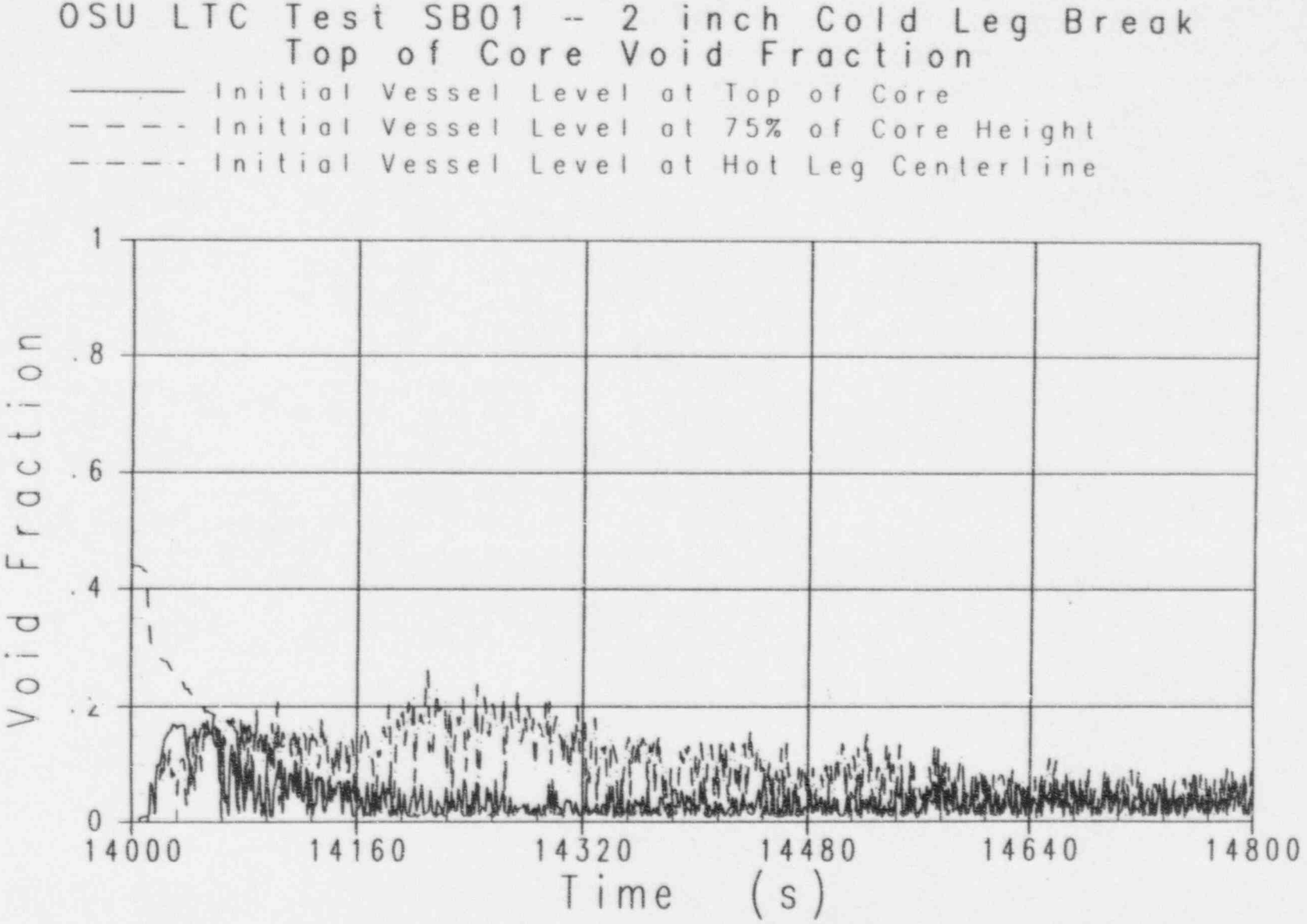
OSU LTC Test SB01 -- 2 inch Cold Leg Break
Top of Core Void Fraction
Initial Vessel Level at Top of Core
Initial Vessel Level at 75% of Core Height
Initial Vessel Level at Hot Leg Centerline
Void Fraction
1
.8
.6
.4
.2
0
14000
14160
14320
14480
14640
14800
Time (s)

Figure 3 – 7

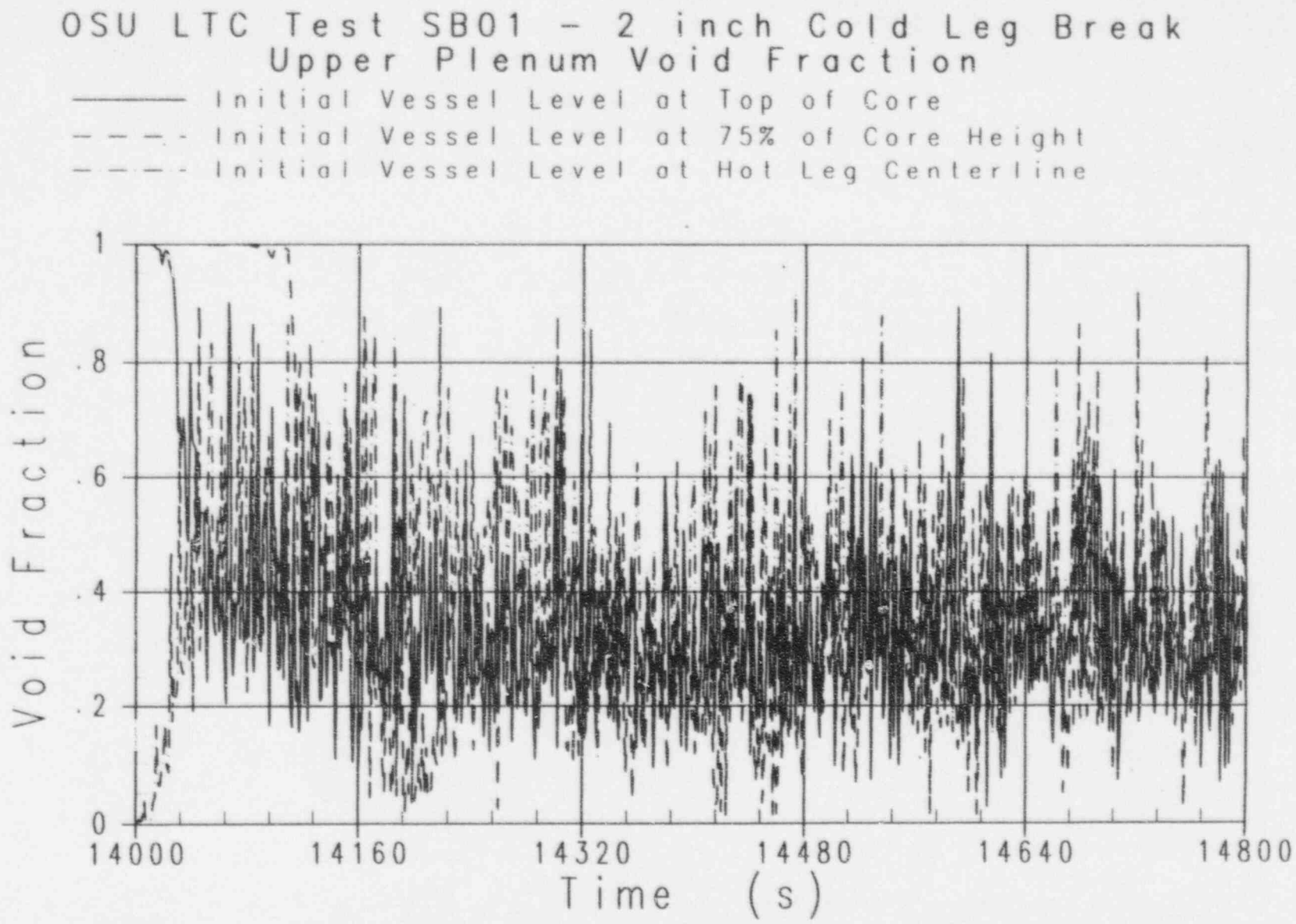
OSU LTC Test SB01 - 2 inch Cold Leg Break
Upper Plenum Void Fraction
Initial Vessel Level at Top of Core
Initial Vessel Level at 75% of Core Height
Initial Vessel Level at Hot Leg Centerline
Void Fraction
1
.8
.6
.4
.2
0
14000
14160
14320
14480
14640
14800
Time (s)

Figure 3 - 8

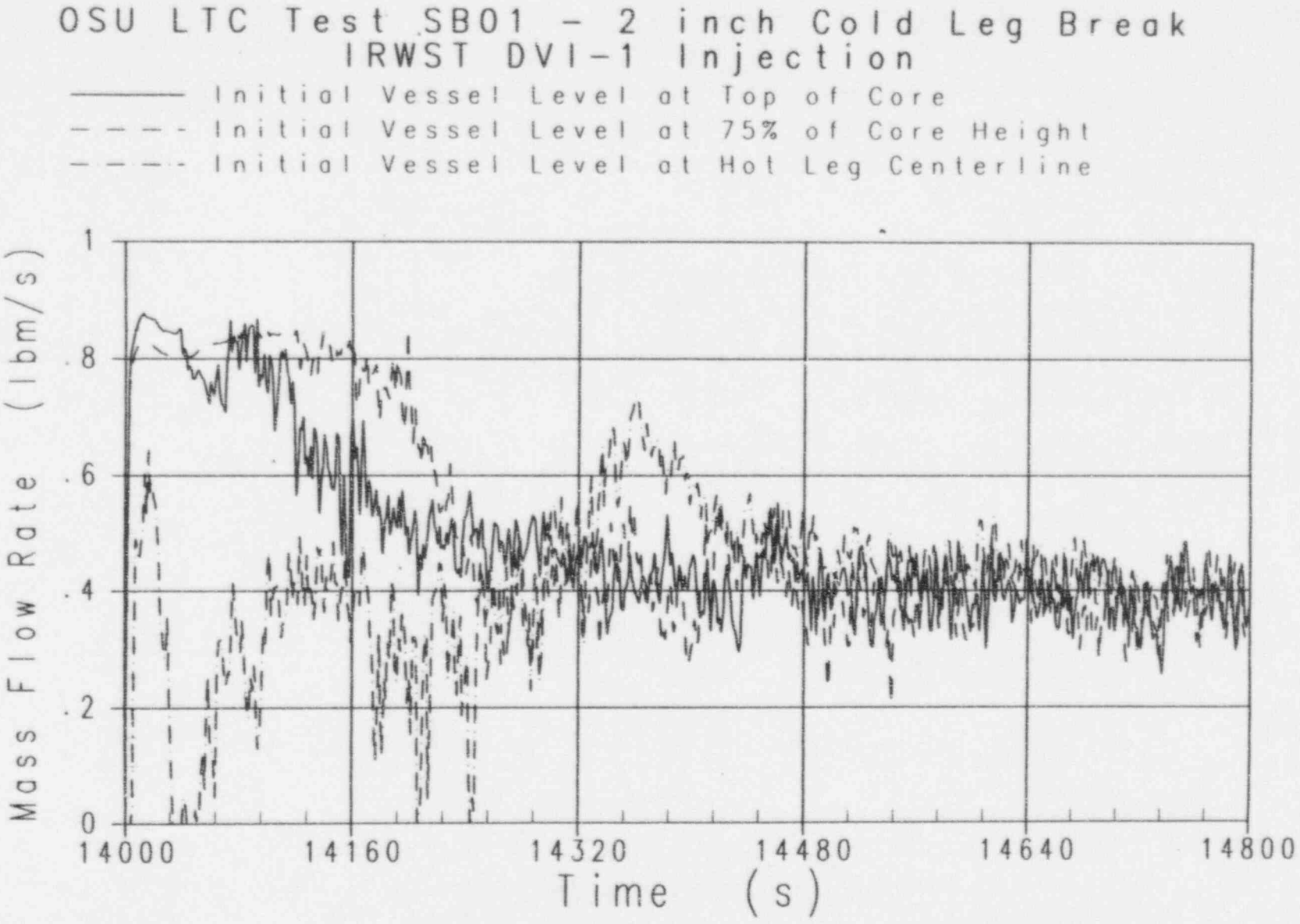
OSU LTC Test SB01 - 2 inch Cold Leg Break
IRWST DVI-1 Injection
Initial Vessel Level at Top of Core
Initial Vessel Level at 75% of Core Height
Initial Vessel Level at Hot Leg Centerline
Mass Flow Rate (lbm/s)
1
.8
.6
.4
.2
0
14000
14160
14320
14480
14640
14800
Time (s)

Figure 3 - 9

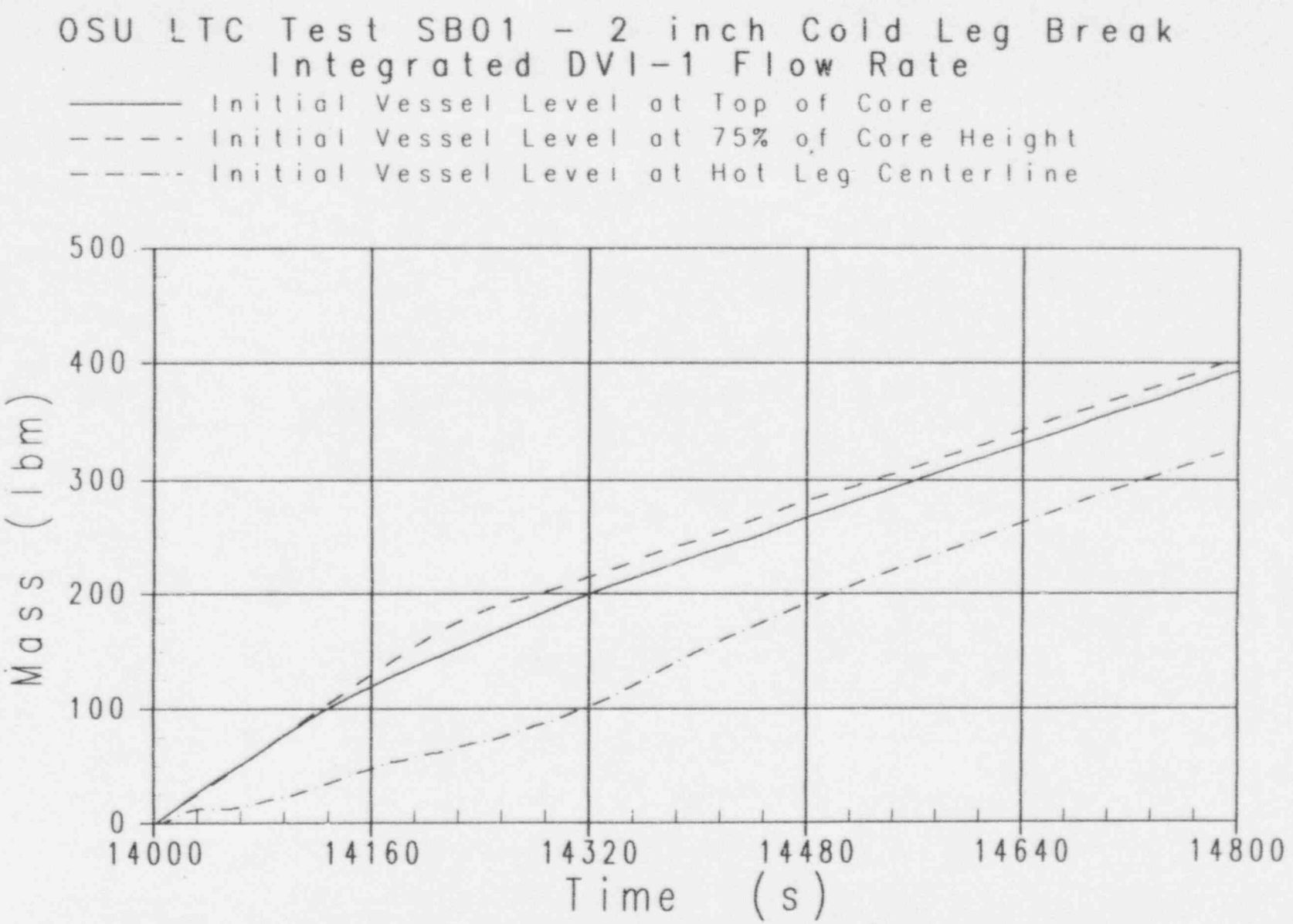
OSU LTC Test SB01 - 2 inch Cold Leg Break
Integrated DVI-1 Flow Rate
Initial Vessel Level at Top of Core
Initial Vessel Level at 75% of Core Height
Initial Vessel Level at Hot Leg Centerline
Mass (lbm)
500
400
300
200
100
0
14000
14160
14320
14480
14640
14800
Time (s)

Figure 3 -10

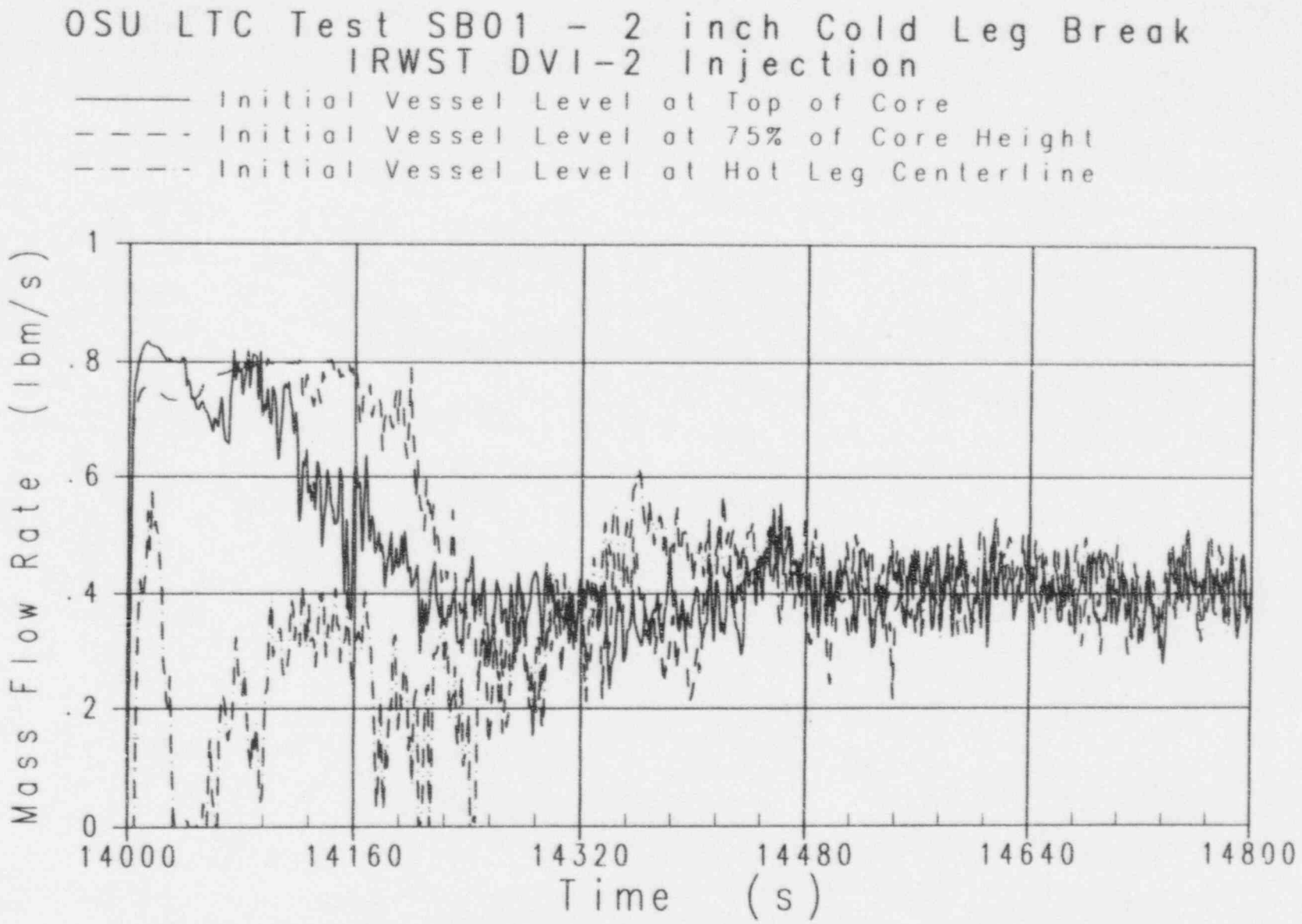
OSU LTC Test SB01 - 2 inch Cold Leg Break
IRWST DVI-2 Injection
Initial Vessel Level at Top of Core
Initial Vessel Level at 75% of Core Height
Initial Vessel Level at Hot Leg Centerline
Mass Flow Rate (lbm/s)
1
.8
.6
.4
.2
0
14000
14160
14320
14480
14640
14800
Time (s)

Figure 3 -11

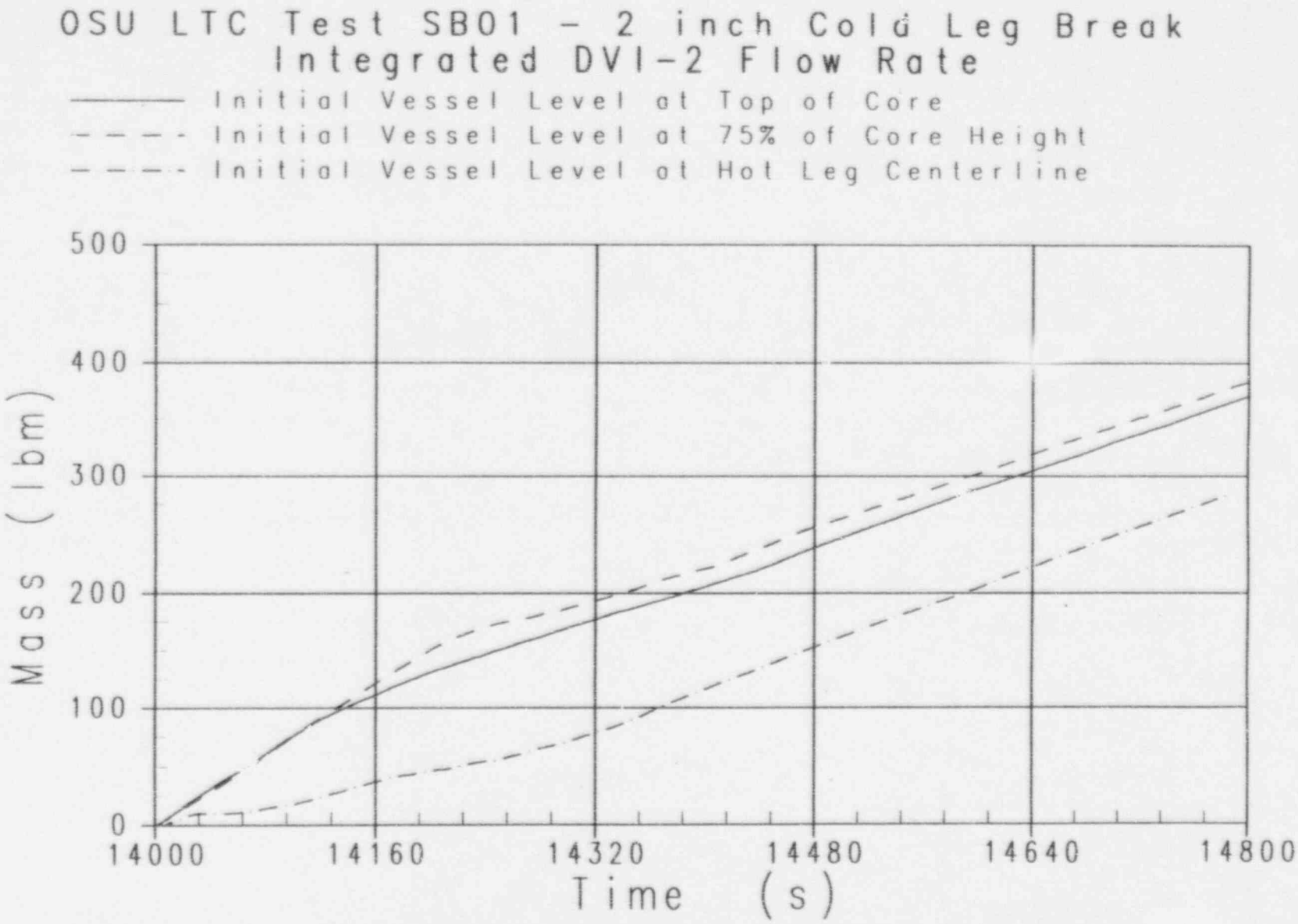
OSU LTC Test SB01 - 2 inch Cold Leg Break
Integrated DVI-2 Flow Rate
Initial Vessel Level at Top of Core
Initial Vessel Level at 75% of Core Height
Initial Vessel Level at Hot Leg Centerline
Mass (lbm)
500
400
300
200
100
0
14000
14160
14320
14480
14640
14800
Time (s)

Figure 3 -12

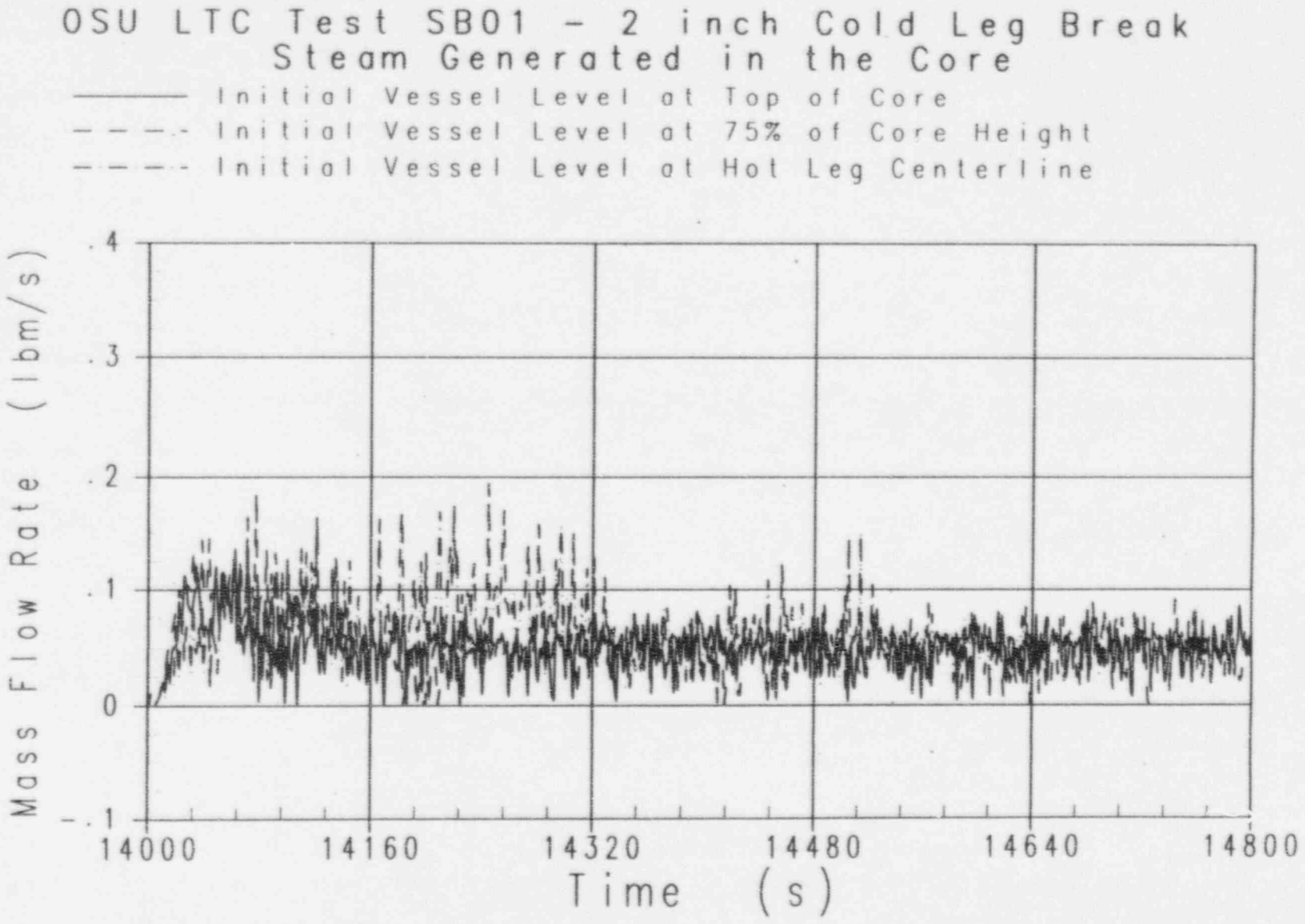
OSU LTC Test SB01 - 2 inch Cold Leg Break
Steam Generated in the Core
Initial Vessel Level at Top of Core
Initial Vessel Level at 75% of Core Height
Initial Vessel Level at Hot Leg Centerline
Mass Flow Rate (lbm/s)
.4
.3
.2
.1
0
-.1
14000
14160
14320
14480
14640
14800
Time (s)

Figure 3 -13

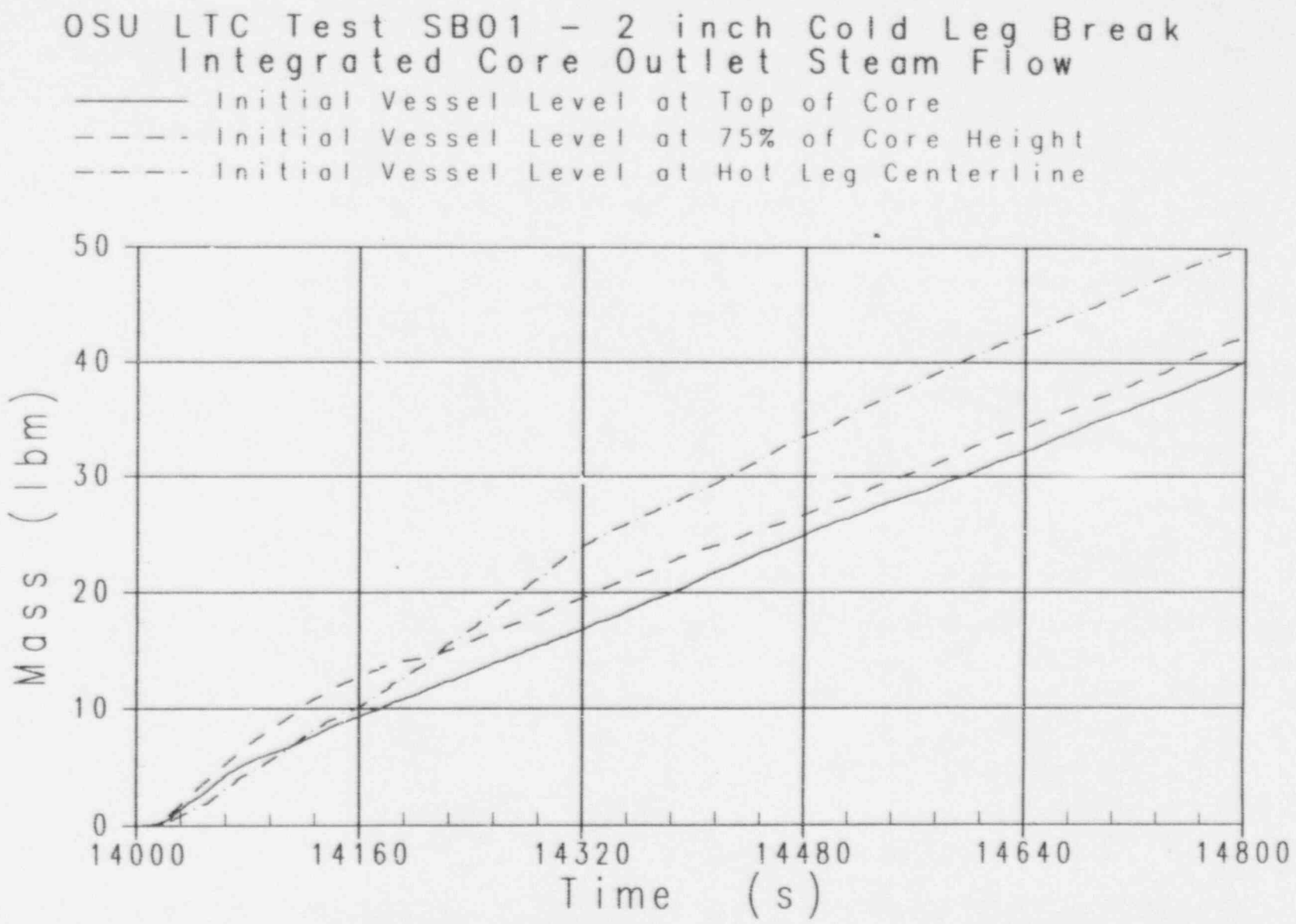
OSU LTC Test SB01 - 2 inch Cold Leg Break
Integrated Core Outlet Steam Flow
Initial Vessel Level at Top of Core
Initial Vessel Level at 75% of Core Height
Initial Vessel Level at Hot Leg Centerline
Mass (lbm)
0
10
20
30
40
50
14000
14160
14320
14480
14640
14800
Time (s)

Figure 3 -14

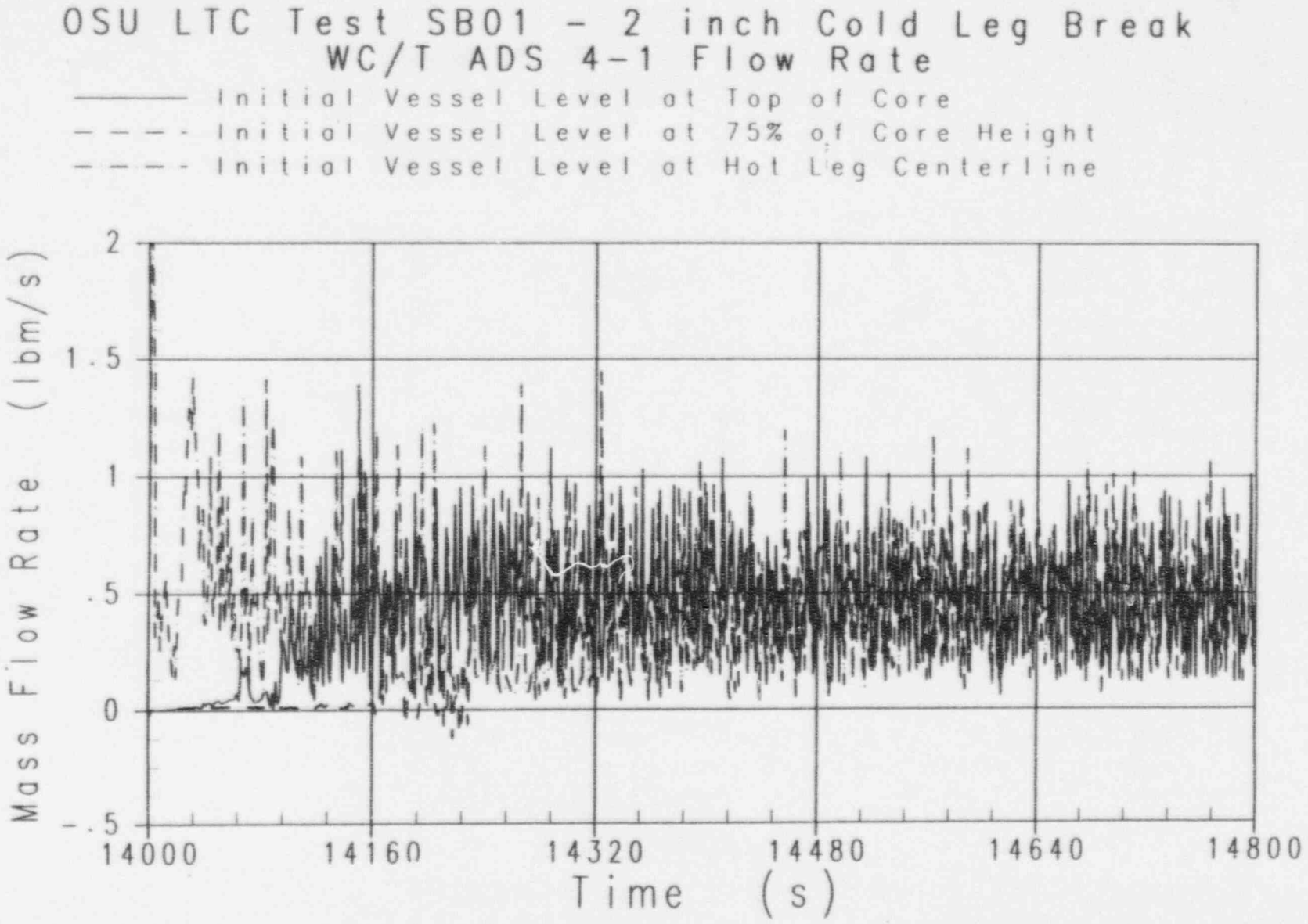
OSU LTC Test SB01 - 2 inch Cold Leg Break
WC/T ADS 4-1 Flow Rate
Initial Vessel Level at Top of Core
Initial Vessel Level at 75% of Core Height
Initial Vessel Level at Hot Leg Centerline
Mass Flow Rate (lbm/s)
2
1.5
1
.5
0
-.5
14000
14160
14320
14480
14640
14800
Time (s)

Figure 3 -15

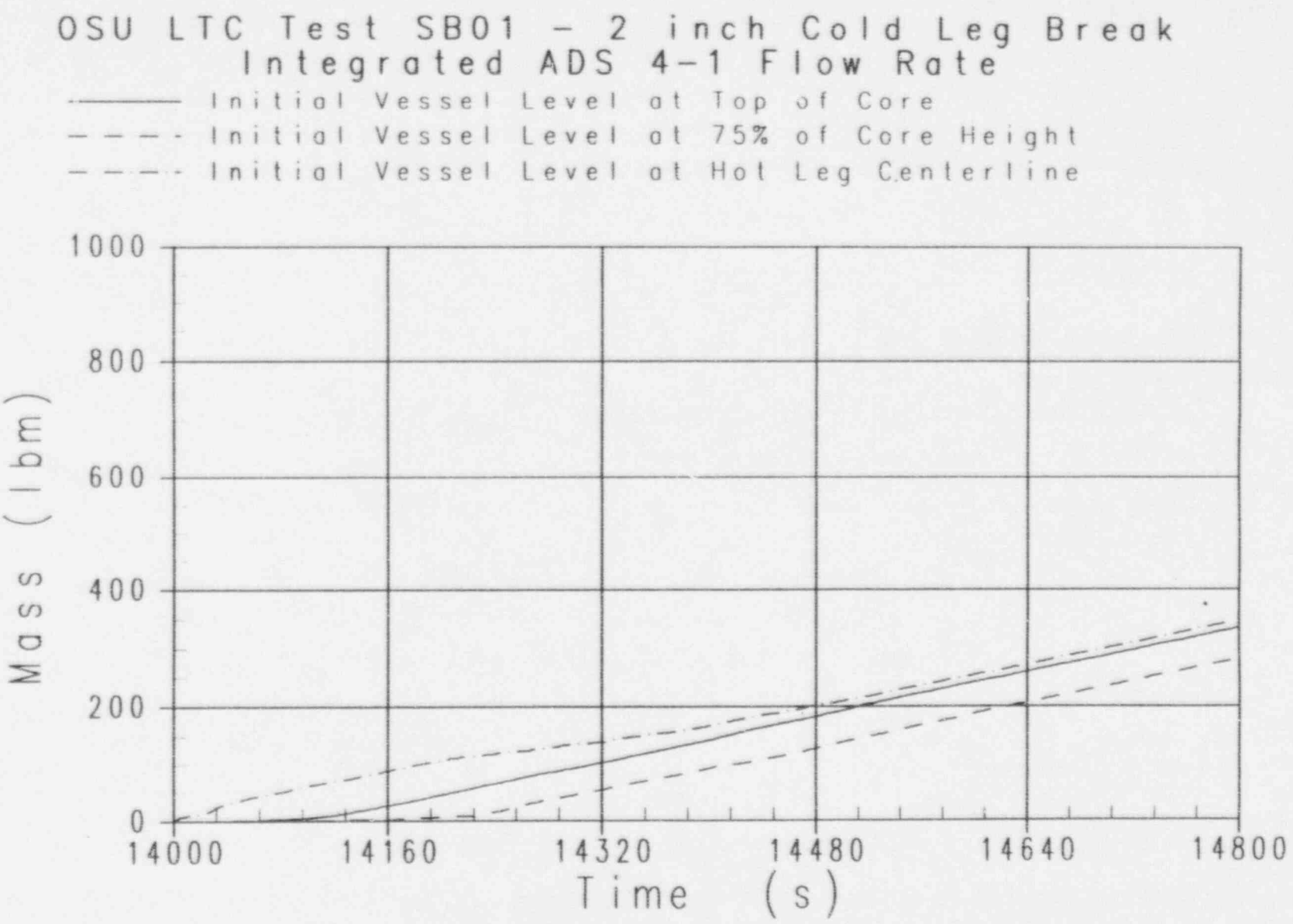
OSU LTC Test SB01 - 2 inch Cold Leg Break
Integrated ADS 4-1 Flow Rate
Initial Vessel Level at Top of Core
Initial Vessel Level at 75% of Core Height
Initial Vessel Level at Hot Leg Centerline
Mass (lbm)
1000
800
600
400
200
0
14000
14160
14320
14480
14640
14800
Time (s)

Figure 3 -16

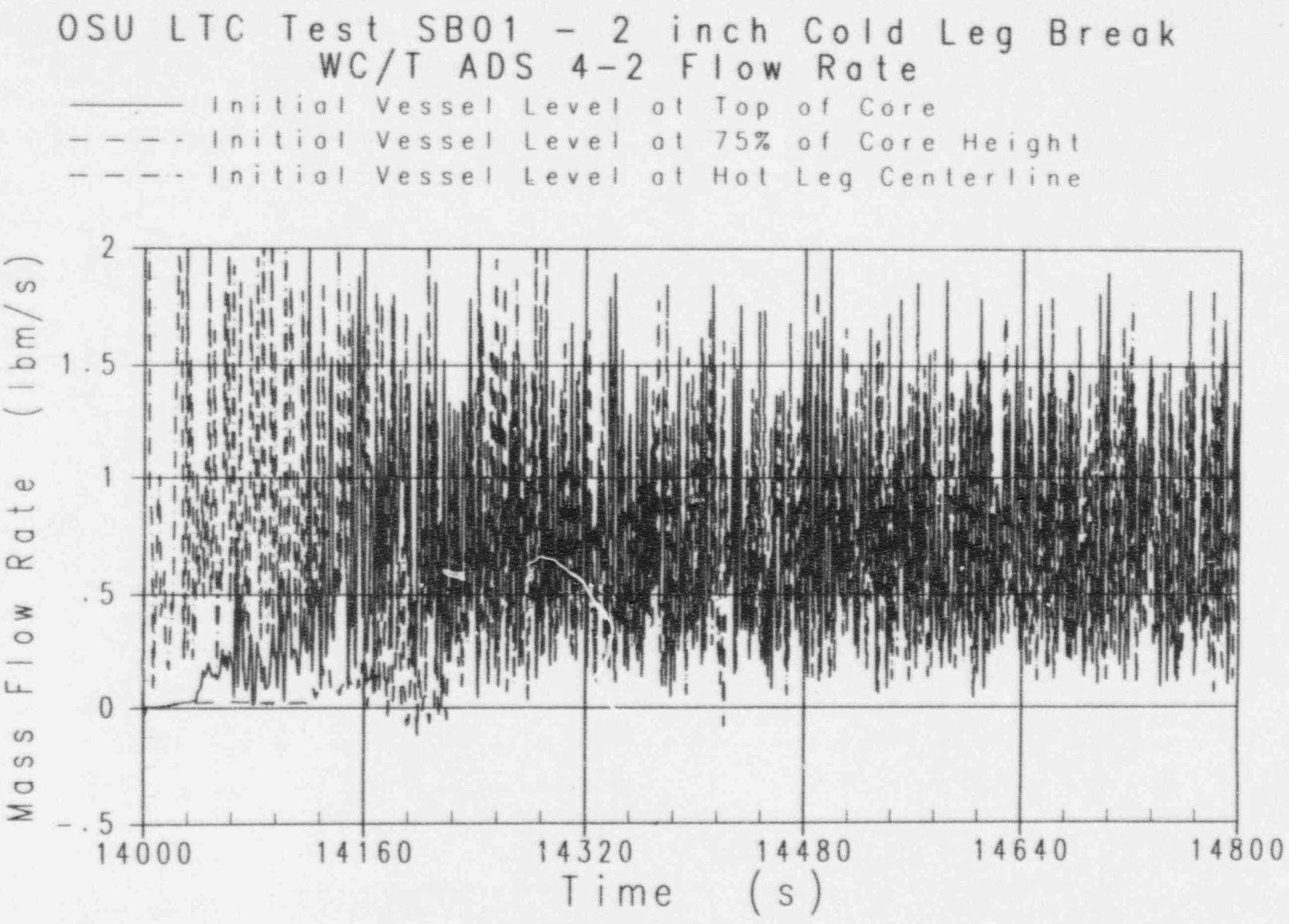
OSU LTC Test SB01 - 2 inch Cold Leg Break
WC/T ADS 4-2 Flow Rate
Initial Vessel Level at Top of Core
Initial Vessel Level at 75% of Core Height
Initial Vessel Level at Hot Leg Centerline
Mass Flow Rate (lbm/s)
2
1.5
1
.5
0
-.5
14000
14160
14320
14480
14640
14800
Time (s)

Figure 3 -17

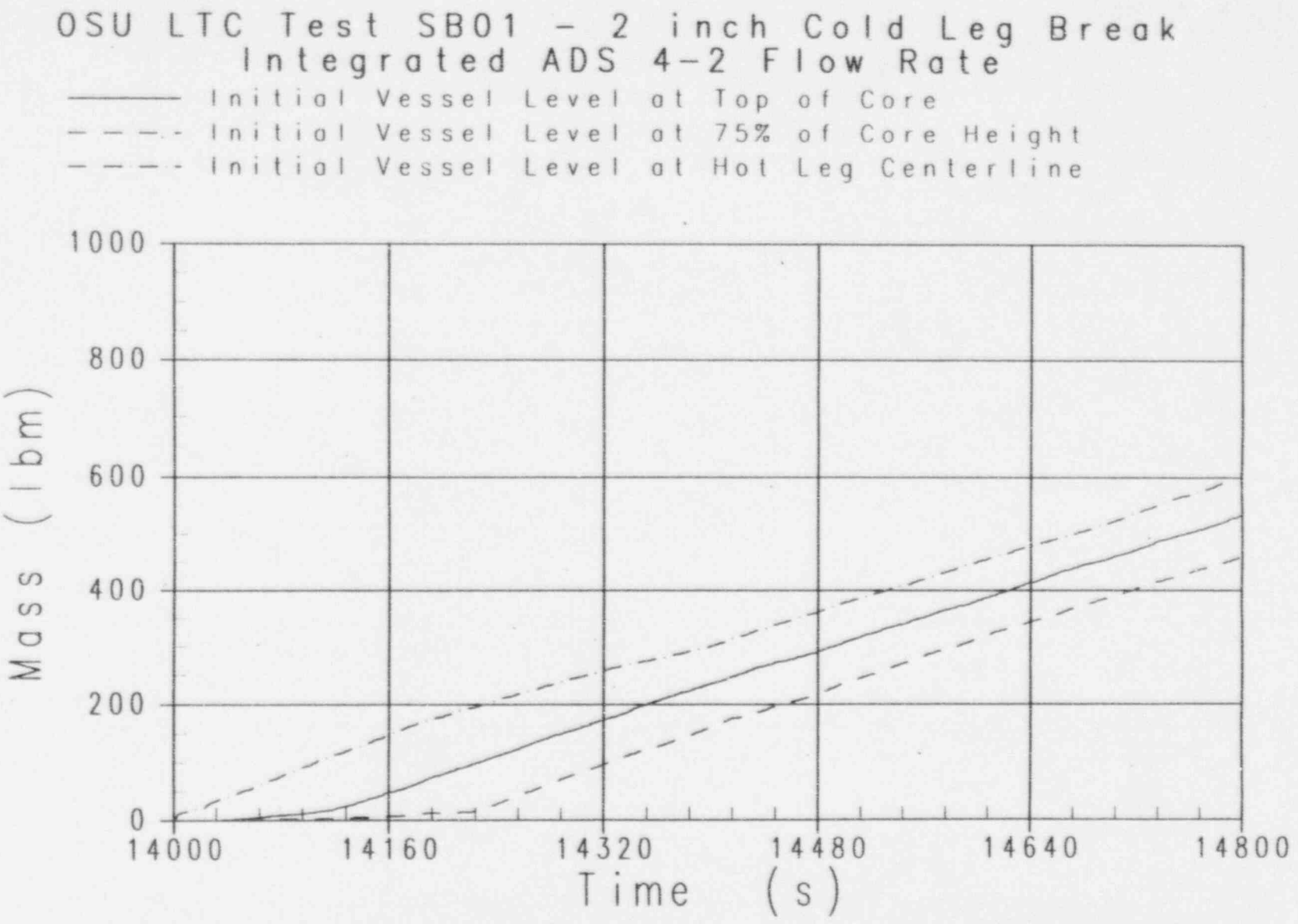
OSU LTC Test SB01 - 2 inch Cold Leg Break
Integrated ADS 4-2 Flow Rate
Initial Vessel Level at Top of Core
Initial Vessel Level at 75% of Core Height
Initial Vessel Level at Hot Leg Centerline
Mass (lbm)
1000
800
600
400
200
0
14000
14160
14320
14480
14640
14800
Time (s)

Figure 3 -18

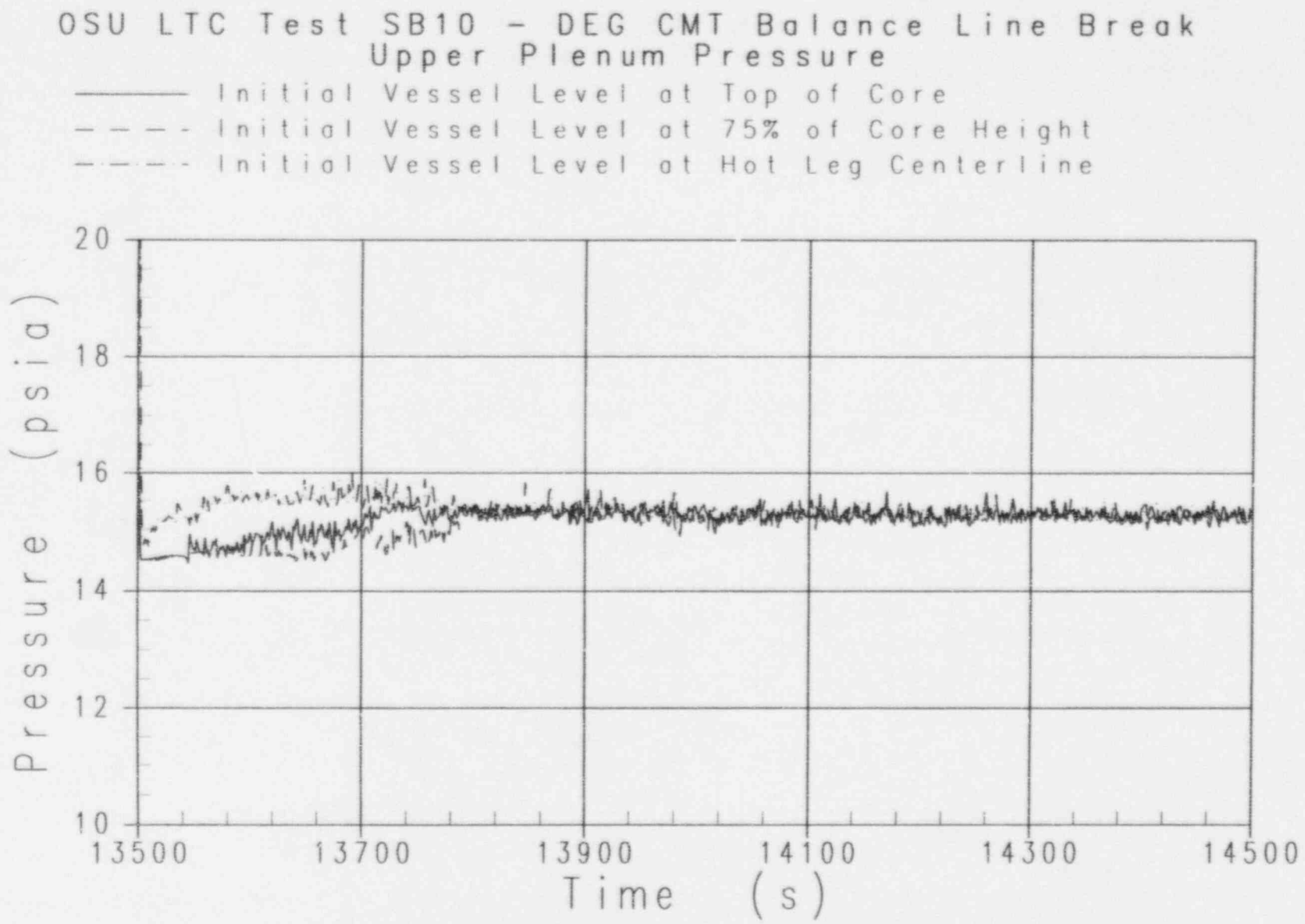
OSU LTC Test SB10 - DEG CMT Balance Line Break
Upper Plenum Pressure
Initial Vessel Level at Top of Core
Initial Vessel Level at 75% of Core Height
Initial Vessel Level at Hot Leg Centerline
Pressure (psia)
20
18
16
14
12
10
13500
13700
13900
14100
14300
14500
Time (s)

Figure 3 -19

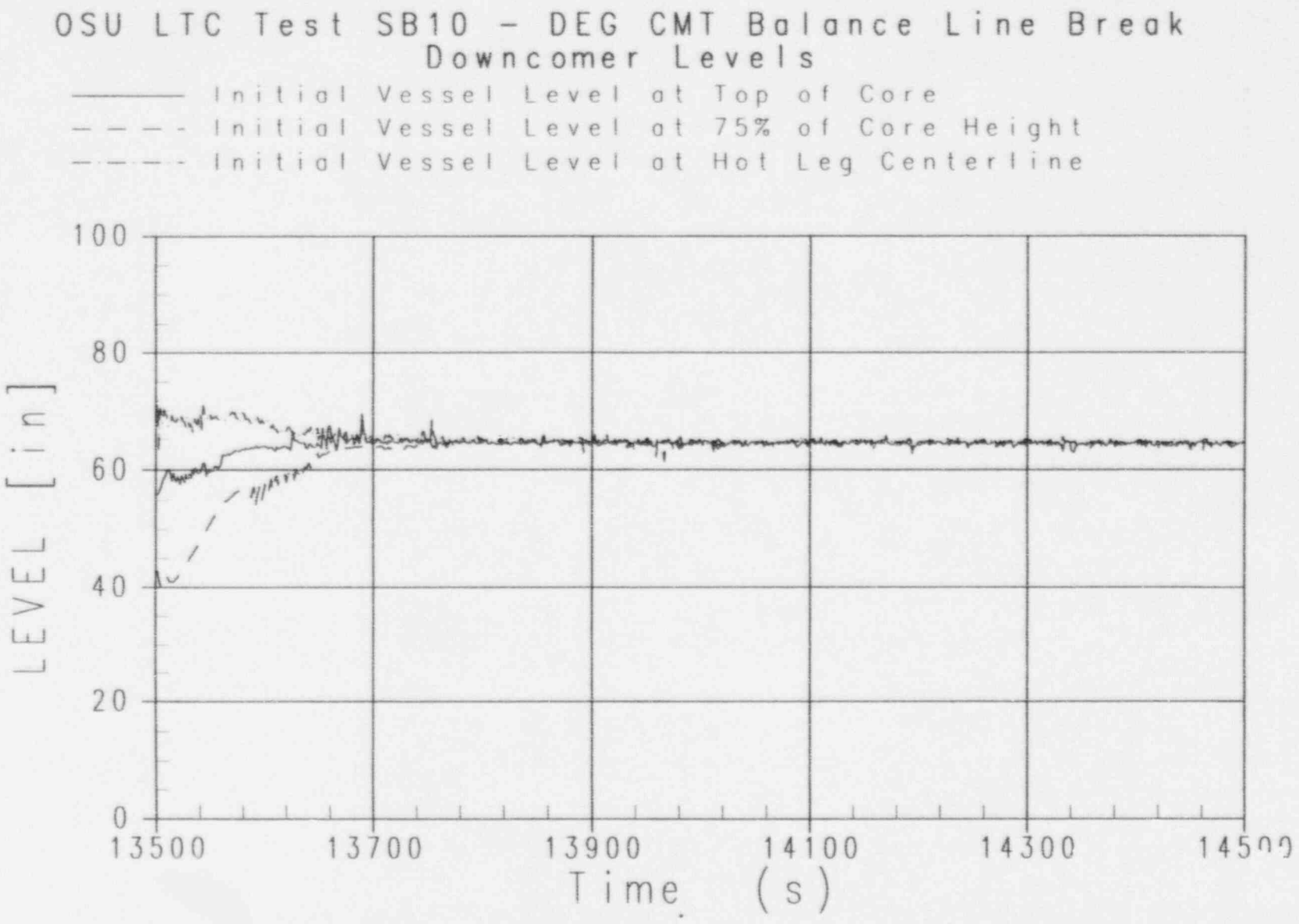
OSU LTC Test SB10 - DEG CMT Balance Line Break
Downcomer Levels
Initial Vessel Level at Top of Core
Initial Vessel Level at 75% of Core Height
Initial Vessel Level at Hot Leg Centerline
LEVEL [in]
100
80
60
40
20
0
13500
13700
13900
14100
14300
Time (s)

Figure 3 -20

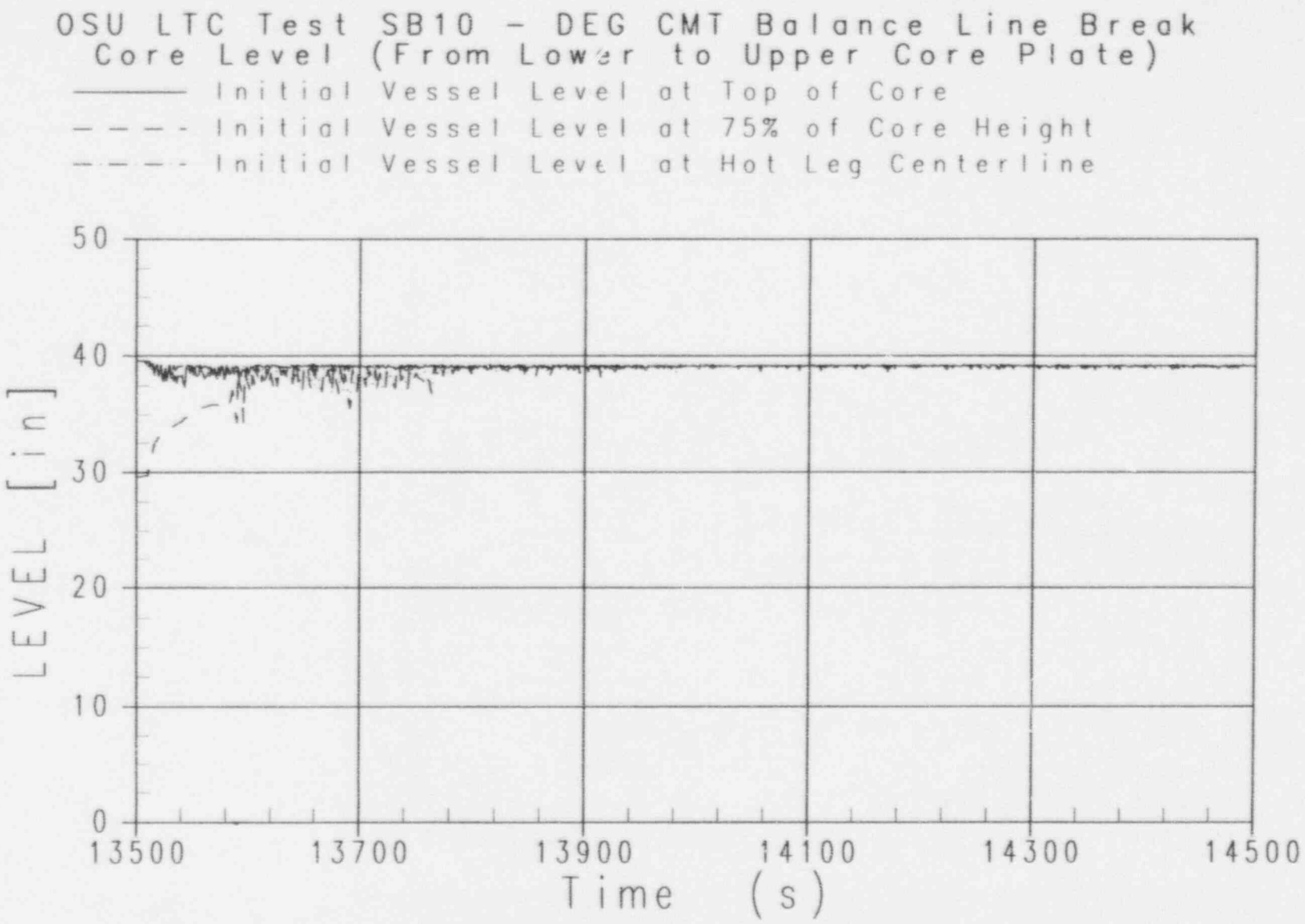
OSU LTC Test SB10 - DEG CMT Balance Line Break
Core Level (From Lower to Upper Core Plate)
Initial Vessel Level at Top of Core
Initial Vessel Level at 75% of Core Height
Initial Vessel Level at Hot Leg Centerline
LEVEL [in]
50
40
30
20
10
0
13500
13700
13900
14100
14300
14500
Time (s)

Figure 3 -21

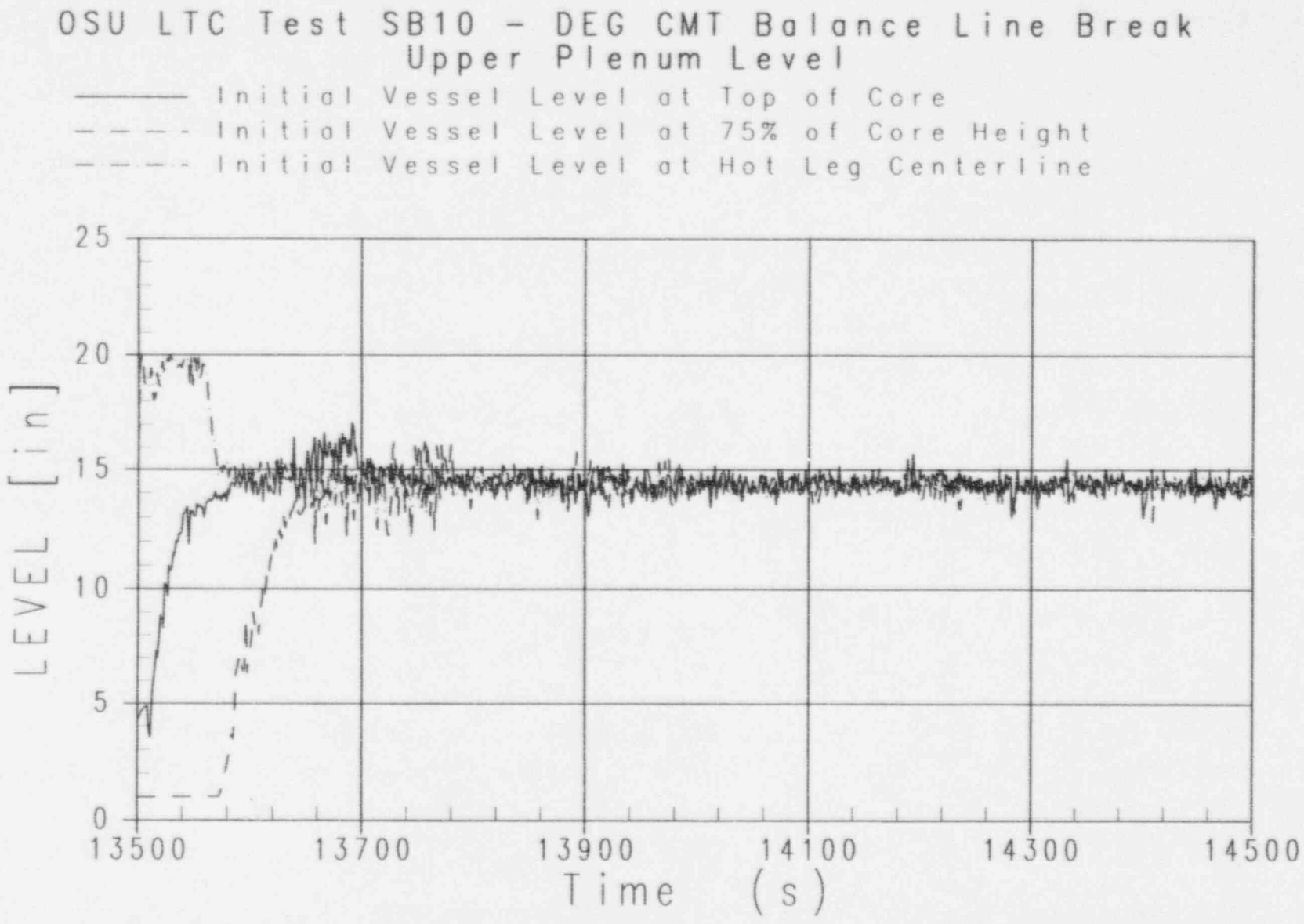
OSU LTC Test SB10 - DEG CMT Balance Line Break
Upper Plenum Level
Initial Vessel Level at Top of Core
Initial Vessel Level at 75% of Core Height
Initial Vessel Level at Hot Leg Centerline
LEVEL [in]
25
20
15
10
5
0
13500
13700
13900
14100
14300
14500
Time (s)

Figure 3 -22

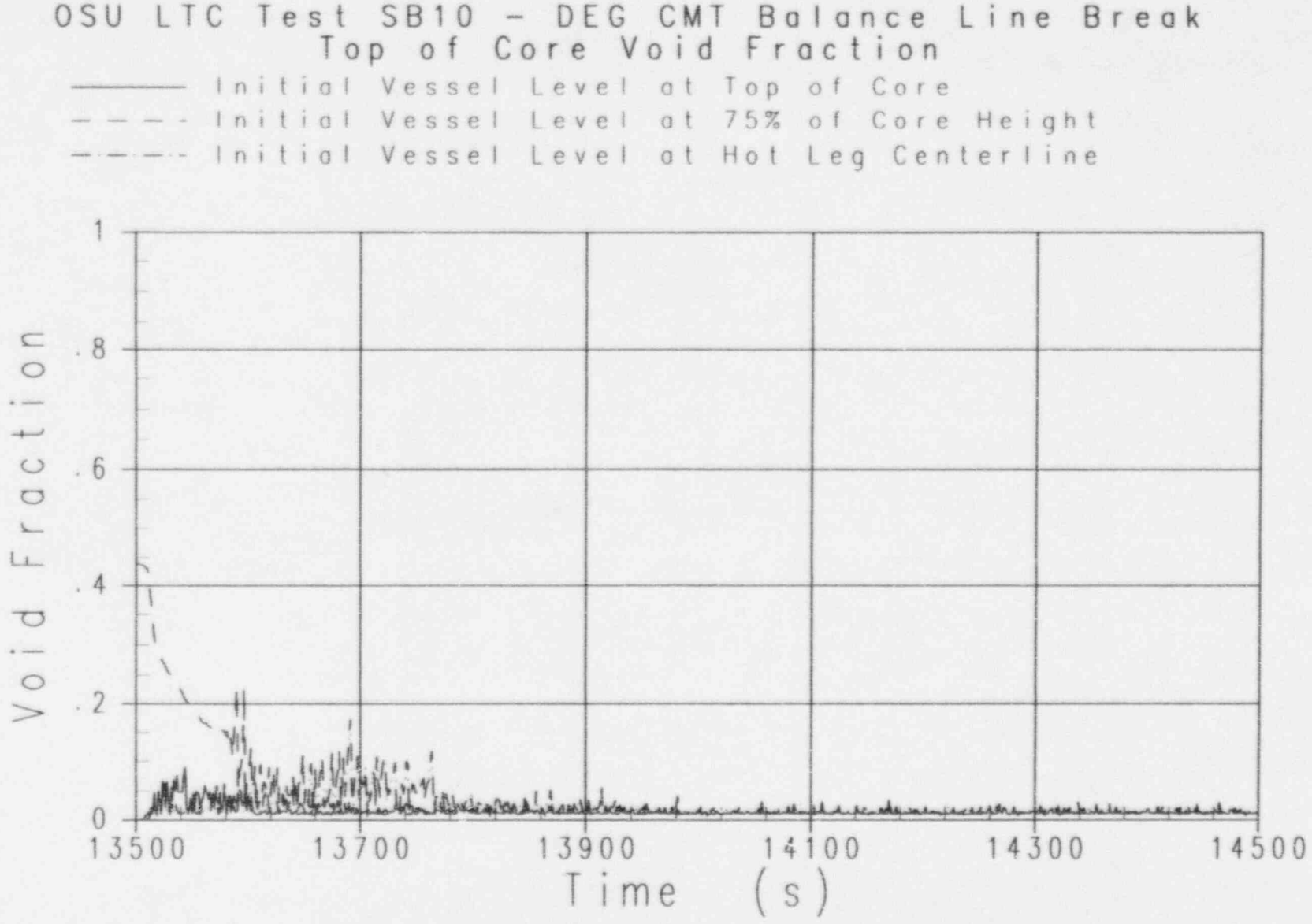
OSU LTC Test SB10 - DEG CMT Balance Line Break
Top of Core Void Fraction
Initial Vessel Level at Top of Core
Initial Vessel Level at 75% of Core Height
Initial Vessel Level at Hot Leg Centerline
Void Fraction
1
.8
.6
.4
.2
0
13500
13700
13900
14100
14300
14500
Time (s)

Figure 3 -23

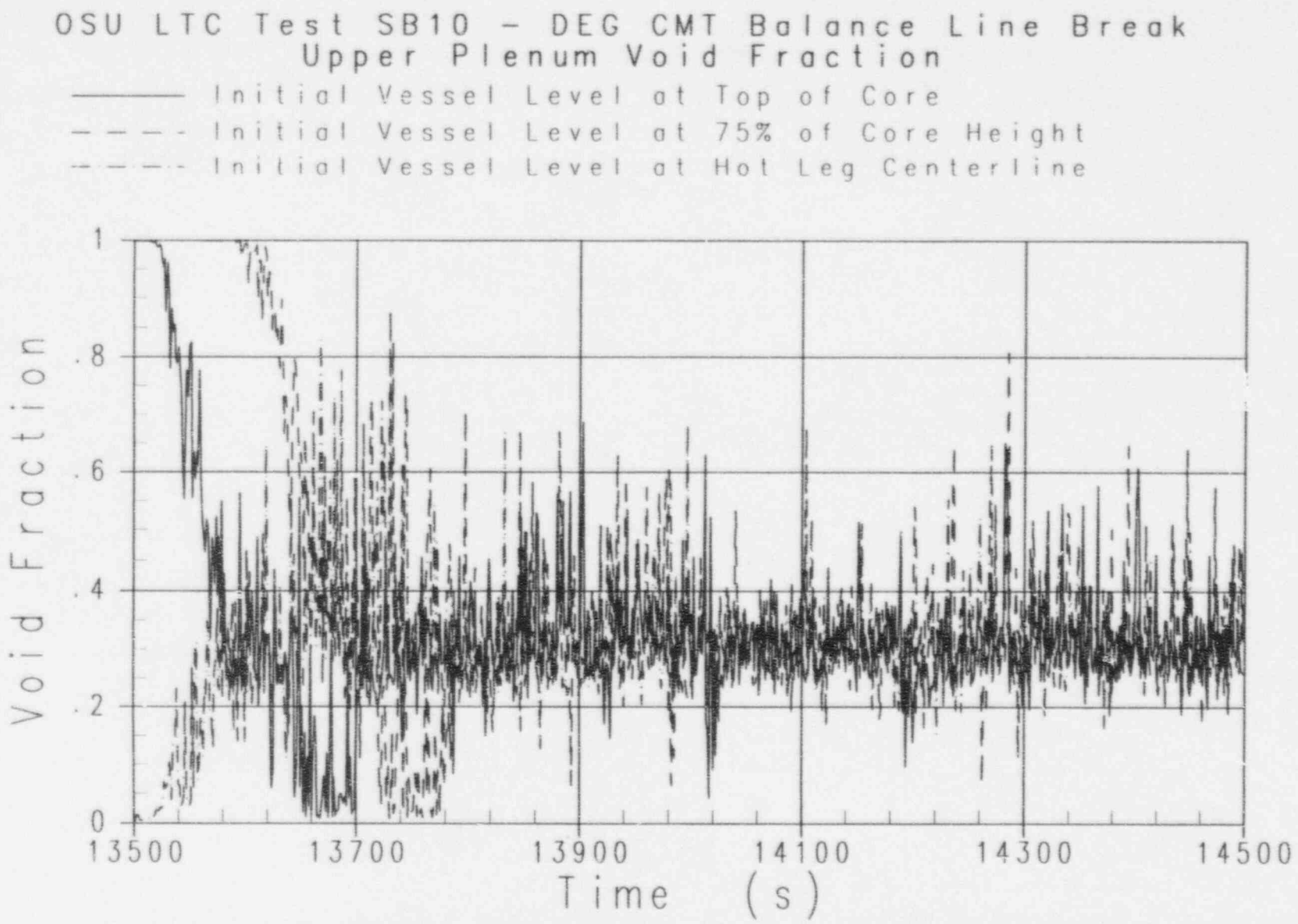
OSU LTC Test SB10 - DEG CMT Balance Line Break
Upper Plenum Void Fraction
Initial Vessel Level at Top of Core
Initial Vessel Level at 75% of Core Height
Initial Vessel Level at Hot Leg Centerline
Void Fraction
1
.8
.6
.4
.2
0
13500
13700
13900
14100
14300
14500
Time (s)

Figure 3 -24

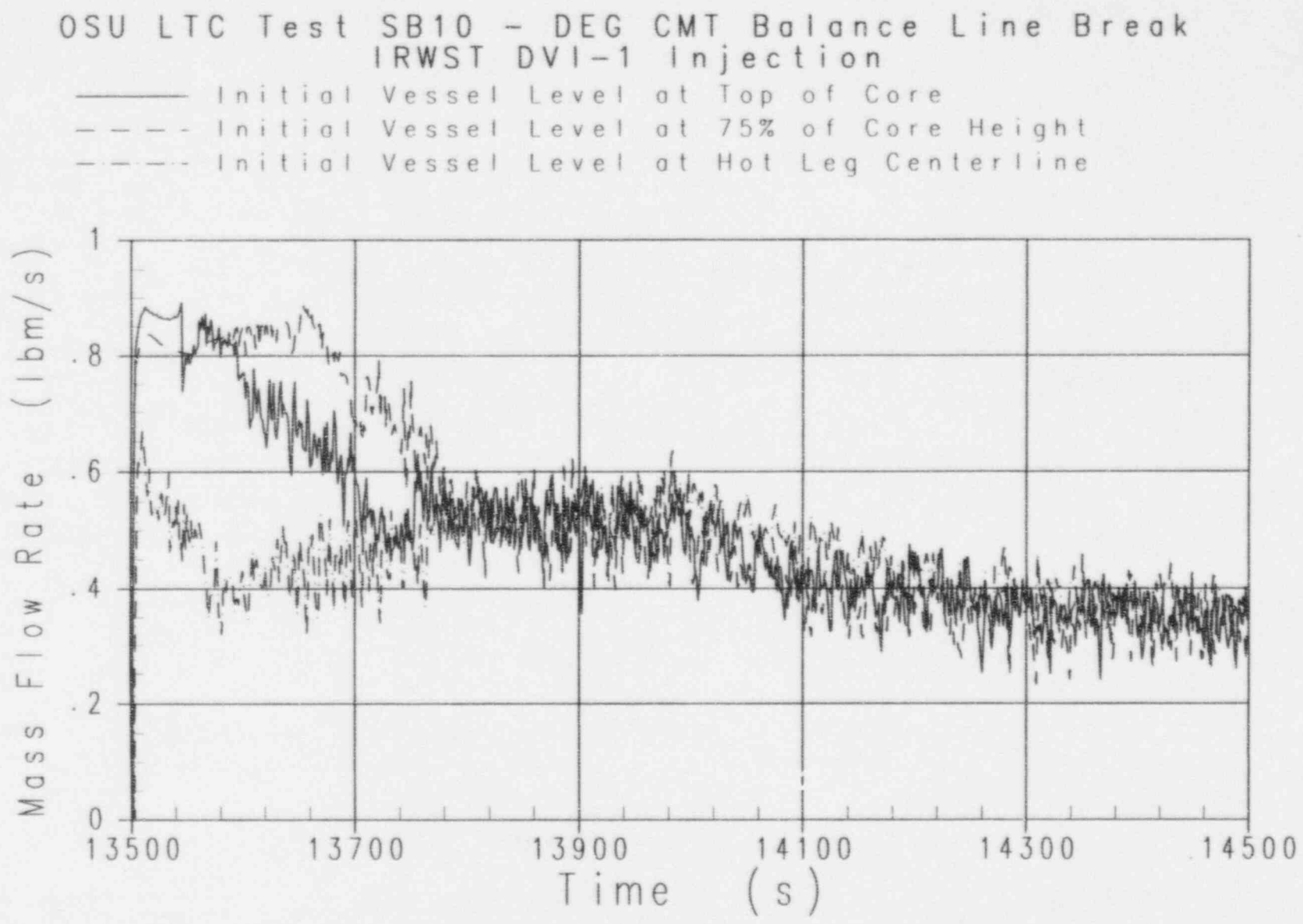
OSU LTC Test SB10 - DEG CMT Balance Line Break
IRWST DVI-1 Injection
Initial Vessel Level at Top of Core
Initial Vessel Level at 75% of Core Height
Initial Vessel Level at Hot Leg Centerline
Mass Flow Rate (lbm/s)
1
.8
.6
.4
.2
0
13500
13700
13900
14100
14300
14500
Time (s)

Figure 3 -25

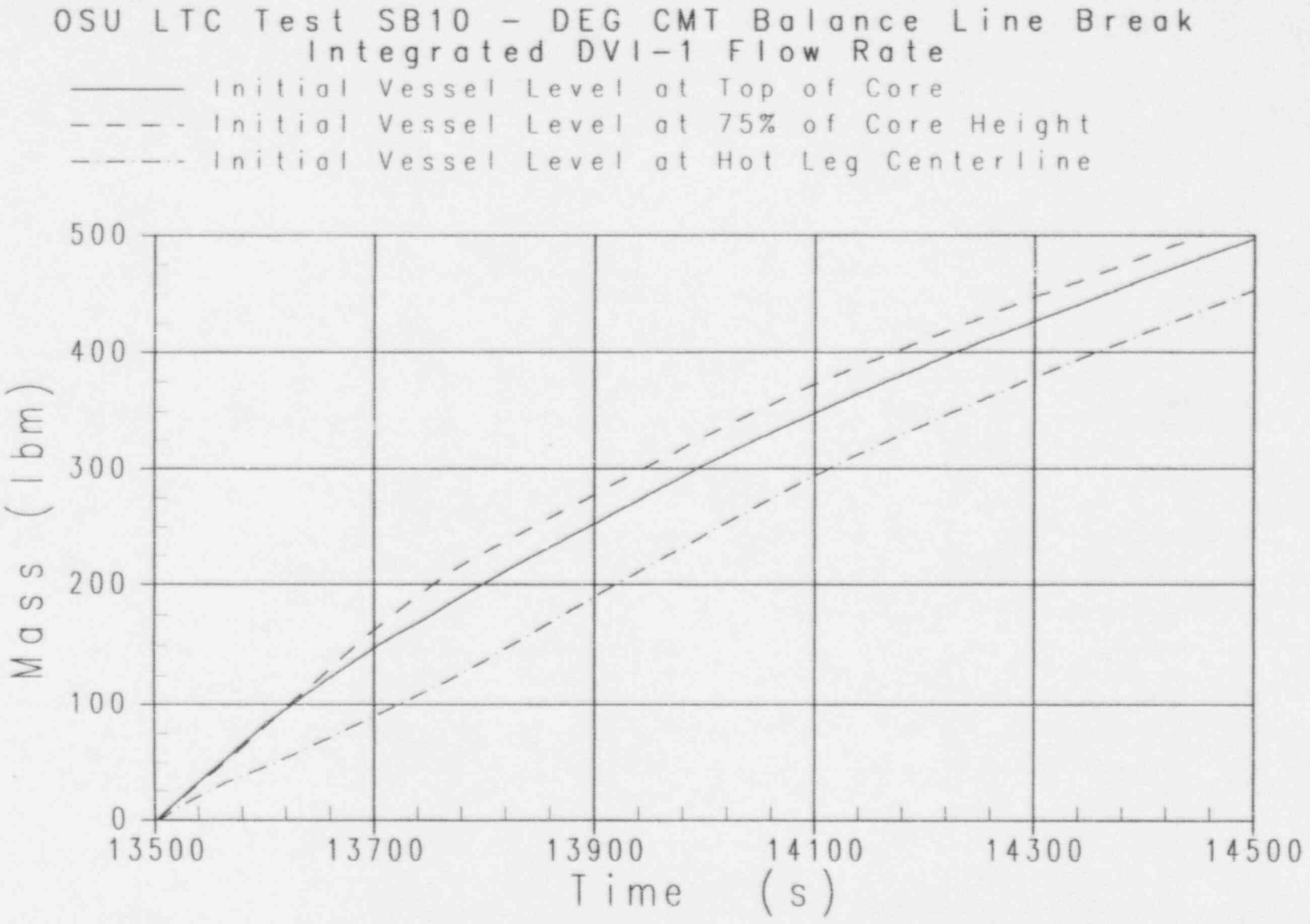
OSU LTC Test SB10 - DEG CMT Balance Line Break
Integrated DVI-1 Flow Rate
Initial Vessel Level at Top of Core
Initial Vessel Level at 75% of Core Height
Initial Vessel Level at Hot Leg Centerline
Mass (lbm)
0
100
200
300
400
500
13500
13700
13900
14100
14300
14500
Time (s)

Figure 3 -26

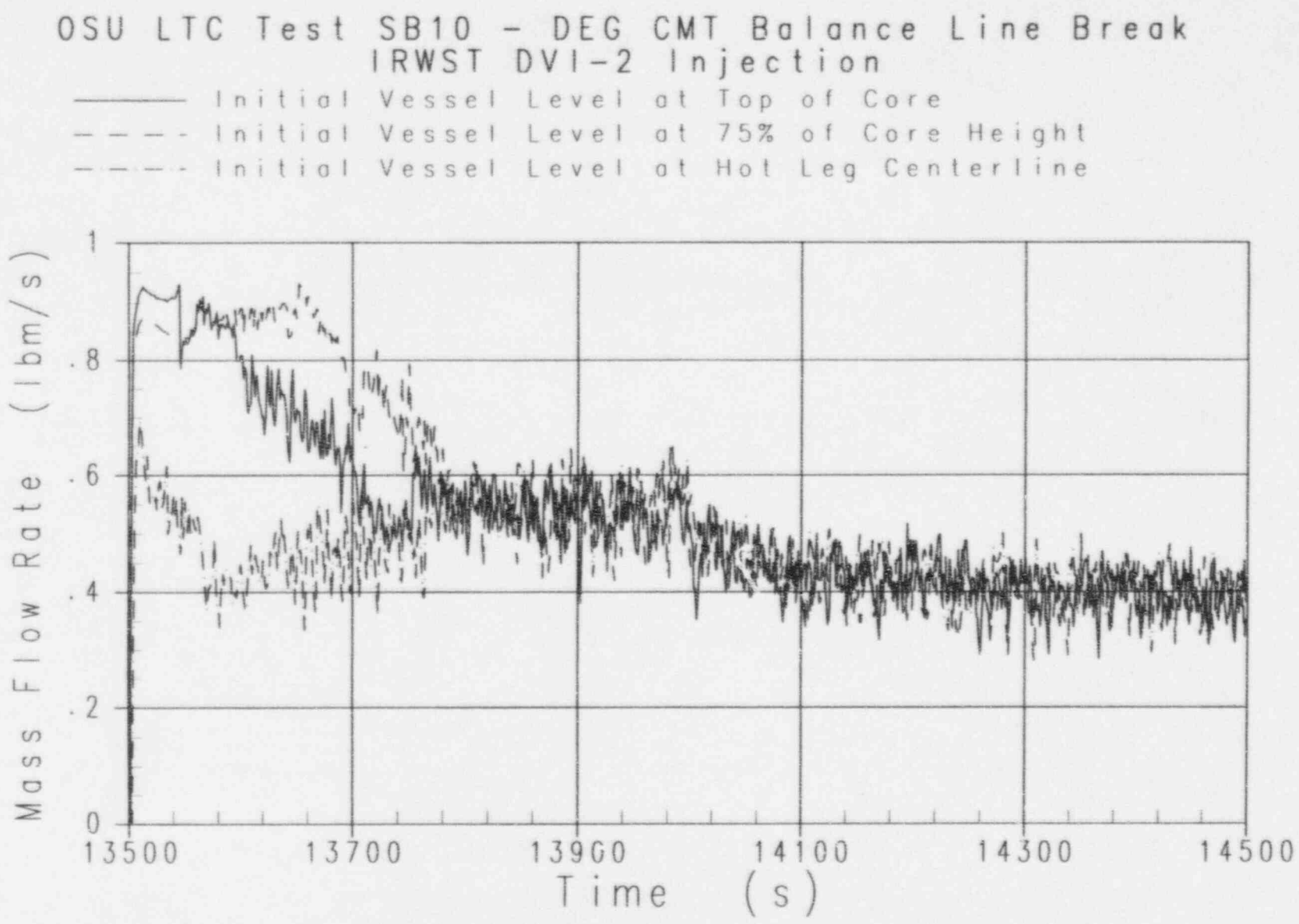
OSU LTC Test SB10 - DEG CMT Balance Line Break
IRWST DVI-2 Injection
Initial Vessel Level at Top of Core
Initial Vessel Level at 75% of Core Height
Initial Vessel Level at Hot Leg Centerline
Mass Flow Rate (lbm/s)
1
.8
.6
.4
.2
0
13500
13700
13900
14100
14300
14500
Time (s)

Figure 3 -27

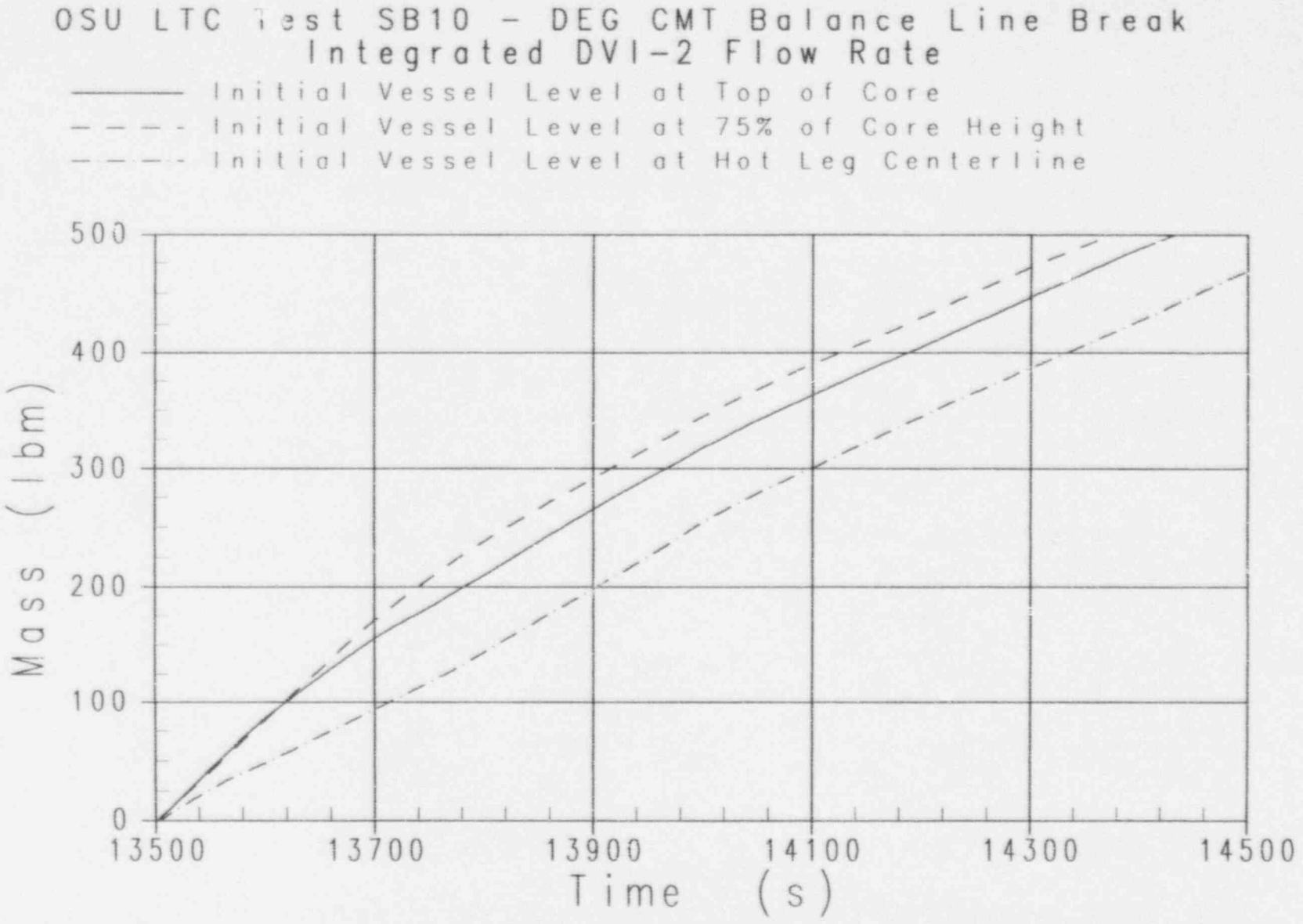
OSU LTC Test SB10 - DEG CMT Balance Line Break
Integrated DVI-2 Flow Rate
Initial Vessel Level at Top of Core
Initial Vessel Level at 75% of Core Height
Initial Vessel Level at Hot Leg Centerline
Mass (lbm)
0
100
200
300
400
500
13500
13700
13900
14100
14300
14500
Time (s)

Figure 3 -28

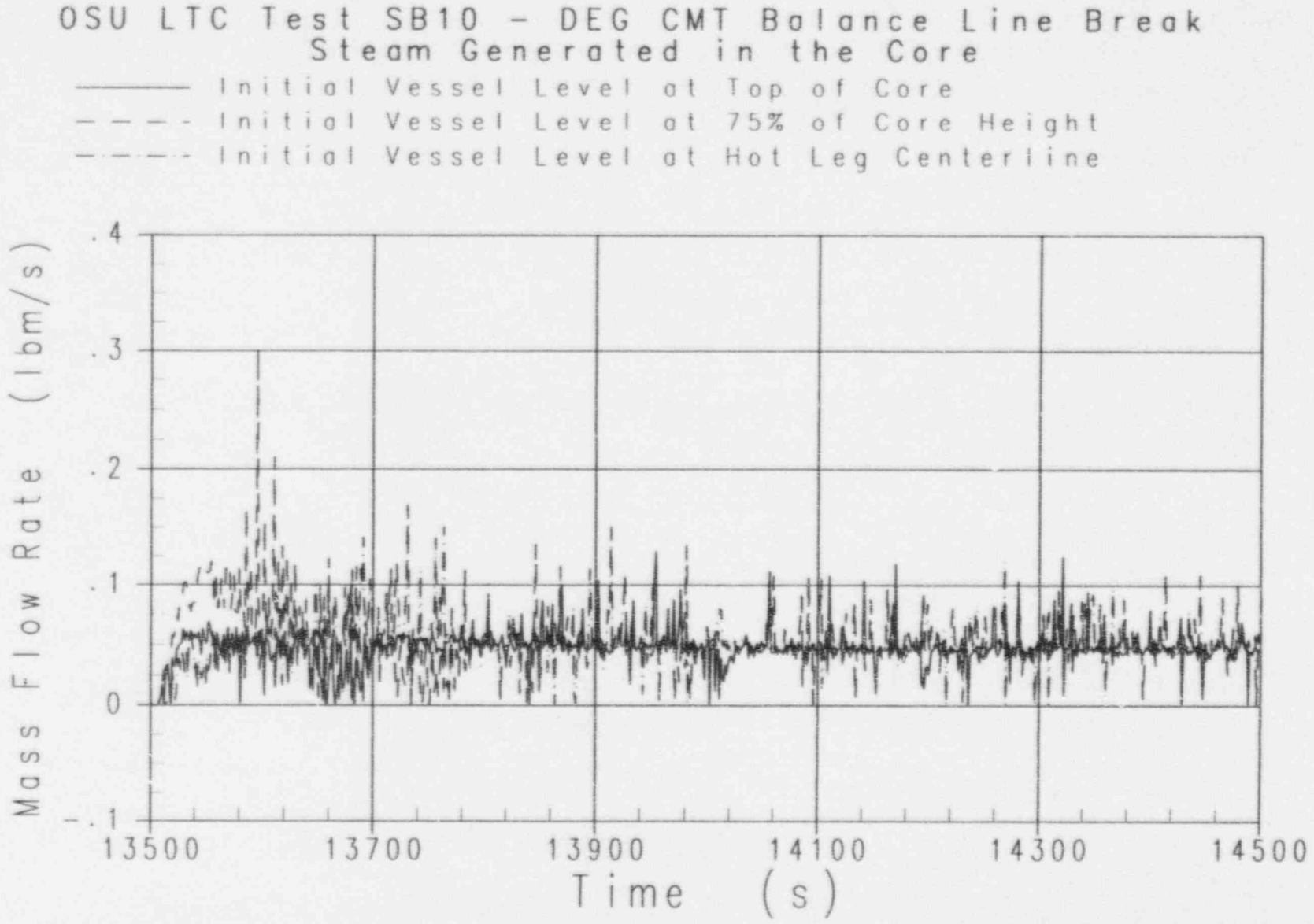
OSU LTC Test SB10 - DEG CMT Balance Line Break
Steam Generated in the Core
Initial Vessel Level at Top of Core
Initial Vessel Level at 75% of Core Height
Initial Vessel Level at Hot Leg Centerline
Mass Flow Rate (lbm/s)
.4
.3
.2
.1
0
-.1
13500
13700
13900
14100
14300
14500
Time (s)

Figure 3 -29

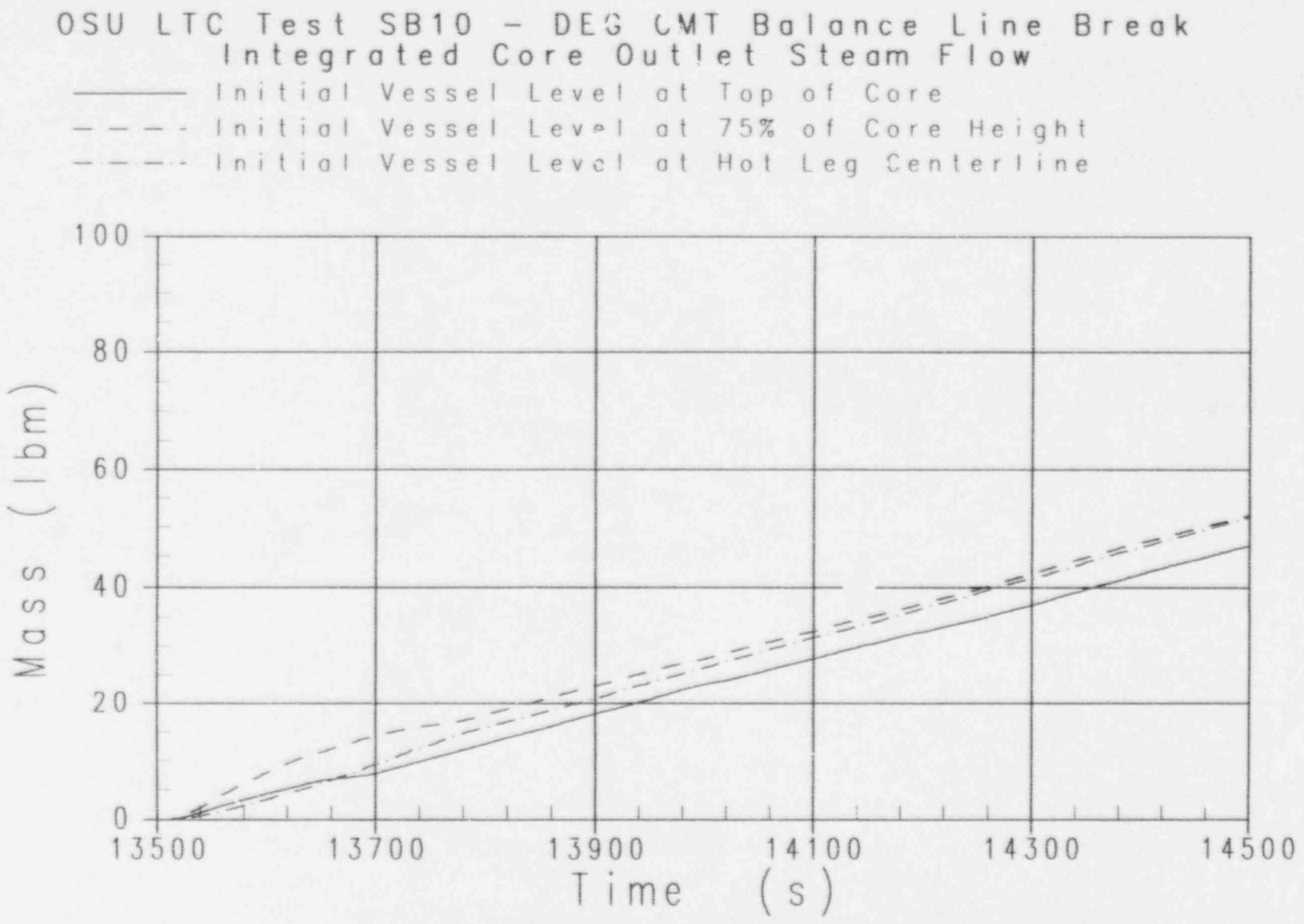
OSU LTC Test SB10 - DEG CMT Balance Line Break
Integrated Core Outlet Steam Flow
Initial Vessel Level at Top of Core
Initial Vessel Level at 75% of Core Height
Initial Vessel Level at Hot Leg Centerline
Mass (lbm)
100
80
60
40
20
0
13500
13700
13900
14100
14300
14500
Time (s)

Figure 3 -30

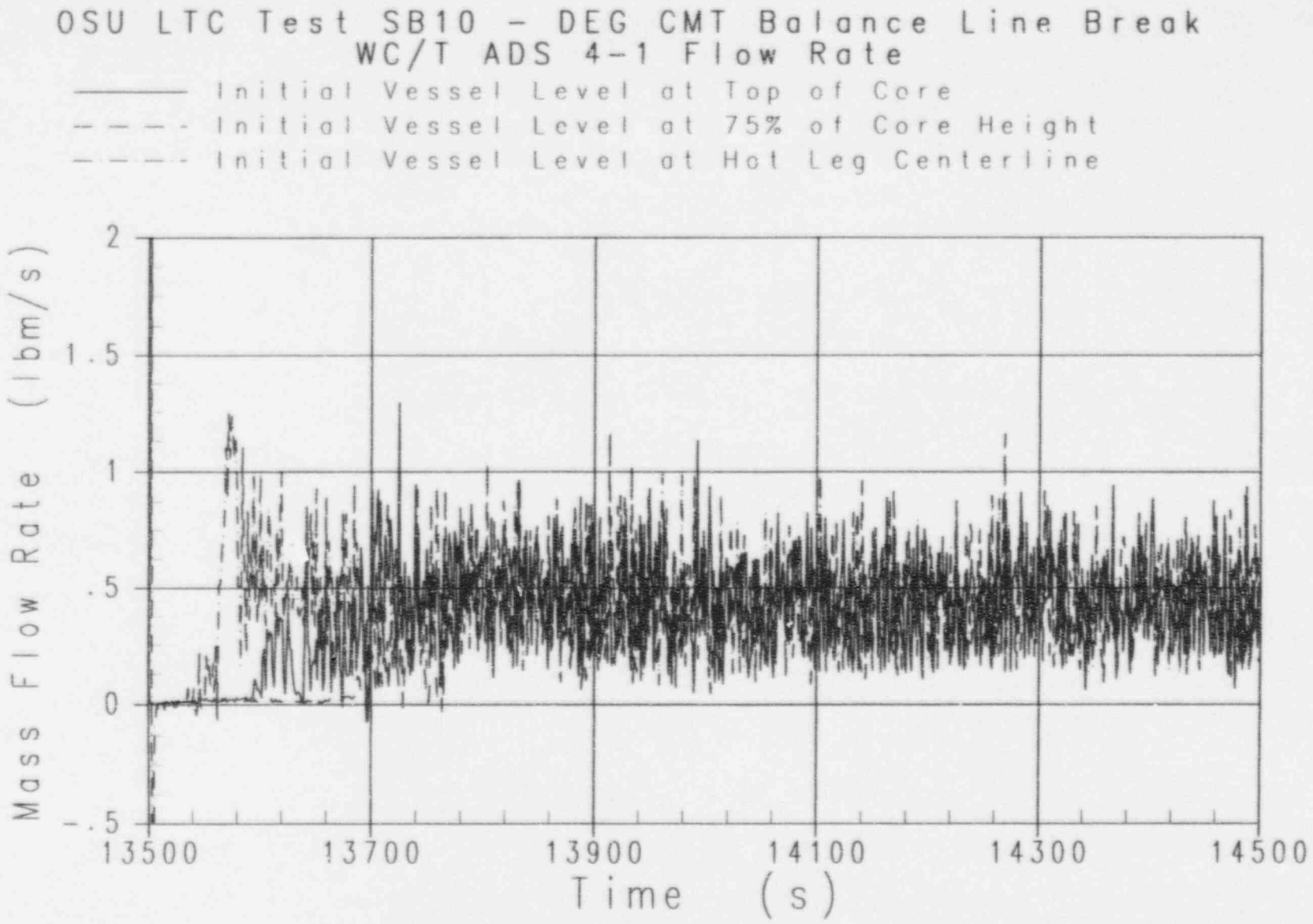
OSU LTC Test SB10 - DEG CMT Balance Line Break
WC/T ADS 4-1 Flow Rate
Initial Vessel Level at Top of Core
Initial Vessel Level at 75% of Core Height
Initial Vessel Level at Hot Leg Centerline
Mass Flow Rate (lbm/s)
2
1.5
1
.5
0
-.5
13500
13700
13900
14100
14300
14500
Time (s)

Figure 3 -31

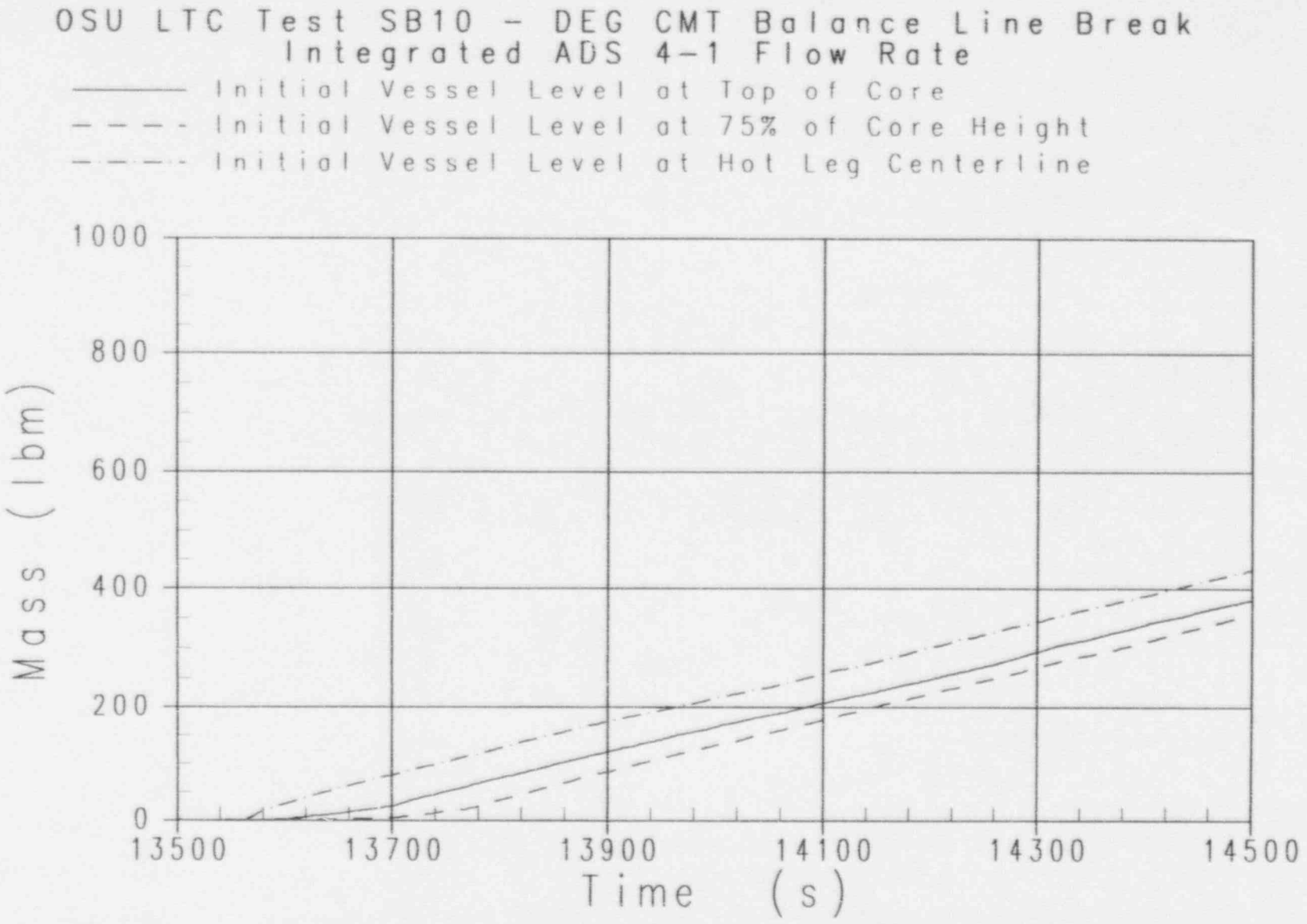
OSU LTC Test SB10 - DEG CMT Balance Line Break
Integrated ADS 4-1 Flow Rate
Initial Vessel Level at Top of Core
Initial Vessel Level at 75% of Core Height
Initial Vessel Level at Hot Leg Centerline
Mass (lbm)
1000
800
600
400
200
0
13500
13700
13900
14100
14300
14500
Time (s)

Figure 3 -32

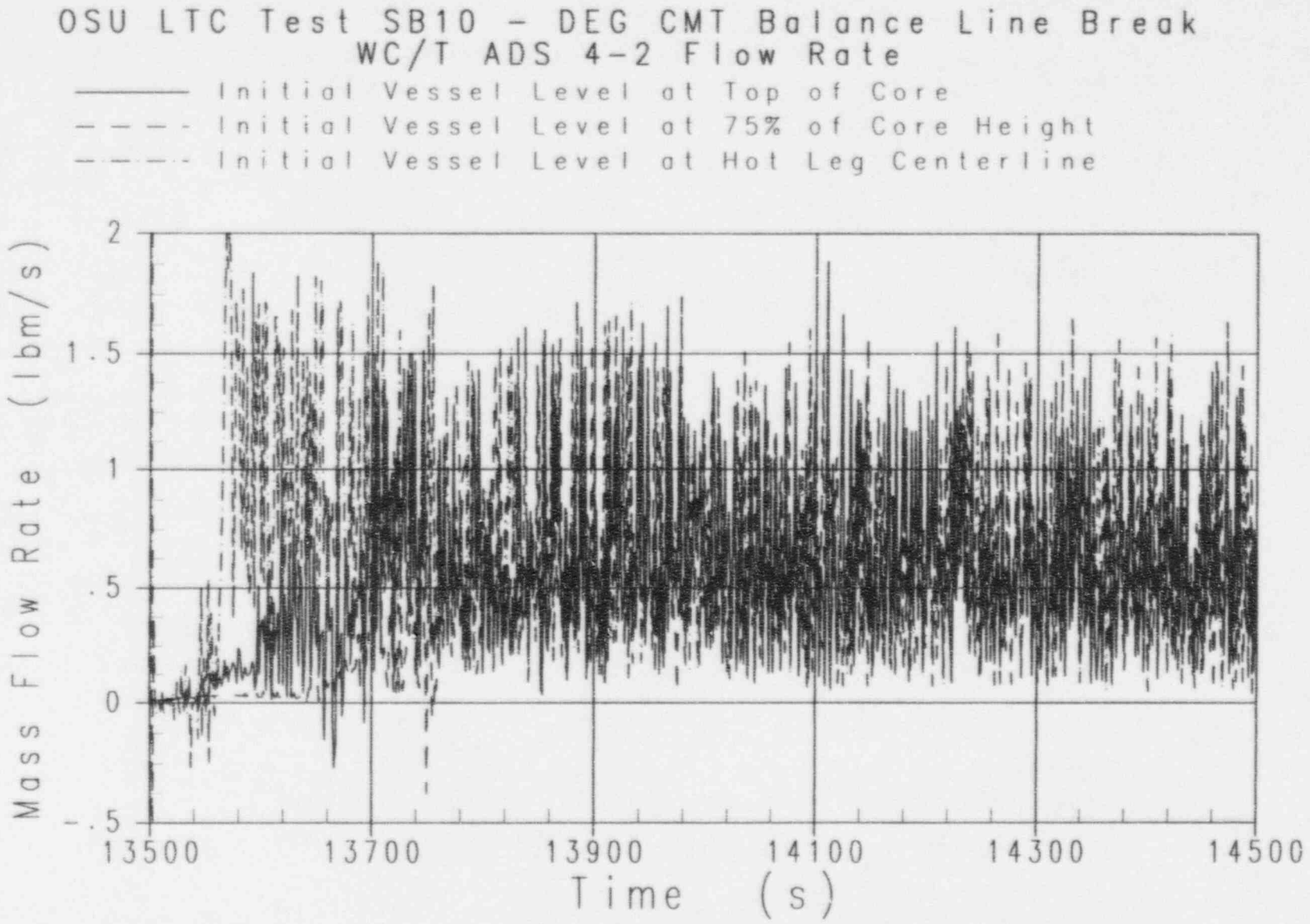
OSU LTC Test SB10 - DEG CMT Balance Line Break
WC/T ADS 4-2 Flow Rate
Initial Vessel Level at Top of Core
Initial Vessel Level at 75% of Core Height
Initial Vessel Level at Hot Leg Centerline
Mass Flow Rate (lbm/s)
2
1.5
1
.5
0
-.5
13500
13700
13900
14100
14300
14500
Time (s)

Figure 3 -33

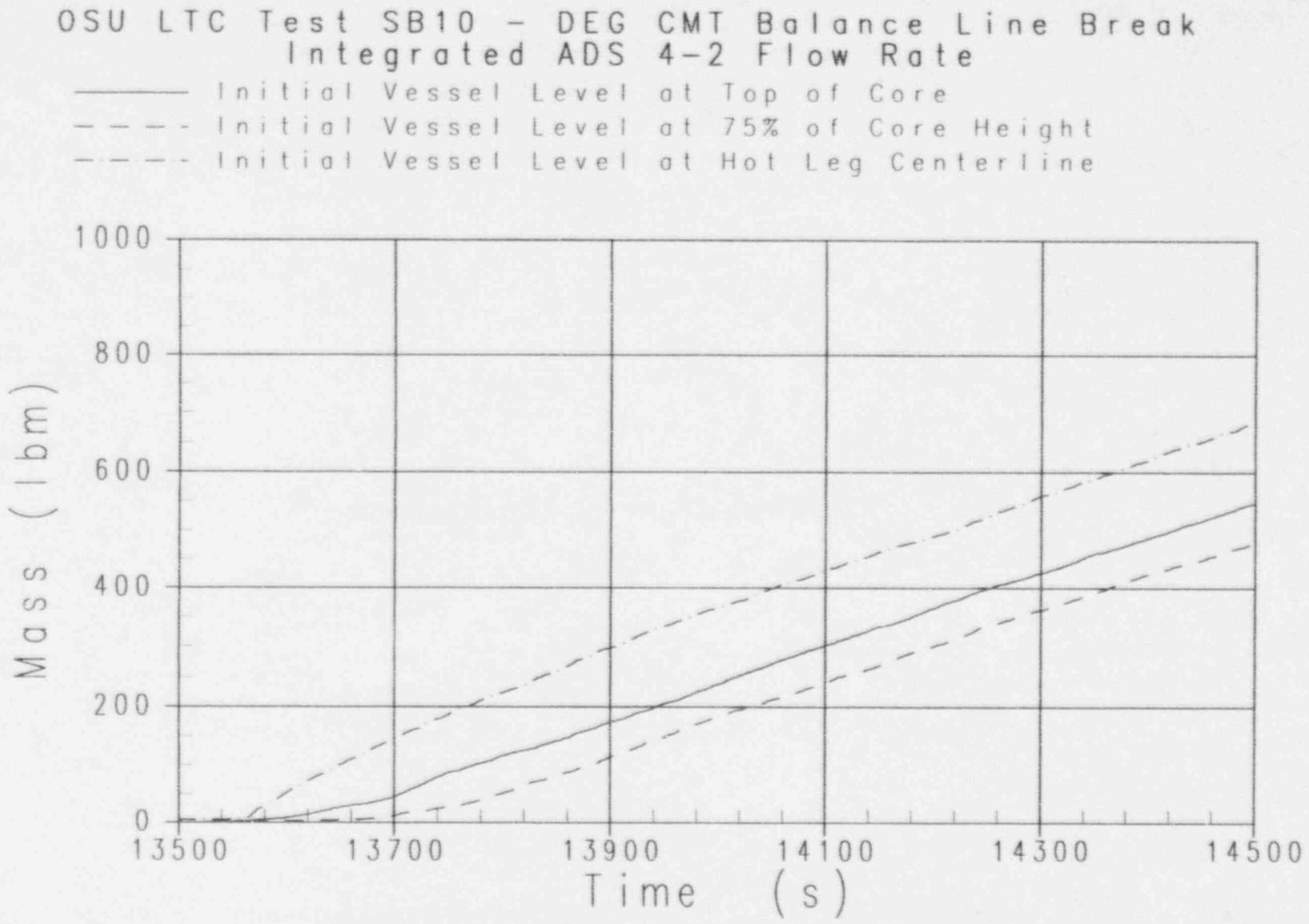
OSU LTC Test SB10 - DEG CMT Balance Line Break
Integrated ADS 4-2 Flow Rate
Initial Vessel Level at Top of Core
Initial Vessel Level at 75% of Core Height
Initial Vessel Level at Hot Leg Centerline
Mass (lbm)
1000
800
600
400
200
0
13500
13700
13900
14100
14300
14500
Time (s)

Figure 3 -34

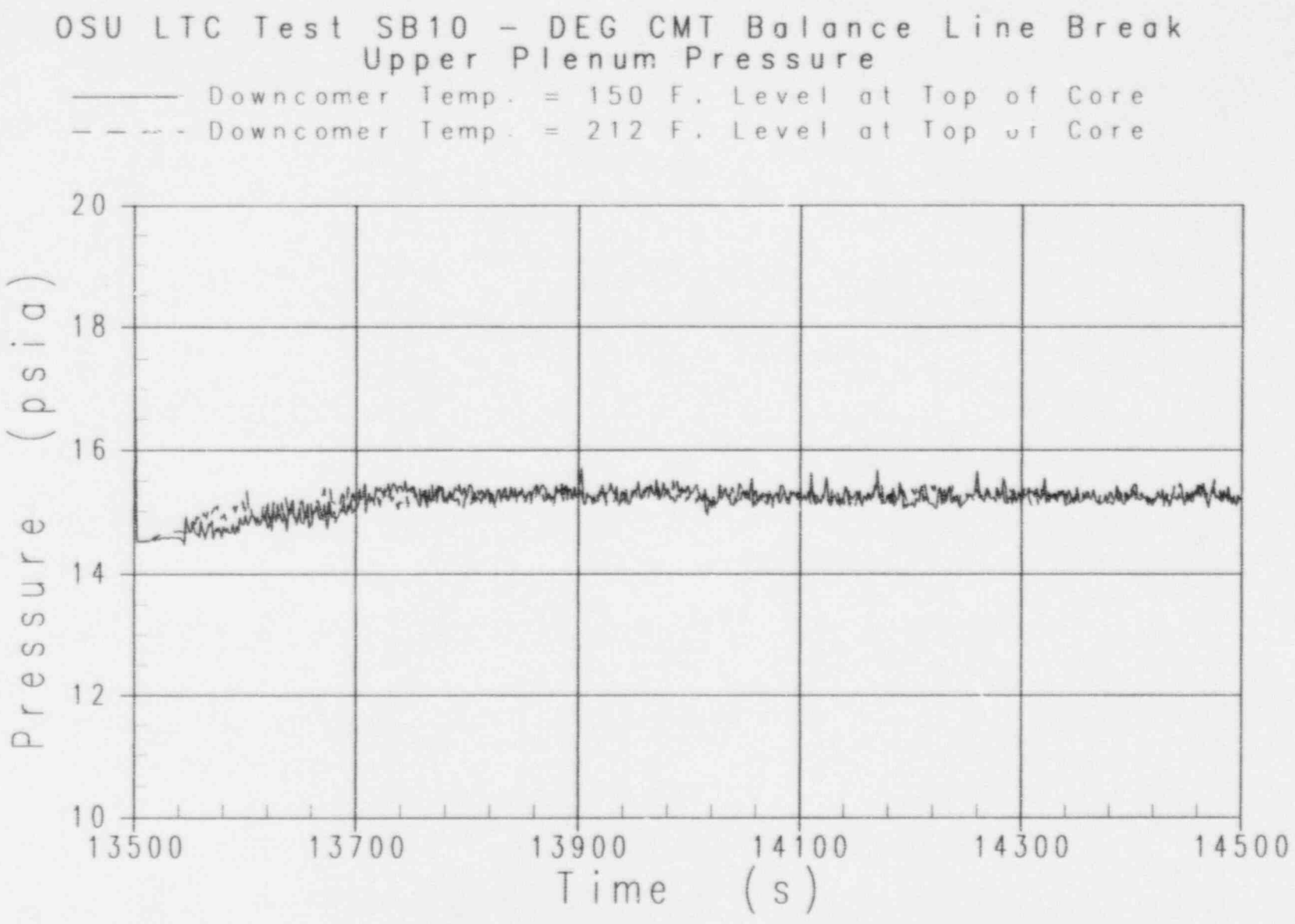
OSU LTC Test SB10 - DEG CMT Balance Line Break
Upper Plenum Pressure
Downcomer Temp. = 150 F. Level at Top of Core
Downcomer Temp. = 212 F. Level at Top of Core
Pressure (psia)
20
18
16
14
12
10
13500
13700
13900
14100
14300
14500
Time (s)

Figure 3–35

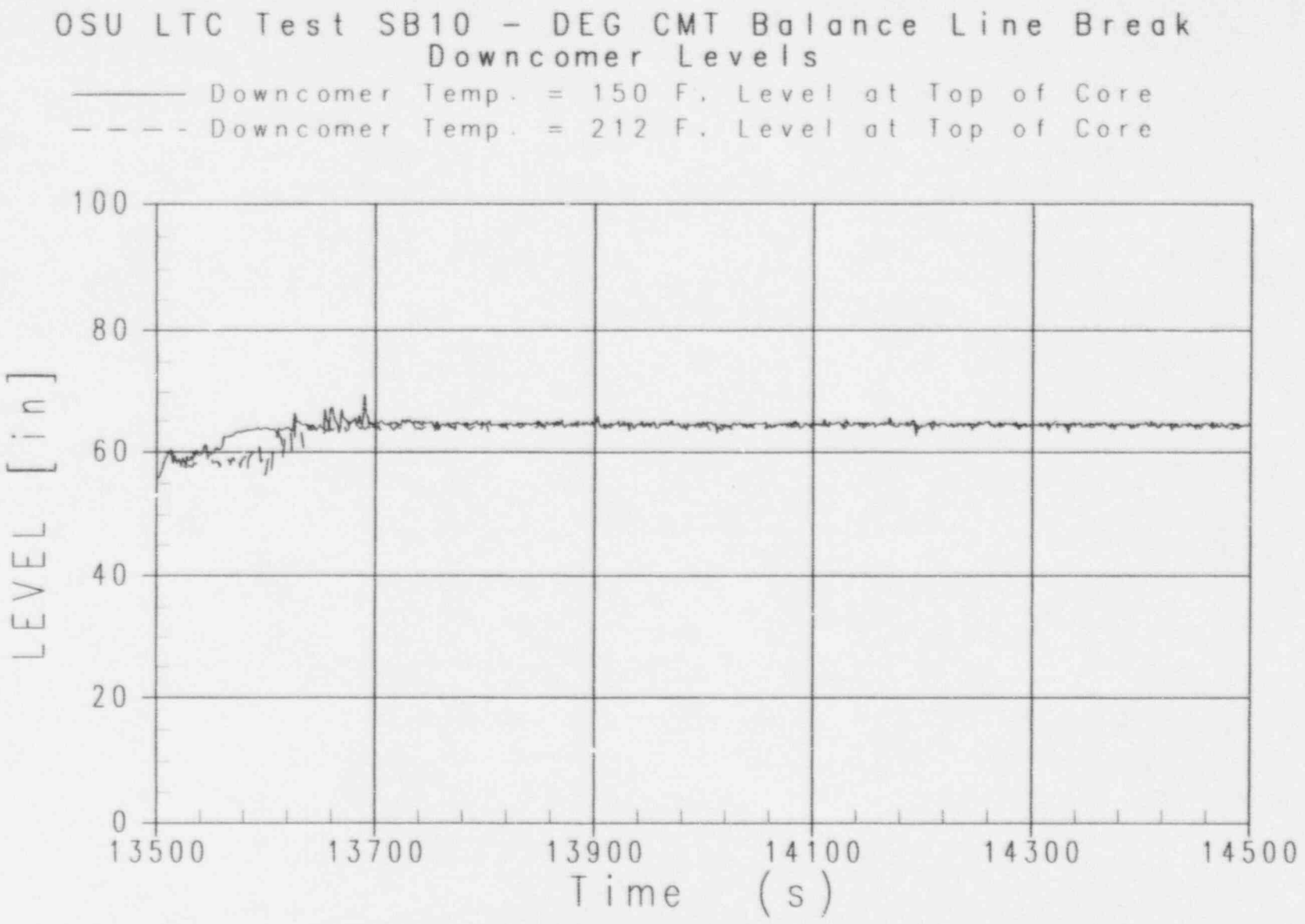
OSU LTC Test SB10 - DEG CMT Balance Line Break
Downcomer Levels
Downcomer Temp. = 150 F. Level at Top of Core
Downcomer Temp. = 212 F. Level at Top of Core
LEVEL [in]
100
80
60
40
20
0
13500
13700
13900
14100
14300
14500
Time (s)

Figure 3-36

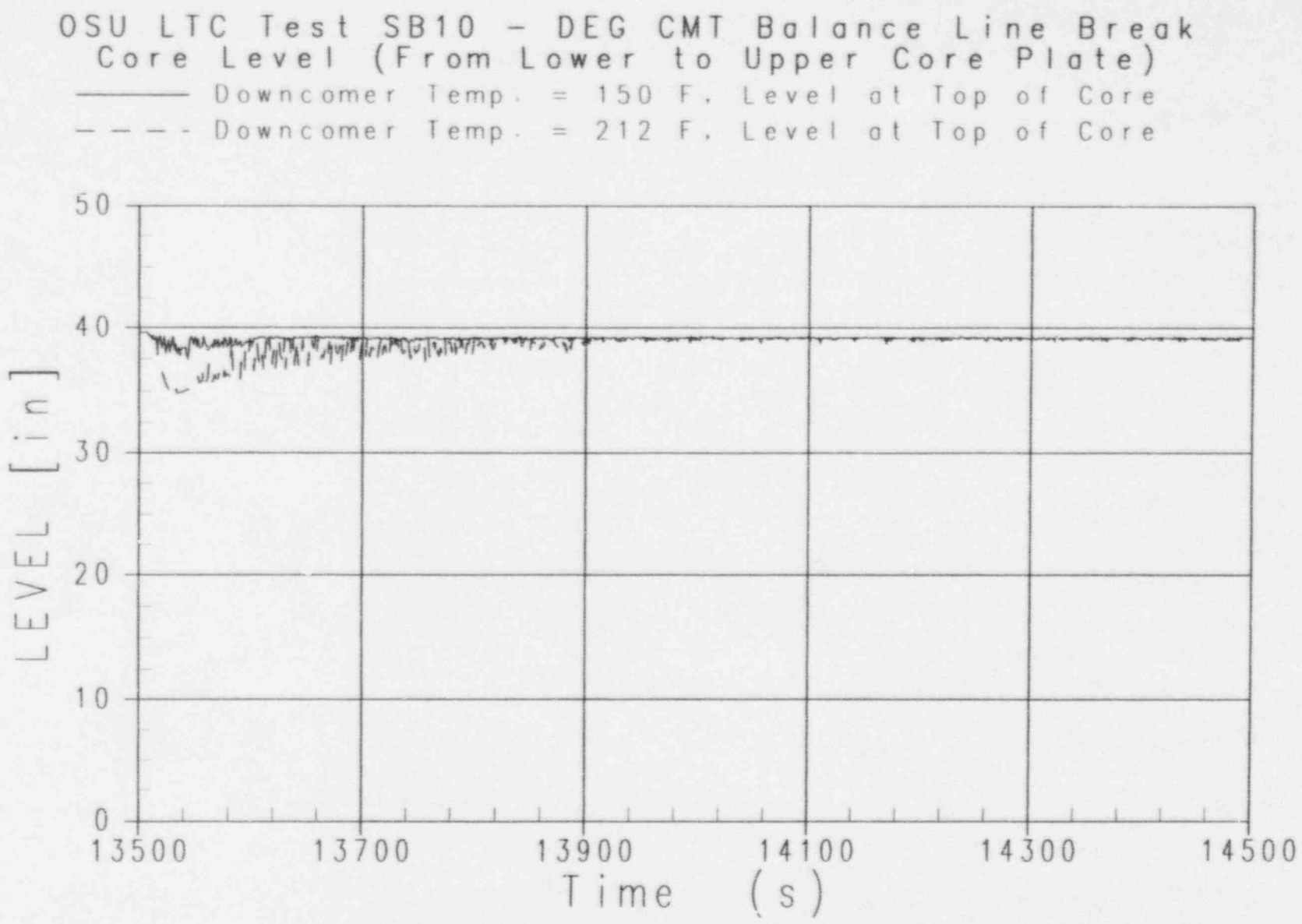
OSU LTC Test SB10 - DEG CMT Balance Line Break
Core Level (From Lower to Upper Core Plate)
Downcomer Temp. = 150 F, Level at Top of Core
Downcomer Temp. = 212 F, Level at Top of Core
LEVEL [in]
50
40
30
20
10
0
13500
13700
13900
14100
14300
14500
Time (s)

Figure 3-37

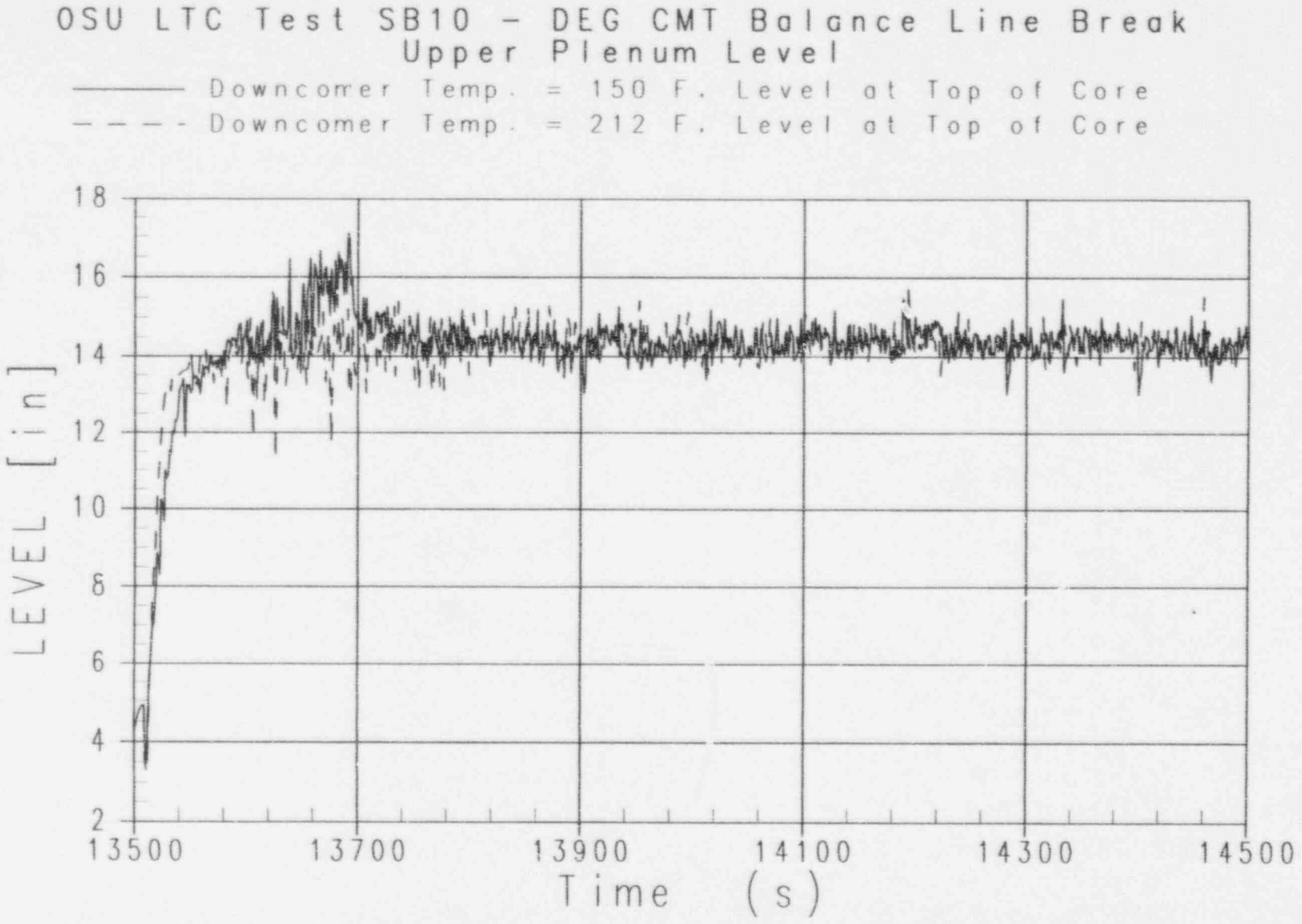
OSU LTC Test SB10 - DEG CMT Balance Line Break
Upper Plenum Level
Downcomer Temp. = 150 F. Level at Top of Core
Downcomer Temp. = 212 F. Level at Top of Core
LEVEL [in]
18
16
14
12
10
8
6
4
2
13500
13700
13900
14100
14300
14500
Time (s)

Figure 3-38

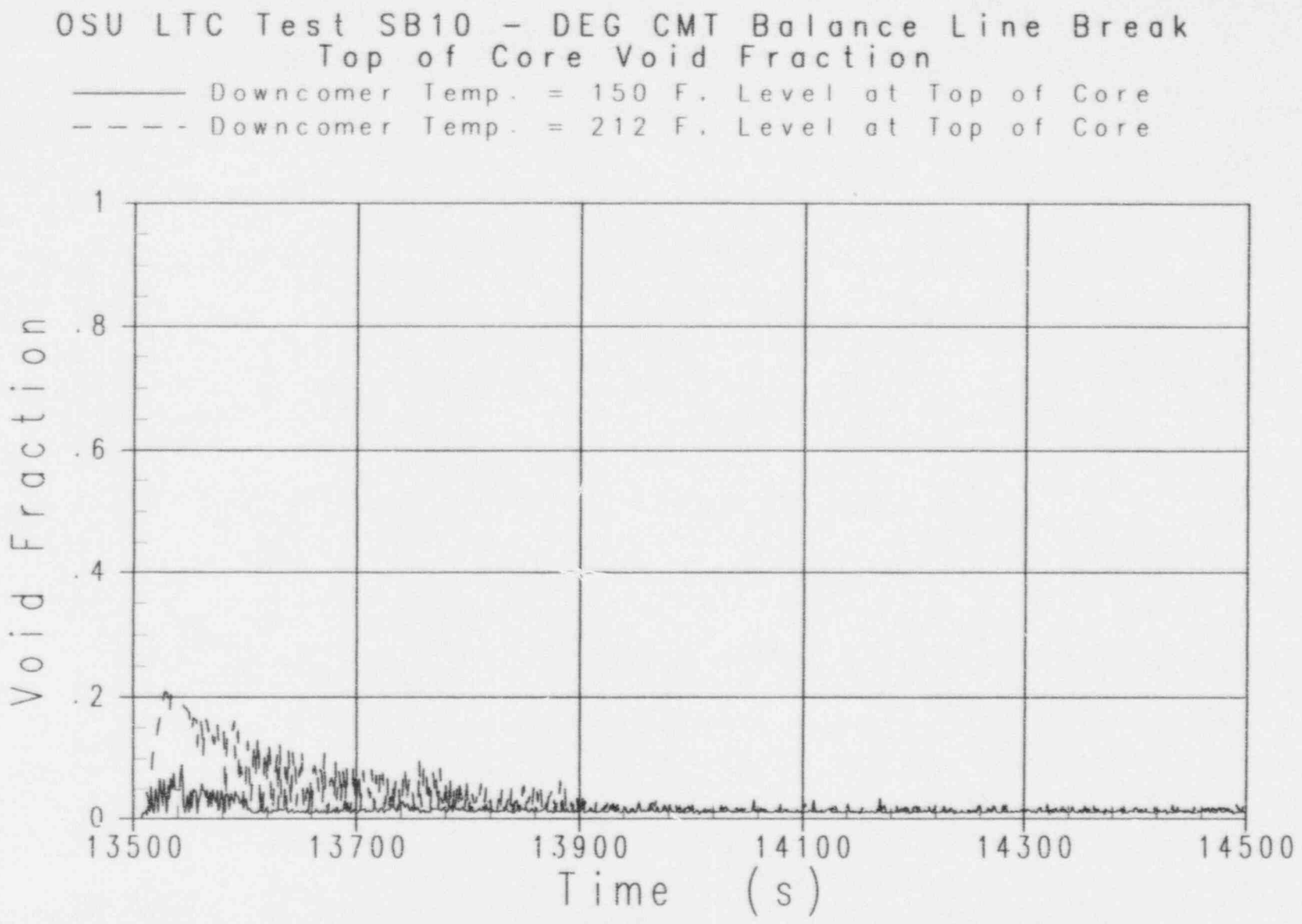
OSU LTC Test SB10 - DEG CMT Balance Line Break
Top of Core Void Fraction
Downcomer Temp. = 150 F. Level at Top of Core
Downcomer Temp. = 212 F. Level at Top of Core
Void Fraction
1
.8
.6
.4
.2
0
13500
13700
13900
14100
14300
14500
Time (s)

Figure 3-39

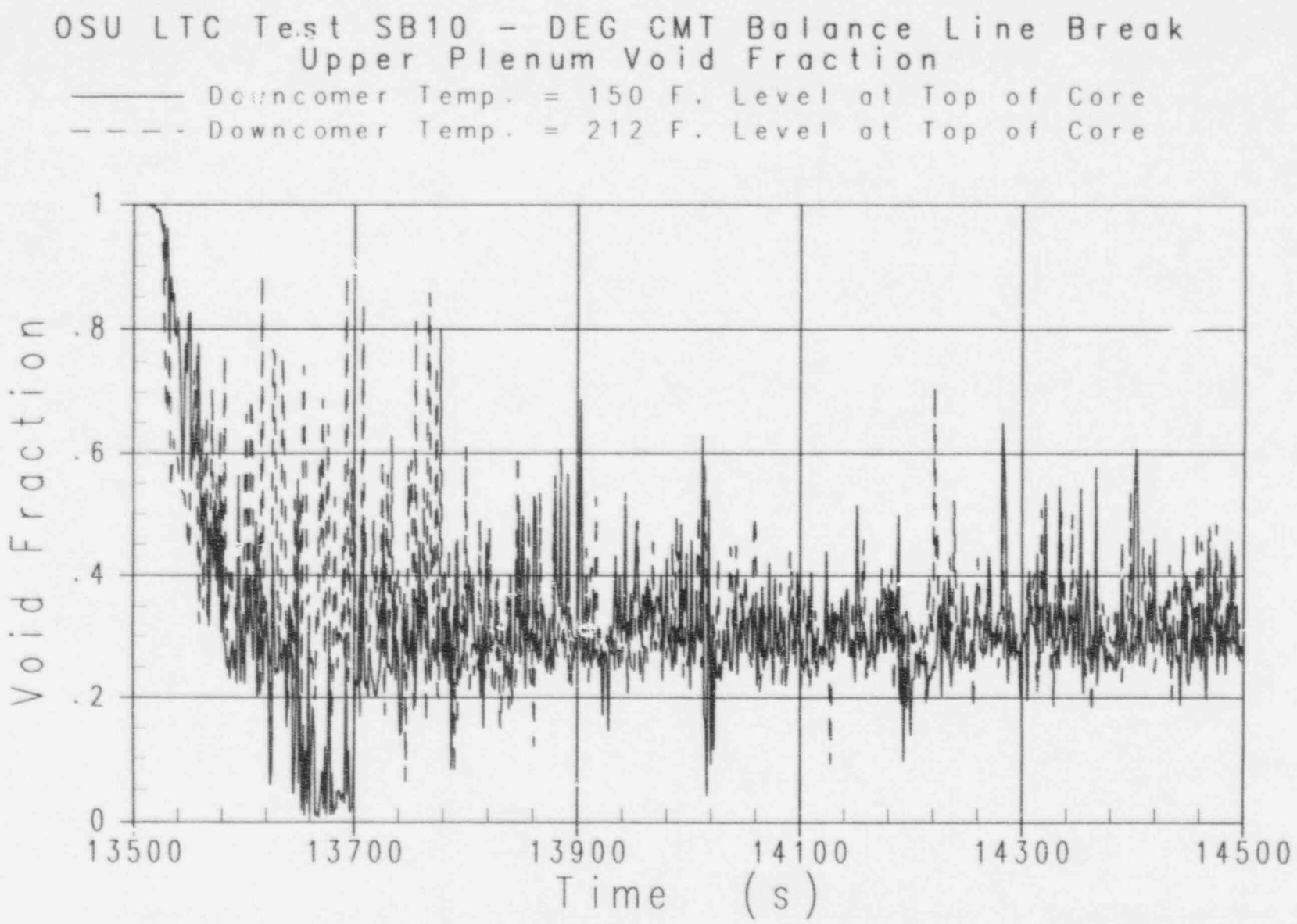
OSU LTC Test SB10 - DEG CMT Balance Line Break
Upper Plenum Void Fraction
Downcomer Temp. = 150 F. Level at Top of Core
Downcomer Temp. = 212 F. Level at Top of Core
Void Fraction
1
.8
.6
.4
.2
0
13500
13700
13900
14100
14300
14500
Time (s)

Figure 3-40

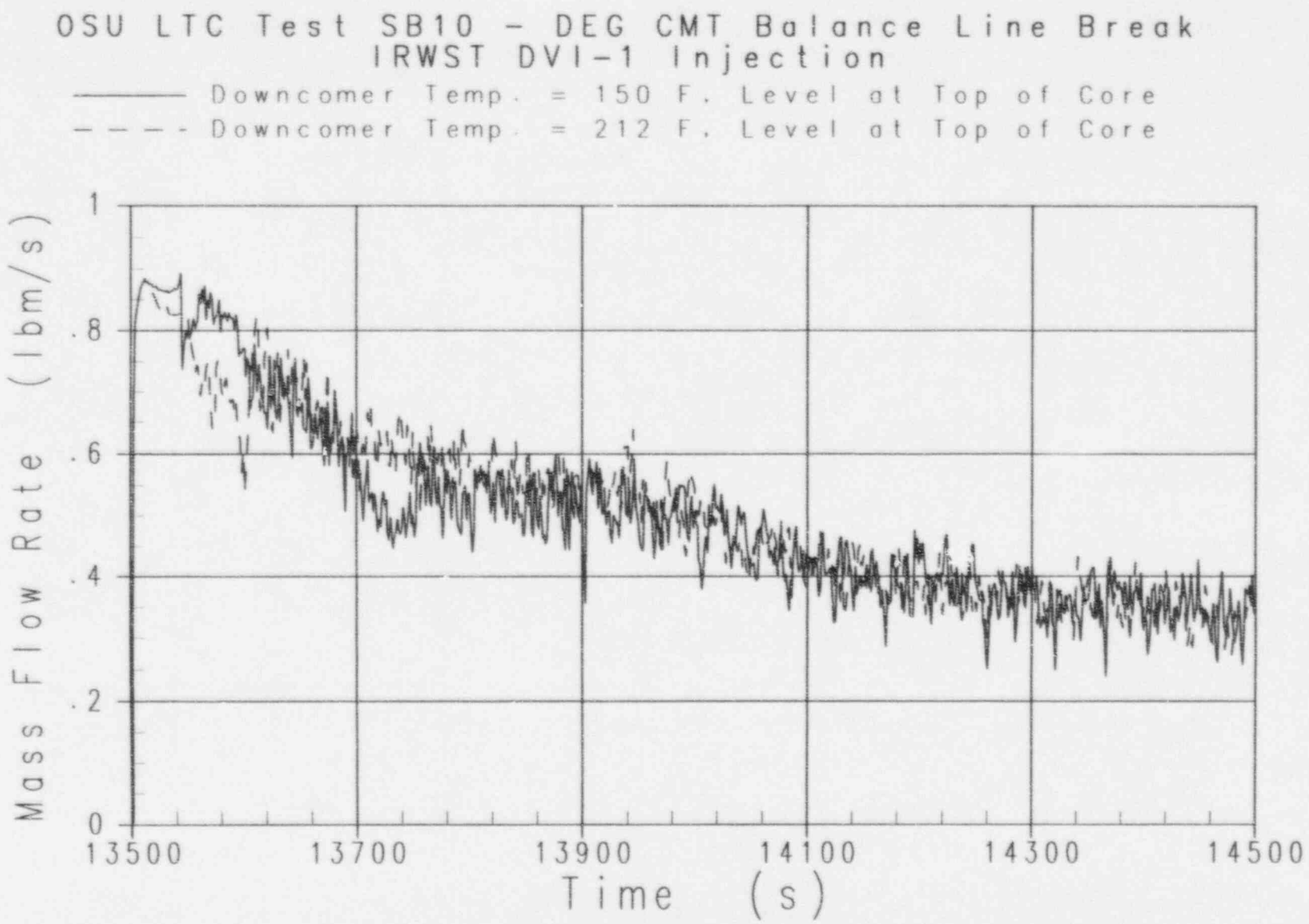
OSU LTC Test SB10 - DEG CMT Balance Line Break
IRWST DVI-1 Injection
Downcomer Temp. = 150 F. Level at Top of Core
Downcomer Temp. = 212 F. Level at Top of Core
Mass Flow Rate (lbm/s)
1
.8
.6
.4
.2
0
13500
13700
13900
14100
14300
14500
Time (s)

Figure 3-41

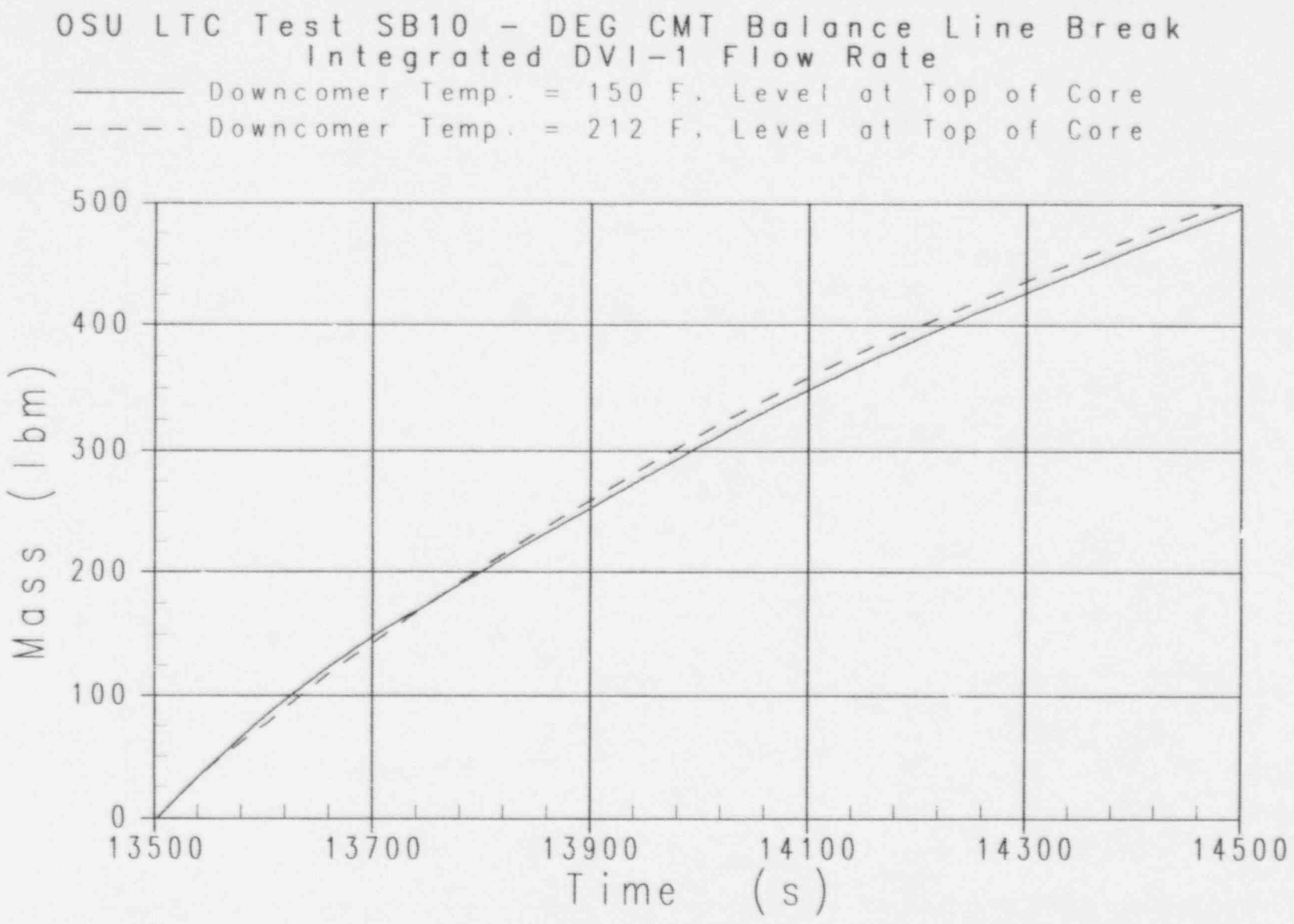
OSU LTC Test SB10 - DEG CMT Balance Line Break
Integrated DVI-1 Flow Rate
Downcomer Temp. = 150 F. Level at Top of Core
Downcomer Temp. = 212 F. Level at Top of Core
Mass (lbm)
500
400
300
200
100
0
13500
13700
13900
14100
14300
14500
Time (s)

Figure 3-42

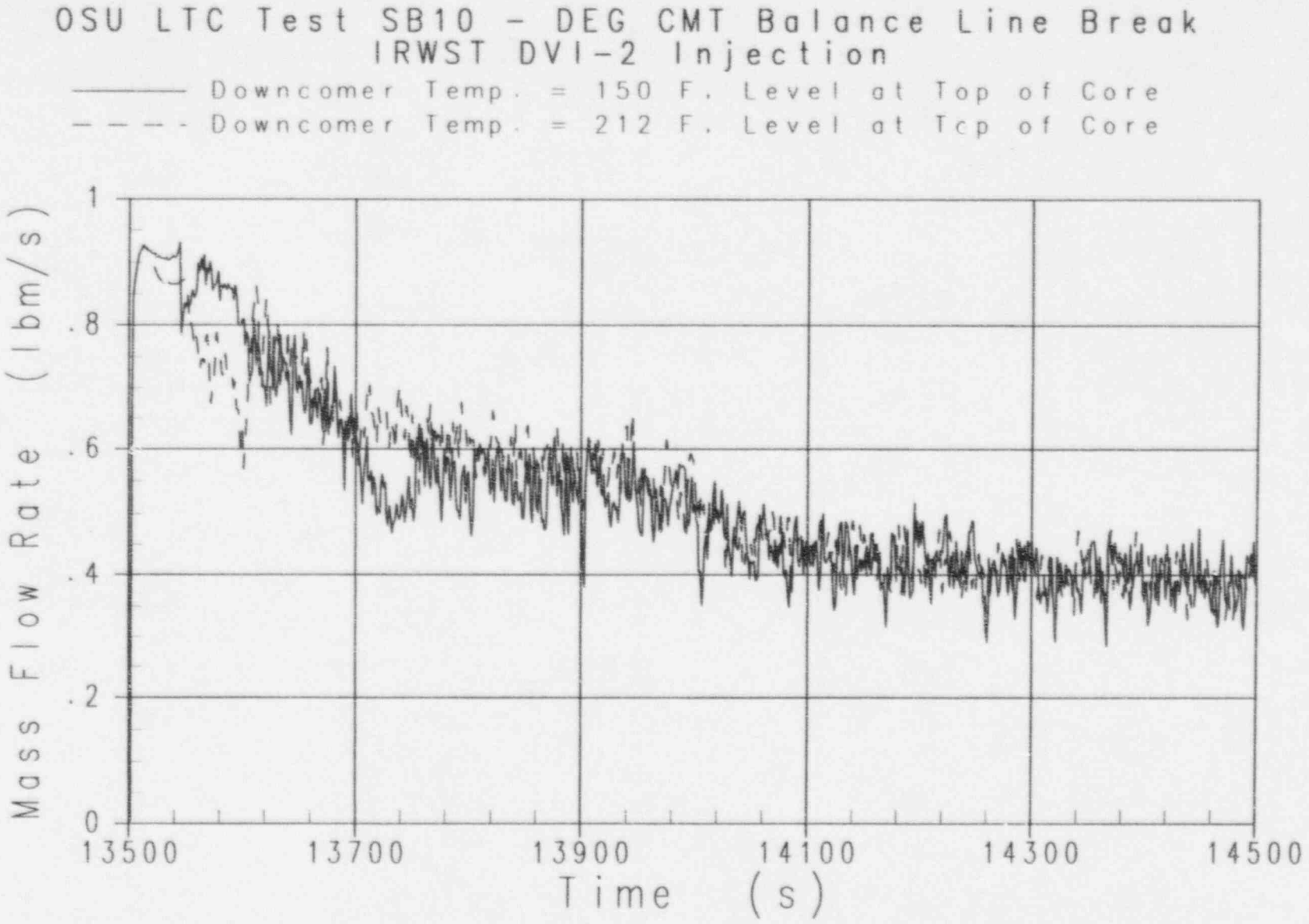
OSU LTC Test SB10 - DEG CMT Balance Line Break
IRWST DVI-2 Injection
Downcomer Temp. = 150 F. Level at Top of Core
Downcomer Temp. = 212 F. Level at Top of Core
Mass Flow Rate (lbm/s)
1
.8
.6
.4
.2
0
13500
13700
13900
14100
14300
14500
Time (s)

Figure 3-43

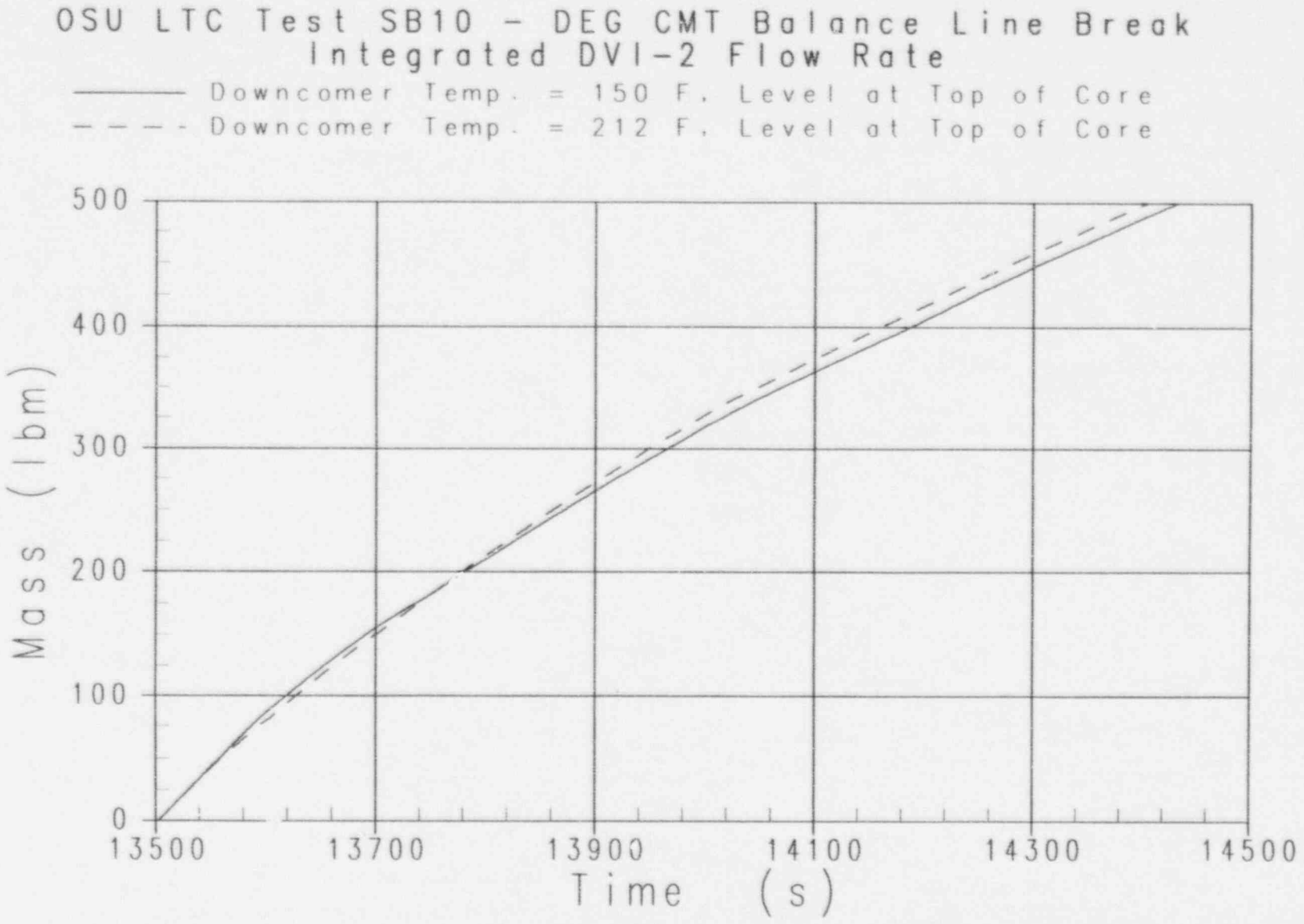
OSU LTC Test SB10 - DEG CMT Balance Line Break
Integrated DVI-2 Flow Rate
Downcomer Temp. = 150 F, Level at Top of Core
Downcomer Temp. = 212 F, Level at Top of Core
Mass (lbm)
0
100
200
300
400
500
13500
13700
13900
14100
14300
14500
Time (s)

Figure 3-44

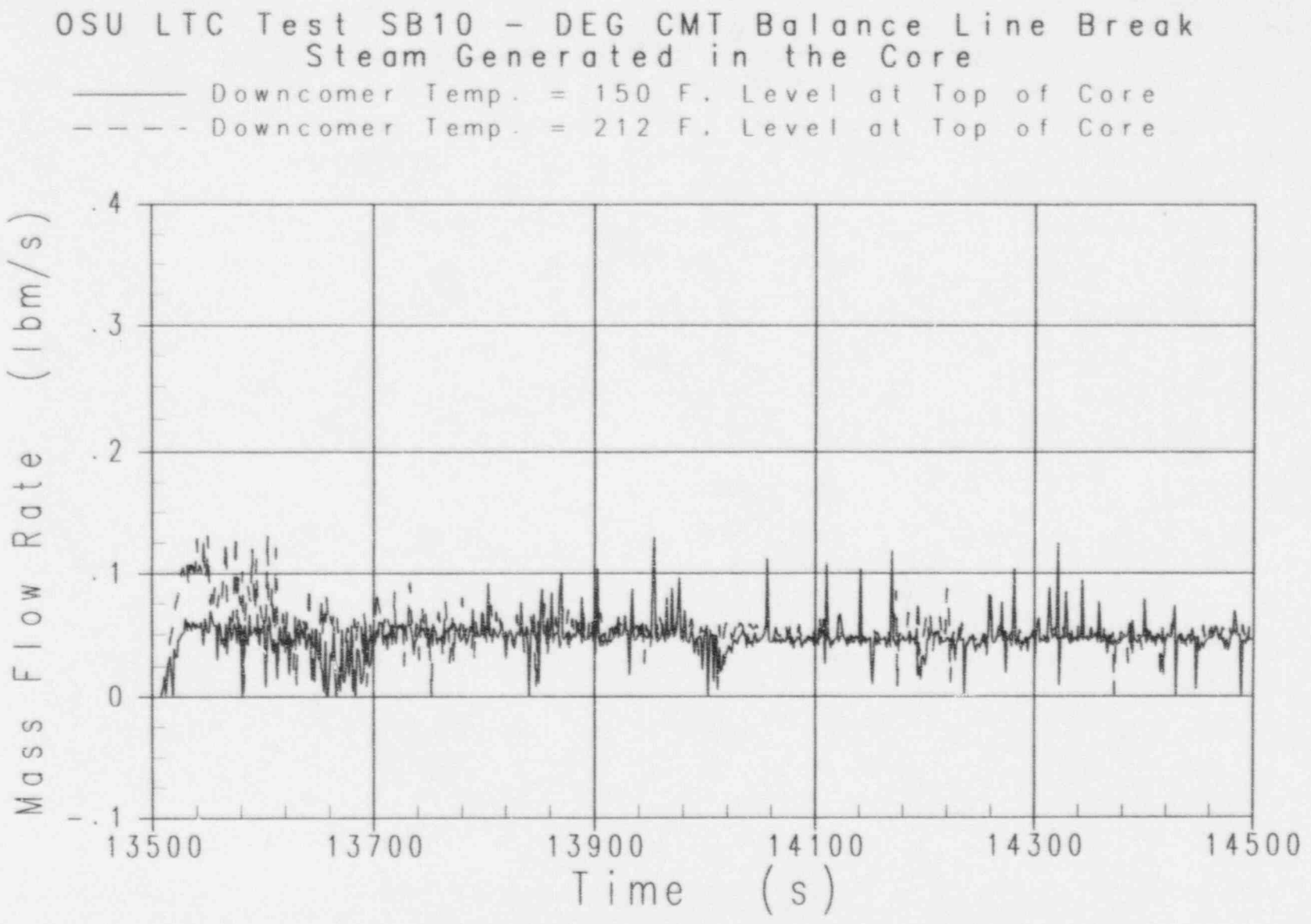
OSU LTC Test SB10 - DEG CMT Balance Line Break
Steam Generated in the Core
Downcomer Temp. = 150 F. Level at Top of Core
Downcomer Temp. = 212 F. Level at Top of Core
Mass Flow Rate (lbm/s)
.4
.3
.2
.1
0
-.1
13500
13700
13900
14100
14300
14500
Time (s)

Figure 3-45

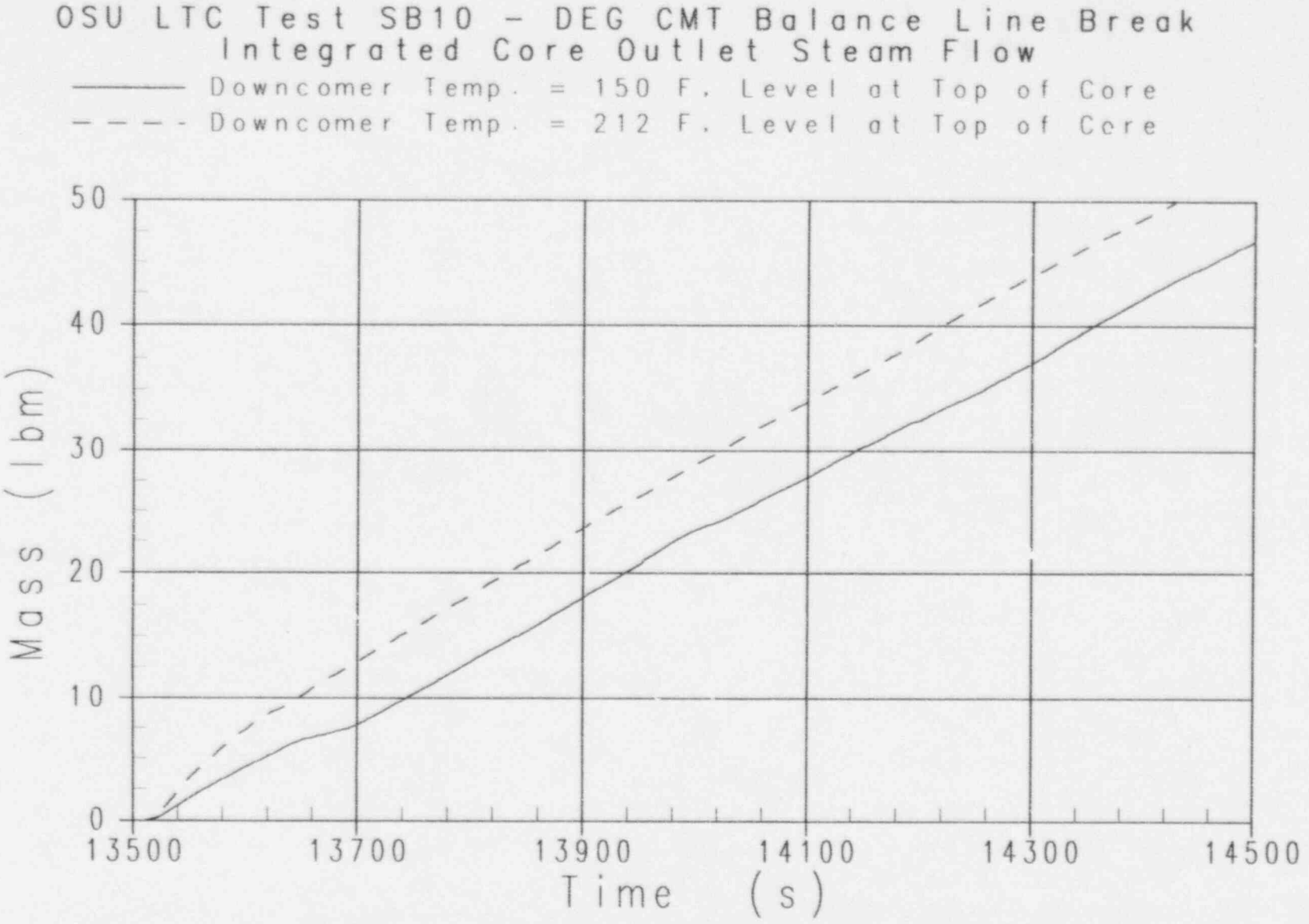
OSU LTC Test SB10 - DEG CMT Balance Line Break
Integrated Core Outlet Steam Flow
Downcomer Temp. = 150 F. Level at Top of Core
Downcomer Temp. = 212 F. Level at Top of Core
Mass (lbm)
0
10
20
30
40
50
13500
13700
13900
14100
14300
14500
Time (s)

Figure 3-46

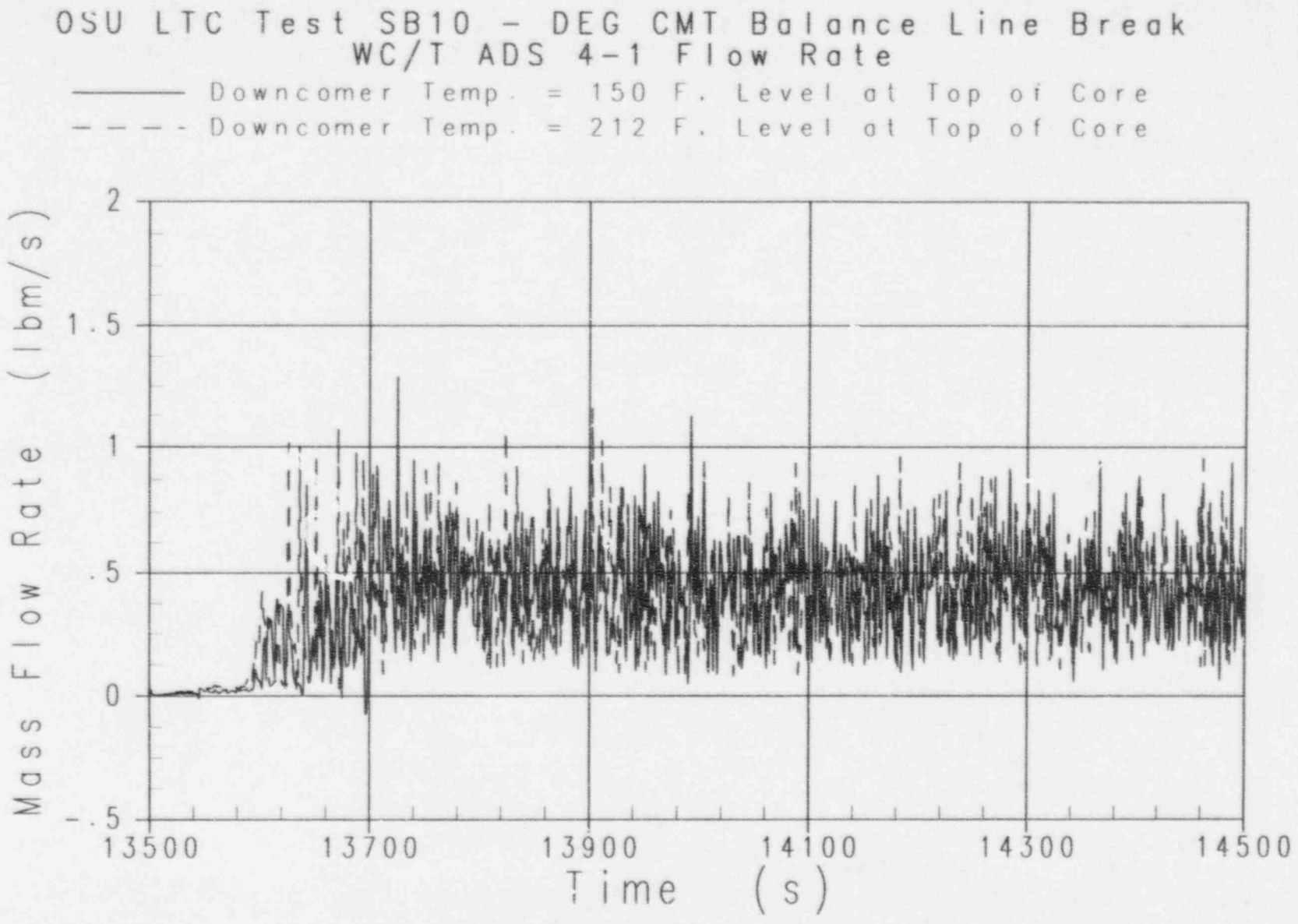
OSU LTC Test SB10 - DEG CMT Balance Line Break
WC/T ADS 4-1 Flow Rate
Downcomer Temp. = 150 F. Level at Top of Core
Downcomer Temp. = 212 F. Level at Top of Core
Mass Flow Rate (lbm/s)
2
1.5
1
.5
0
-.5
13500
13700
13900
14100
14300
14500
Time (s)

Figure 3-47

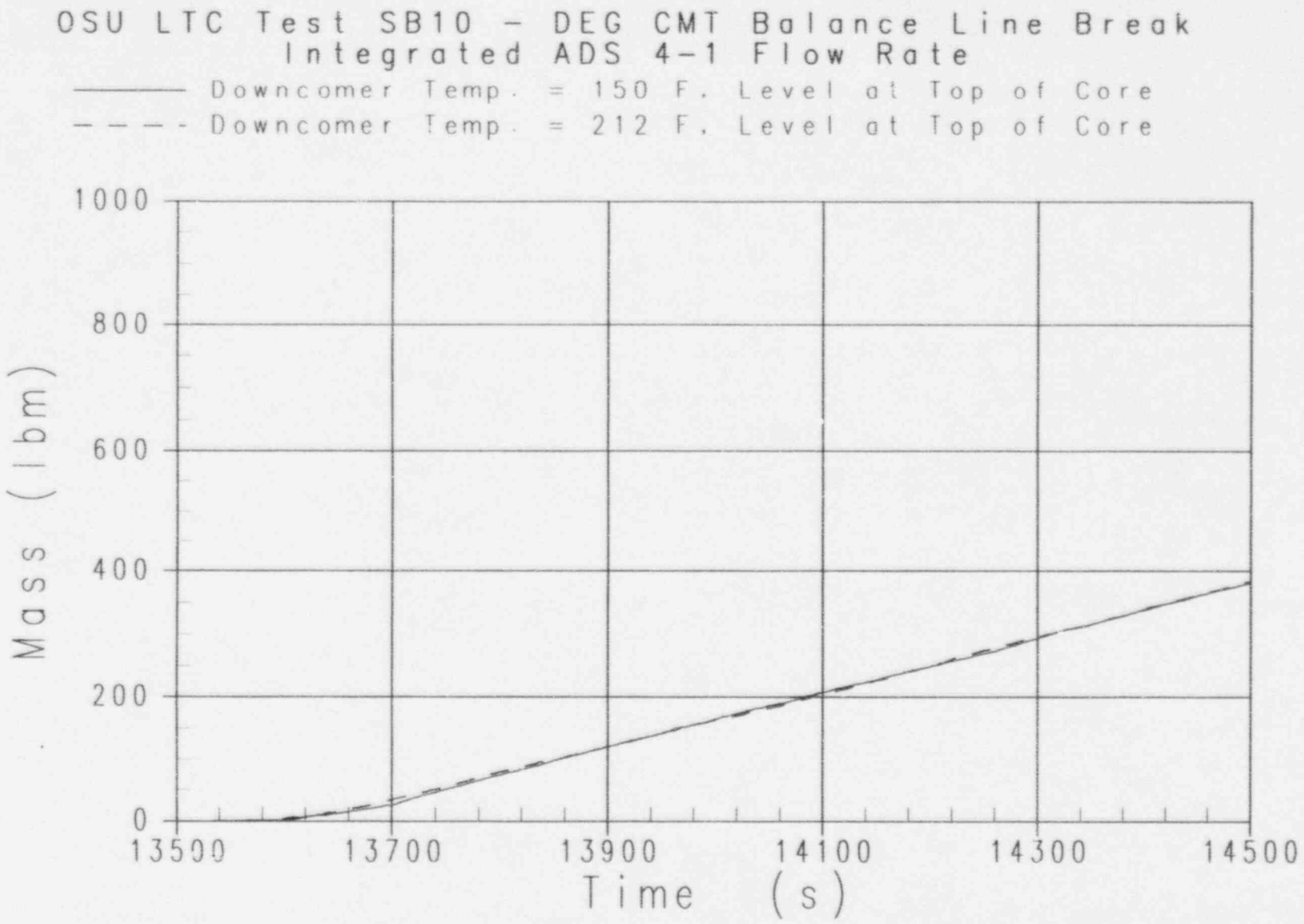
OSU LTC Test SB10 - DEG CMT Balance Line Break
Integrated ADS 4-1 Flow Rate
Downcomer Temp. = 150 F. Level at Top of Core
Downcomer Temp. = 212 F. Level at Top of Core
Mass (lbm)
1000
800
600
400
200
0
13500
13700
13900
14100
14300
14500
Time (s)

Figure 3-48

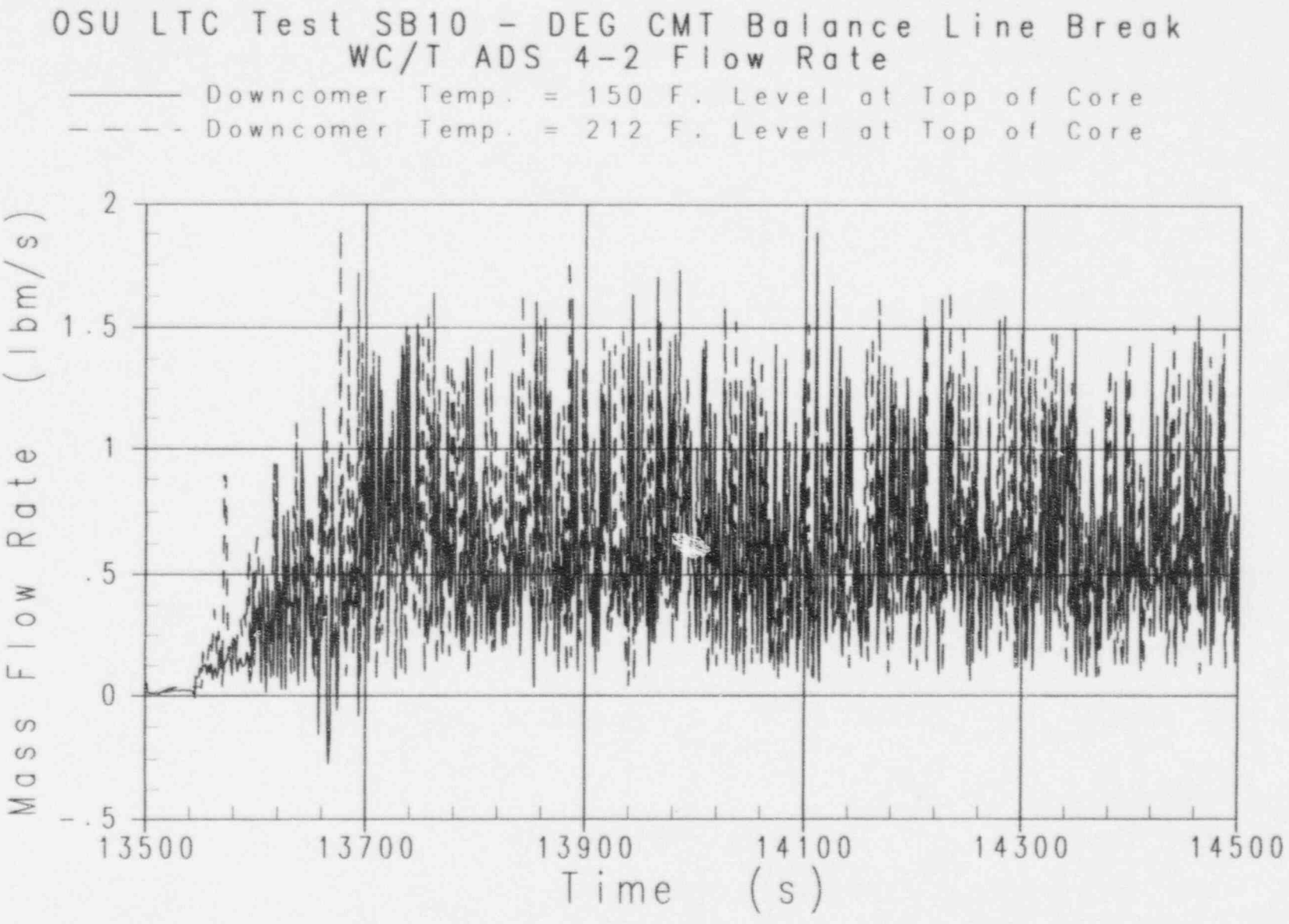
OSU LTC Test SB10 - DEG CMT Balance Line Break
WC/T ADS 4-2 Flow Rate
Downcomer Temp. = 150 F. Level at Top of Core
Downcomer Temp. = 212 F. Level at Top of Core
Mass Flow Rate (lbm/s)
2
1.5
1
.5
0
-.5
13500
13700
13900
14100
14300
14500
Time (s)

Figure 3-49

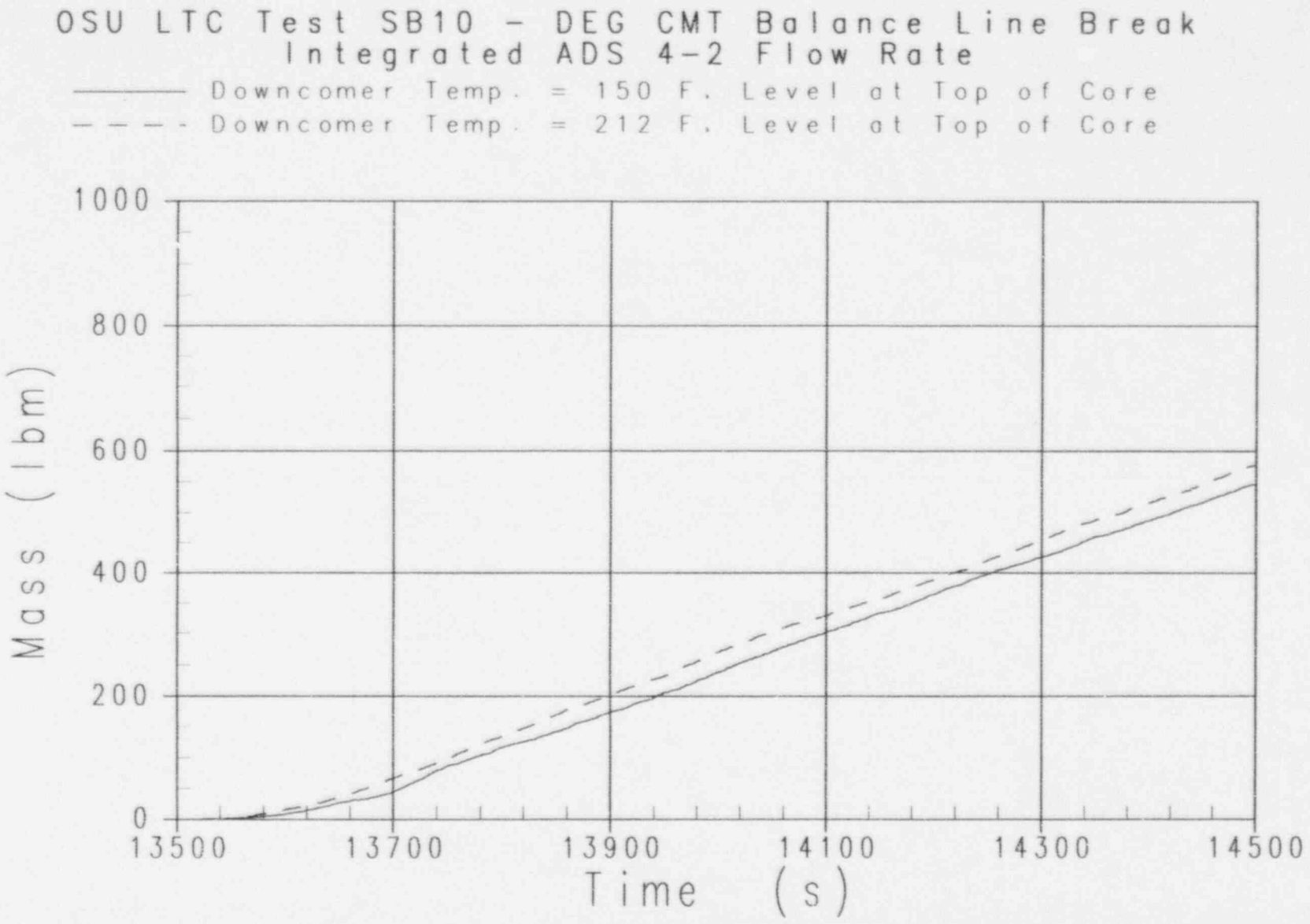
OSU LTC Test SB10 - DEG CMT Balance Line Break
Integrated ADS 4-2 Flow Rate
Downcomer Temp. = 150 F. Level at Top of Core
Downcomer Temp. = 212 F. Level at Top of Core
Mass (lbm)
1000
800
600
400
200
0
13500
13700
13900
14100
14300
14500
Time (s)

Figure 3-50

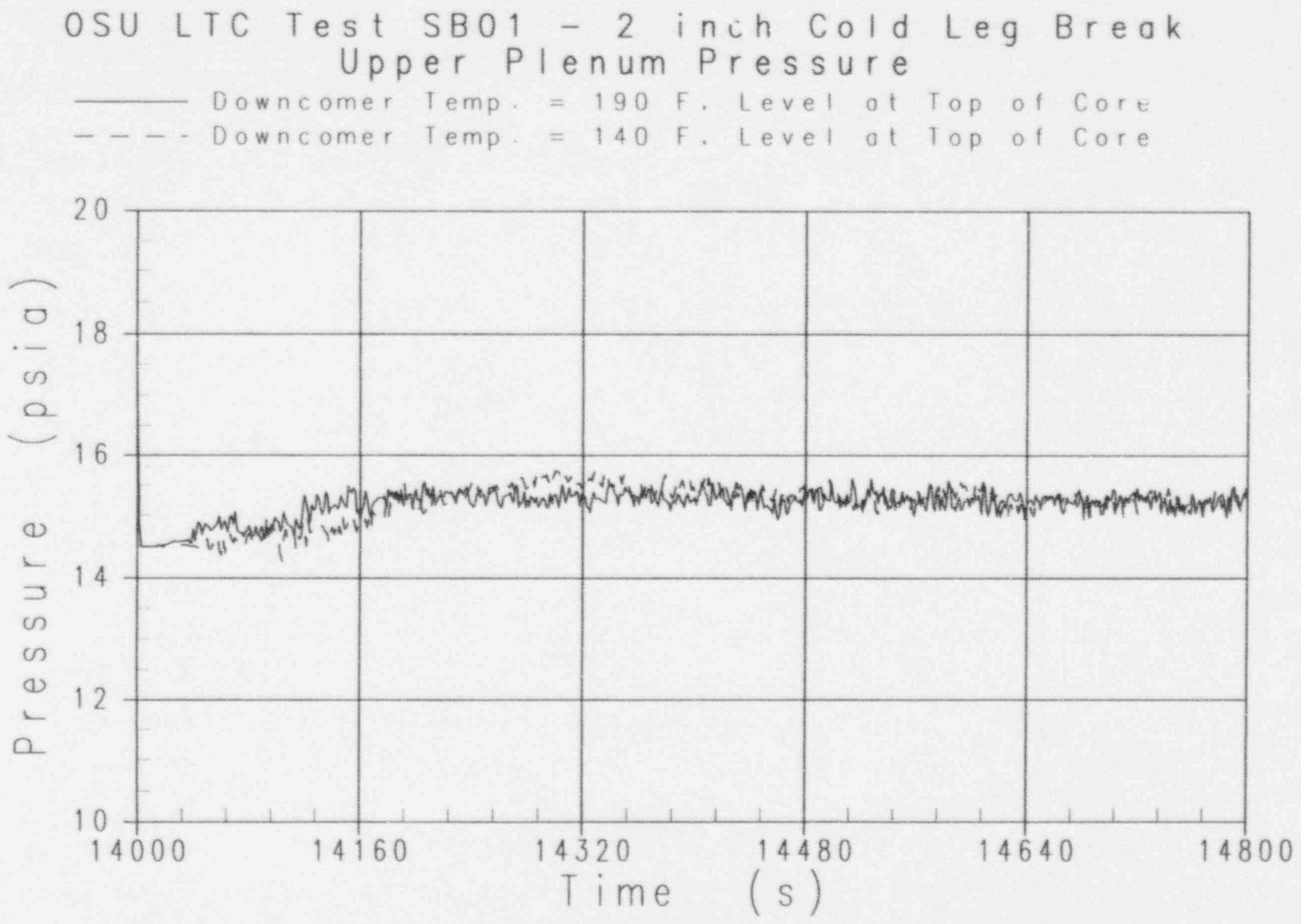
OSU LTC Test SB01 - 2 inch Cold Leg Break
Upper Plenum Pressure
Downcomer Temp. = 190 F. Level at Top of Core
Downcomer Temp. = 140 F. Level at Top of Core
Pressure (psia)
20
18
16
14
12
10
14000
14160
14320
14480
14640
14800
Time (s)

Figure 3 -51

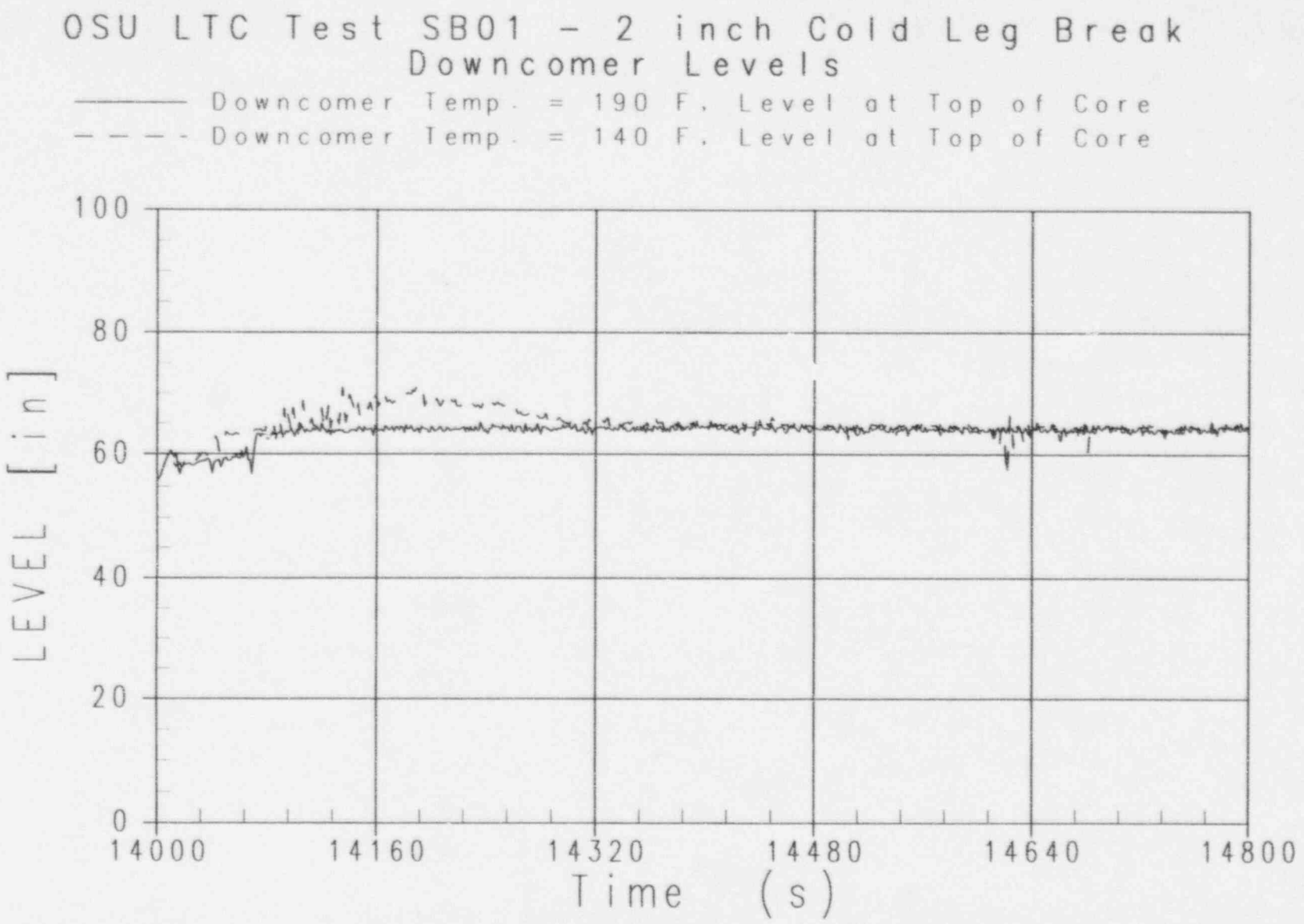
OSU LTC Test SB01 - 2 inch Cold Leg Break
Downcomer Levels
Downcomer Temp. = 190 F, Level at Top of Core
Downcomer Temp. = 140 F, Level at Top of Core
LEVEL [in]
100
80
60
40
20
0
14000
14160
14320
14480
14640
14800
Time (s)

Figure 3 -52

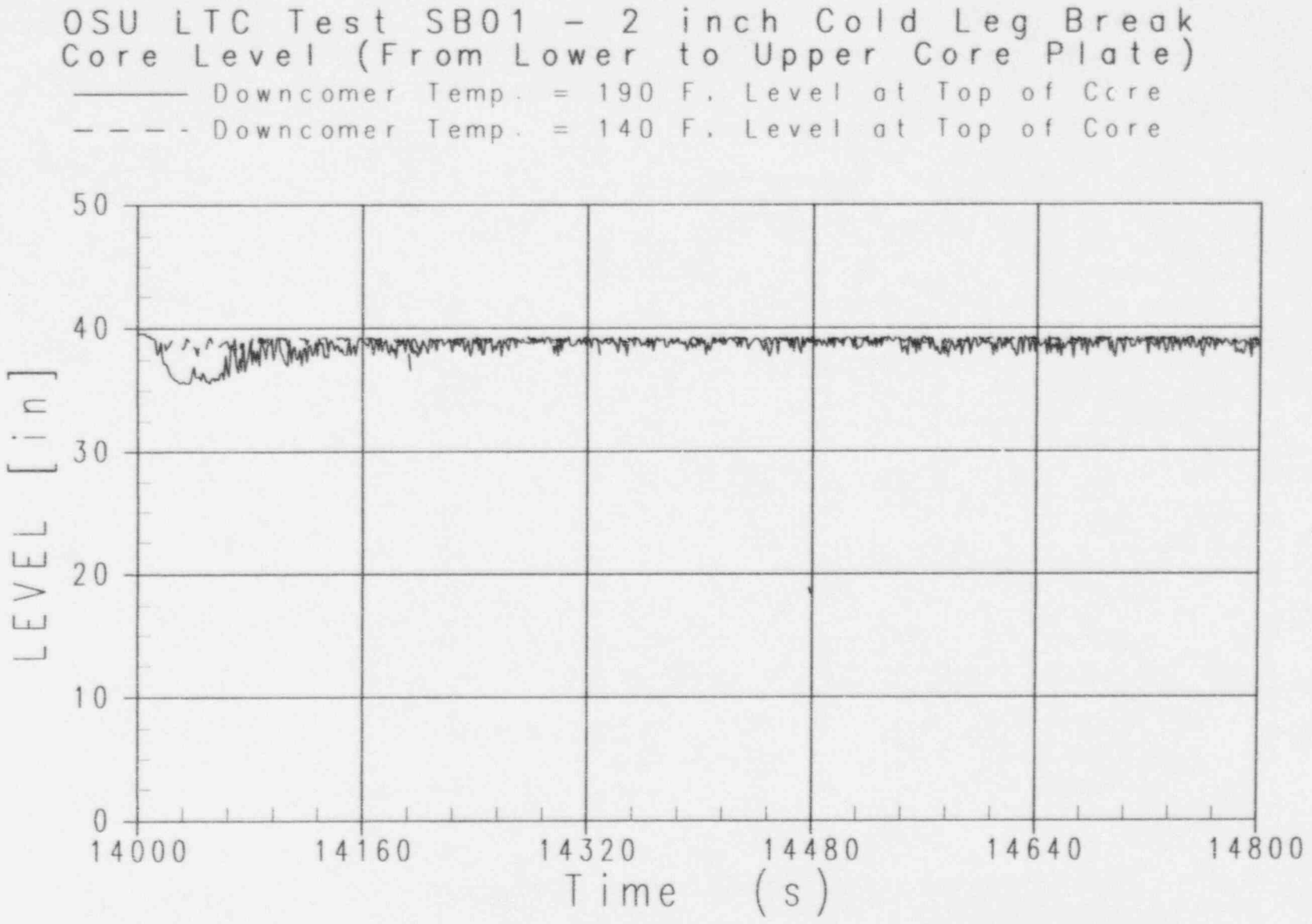
OSU LTC Test SB01 - 2 inch Cold Leg Break
Core Level (From Lower to Upper Core Plate)
Downcomer Temp. = 190 F. Level at Top of Core
Downcomer Temp. = 140 F. Level at Top of Core
LEVEL [in]
50
40
30
20
10
0
14000
14160
14320
14480
14640
14800
Time (s)

Figure 3 -53

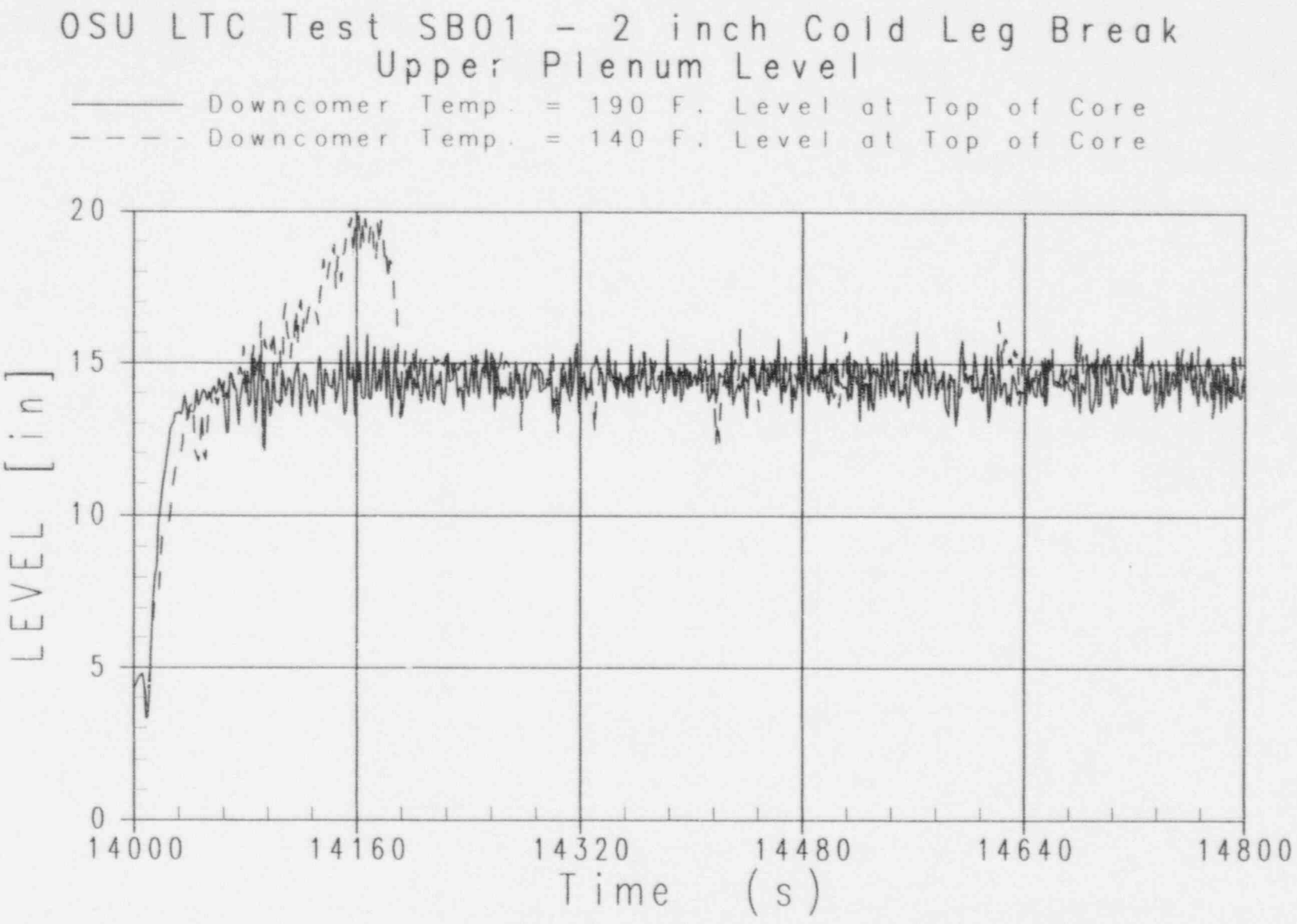
OSU LTC Test SB01 - 2 inch Cold Leg Break
Upper Plenum Level
Downcomer Temp. = 190 F. Level at Top of Core
Downcomer Temp. = 140 F. Level at Top of Core
LEVEL [in]
20
15
10
5
0
14000
14160
14320
14480
14640
14800
Time (s)

Figure 3 -54

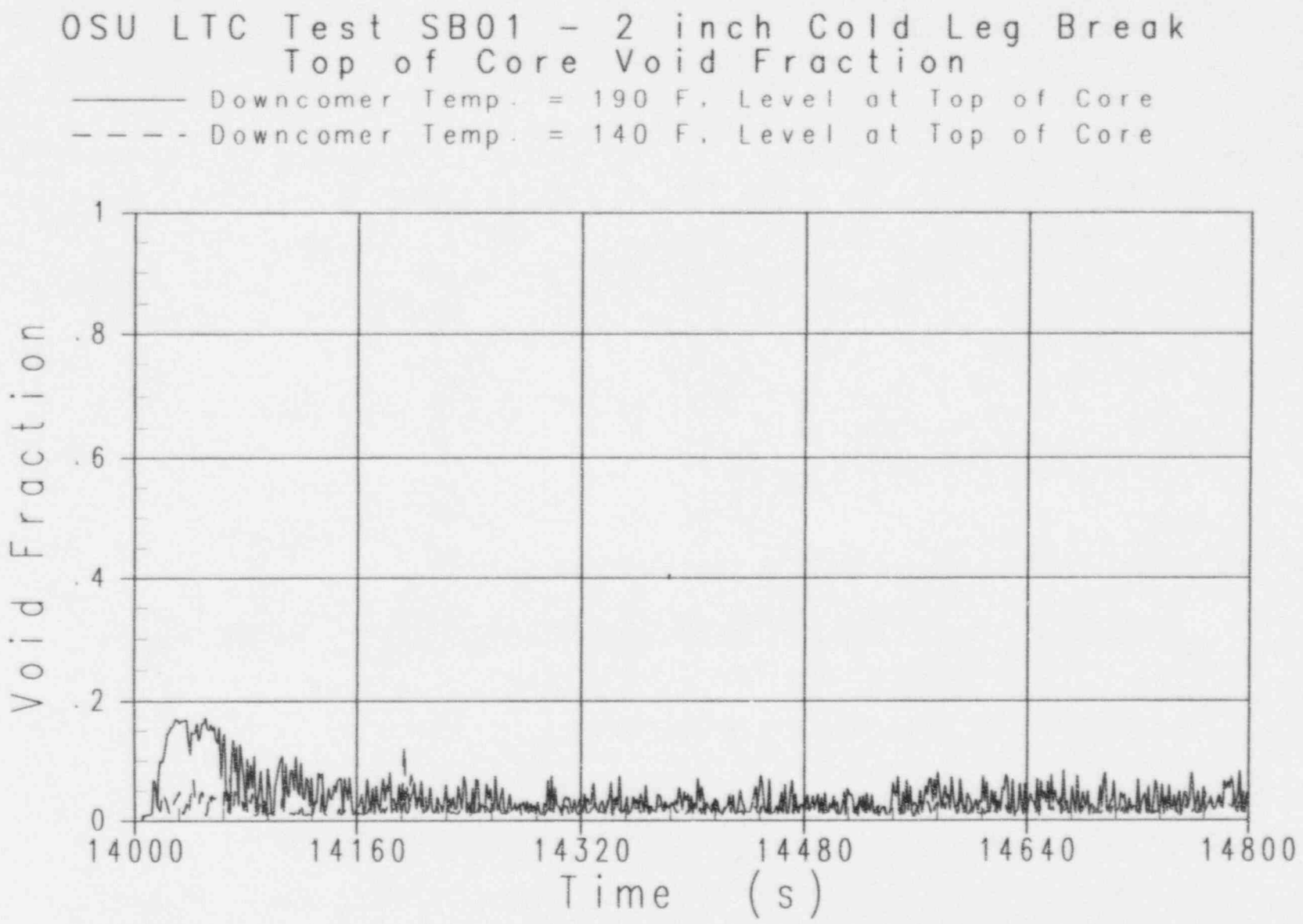
OSU LTC Test SB01 - 2 inch Cold Leg Break
Top of Core Void Fraction
Downcomer Temp. = 190 F. Level at Top of Core
Downcomer Temp. = 140 F. Level at Top of Core
Void Fraction
1
.8
.6
.4
.2
0
14000
14160
14320
14480
14640
14800
Time (s)

Figure 3 -55

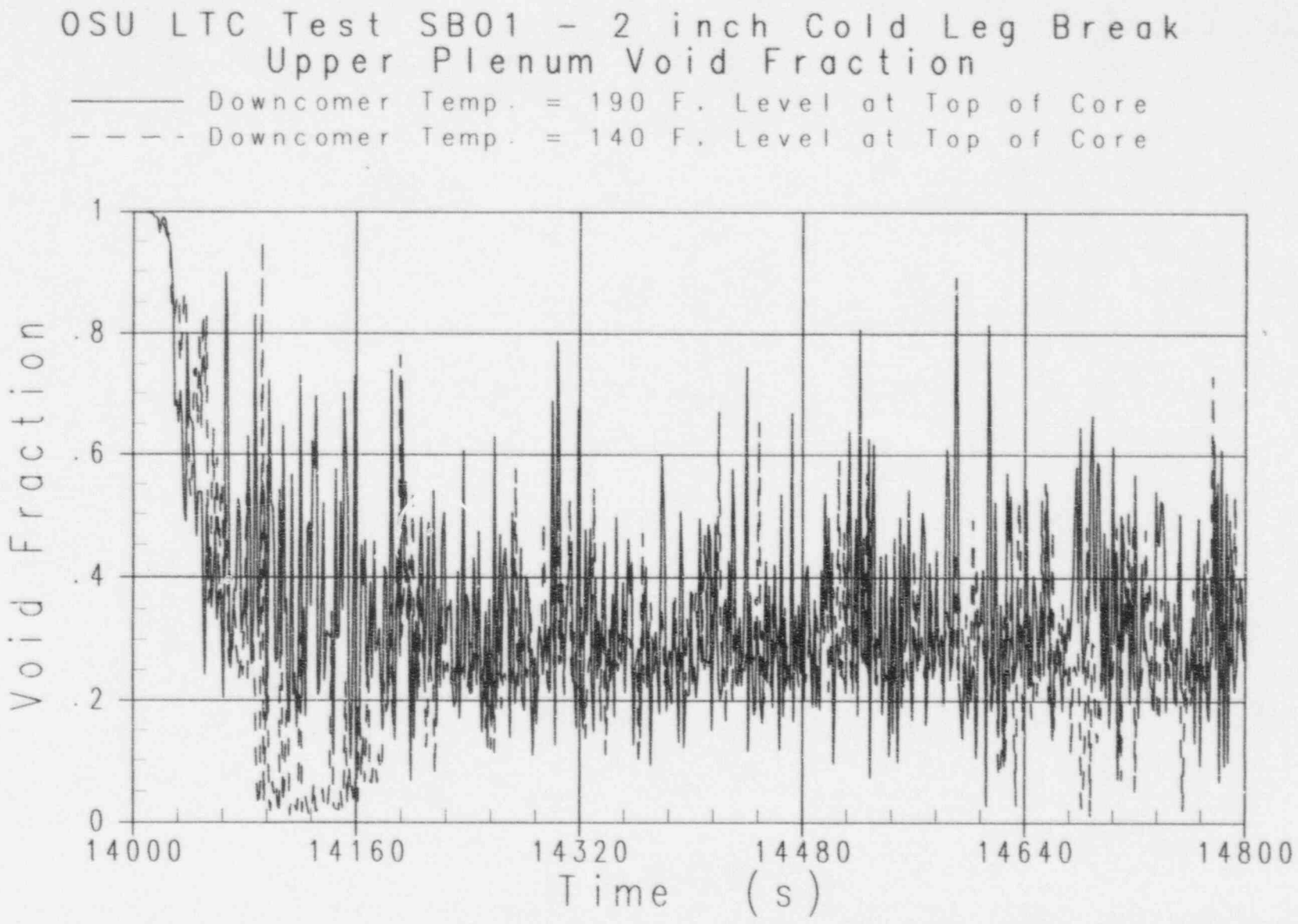
OSU LTC Test SB01 - 2 inch Cold Leg Break
Upper Plenum Void Fraction
Downcomer Temp. = 190 F. Level at Top of Core
Downcomer Temp. = 140 F. Level at Top of Core
Void Fraction
1
.8
.6
.4
.2
0
14000
14160
14320
14480
14640
14800
Time (s)

Figure 3 -56

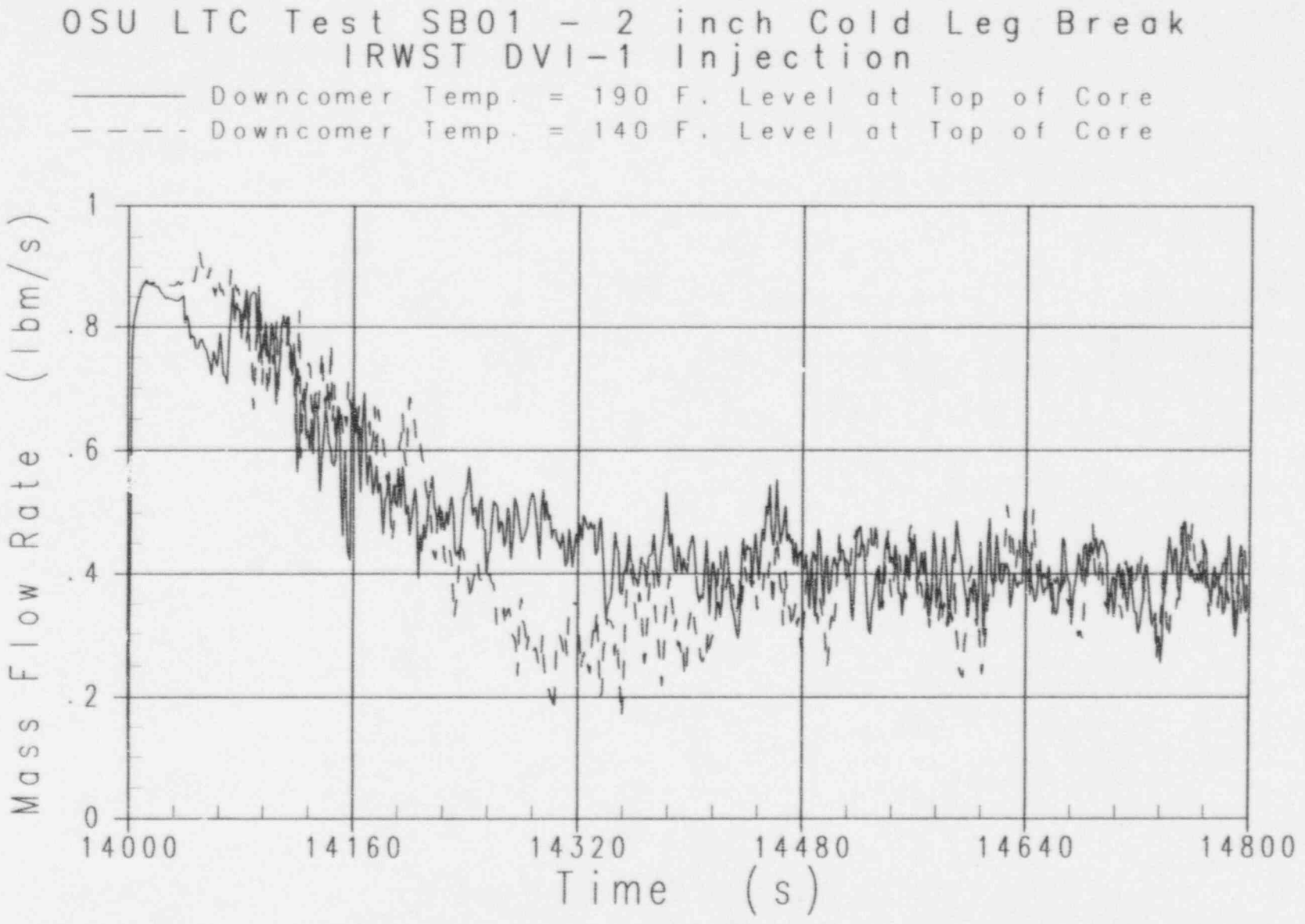
OSU LTC Test SB01 - 2 inch Cold Leg Break
IRWST DVI-1 Injection
Downcomer Temp. = 190 F. Level at Top of Core
Downcomer Temp. = 140 F. Level at Top of Core
Mass Flow Rate (lbm/s)
1
.8
.6
.4
.2
0
14000
14160
14320
14480
14640
14800
Time (s)

Figure 3 -57

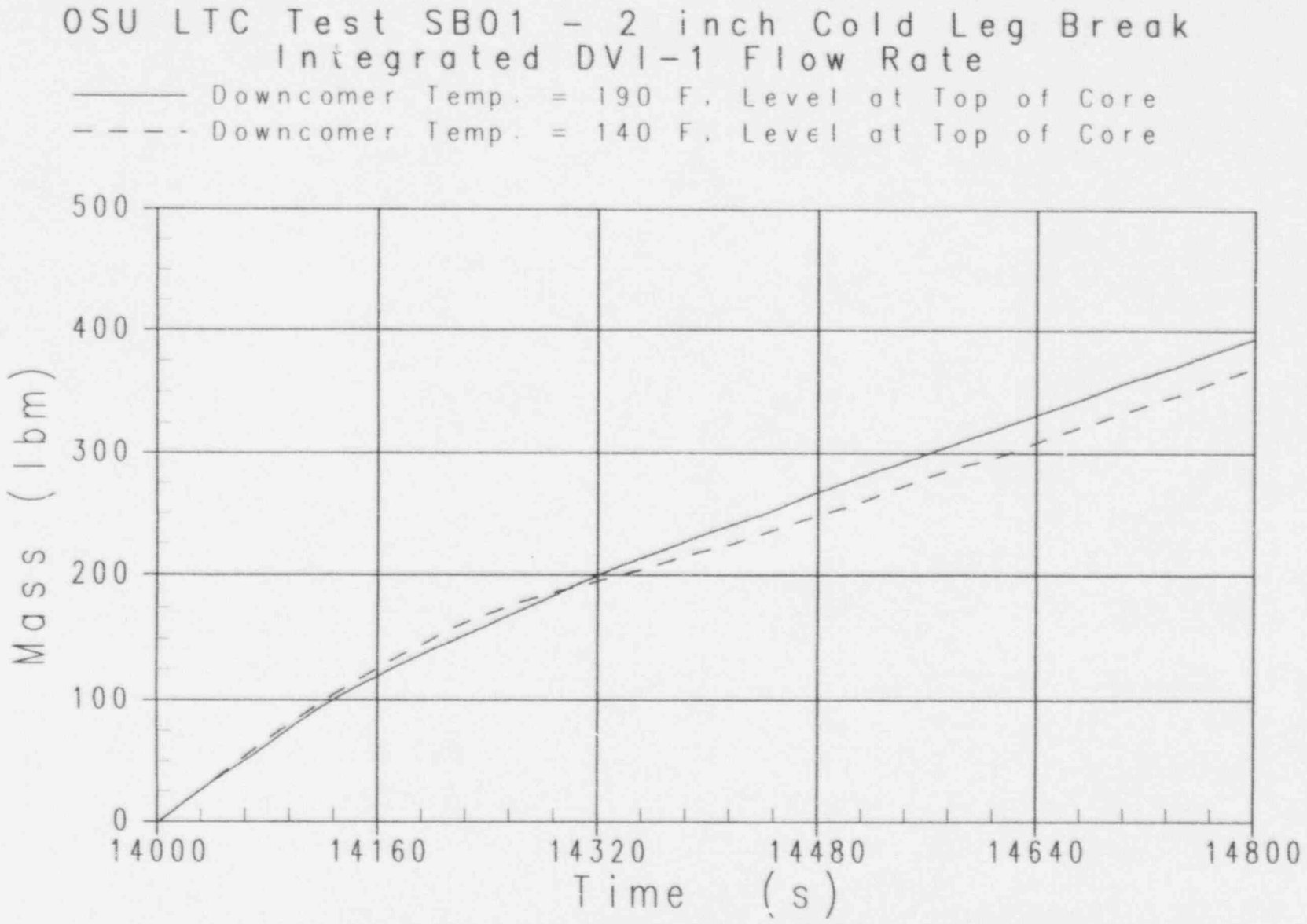
OSU LTC Test SB01 - 2 inch Cold Leg Break
Integrated DVI-1 Flow Rate
Downcomer Temp. = 190 F. Level at Top of Core
Downcomer Temp. = 140 F. Level at Top of Core
Mass (lbm)
500
400
300
200
100
0
14000
14160
14320
14480
14640
14800
Time (s)

Figure 3 -58

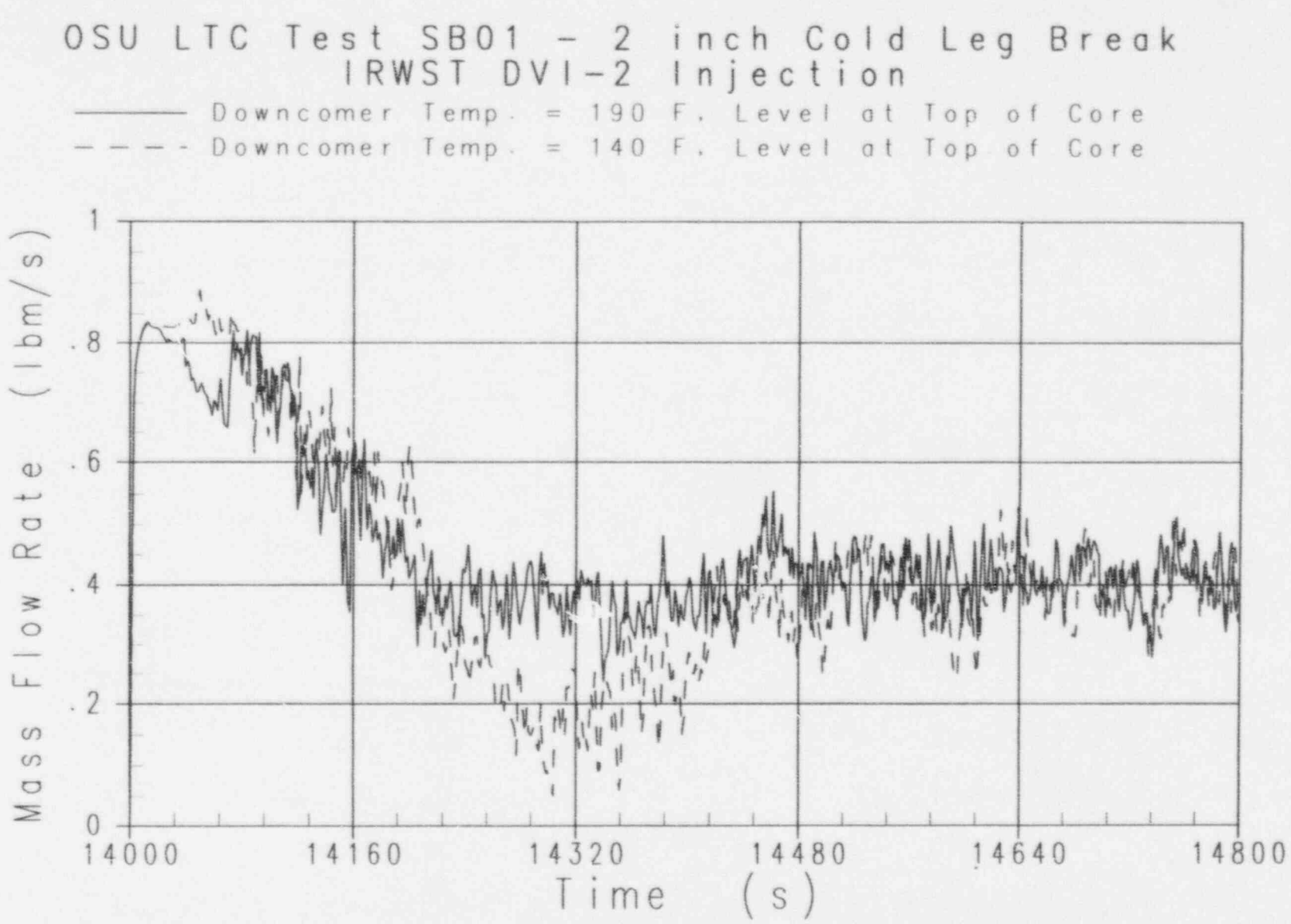
OSU LTC Test SB01 - 2 inch Cold Leg Break
IRWST DVI-2 Injection
Downcomer Temp. = 190 F. Level at Top of Core
Downcomer Temp. = 140 F. Level at Top of Core
Mass Flow Rate (lbm/s)
1
.8
.6
.4
.2
0
14000
14160
14320
14480
14640
14800
Time (s)

Figure 3 -59

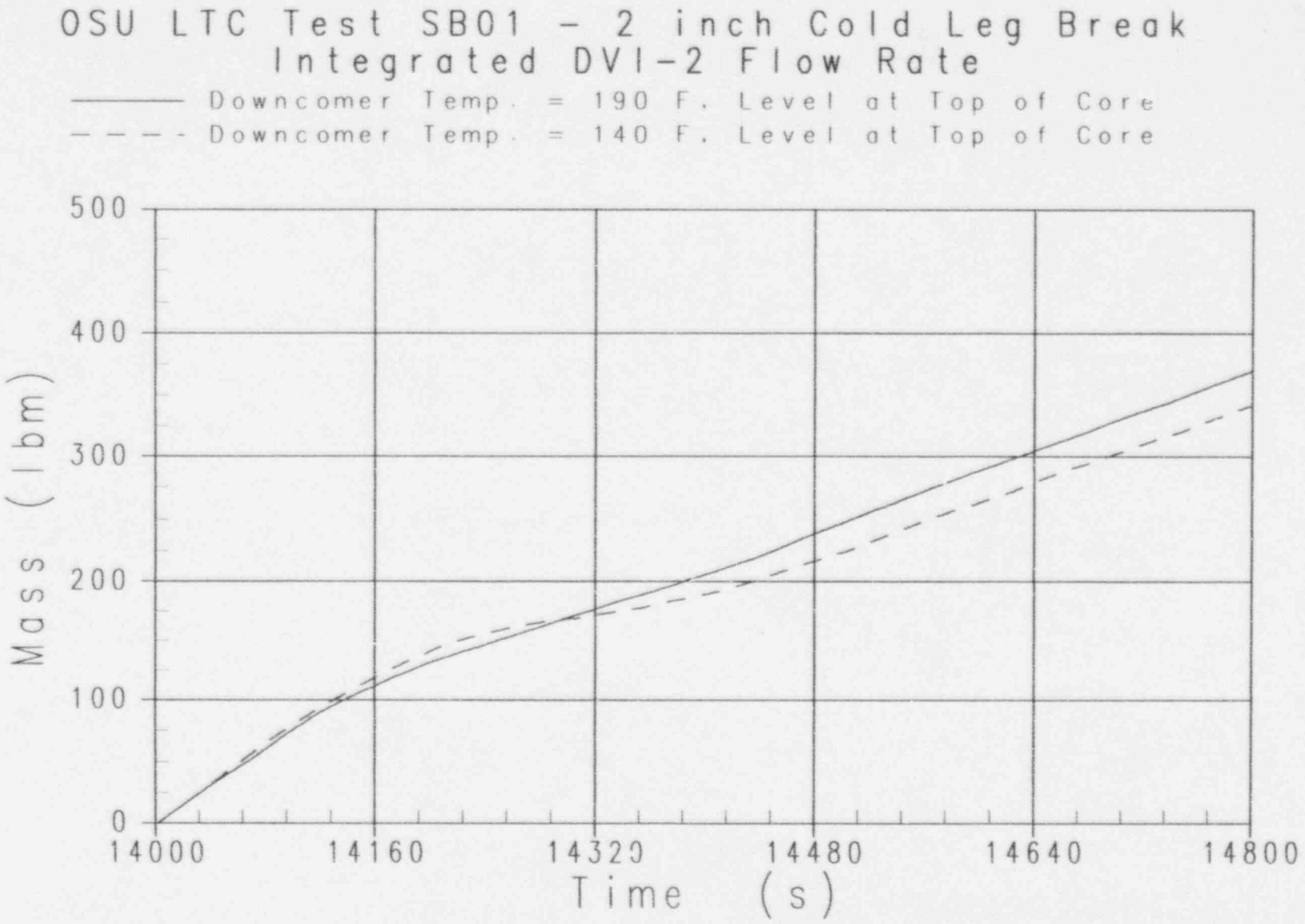
OSU LTC Test SB01 - 2 inch Cold Leg Break
Integrated DVI-2 Flow Rate
Downcomer Temp. = 190 F. Level at Top of Core
Downcomer Temp. = 140 F. Level at Top of Core
Mass (lbm)
500
400
300
200
100
0
14000
14160
14320
14480
14640
14800
Time (s)

Figure 3 -60

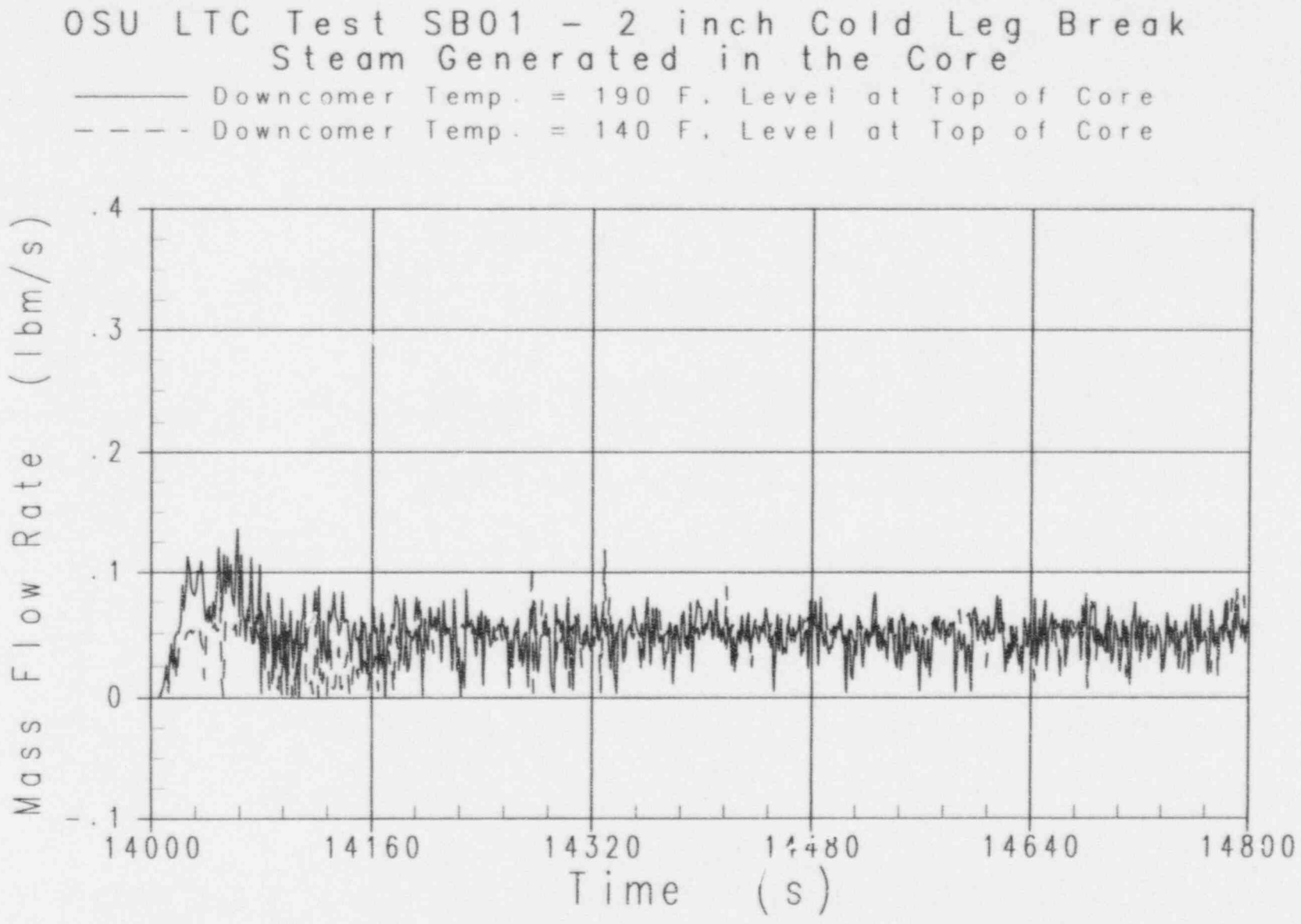
OSU LTC Test SB01 - 2 inch Cold Leg Break
Steam Generated in the Core
Downcomer Temp. = 190 F. Level at Top of Core
Downcomer Temp. = 140 F. Level at Top of Core
Mass Flow Rate (lbm/s)
.4
.3
.2
.1
0
-.1
14000
14160
14320
14480
14640
14800
Time (s)

Figure 3 -61

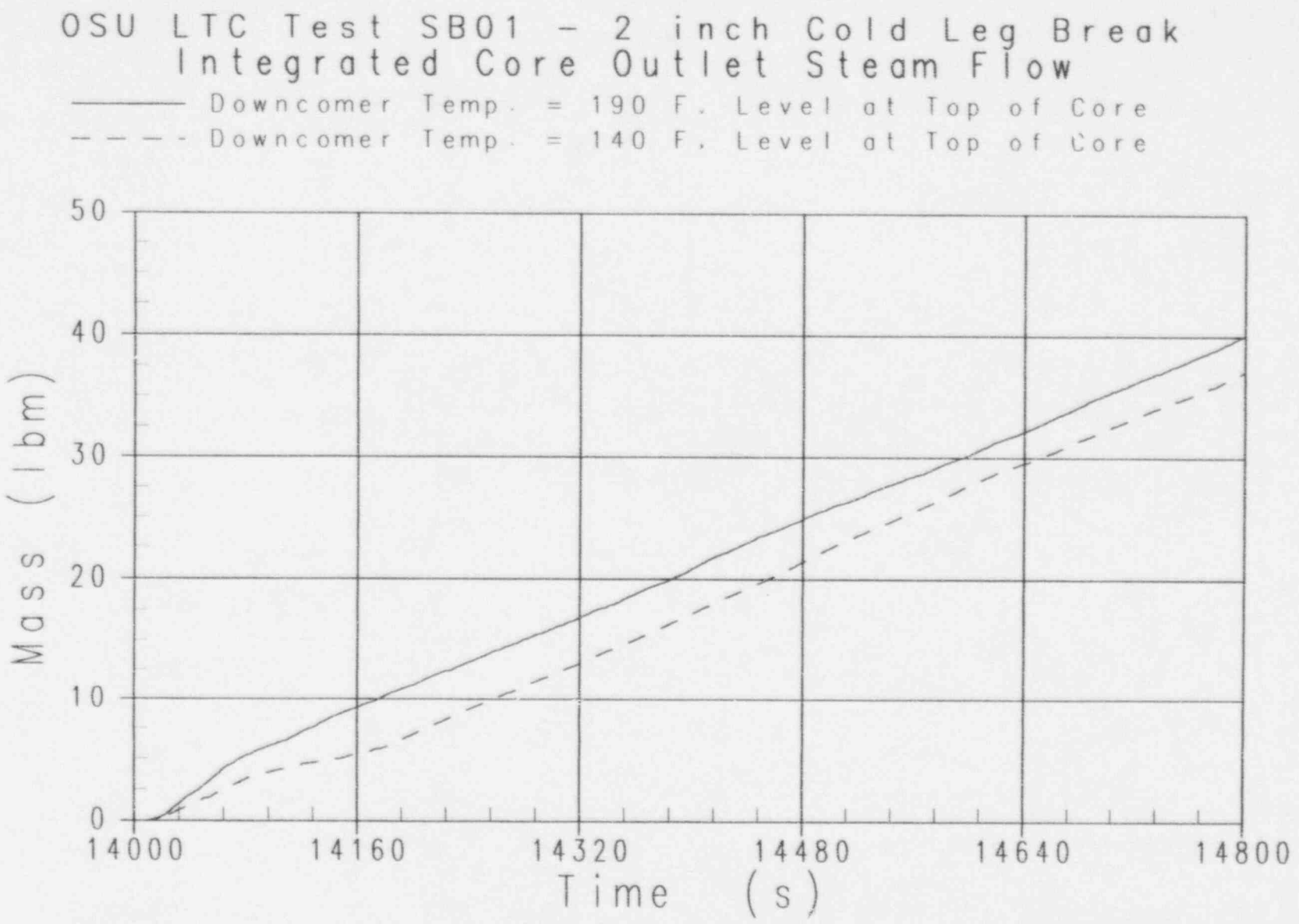
OSU LTC Test SB01 - 2 inch Cold Leg Break
Integrated Core Outlet Steam Flow
Downcomer Temp. = 190 F. Level at Top of Core
Downcomer Temp. = 140 F. Level at Top of Core
Mass (lbm)
50
40
30
20
10
0
14000
14160
14320
14480
14640
14800
Time (s)

Figure 3 -62

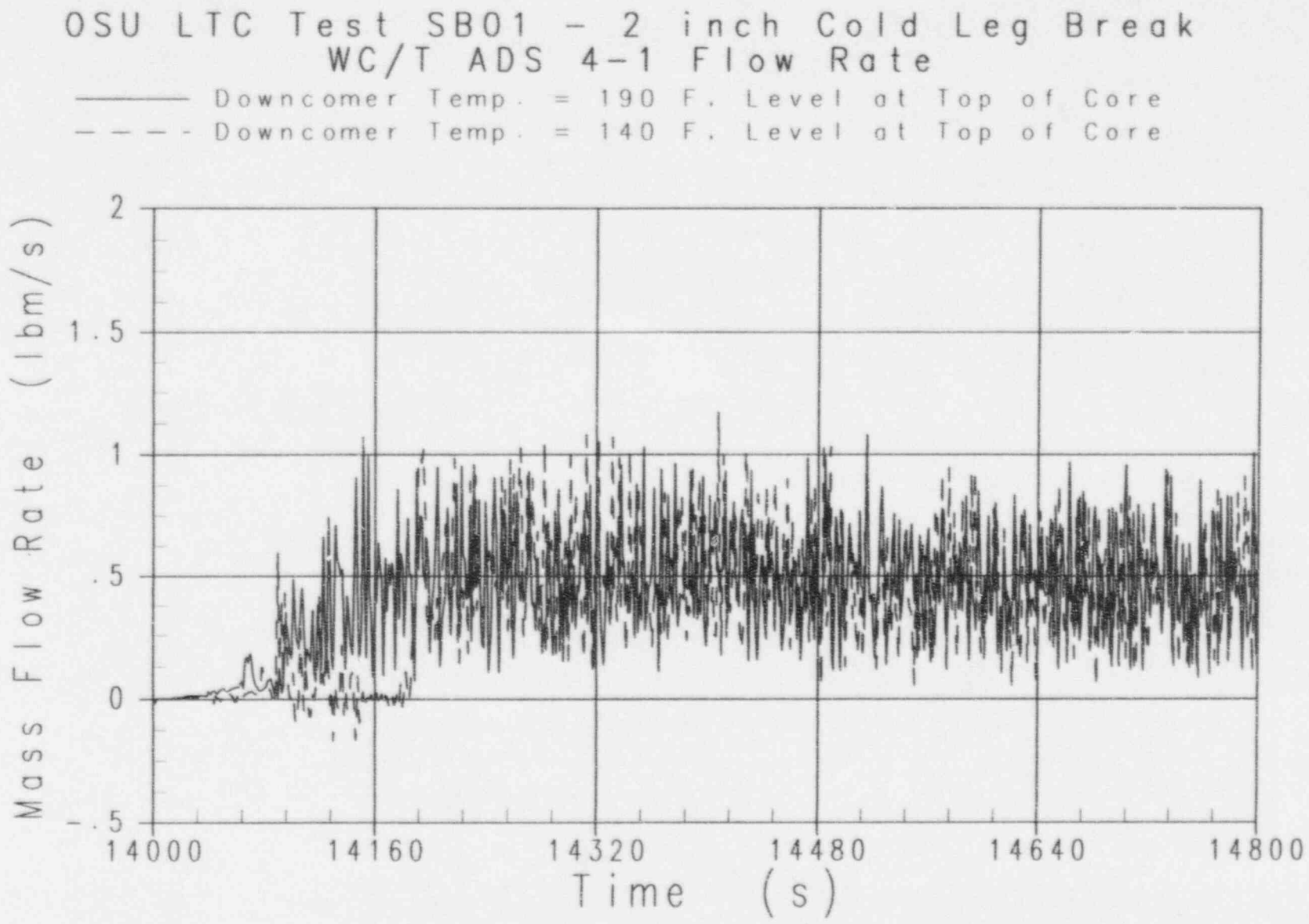
OSU LTC Test SB01 - 2 inch Cold Leg Break
WC/T ADS 4-1 Flow Rate
Downcomer Temp. = 190 F. Level at Top of Core
Downcomer Temp. = 140 F. Level at Top of Core
Mass Flow Rate (lbm/s)
2
1.5
1
.5
0
-.5
14000
14160
14320
14480
14640
14800
Time (s)

Figure 3 -63

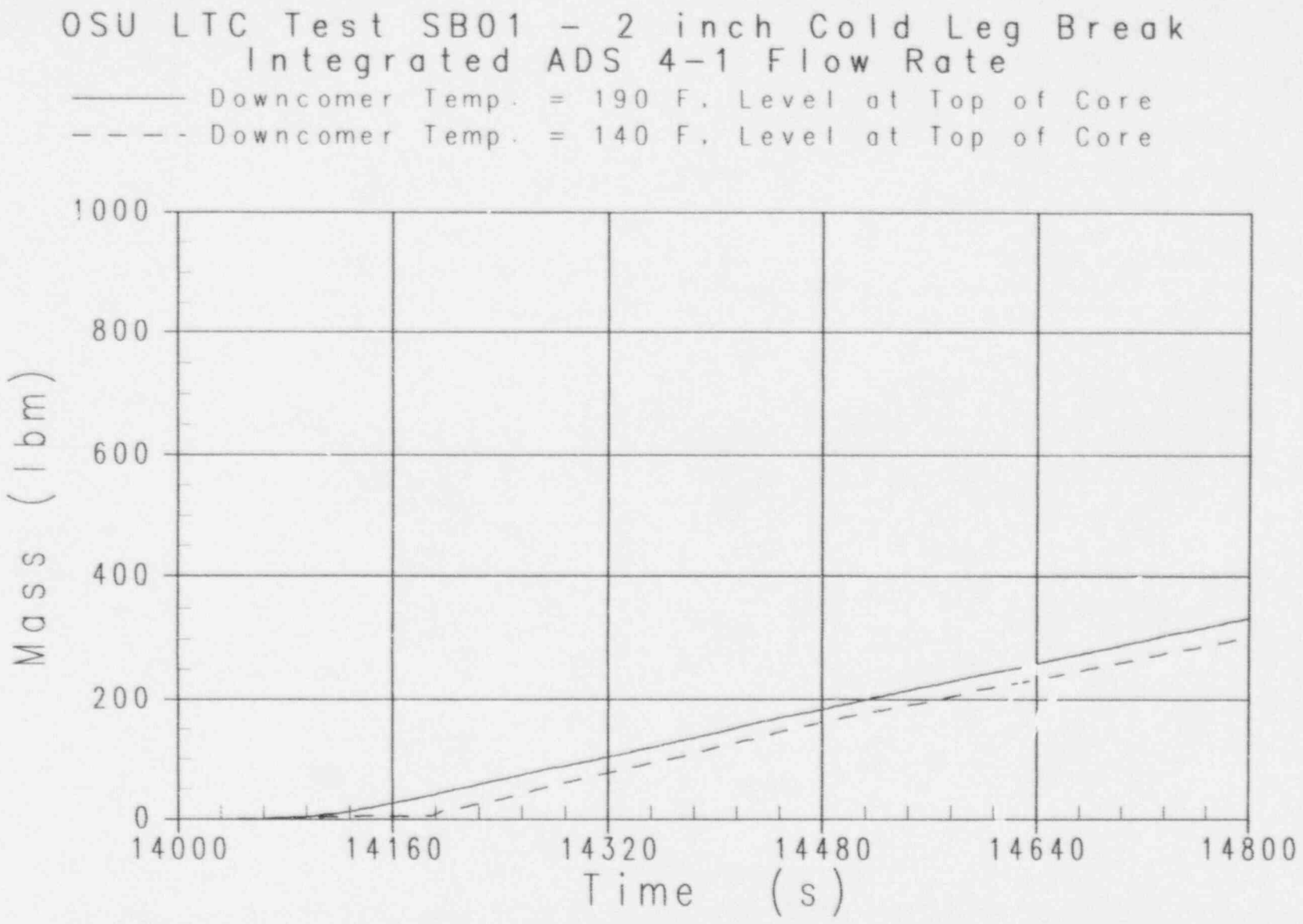
OSU LTC Test SB01 - 2 inch Cold Leg Break
Integrated ADS 4-1 Flow Rate
Downcomer Temp. = 190 F. Level at Top of Core
Downcomer Temp. = 140 F. Level at Top of Core
Mass (lbm)
1000
800
600
400
200
0
14000
14160
14320
14480
14640
14800
Time (s)

Figure 3 -64

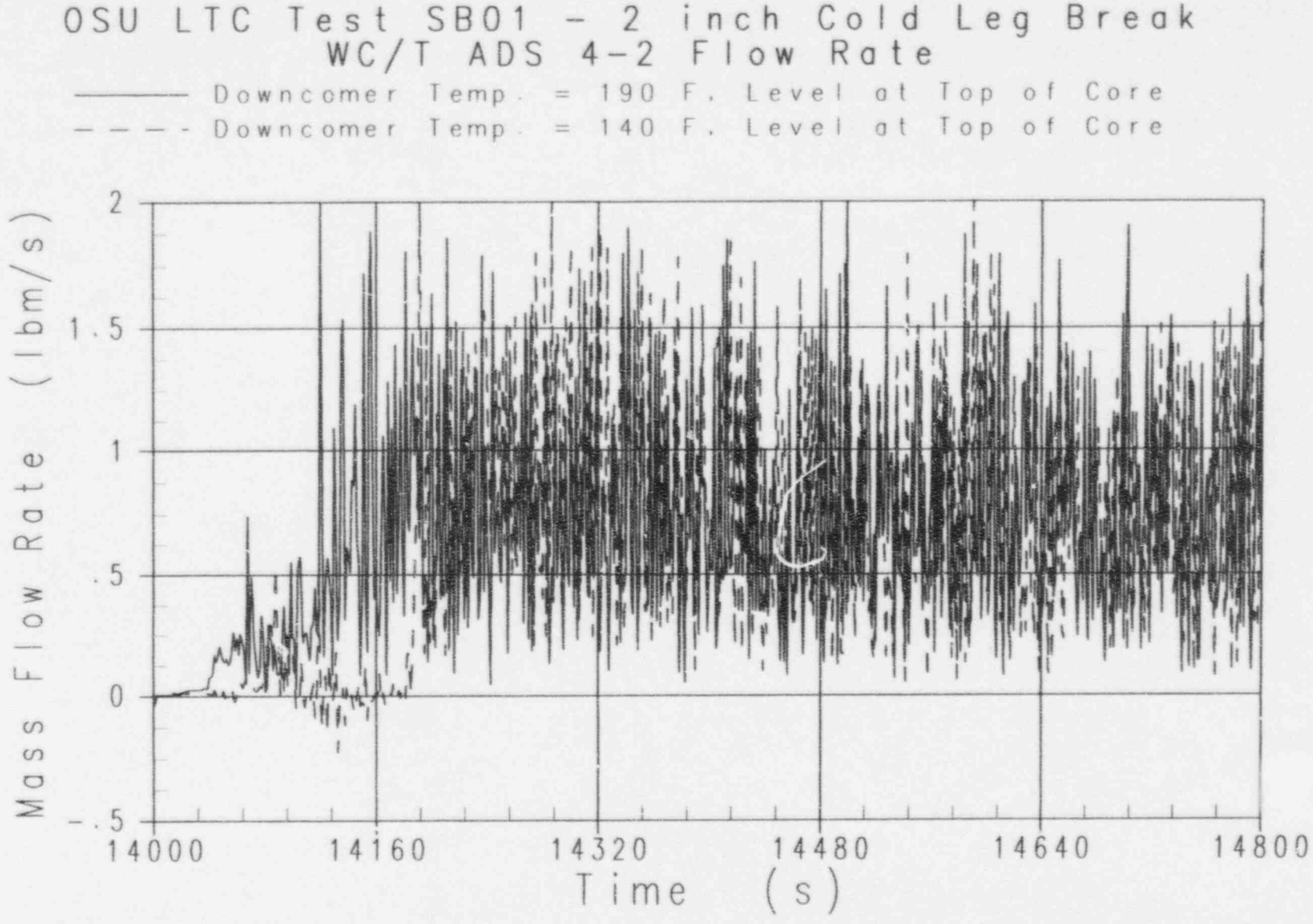
OSU LTC Test SB01 - 2 inch Cold Leg Break
WC/T ADS 4-2 Flow Rate
Downcomer Temp. = 190 F. Level at Top of Core
Downcomer Temp. = 140 F. Level at Top of Core
Mass Flow Rate (lbm/s)
2
1.5
1
.5
0
-.5
14000
14160
14320
14480
14640
14800
Time (s)

Figure 3 -65

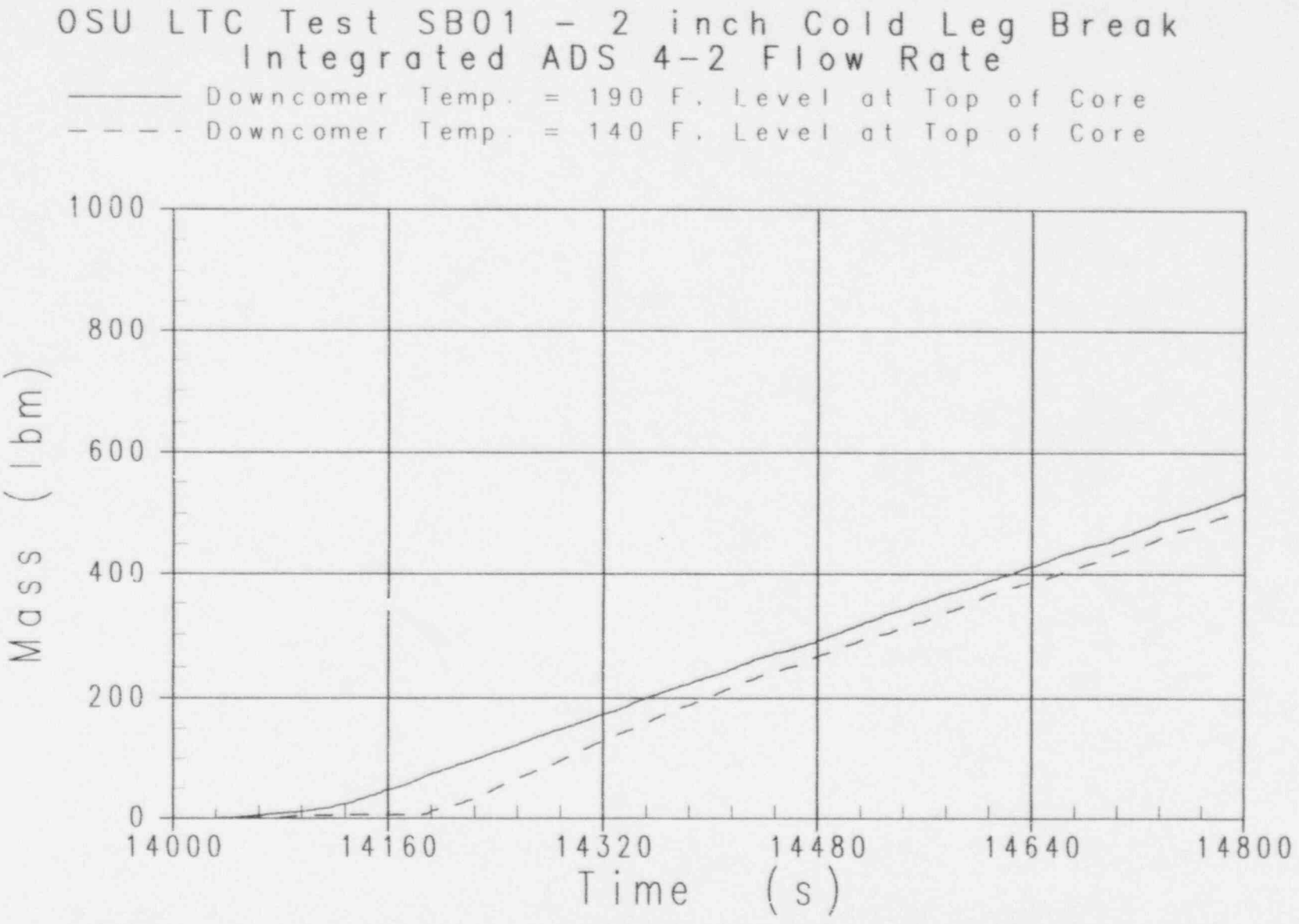
OSU LTC Test SB01 - 2 inch Cold Leg Break
Integrated ADS 4-2 Flow Rate
Downcomer Temp. = 190 F. Level at Top of Core
Downcomer Temp. = 140 F. Level at Top of Core
Mass (lbm)
1000
800
600
400
200
0
14000
14160
14320
14480
14640
14800
Time (s)

Figure 3 -66

4.0 MODEL IMPROVEMENTS ADDED TO WCOBRA/TRAC

This section describes the various code modifications made to the NRC-approved MOD7A version of WCOBRA/TRAC for AP600. Most of the MOD7A code modifications represent new model options implemented for AP600 loss-of-coolant accident (LOCA) analysis applications. References 4-1 and 4-2 describe the MOD7A code version.

4.1 Check Valve Option, Type 6

The MOD7A code has five valve-type options for the VALVE component. These options are described in Section 9.7 of Reference 4-1. Type 5 is used for check valve operation.

In the original subroutine, a specified ramp opens or closes the valve, taking several hundred time steps. Under certain circumstances, the valve stays partially open and allows flow in both directions.

A Type 6 check valve has been added to the WCOBRA/TRAC code. The Type 6 valve is either fully opened or fully closed in one time step. The check valve opens when the pressure gradient across the valve reaches a user-specified value and closes when the pressure gradient is less than the specified value, or when reverse flow is detected.

4.2 PIPE One-Dimensional Component Model Changes

The following changes made to the TRAC PIPE logics improve the modeling capability. User inputs control the options that apply to the following modifications.

4.2.1 Condensation Blocking

Standard code logic condenses steam entering a computational cell using an interfacial heat transfer correlation until the liquid in the cell reaches saturation temperature. The code also allows steam to penetrate into cells below this cell and cause increased condensation. In a water-filled core makeup tank (CMT), significant interfacial condensation occurs only near the steam distributor. Therefore, an option has been added to block interfacial condensation due to liquid subcooling in a user-specified range of cells within selected PIPE components. The top CMT cell size should be chosen for each geometry based on the zone where steam mixing is expected to occur.

4.2.2 Level Sharpening

The level sharpening logic, as discussed in Section 9.6 of Reference 4-1 and used in the TRAC PD-2 PRIZER (pressurizer) component, was added as an option to the PIPE component. This feature forces the vapor and liquid to separate so that a more distinct liquid level is calculated.

The level sharpening model applies to a range of user-specified cells within the PIPE component.

4.2.3 Wall Condensation

As reported in subsection 6.3.10 of Reference 4-1, the TRAC one-dimensional component standard direct wall condensation is calculated as the maximum of a free-convection coefficient using the McAdams correlation or the Dittus-Boelter correlation corrected by a multiplier linear with quality that goes to zero at quality equal to 0.71. It applies only for vapor fractions greater than 0.05 and quality greater than 0.71. Further condensation results from convective heat transfer from the liquid phase followed by interfacial condensation. These convective heat transfer coefficients underestimate wall condensation effects for low-velocity steam, as observed in Reference 4-3. This underestimation is addressed by providing an optional user-defined wall condensation heat transfer coefficient, which is internally multiplied by the vapor fraction. For CMT applications, a value of [ ]^{a,c} is recommended, based on the heat transfer analysis in Reference 4-4.

4.2.4 Level Trip Signal Generation

While the original TRIP subroutine in WCOBRA/TRAC adequately models pressurizer (PRIZER one-dimensional component) setpoints, it is unable to use the trip points with the PIPE one-dimensional components. For example, the original TRIP subroutine could not handle CMT level setpoints that trigger automatic depressurization system (ADS) valve operation. A new subroutine (PIPE1X) was added that calculates PIPE component water level for inclined pipes to allow PIPE component water level trip signal generation. The generated signal is passed to the existing logic and processed so that response actions can be taken via the TRIP and TRIPSET subroutines. The user can select this modification for each PIPE component.

4.3 Small-Break LOCA Break Model

A modification to the TRAC-PF1/MOD1 critical flow model, discussed in subsection 4.8.2 of Reference 4-1, has been implemented. Generally, AP600 test facilities use orifices of small relative flow area to simulate small breaks. The TRAC-PF1/MOD1 critical flow model assumes the piping layout geometry is preserved by the input noding development. For example, if a piping layout includes an orifice, a separate cell is used to preserve the geometry of the orifice (length, hydraulic diameter, flow area, and the like) In this example, donor cell properties used by the break model are governed by code-calculated conditions inside the orifice, which may be completely different from the upstream pipe conditions. This is especially true for small orifices. In this example, uncertainty in evaluations of orifice local conditions could dominate the choked flow solution. The new model uses the upstream conditions in the pipe to evaluate critical velocity. To preserve the application of the Alamgir, Lienhard, and Jones nucleation delay correlation used in the subcooled critical flow model (Reference 4-1, Equations 4-272 and 4-273), the U_{le} and ΔX terms are scaled from the upstream values to the orifice geometry as follows:

$$U_{le} = (U_{le} \text{ as previously defined in Reference 4-1})/CHM$$

and

$$\Delta X = (\Delta X \text{ as previously defined in Reference 4-1})/(CHM)^{1/2}$$

where:

discharge multiplier, CHM = Cd * (flow area orifice/flow area pipe)

and

Cd = orifice entrance contraction coefficient

CHM is a user-defined term. In MOD7A, ΔX is the length of cell where critical flow is calculated. In small-break LOCA applications where the critical flow occurs in the orifice, ΔX should equal orifice thickness; however, because orifice geometry is not explicitly preserved in one-dimensional component input, the above scaling is performed in conjunction with the following input specification process, preserving the Alamgir, Lienhard, and Jones nucleation delay correlation:

$$\text{Cell length (DX) of the orifice cell} = \text{Hydraulic diameter } (HD)_{pipe} * (L/D)_{orifice}$$
$$\text{Flow area (FA) of the orifice cell} = \text{Flow area } (FA)_{pipe}$$
$$\text{Hydraulic diameter (HD) of the orifice cell} = (HD)_{pipe}$$
$$\text{Volume (VOL) of the orifice cell} = (FA)_{pipe} * DX$$

The above three specifications (DX, VOL, FA) will additionally satisfy the choked flow package, specifying that A_e/A_c be less than 1.01. In this ratio, A_e is the cell area calculated as VOL/DX. Using this approach, Reference 4-1, Equation 4-25, which evaluates the L/D of the adjacent donor cell, is consistent with the geometry of the orifice.

The above input specification (DX, FA, VOL, HD) for the orifice cell must be rigorously preserved in applications where subcooled discharge is expected (void fraction less than 0.1), because the subcooled Alamgir, Lienhard, and Jones nucleation delay correlation represents the local orifice condition dependence.

In application, critical velocity based on upstream pipe conditions is calculated using the existing model. Scaled critical velocity is then calculated as critical velocity multiplied by the CHM multiplier. Finally, the momentum equation velocity solution is limited to scaled critical velocity. Note that this modeling is not activated in the Oregon State University (OSU) long-term cooling (LTC) calculations herein because critical flow does not occur.

4.4 Time-Dependent Choked Flow Multipliers Model

This model is an extension of the small-break LOCA model described in the previous subsection. In certain applications, break flow area may depend not only on orifice geometry but on time. An option has been added to the code that allows the user to supplement the total break flow area multiplier with a time-dependent fractional flow area multiplier. The model is initiated in a single user-specified one-dimensional component when trip number 200 is activated. This model can only be used in conjunction with the small-break LOCA model (that is, when IBRKMOD is specified non-zero). An example of this application is a noding that puts the Stages 1 through 3 of the ADS into a single one-dimensional component. The time-dependent multiplier array models the sequential time-dependent opening of each stage of ADS when the CMT low-level trip is activated.

4.5 VALVE Component Choke Flow Model

Hydraulic choking is computed using input data in most TRAC one-dimensional components, such as PIPE and TEE. Originally, MOD7A code choking capability did not exist for VALVE components; however, for primary AP600 valves (such as ADS and check valves), a valve choking simulation is necessary. Therefore, the code was extended to include choking capability for the VALVE component. The extension is coded the same way that PIPE component choking is coded, as described in subsection 4.8.2 of Reference 4-1. Potential VALVE component choking locations are specified by input the same way that the PIPE component choking locations are specified. No such locations are specified in the OSU LTC simulations.

4.6 User-Specified One-Dimensional PIPE Wall Area

In the MOD7A code, the PIPE inside wall area is determined from an internal calculation based on user-specified values for cell length and volume. To make the code more flexible for complex geometries and noding applications, an added option allows the user to directly specify a cell inside-wall area that overwrites the code internal calculation. Such input flexibility is already included in the STGEN 1-D component. This option is not employed in the OSU test simulations.

4.7 One-Dimensional Component Improved Mass Conservation

Mass conservation can be violated in the one-dimensional WCOBRA/TRAC components when pure liquid slowly injects into a vapor region. More specifically, the donor velocity could reverse at every time step. The donor node is determined at the beginning of a time step, while the velocity is computed opposite to it within the same time step. Consequently, the mass convected from one cell is deposited into the same cell and the mass increases. To solve this problem, when slow liquid injection into a large tank takes place, the relative velocity was set equal to zero. This stabilizes the computation. As a result, the mass increase is reduced by a factor of 30. This code update was not used in the WCOBRA/TRAC simulations of OSU tests.

4.8 References

4-1. Bajorek, S. M., Hochreiter, L. E., Young, M. Y., Dederer, S. I., Nissley, M. E., Tsai, C. K., Yeh, H. C., Chow, S. K., Takeuchi, K., Cunningham, J. P., and Stucker, D. L., WCAP-12945P, Vols. 1-5, *Code Qualification Document for Best Estimate LOCA Analysis*, June 1992.

4-2. NTD-NSD-MYY-94-65, *Submittal U*, MOD7A Code Version, S. Bajorek (W) to C. Fineman (INEL), November 11, 1994.

4-3. Collier, J. G., *Convective Boiling and Condensation*, First Edition, McGraw-Hill Inc., New York, 1972, pp. 315.

4-4. Cunningham, J. P., Haberstroh, R. C., Hochreiter, L. E., and Wright, R. F., WCAP-14215, *AP600 Core Makeup Tank Test Analysis*, December 1994.

5.0 OSU TEST DATA COMPARISONS WITH WCOBRA/TRAC CALCULATIONS

To demonstrate the adequacy of WCOBRA/TRAC to perform long-term cooling (LTC) analysis for the AP600 plant, a set of calculations was performed with WCOBRA/TRAC and compared to the Oregon State University (OSU) test data. The window-mode approach was used with the time periods selected just prior to, during, or immediately following the switchover from in-containment refueling water storage tank (IRWST) injection to sump injection. Calculations were performed for 1000 seconds in each case, with approximately the first 400 seconds defined as the initialization period that was required to transition from the vessel initial conditions to a quasi-equilibrium condition that would compare to the test data. The remaining 600 seconds showed a quasi-steady-state condition that could be compared to the measured data. To show a representative selection of small breaks, calculations and test data comparisons were performed for the following four tests:

- SB01 - 2-inch Cold Leg (CL) Break
- SB10 - Balance Line Break
- SB12 - Direct Vessel Injection (DVI) Line Break
- SB23 - 1/2-inch Cold Leg Break

In each of the calculations, the boundary conditions appropriate to that time period were established from the test data. The boundary conditions included:

- IRWST level, temperature, and pressure
- Sump level, temperature, and pressure
- Steam generator secondary-side conditions
- Core makeup tank (CMT) level and temperature
- Break separator level, temperature, and pressure
- Core decay heat level

Initial conditions, typically within the vessel, are those that do not influence the quasi-equilibrium state. In these calculations, the following initial conditions were identified:

- Vessel initial fluid levels in downcomer, core, and upper plenum
- Vessel initial fluid temperatures in downcomer, core, and upper plenum
- Initial vessel and internals metal temperatures
- Heater rod temperatures
- Initial system pressure

Initial conditions within the vessel were selected either from conditions observed during the test at the start of IRWST flow or in a fashion that was conservative for the particular parameter. Specifically, the downcomer fluid temperature was set at the test value observed at the start of IRWST flow. In all cases this value was above the values observed subsequently during the tests and was considered an upper bound temperature. The core liquid and heater rod temperatures were set slightly below

saturation temperature at the test pressure, primarily to minimize liquid level perturbations at the start of the calculations. The vessel collapsed liquid level was set at the top of the core in all calculations. This level is below the levels observed in the test data and results in high DVI line flows until the proper vessel level is achieved. Consistent with the vessel collapsed liquid level, no liquid is assumed in the loops, pressurizer, surge line, steam generator (primary side), or reactor coolant pumps. As shown in Section 3, this assumption does not impact the results since these effects persist for typically less than 400 seconds into the calculation.

For all tests except SB01, the CMTs were empty during the periods of calculational comparisons. In the case of SB01, both CMTs contained liquid during the period of interest; however, only CMT-2 was discharging a significant amount, approximately 0.1 lbm/sec during the post-initialization phase. Because the CMT behavior during this period would not occur in the plant, as verified in Reference 5-1, the CMT flow was treated as a boundary condition in SB01 with the mean of the test flow rate input to the calculation.

Break location and geometry were adjusted as appropriate for each test while other facility parameters, such as geometry and hydraulic line resistances, were held constant for all comparisons.

Of the four calculations performed, two showed good comparison with the test data: SB10 and SB23. Of the other two, the SB01 calculation predicted a more rapid draindown of the IRWST than indicated by the data, while the SB12 calculation predicted a slower draindown than indicated by the data. In all cases, however, the core and upper plenum levels were predicted accurately and the core remained covered as indicated by the test data.

5.1 Long-Term Cooling Calculation – SB01

This section compares the test results and the WCOBRA/TRAC simulations for the LTC period of the 2-in. cold leg break transient (test SB01) at the initiation of the sump injection phase.

The window-mode approach was employed to analyze the sump injection part of the SB01 test. The basis of this approach is described in Section 3. The modeling of the OSU facility for the window mode is the same as described in Section 3, but with simplifications that reduce the amount of computation and avoid excessively small time steps. For example, during the sump injection part of the tests, the passive residual heat removal heat exchanger (PRHR HX) tubes contained water, but there was no significant flow into or out of the PRHR HX. Also, during this period, the accumulators were fully discharged. Consequently, the PRHR HX and accumulators were not modeled in the simulations. The sump injection began when the IRWST reached the appropriate level to allow opening of the check valves. The automatic depressurization system Stages 1 through 3 (ADS1–3) valves discharged into the containment rather than into the IRWST, and the IRWST was represented as a simple tank by a WCOBRA/TRAC pipe component. Since the IRWST was nearly empty, there was no significant heat transfer to the secondary side of the PRHR HX; this was an additional justification for not modeling the PRHR HX.

In this test, CMT-2 delivers a significant volume of fluid during the period of WCOBRA/TRAC simulation, while CMT-1 shows no significant draining during this period. Both CMTs empty at approximately 1500 seconds after the start of sump injection. Thus, the CMT-2 draining was modeled in the simulation. Because the CMT behavior during this period would not occur in the plant, as verified in Reference 5-1, the CMT flow was treated as a boundary condition with the mean of the test flow rate input to the calculation. During the quasi-equilibrium portion of the calculation, the CMT-2 discharge rate was [ ]^{a,b,c} lbm/sec.

The SB01 test was simulated for the time period of 14,000 to 15,000 seconds. The primary sump injection began through the check valves at approximately 14,200 seconds. As discussed in Section 3, the objective of the window-mode approach was to obtain quasi-equilibrium conditions that represented the OSU test facility state in the time period near that of sump injection initiation. In this test simulation, the initialization period of 400 seconds, which is required to reach the quasi-equilibrium phase, was completed at 14,400 seconds, just following the initiation of sump injection flow through the check valves. During this simulation, the IRWST level did not reach the level required to open the sump motor-operated isolation valves.

Quasi-equilibrium calculation results were taken from the time period of 14,400 to 15,000 seconds. The SB01 window analyzed is later in time than the pressure and liquid level oscillations discussed in subsection 6.1.3 of Reference 5-1.

5.1.1 WCOBRA/TRAC Comparison with Test Results

Figure 5.1-1 shows that the WCOBRA/TRAC calculated and measured IRWST liquid levels are in fair agreement, with the calculation indicating a more rapid draining of the IRWST. Similar comparisons for SB10, SB12, and SB23 show substantially better comparisons with the average of the remaining three tests being within 10 percent of the average measured IRWST drain-down rate.

The comparison between WCOBRA/TRAC and measured pressure in the upper plenum is shown in Figure 5.1-2. The quasi-equilibrium WCOBRA/TRAC value of 15.2 psia is in reasonable agreement with the test data of approximately [ ]^{a,b,c} psia.

During LTC, water enters the vessel through the DVI nozzles first from the IRWST and then from the sump. As IRWST level falls below the sump level, the sump check valves open; as the IRWST level falls to the low-low level (15 percent full), the sump isolation valves also open. The distribution of the flow between the sump lines and the IRWST lines is then dependent on the hydraulic resistance of each line. The calculated and measured IRWST flow rates to the DVI lines are compared in Figures 5.1-3 and 5.1-4. While the trends of the measured IRWST flow were predicted, the magnitude of the IRWST flow rate was over-predicted by WCOBRA/TRAC. The calculated and measured sump flow rates to the DVI lines are compared in Figures 5.1-5 and 5.1-6. From 14,400 seconds until 14,800 seconds, the calculated sump flows were under-predicted compared to the measured values. The deviations of the IRWST and sump flows tend to be offsetting so that the deviation in the total

DVI-1 line flows, shown in Figures 5.1.7 and 5.1.8, is less than either of the components. After the initialization transient, the total DVI-2 flow is predicted reasonably well, as indicated in Figures 5.1-9 and 5.1-10.

The comparison of the liquid temperatures at the DVI-1 and DVI-2 nozzles is shown in Figures 5.1-11 and 5.1-12. The temperature at the nozzles depended on the relative proportion of the sump water to the colder IRWST water. After 14,400 seconds, when the sump injection had started, the DVI-1 injection temperature was predicted within 20°F to 30°F. Similarly, the DVI-2 injection temperature was predicted within 15°F to 25°F. The discrepancy in the temperatures relates directly to the relatively high IRWST flow and the correspondingly low sump flow. Again, however, the calculations correctly predict the trends of the data.

The break flow comparison is shown in Figure 5.1-13. The integrated break mass flow rate is shown in Figure 5.1-14. The calculated break flow rate was negligible (< 0.02 lbm/sec). The measured break flow oscillated between positive and negative values, but the integral indicates that the flow was generally negative, that is, the average rate of flow from the break separator into the cold leg over the period of 14,400 to 15,000 seconds was [ ]^{a,b,c} lbm/sec. As discussed in subsection 5.1.1.2 of Reference 5-2, the primary sump and break separator levels exceeded the elevation of the break at the bottom of CL-3 as the test transient proceeded. When this occurred, the break flow measured by instrument FMM-905 reversed, rendering the measurement invalid. Thus, the negative measured break flow may be taken into consideration as a trend but not as an absolute value. The simulation did not model the break separator, so reverse flow into the cold leg because of the break separator filling cannot be predicted.

The ADS1–3 flow was negligible during the comparison period (Figures 5.1-15 and 5.1-16) in both the prediction and the test (0.004 and [ ]^{a,b,c} lbm/sec). The ADS Stages 4-1 and 4-2 flow rate comparisons are shown in Figures 5.1-17 through 5.1-20. After the establishment of the quasi-equilibrium condition, the predicted ADS Stages 4-1 and 4-2 average flow rates were 0.49 lbm/sec and 0.74 lbm/sec, respectively, while the corresponding test values were [ ]^{a,b,c} lbm/sec and [ ]^{a,b,c} lbm/sec. Both the predictions and the test measurements showed oscillations during the quasi-equilibrium phase, reflecting the intermittent discharge of water from ADS Stages 4-1 and 4-2. In this test, the flow area of ADS Stage 4-1 was reduced by 50 percent to represent the failure of one ADS valve. The predictions showed a 33 percent reduction in ADS Stage 4-1 flow rate while the test measurements showed only a 10 percent reduction in ADS Stage 4-1 flow rate.

The amount of steam generated in the core is shown in Figure 5.1-21. The predicted rate of steam generation was somewhat lower than the rate evaluated from the test data. This is consistent with the overprediction of DVI injection flow during this period.

The collapsed core liquid level is shown in Figure 5.1-22. The top of the heater rods corresponded to a level of 36 in., and the instrument span for the core level measurement was 40 in. The core was completely covered in both the calculation and the test after the quasi-equilibrium condition was

established. The predicted upper plenum collapsed liquid level relative to the upper core plate (Figure 5.1-23) was in very good agreement with the data at [ ]^{a,b,c} to [ ]^{a,b,c} in., after the quasi-equilibrium condition was established. The hot legs are between elevations of 11.9 in. and 16.9 in. Thus, the collapsed water level in the upper plenum implies liquid levels in the hot legs. The collapsed downcomer liquid level relative to the bottom of the vessel is shown at approximately 64 in. in Figure 5.1-24. The cold legs were between elevations of 69.7 in. and 73.3 in. The measured downcomer collapsed liquid level was [ ]^{a,b,c}, while the WCOBRA/TRAC calculated level was 6 in. below. In the test, the total collapsed level of the lower plenum, core, and upper plenum was [ ]^{a,b,c} in. less than the collapsed level in the downcomer, corresponding to a differential pressure of [ ]^{a,b,c} psi; in the simulation, the total collapsed level of the lower plenum, core, and upper plenum was approximately the same as the collapsed level in the downcomer.

The predicted liquid levels in the hot legs (HLs) are shown in Figures 5.1-25 through 5.5-28. HL-1 was in the broken loop, and HL-2 was in the intact loop. To present the liquid levels in the hot legs, the horizontal and inclined portions of the hot legs were considered separately. In Figures 5.1-25 and 5.1-26, full hot legs in the horizontal section corresponded to a level of 5 in. The predictions showed average levels of 4.5 in. in both hot legs. Figures 5.1-27 and 5.1-28 show the collapsed liquid level in the inclined section of the hot legs. No significant buildup of water was calculated in the sloping section of either of the hot legs. Comparison with test measurements was only available for the HL-2, where the data also showed minimal liquid buildup.

Considering the global mass balance, the WCOBRA/TRAC prediction showed a total injection from the DVI lines of 1.20 lbm/sec and a total discharge through the ADS4 valves of 1.23 lbm/sec; in the test, the injection was [ ]^{a,b,c} lbm/sec, and the discharge was [ ]^{a,b,c} lbm/sec. In both the calculations and the test data, reverse flow was indicated at the break, which may partially explain the deviations in the global mass balances. In the calculations, the total of the break flow and the ADS1–3 was estimated to be less than 0.03 lbm/sec; therefore, these components are excluded from the mass balance comparisons. The variation between the calculated and the measured flow rates (1.21 and [ ]^{a,b,c} lbm/sec, respectively) is fair.

OSU LTC Test SB01 – 2-in. Cold Leg Line Break Figures

The following figures are proprietary and therefore are not provided:

Figure	Title
5.1-1	IRWST Level
5.1-2	Upper Plenum Pressure
5.1-3	IRWST DVI-1 Injection
5.1-4	IRWST DVI-2 Injection
5.1-5	Sump Injection 1 Flow
5.1-6	Sump Injection 2 Flow
5.1.7	Total DVI-1 Flow Rate
5.1-8	Total Integral Flow DVI-1
5.1-9	Total DVI-2 Flow Rate
5.1-10	Total Integral Flow DVI-2
5.1-11	Liquid Temperature at the DVI-1 Nozzle
5.1-12	Liquid Temperature at the DVI-2 Nozzle
5.1-13	Break Flow Rate
5.1-14	Break Flow Integral
5.1-15	ADS 1, 2, 3 Flow
5.1-16	ADS 1, 2, 3 Flow Integral
5.1-17	WC/T ADS 4-1 Flow Rate
5.1-18	Total ADS 4-1 Flow Integral
5.1-19	WC/T ADS 4-2 Flow Rate
5.1-20	Total ADS 4-2 Flow Integral
5.1-21	Steam Generated in the Core
5.1-22	Core Level (From Lower to Upper Core Plate)
5.1-23	Upper Plenum Level
5.1-24	Downcomer Levels
5.1-25	HL-1 Liquid Level (Horizontal Section)
5.1-26	HL-2 Liquid Level (Horizontal Section)
5.1-27	HL-1 Level (Inclined Section)
5.1-28	HL-2 Level (Inclined Section)

5.2 Long-Term Cooling Window Model – SB10

This section compares the test results and the WCOBRA/TRAC predictions for the LTC part of the double-ended guillotine (DEG) CMT/cold leg balance line break transient (test SB10) during the transition to sump injection.

The window-mode approach was employed to analyze the sump injection part of the SB10 test. The basis of this approach is described in Section 3. The modeling of the OSU facility for the window mode is the same as described in Section 3, including the simplifications discussed in Section 5.1 that reduce the amount of computation and avoid excessively small time steps. In test SB10, balance line 1 was broken and there was no flow in DVI-1 from the CMT to the vessel. For this reason, CMT-1 and DVI-1 to the sump/IRWST injection line were not modeled. Also, DVI-2 between the CMT and the sump injection line was not modeled since CMT-2 was empty at the start of the window simulation.

The WCOBRA/TRAC calculation simulated the test from time 13,500 to 14,500 seconds. In test SB10, sump injection started at 14,000 seconds. The first 400 seconds of this simulation were required to dissipate the effects of the assumed vessel initial conditions and reach the appropriate quasi-equilibrium solution. Quasi-equilibrium values were calculated in the period from 13,900 to 14,500 seconds.

5.2.1 WCOBRA/TRAC Comparison with Test Results

Figure 5.2-1 shows that the WCOBRA/TRAC calculated and measured IRWST liquid levels are in good agreement, with the calculation indicating an IRWST draining rate nearly equal to that of the test.

The comparison between the WCOBRA/TRAC and measured pressure in the upper plenum is shown in Figure 5.2-2. The calculated pressure was 15.2 psia, which was [ ]^{a,b,c} psia lower than the measured pressure. This discrepancy in pressure is due to uncertainty in the measured pressure values observed in this test.

The IRWST flow rates to the DVI nozzles are compared in Figures 5.2-3 and 5.2-4. In both plots, the calculated flow rates compared favorably with the trends of the measured values following the initialization phase and showed a calculated flow-to-measured flow ratio of 1.10 to 1.15.

In the test, the pressure in the DVI lines fell below the pressure corresponding to the water level of the primary sump at 14,000 seconds, and water flowed through the sump check valves to the DVI lines (Figures 5.2-5 and 5.2-6). Also, the IRWST level reached the low-low level setpoint, which opened the motor-operated sump isolation valves at 14,800 seconds. This occurred after the end of the quasi-equilibrium simulation at 14,500 seconds.

The total DVI flow (sump and IRWST) and the integrated values for each DVI line are shown in Figures 5.2-7 through 5.2-10. Considering the time interval between 13,900 seconds and 14,500 seconds, the calculated DVI-1 and DVI-2 average flow rates were 0.52 lbm/sec and 0.54 lbm/sec; the corresponding test values were [ ]^{a,b,c} lbm/sec and [ ]^{a,b,c} lbm/sec, respectively. Thus, the calculated total injection rate (1.06 lbm/sec) was in good agreement with the measured total injection rate ([ ]^{a,b,c} lbm/sec).

The comparison of the liquid temperatures at the DVI-1 and DVI-2 nozzles is shown in Figures 5.2-11 and 5.2-12. The temperature at the nozzles depended on the relative proportion of the sump water to the colder IRWST water. At the end of the simulation, the DVI-1 temperature was underpredicted by 15°F, and the DVI-2 temperature was underpredicted by 10°F.

The flow out of the cold leg side of the break is shown in Figures 5.2-13 and 5.2-14. The predicted average flow rate after 13,900 seconds was 0.02 lbm/sec, which was small relative to the discharge from ADS4. In the test, the measured flow was oscillating with positive and negative flows. The mean test flow rate after 13,900 seconds ([ ]^{a,b,c} lbm/sec) was also small relative to the ADS4 discharge. However, the predicted and measured break flow provided small contributions to the test facility mass inventory during LTC.

The ADS1–3 flow was negligible in both calculation and test during sump injection (Figures 5.2-15 and 5.2-16). However, the comparison of the two values in the quasi-equilibrium phase was excellent in that both showed rates of [ ]^{a,b,c} lbm/sec.

The ADS Stages 4-1 and 4-2 predicted flow rates are shown in Figures 5.2-17 and 5.2-18. In this test, only the data for the total ADS4 measured discharge was available (Figure 5.2-19). No measurements were available for the distribution of the flow between ADS Stages 4-1 and 4-2. The total integrated ADS4 flow is compared in Figure 5.2-20. The agreement between the prediction and the test data was good. The measured mean total flow rate was [ ]^{a,b,c} lbm/sec, and the predicted mean total flow rate was 1.09 lbm/sec. Both the predictions and the test measurements showed oscillations reflecting the intermittent discharge of water from ADS Stages 4-1 and 4-2.

The amount of steam generated in the core is shown in Figure 5.2-21. The predicted rate of steam generation duplicated the calculated value from the test data (Reference 5-1) over the quasi-equilibrium portion of the calculation, from 13,900 seconds to 14,500 seconds. This is expected given the excellent comparison of the measured and calculated total DVI flow rates.

The core collapsed liquid levels are compared in Figure 5.2-22. The top of the heater rods corresponded to a level of 36 in. and the instrument span for core level measurement was 40 in. The core was completely covered in both the test and the simulation. The predicted upper plenum collapsed liquid level relative to the upper core plate level (Figure 5.2-23) was in excellent agreement with the data with no observable difference in the two levels. The hot legs were between elevations of 11.9 in., and 16.9 in. in the upper plenum, so that a collapsed liquid level of [ ]^{a,b,c} in. indicates

liquid levels in the hot legs. The collapsed downcomer liquid level relative to the bottom of the vessel is shown in Figure 5.2-24. The cold legs were between elevations 69.7 in. and 73.3 in. The measured downcomer collapsed liquid level was [ ]^{a,b,c}, while the calculated level was 5 in. lower.

The calculated liquid levels in the hot legs are shown in Figures 5.2-25 through 5.2-28. HL-1 was in the broken loop and HL-2 was in the intact loop. To present the liquid levels in tne hot legs, the horizontal and inclined sections were considered separately. In Figures 5.2-25 and 5.2-26, full hot legs in the horizontal section corresponded to a level of 5 in. The predictions showed average levels of 3.5 in. in both hot legs. Figures 5.2-27 and 5.2-28 show the calculated collapsed liquid level in the inclined sections of the hot legs compared to the measured values. The calculations show levels of approximately 5 in., while the measured values are [ ]^{a,b,c} in. to [ ]^{a,b,c} in. higher.

Considering the global mass balance, the WCOBRA/TRAC prediction showed a total injection from the DVI lines of 1.06 lbm/sec and a total discharge through ADS4 of 1.09 lbm/sec; in the test, the injection was [ ]^{a,b,c} lbm/sec and the ADS4 discharge was [ ]^{a,b,c} lbm/sec. In the calculations, the total of the break flow and the ADS1–3 was estimated to be less than 0.03 lbm/sec; therefore, these components are excluded from the mass balance comparisons. The variation between the calculated and measured flow rates (1.075 and [ ]^{a,b,c} lbm/sec, respectively) is good.

OSU LTC Test SB10 – DEG CMT Balance Line Break Figures

The following figures are proprietary and therefore are not provided:

Figure	Title
5.2-1	IRWST Level
5.2-2	Upper Plenum Pressure
5.2-3	IRWST DVI-1 Injection
5.2-4	IRWST DVI-2 Injection
5.2-5	Sump Injection 1 Flow
5.2-6	Sump Injection 2 Flow
5.2.7	Total DVI-1 Flow Rate
5.2-8	Total Integral Flow DVI-1
5.2-9	Total DVI-2 Flow Rate
5.2-10	Total Integral Flow DVI-2
5.2-11	Liquid Temperature at the DVI-1 Nozzle
5.2-12	Liquid Temperature at the DVI-2 Nozzle
5.2-13	Break Flow Rate
5.2-14	Break Flow Integral
5.2-15	ADS 1, 2, 3 Flow
5.2-16	ADS 1, 2, 3 Flow Integral
5.2-17	WC/T ADS 4-1 Flow Rate
5.2-18	WC/T ADS 4-2 Flow Rate
5.2-19	Measured Total ADS 4 Flow Rate
5.2-20	Total ADS 4 Flow Integral
5.2-21	Steam Generated in the Core
5.2-22	Core Level (From Lower to Upper Core Plate)
5.2-23	Upper Plenum Level
5.2-24	Downcomer Levels
5.2-25	HL-1 Liquid Level (Horizontal Section)
5.2-26	HL-2 Liquid Level (Horizontal Section)
5.2-27	HL-1 Level (Inclined Section)
5.2-28	HL-2 Level (Inclined Section)

5.3 Long-Term Cooling Window Model – SB12

This section compares the test results and the WCOBRA/TRAC predictions for the LTC part of the DEG DVI line break transient (test SB12) at the end of the IRWST injection phase.

In test SB12, the data collection system failed shortly after the start of the sump injection phase of the test. Consequently, for this test, the window-mode analysis was performed on the last 1000 seconds of IRWST injection. The test was simulated from 8500 to 9500 seconds. The basis of this approach is described in Section 3. As discussed in that section, the objective of the window-mode approach is to obtain a quasi-equilibrium condition representing the OSU test facility behavior during LTC, in this case, during the final phase of IRWST discharge. The initial 400 seconds of this simulation, up to 8900 seconds, were considered the initialization phase in this analysis, since the calculated results were stabilizing during this period. Average values for comparative purposes were calculated from 8900 to 9500 seconds.

The modeling of the OSU facility for the window mode is the same as described in Section 3, including the simplifications discussed in Section 5.1 that reduce the amount of computation and avoid excessively small time steps. In test SB12, the DVI-1 and DVI-2 lines between the CMTs and the sump/IRWST injection lines were fully modeled. There was a break in DVI-1 between the sump/IRWST injection TEE and the DVI nozzle at the vessel. Thus, the vessel discharges directly through the vessel side of the DVI nozzle break, and indirectly through the balance line to the CMT side of the break.

5.3.1 WCOBRA/TRAC Comparison with Test Results

Figure 5.3-1 shows that the WCOBRA/TRAC calculated and measured IRWST liquid levels and are in fair agreement, with the calculation indicating an IRWST draining rate slower than that of the test.

The comparison between WCOBRA/TRAC and measured pressure in the upper plenum is shown in Figure 5.3-2. The quasi-equilibrium WCOBRA/TRAC value of 15.6 psia is in excellent agreement with the test data value of approximately [ ]^{a,b,c} psia.

The break flow at the broken DVI-1 nozzle is shown in Figures 5.3-3 and 5.3-4. During the quasi-equilibrium phase, agreement between calculated and measured flow was good, with the calculated value of 0.87 lbm/sec and the measured value of [ ]^{a,b,c} lbm/sec.

The IRWST flow rates to the unbroken DVI-2 nozzle are compared in Figures 5.3-5 and 5.3-6. The calculated flow rate is in fair agreement with the trend of the measured value, following the initialization phase, with a value of 0.25 lbm/sec versus a measured value of [ ]^{a,b,c} lbm/sec.

In the test, the pressure in the DVI lines fell below the pressure corresponding to the water level of the primary sump at 9350 seconds, and flow was initiated through the sump check valves to the DVI

lines. Since the calculation was to be terminated at 9500 seconds, insufficient time was available to obtain a meaningful comparison of sump flow rates. To simplify the calculation and still have 450 seconds of quasi-equilibrium flow calculations (8900 to 9350 seconds), the sump flow was inhibited in this calculation.

The comparisons of the liquid temperatures at the DVI-1 and DVI-2 nozzles are shown in Figures 5.3-7 and 5.3-8. Temperature spikes in the DVI-1 calculated temperatures indicate brief periods of reverse flow at the broken nozzle. The period of the spikes was not sufficiently long, however, to have a significant influence on the average DVI-1 flow rate (Figures 5.3-3 and 5.3-4).

The flow out of the IRWST side of the broken DVI-1 line is shown in Figures 5.3-9 and 5.3-10. The comparison of calculated and measured values is considered good but of minor influence on vessel conditions since it only feeds into the IRWST drain down calculation.

The ADS1–3 flow was negligible (< [ ]^{a,b,c} lbm/sec) in both calculation and test during IRWST injection (Figures 5.3-11 and 5.3-12). However, the comparison of the two values in the quasi-equilibrium phase was at best fair since only the trend of the measured data was calculated.

The ADS Stages 4-1 and 4-2 calculated and measured flow rates are shown in Figures 5.3-13 and 5.3-15. The integrated ADS4 flows are compared in Figures 5.3-14 and 5.3-16. The agreement between the total calculated (ADS Stage 4-1 plus 4-2) and the total measured data was good. The measured total flow rate was [ ]^{a,b,c} lbm/sec, and the calculated total flow rate was 1.12 lbm/sec. Both the predictions and the test measurements showed oscillations reflecting the intermittent discharge of water from ADS Stages 4-1 and 4-2.

The amount of steam generated in the core is shown in Figure 5.3-17. The calculated rate of steam generation under-predicts the test data over the quasi-equilibrium portion of the calculation, from 8900 seconds to 9500 seconds.

The core collapsed liquid levels are compared in Figure 5.3-18. The top of the heater rods corresponded to a level of 36 in. and the instrument span for core level measurement was 40 in. The core was essentially covered in both the test and the simulation. The predicted upper plenum collapsed liquid level relative to the upper core plate level (Figure 5.3.19) was in good agreement with the data with an average deviation in the two levels of 2 to 3 inches. The hot legs were between elevations of 11.9 in., and 16.9 in. in the upper plenum, so that a collapsed liquid level of [ ]^{a,b,c} in. indicates liquid levels in the hot legs. The collapsed downcomer liquid level relative to the bottom of the vessel is shown in Figure 5.3-20. The cold legs were between elevations of 69.7 in. and 73.3 in. The measured downcomer collapsed liquid level was [
]^{a,b,c}, while the predicted level was approximately 5 in. lower.

The predicted liquid levels in the hot legs are shown in Figures 5.3-21 through 5.3-26. To present the liquid levels in the hot legs, the horizontal and inclined sections were considered separately. In

Figures 5.3-21 and 5.3-22, full hot legs in the horizontal section corresponded to a level of 5 in. The predictions showed average levels of 3.5 in. in both hot legs. Figures 5.3-23 and 5.3-24 show the calculated collapsed liquid level in the inclined sections of the hot legs compared to the measured values. The calculations show levels of approximately 6 in. to 8 in. while the measured values are [ ]^{a,b,c} in. to [ ]^{a,b,c} in. higher.

Considering the global mass balance, the WCOBRA/TRAC prediction showed a total injection from the broken and unbroken DVI lines of 1.12 lbm/sec and a total discharge through ADS4 of 1.12 lbm/sec; in the test, the injection was [ ]^{a,b,c} lbm/sec and the ADS4 discharge was [ ]^{a,b,c} lbm/sec. In the calculations, the total of the break flow and ADS1–3 was estimated to be less than 0.01 lbm/sec; therefore, these components are excluded from the mass balance comparisons. The variation between the calculated and measured flow rates (1.12 and [ ]^{a,b,c} lbm/sec, respectively) is good.

OSU LTC Test SB12 – DEG DVI-1 Line Break Figures

The following figures are proprietary and therefore are not provided:

Figure	Title
5.3-1	IRWST Level
5.3-2	Upper Plenum Pressure
5.3-3	Vessel Side Break (DVI-1) Flow Rate
5.3-4	Vessel Side Break (DVI-1) Flow Integral
5.3-5	Total DVI-2 Flow Rate
5.3-6	Total Integral Flow DVI-2
5.3-7	Liquid Temperature at the DVI-1 Nozzle
5.3-8	Liquid Temperature at the DVI-2 Nozzle
5.3-9	Total DVI-1 Flow (DVI Side Break Flow)
5.3-10	Total Integral Flow DVI-1 (DVI Side Break Flow Integral)
5.3-11	ADS 1, 2, 3 Flow
5.3-12	ADS 1, 2, 3 Flow Integral
5.3-13	ADS 4-1 Flow Rate
5.3-14	ADS 4-1 Flow Integral
5.3-15	ADS 4-2 Flow Rate
5.3-16	ADS 4-2 Flow Integral
5.3-17	Steam Generated in the Core
5.3-18	Core Level (From Lower to Upper Core Plate)
5.3-19	WC/T Upper Plenum Level
5.3-20	Downcomer Levels
5.3-21	HL-1 Liquid Level (Horizontal Section)
5.3-22	HL-2 Liquid Level (Horizontal Section)
5.3-23	HL-1 Level (Inclined Section)
5.3-24	HL-2 Level (Inclined Section)

5.4 Long-Term Cooling Calculation – SB23

This section compares the test results and the WCOBRA/TRAC simulations for the LTC period of the 2-in. cold leg break transient (test SB23) during the transition to sump injection.

The window-mode approach was employed to analyze the sump injection part of the SB23 test. The basis of this approach is described in Section 3. The modeling of the OSU facility for the window mode is the same as described in Section 3, but with simplifications that reduce the amount of computation and avoid excessively small time steps. During the sump injection part of the tests, the PRHR HX tubes contained water, but there was no significant flow into or out of the PRHR HX. Also, during this period, the accumulators were fully discharged. Consequently, the PRHR HX and accumulators were not modeled in the simulations. The sump injection began when the IRWST reached the appropriate level to allow opening of the check valves. ADS1–3 discharged into the containment rather than into the IRWST, and the IRWST was simply represented by a pipe component. Since the IRWST was nearly empty, there was no significant heat transfer to the secondary side of the PRHR HX; this was an additional justification for not modeling the PRHR HX.

The SB23 test was simulated for the time period of 14,000 to 15,000 seconds. The primary sump injection began through the check valves at approximately 14,700 seconds. As discussed in Section 3, the objective of the window-mode approach was to obtain quasi-equilibrium conditions that represented the OSU test facility state in the time period near sump injection initiation. In this test simulation, the initialization period of 400 seconds, which is required to reach the quasi-equilibrium phase, was completed at 14,400 seconds, prior to the initiation of sump injection flow through the check valves. During this simulation, the IRWST level did not reach the level required to open the sump motor-operated isolation valves. Quasi-equilibrium calculation results were taken from the time period of 14,400 to 15,000 seconds. The SB23 window analyzed is later in time than the pressure and liquid level oscillations discussed in subsection 6.1.3 of Reference 5-1.

5.4.1 WCOBRA/TRAC Comparison with Test Results

Figure 5.4-1 shows that the WCOBRA/TRAC calculated and measured IRWST liquid levels are in excellent agreement, with the calculation indicating an IRWST draining rate equal to that of the test.

The comparison between WCOBRA/TRAC and measured pressure in the upper plenum is shown in Figure 5.4-2. The quasi-equilibrium WCOBRA/TRAC value of 15.4 psia is in reasonable agreement with the test value of approximately [ ]^{a,b,c} psia.

The IRWST flow rates to the DVI nozzles are compared in Figures 5.4-3 and 5.4-4. In both lines, the calculated flow rates compared favorably with the trends of the measured values following the initialization phase and showed a calculated-to-measured flow ratio of approximately 1.05 to 1.10.

In the test, the pressure in the DVI lines fell below the pressure corresponding to the water level of the primary sump at 14,600 to 14,700 seconds, and water flowed through the sump check valves to the DVI lines (Figures 5.4-5 and 5.4-6). The IRWST level reached the low-low level setpoint after the end of the quasi-equilibrium simulation at 15,000 seconds. As a consequence, the related increased sump injection flow rate was not calculated.

The sump and IRWST total flow rate, and the integrated sump and IRWST total flow rate to the DVI lines, are shown in Figures 5.4-7 through 5.4-10. Considering the time interval between 14,400 seconds and 15,000 seconds, the calculated DVI-1 and DVI-2 average flow rates were 0.54 lbm/sec and 0.56 lbm/sec; the corresponding test values were [ ]^{a,b,c} lbm/sec and [ ]^{a,b,c} lbm/sec, respectively. Thus, the calculated total injection rate (1.10 lbm/sec) was in good agreement with the measured total injection rate ([ ]^{a,b,c} lbm/sec).

The comparison of the liquid temperatures at the DVI-1 and DVI-2 nozzles are shown in Figures 5.4-11 and 5.4-12. The temperature at the nozzles depended on the relative proportion of the sump water to the colder IRWST water. After 14,700 seconds, when the sump injection had started, the DVI-1 and DVI-2 injection temperatures were predicted within 15°F. At the end of the simulation, the DVI-1 and DVI-2 temperatures were under-predicted by less than 10°F.

The break flow comparison is shown in Figure 5.4-13. The integrated break mass flow rate is shown in Figure 5.4-14. The predicted break flow rate was relatively small at -0.04 lbm/sec. The measured break flow oscillated between positive and negative values, but the integral shows that the flow was generally negative, that is, the average rate of flow from the break separator into the cold leg over the period of 14,000 to 14,500 seconds was [ ]^{a,b,c} lbm/sec. As discussed in subsection 5.1.1.2 of Reference 5-2, the primary sump and break separator levels exceeded the elevation of the break at the bottom of CL-3 as the test transient proceeded. When this occurred, the break flow measured by instrument FMM-905 reversed, rendering the measurement invalid. Thus, the negative measured break flow should be taken into consideration as a trend but not as an absolute value. The simulation did not model the break separator, so reverse flow into the cold leg because of the break separator filling cannot be predicted.

The ADS1–3 flow was minimal during the comparison in both the calculation and test (0.012 and [ ]^{a,b,c} lbm/sec) (Figures 5.4-15 and 5.4-16). However, the comparison of the two values in the quasi-equilibrium phase was good in that the difference was very small.

The ADS Stages 4-1 and 4-2 flow rate comparisons are shown in Figures 5.4-17 through 5.4-20. After the establishment of a quasi-equilibrium state, the predicted ADS Stages 4-1 and 4-2 average flow rates were 0.30 lbm/sec and 0.73 lbm/sec, respectively, while the corresponding test values were [ ]^{a,b,c} lbm/sec and [ ]^{a,b,c} lbm/sec. The measured total flow rate was [ ]^{a,b,c} lbm/sec, and the calculated total flow rate was 1.03 lbm/sec. The agreement between the calculated and the test total flow rates was good; however, the comparison of the individual rates was at best fair. However, total

flow out of ADS4 is the more important parameter. Both the predictions and the test measurements showed oscillations reflecting the intermittent discharge of water from ADS Stages 4-1 and 4-2.

The amount of steam generated in the core is shown in Figure 5.4-21. The calculated steam generation rate duplicated the test data over the quasi-equilibrium portion of the calculation, from 14,400 seconds to 15,000 seconds. This would be expected given the good comparison of the measured and calculated total DVI flow rates.

The core collapsed liquid levels are compared in Figure 5.4-22. The top of the heater rods corresponded to a level of 36 in. and the instrument span for core level measurement was 40 in. The core was completely covered in both the test and the simulation. The measured collapsed liquid level was [ ]^{a,b,c} in. while the calculated collapsed liquid level was 37 in. or about [ ]^{a,b,c} in. lower. The measured upper plenum collapsed liquid level relative to the upper core plate level (Figure 5.4-23) was at approximately [ ]^{a,b,c} in., while the calculated level was at 13 in. The hot legs were between elevations of 11.9 in., and 16.9 in. in the upper plenum, so that a collapsed liquid level of 13 in. indicates significant liquid levels in the hot legs. The collapsed downcomer liquid level relative to the bottom of the vessel is shown in Figure 5.4-24. The cold legs were between elevations 69.7 in. and 73.3 in. The measured downcomer collapsed liquid level was [ ]^{a,b,c}, while the predicted level was 58 in.

The predicted liquid levels in the hot legs are shown in Figures 5.4-25 through 5.4-28. HL-1 was in the broken loop, and HL-2 was in the intact loop. To present the liquid levels in the hot legs, the horizontal and inclined portions of the hot legs were considered separately. In Figures 5.4-25 and 5.4-26, the horizontal section calculations showed average levels of 2.0 in. in HL-1 and 3.1 in. in HL-2 compared to a full hot legs level of 5 in. Figures 5.4-27 and 5.4-28 show the collapsed liquid level in the inclined section of the hot legs. There was limited buildup of liquid calculated in the inclined section of either of the hot legs, with the measured data showing levels approximately [ ]^{a,b,c} in. above the calculated values.

Considering the global mass balance, the WCOBRA/TRAC prediction showed a total injection from the broken and unbroken DVI lines of 1.10 lbm/sec and a total discharge through the ADS4 of 1.03 lbm/sec; in the test, the injection was [ ]^{a,b,c} lbm/sec and the ADS4 discharge was [ ] lbm/sec. In the calculations, the total break and the ADS1–3 flow was estimated to be less than 0.01 lbm/sec; therefore, these components are excluded from the mass balance comparisons. The variation between the calculated and measured flow rates (1.06 and [ ]^{a,b,c} lbm/sec, respectively) is considered good.

OSU LTC Test SB23 – 1/2-in. Cold Leg Line Break Figures

The following figures are proprietary and therefore are not provided:

Figure	Title
5.4-1	IRWST Level
5.4-2	Upper Plenum Pressure
5.4-3	IRWST DVI-1 Injection
5.4-4	IRWST DVI-2 Injection
5.4-5	Sump Injection 1 Flow
5.4-6	Sump Injection 2 Flow
5.4.7	Total DVI-1 Flow Rate
5.4-8	Total Integral Flow DVI-1
5.4-9	Total DVI-2 Flow Rate
5.4-10	Total Integral Flow DVI-2
5.4-11	Liquid Temperature at the DVI-1 Nozzle
5.4-12	Liquid Temperature at the DVI-2 Nozzle
5.4-13	Break Flow Rate
5.4-14	Break Flow Integral
5.4-15	ADS 1, 2, 3 Flow
5.4-16	ADS 1, 2, 3 Flow Integral
5.4-17	WC/T ADS 4-1 Flow Rate
5.4-18	Total ADS 4-1 Flow Integral
5.4-19	WC/T ADS 4-2 Flow Rate
5.4-20	Total ADS 4-2 Flow Integral
5.4-21	Steam Generated in the Core
5.4-22	Core Level (From Lower to Upper Core Plate)
5.4-23	Upper Plenum Level
5.4-24	Downcomer Levels
5.4-25	HL-1 Liquid Level (Horizontal Section)
5.4-26	HL-2 Liquid Level (Horizontal Section)
5.4-27	HL-1 Level (Inclined Section)
5.4-28	HL-2 Level (Inclined Section)

5.5 References

5-1. Andreychek, T. S., Chismar, S. A., Delose, F., Fanto, S. V., Fittante, R. L., Frepoli, C., Friend, M. T., Haberstroh, R. C., Hochreiter, L. E., Morrison, W. R., Ogrinsh, M., Peters, F. E., Wright, R. F., and Yeh, H. C., WCAP-14292, Rev. 1, *AP600 Low-Pressure Integral Systems Test at Oregon State University Test Analysis Report,* September 1995.

5-2. Dumsday, C. L., Carter, M., Copper, M. H., Lau, L. K., Loftus, M. J., Nayyar, V. K., Tupper, R. B., and Willis, J. W., WCAP-14252, Volumes 1-4, *AP600 Low-Pressure Integrated Systems Test at Oregon State University Final Data Report,* May 1995.

6.0 ASSESSMENT OF THE WINDOW-MODE CALCULATIONS AND THE LTC PIRT PHENOMENA

6.1 Validation of the Window-Mode Approach

The strategy of the window-mode calculations is that the long-term cooling (LTC) period is a slowly varying transient in which any variation in the initial conditions of the reactor system would be damped out, over time, by the imposed boundary conditions. There are time constants in the reactor system that reflect the transient time of the flow through the system and the response of the system to different initial levels and different initial temperatures. The Oregon State University (OSU) sensitivity calculations in Section 3 show that variations in the initial vessel level and fluid temperatures are damped out by the imposed in-containment refueling water storage tank (IRWST) boundary conditions such that the calculations converge to the same end point. This is possible since the time period used in the window-mode calculation is longer than the time constant for the flow through the system. Therefore, the effects of the initial conditions will diminish with time as the boundary conditions, which are imposed on the calculation, dominate the system response. This implies that any uncertainty in the selected initial conditions for the LTC transient will be damped out by the imposed boundary conditions from the IRWST head, fluid temperature, and power level in the rod bundle, and the containment pressure condition; therefore, the calculations converge to the same point as determined by the boundary conditions. As a result, the LTC transient can be divided into periods to simulate selected portions of the transient of interest, without having to model the entire transient. Each portion of the transient can constitute a separate calculation using reasonable selected values for the initial conditions. If the window-mode calculation is run long enough, the solution becomes converged.

The window-mode process was validated using the OSU test data, which models the AP600 LTC transient. The sensitivity studies performed confirmed that differences in initial conditions would be damped out over time, such that different initial cases would converge to the same end point. The cases were run long enough, approximately three time constants for the primary system, as determined by the transient time of the flow through the system. Some initial conditions stabilized more quickly than others in these calculations. The levels in the system more easily stabilized since there was a direct feedback of the levels and the injection flows as seen in the figures in Section 3. The fluid temperatures took a longer time to stabilize, but the convergence was aided by the heat transfer to the structures.

The sensitivity calculations presented in Section 3 confirm that the window-mode approach is a valid method for analyzing the AP600 LTC transient.

6.2 Assessment of the LTC PIRT Phenomena

The LTC Phenomena Identification Ranking Table (PIRT) phenomena are given in Table 1-1. The highly ranked items reflect the mass inventories in the different components, such as the mixture

inventories in the core, downcomer, and upper plenum. The mixture inventories indicate the degree of core cooling and are very important. As shown in Section 5, WCOBRA/TRAC accurately predicts the collapsed levels in the different components for the different tests. The core decay heat is also highly ranked since it represents the heat source. For the tests, the decay power is a boundary condition that is accurately known and used in the WCOBRA/TRAC calculations. The pressure in the downcomer and the remainder of the system is also highly ranked since it impacts the volumetric venting capability of the automatic depressurization system (ADS) Stage 4 valves and the calculated void fractions within the core. The pressure also impacts the flow regimes that exist in the different components of the system, and therefore, the capability of WCOBRA/TRAC to predict the different flow regimes. The low pressure aspect of the OSU tests, nearly atmospheric, is more severe than the conditions expected for LTC for the AP600 plant. Therefore, the low pressure effects on the flow regimes that WCOBRA/TRAC will calculate are captured in the tests. The flows into and out of the primary system are also highly ranked since they affect the inventories within the system and hence, the core coolability. The flows are measured in the tests and have been compared to the WCOBRA/TRAC calculations.

The hot leg flow pattern and transition was initially ranked as high on the LTC PIRT. The reason for the ranking was a concern related to the pressure drop and venting capability of the ADS Stage 4 flow path. If the pressure drop or the uncertainty in its prediction is high, the primary system can pressurize and the IRWST or sump injection flow will be reduced. The ranking of this parameter has been reduced from high to medium. The basis for the reduction is the relatively low pressure drop of the ADS Stage 4 lines relative to the resistance of the direct vessel injection (DVI) lines. Sensitivity studies varying the ADS Stage 4 line losses indicated no significant effects on the levels and core coolability during LTC. Therefore, the uncertainty in parameters such as the flow regime and separation at the ADS tee are of reduced importance, and comparisons of the ADS Stage 4 flow rates with WCOBRA/TRAC are sufficient for the validation of the code pressure drop calculation.

6.3 Assessment of the Verification Results

The comparisons of the window-mode WCOBRA/TRAC code calculations to the OSU LTC test data are presented in Section 5. The comparisons concentrated on the highly ranked PIRT items identified in Table 1.1. These items reflect the capability of the code to predict the mass distributions within the system as well as the mass inflows and outflows through the DVI lines and ADS Stage 4 valves. In general, WCOBRA/TRAC did agree well with the test data for nearly all parameters investigated. The individual test comparisons given in Section 5 are summarized using composite "measured-to-predicted" plots that indicate the overall agreement of WCOBRA/TRAC with the test data.

Figures 6-1 and 6-2 show the comparisons of the measured-to-predicted individual DVI injection flows for the four tests analyzed. The code calculated values are the quasi-steady-state flow values. Figure 6-3 shows the total DVI flow from both injection lines into the vessel. As the figures indicate, WCOBRA/TRAC is predicting the individual flows reasonably well. The DVI-1 flows are predicted, on average, within 20 percent. The WCOBRA/TRAC-predicted flows are biased slightly higher than

the data. The average of the DVI-2 flows shown in Figure 6-2 are also predicted with an average deviation of 20 percent. However, this is due to the under-prediction of test SB12 DVI-2 flow. Most of the DVI-2 flows are over-predicted by WCOBRA/TRAC. The combined DVI flow comparisons are given in Figure 6-3 and WCOBRA/TRAC over-predicts the combined flows with an average deviation of 15 percent.

Figures 6-4 through 6-8 present similar summary comparisons for the ADS Stage 4 flow rates. Figure 6-4 presents the flow comparisons for ADS Stage 4-1. WCOBRA/TRAC is predicting the flows within an average of 40 percent and is under-predicting the flows out of the system. Figure 6-5 shows the comparisons of ADS Stage 4-2 with these flows over-predicted by WCOBRA/TRAC. The predictions for ADS Stage 4-2 is within an average of 28 percent. The total ADS4 flow comparison is given in Figure 6-6 and indicates scatter above and below the line with WCOBRA/TRAC predicting the average of the total flow within 6 percent over all tests simulated. This indicates that the individual ADS4 line resistances are not as modeled, but the combined resistance is well modeled.

Figure 6-7 shows a composite plot of all the predicted and measured flows for the four OSU tests analyzed by WCOBRA/TRAC. The average deviation of the measured-to-predicted flows is 5 percent for these tests. Figure 6-8 shows the ratios of both the measured and predicted ADS4 to DVI injection flows. With the exception of test SB01, the agreement is excellent, indicating that although the individual line flows are not calculated precisely, the total flow in and out of the system is calculated very well.

Numerical comparisons of the predicted and measured levels were not performed since the agreement was excellent.

The comparisons indicate that WCOBRA/TRAC is predicting the flows measured in the tests reasonably well. The levels, pressures, and steam generation rate are also predicted well by the code. Therefore, WCOBRA/TRAC can be used with confidence to predict the AP600 LTC transient phenomena, including not only vessel mass inventory, but also the flow of liquid injected via the DVI lines to the core and out the ADS vent paths.

(a,b,c)

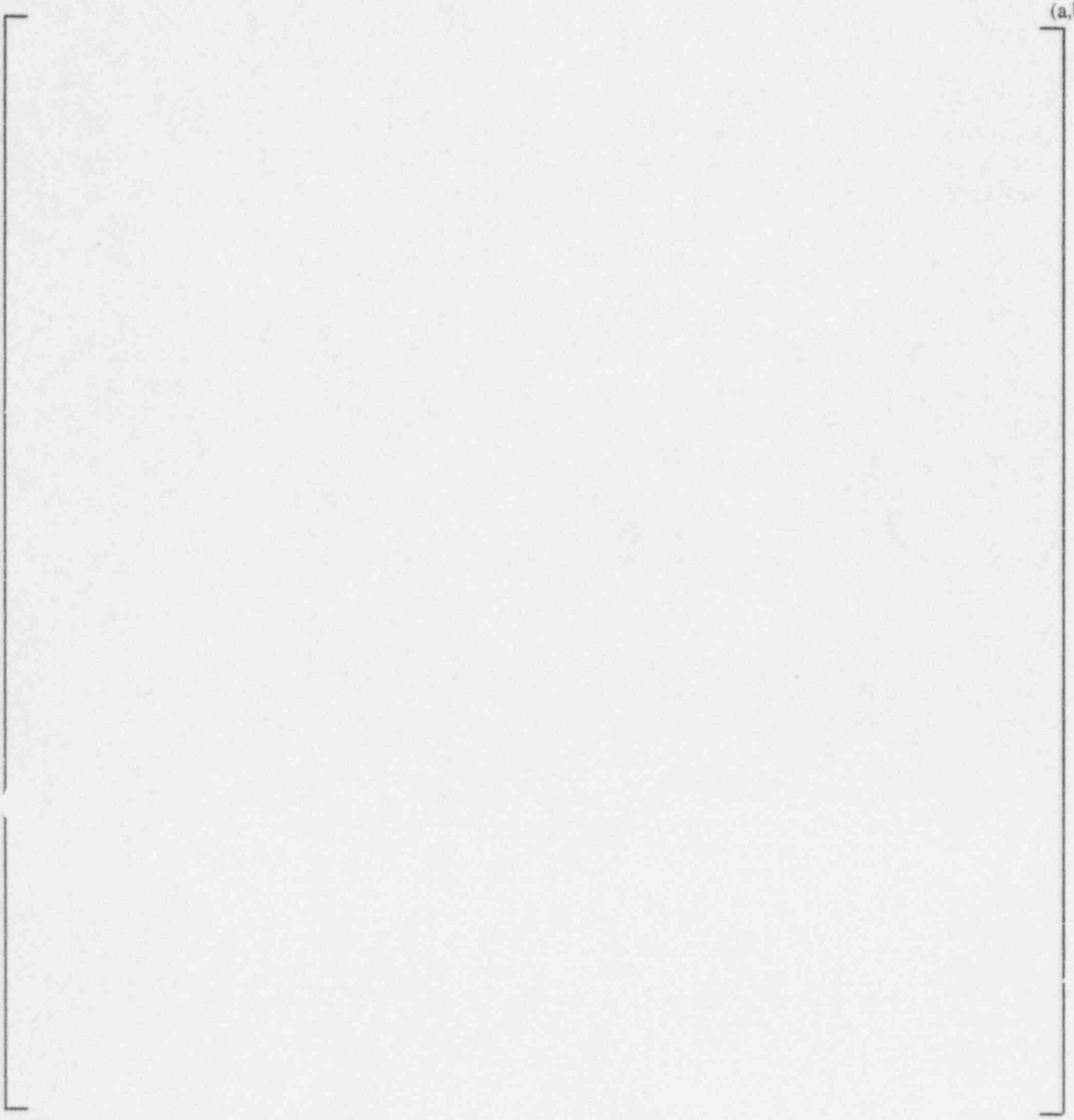

Figure 6-1 Summary Comparisons of DVI-1 Flows

(a,b,c)

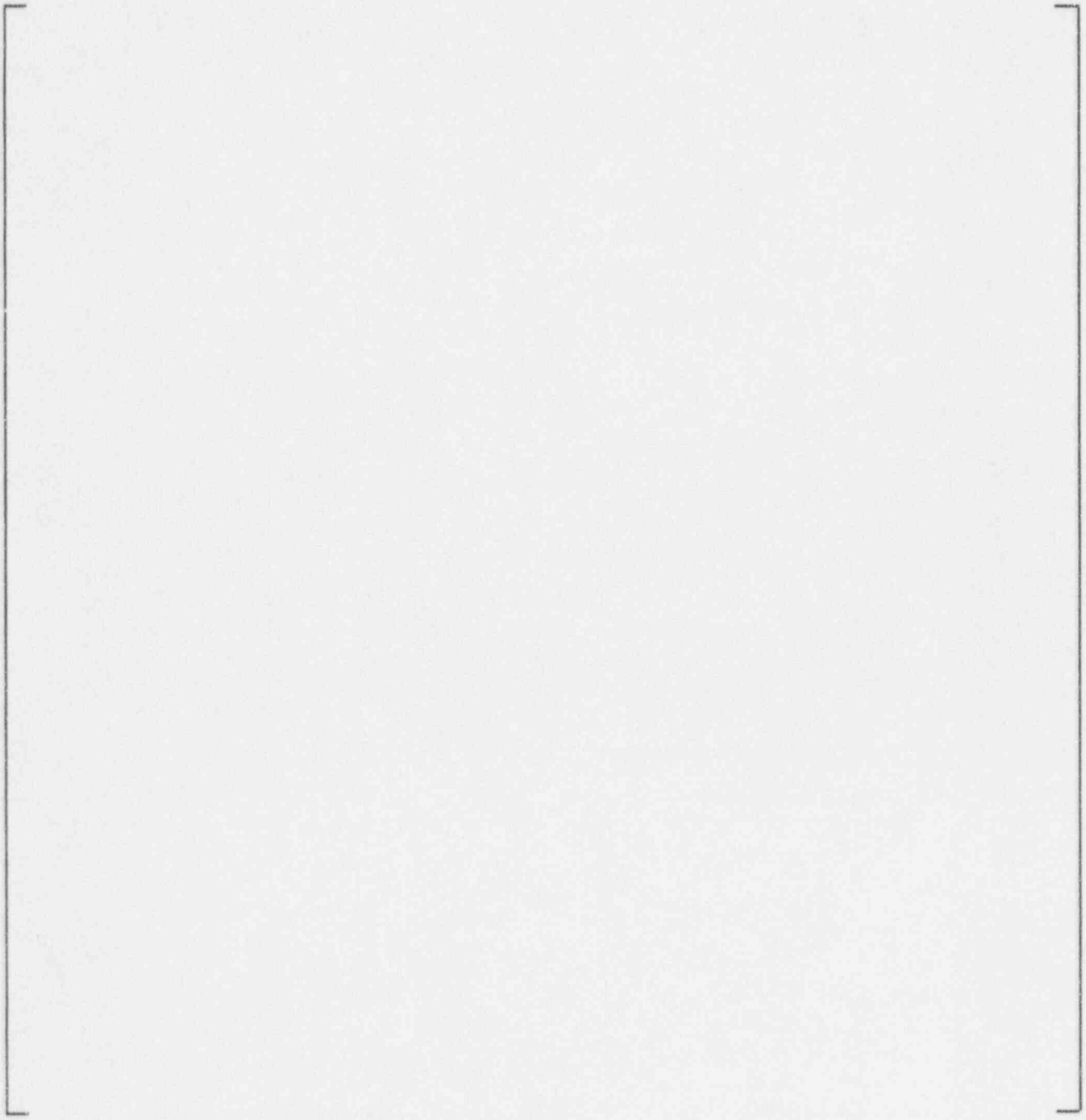

Figure 6-2 Summary Comparisons of DVI-2 Flows

(a,b,c)

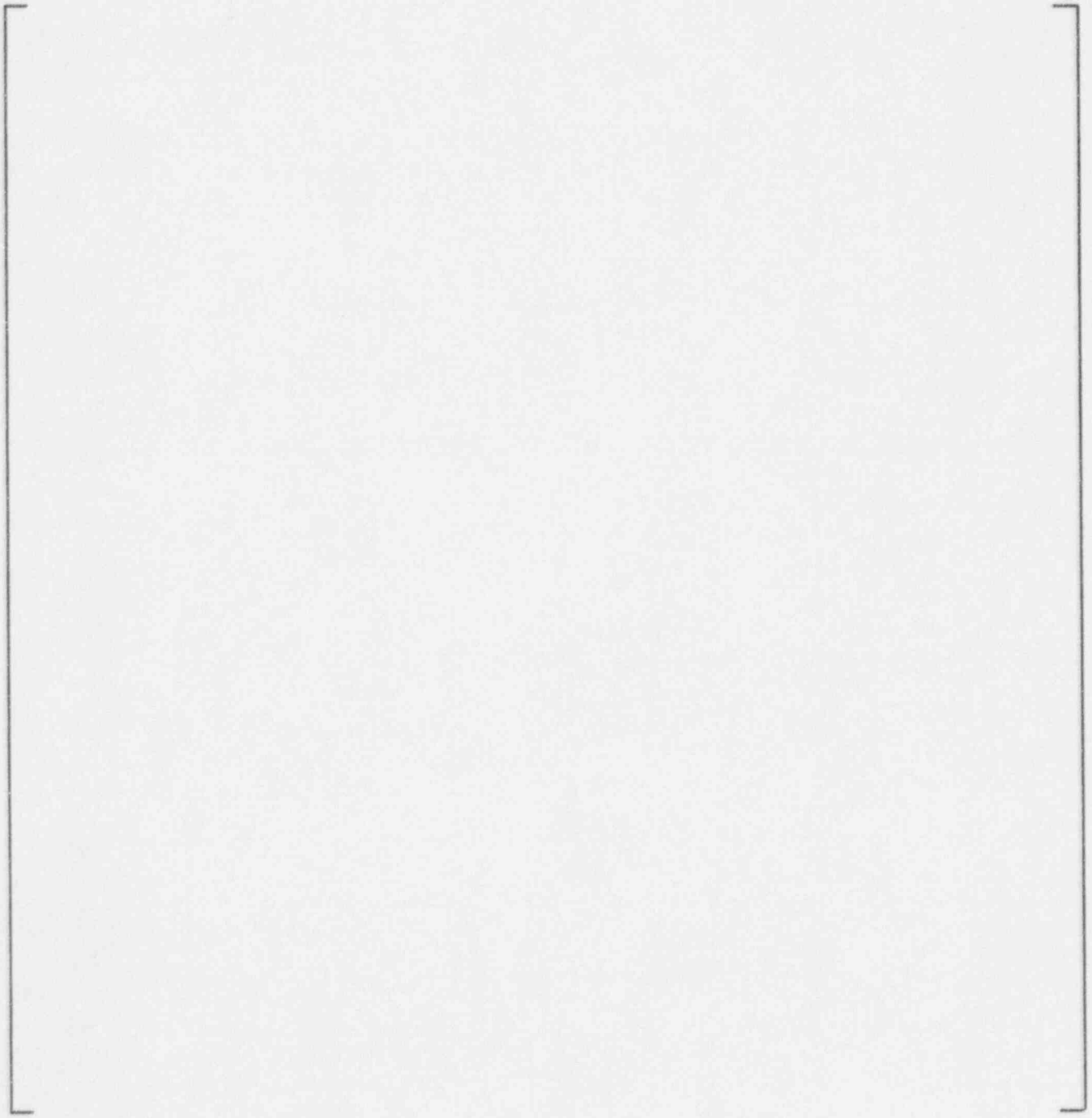

Figure 6-3 Summary Comparisons of All DVI Flows

(a,b,c)

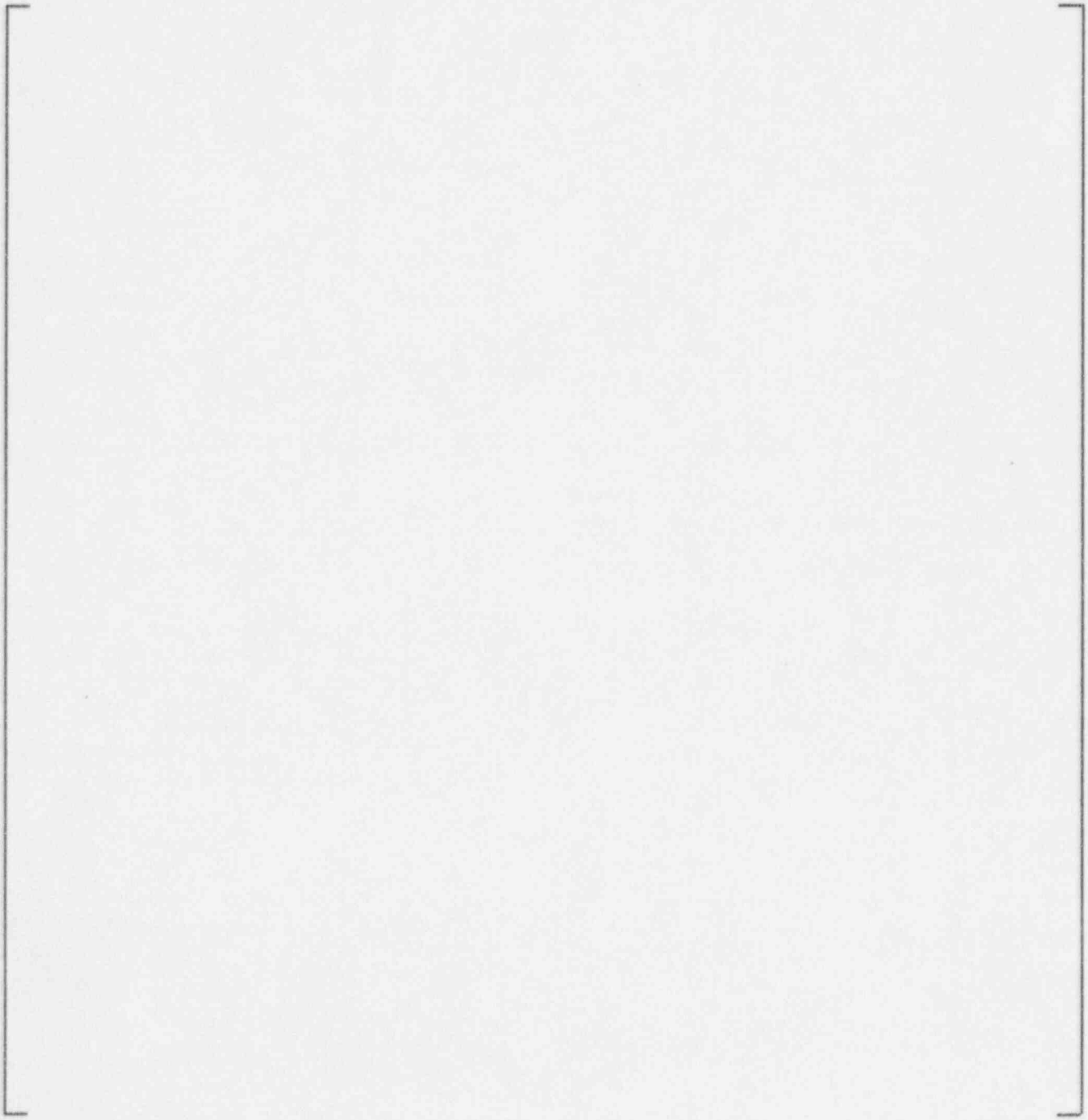

Figure 6-4 Summary Comparisons of ADS4-1 Flows

(a,b,c)

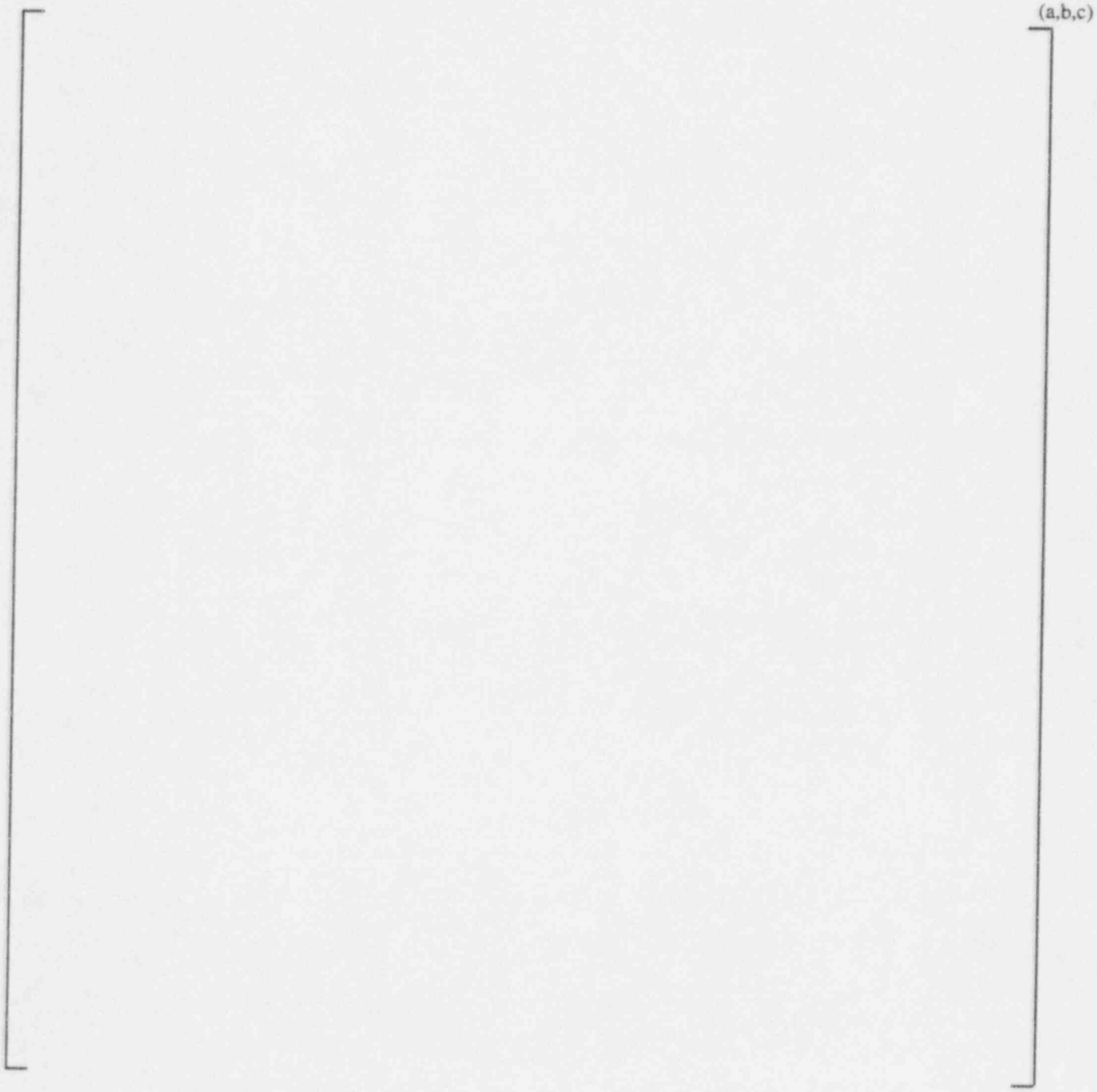

Figure 6-5 Summary Comparisons of ADS4-2 Flows

(a,b,c)

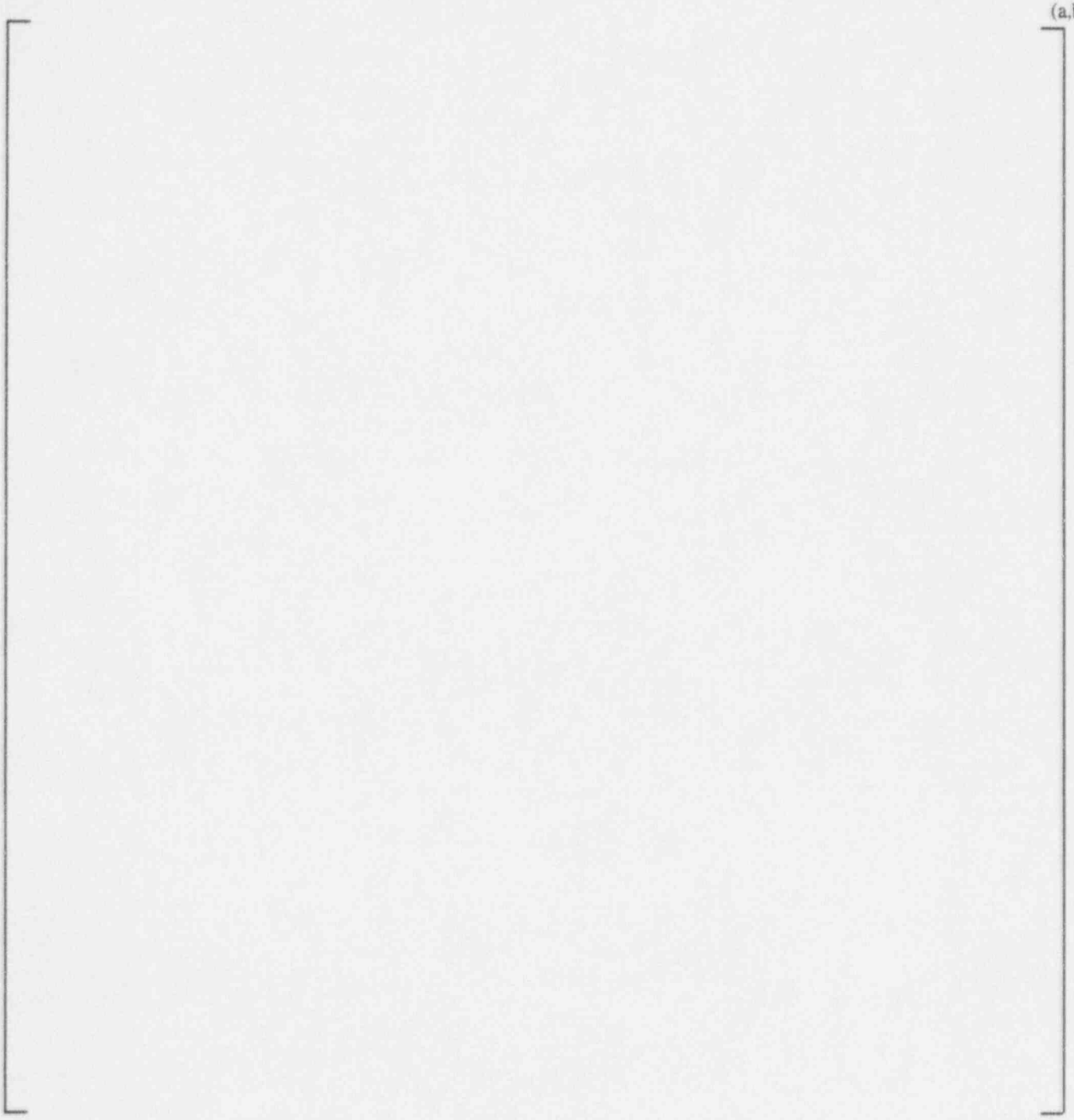

Figure 6-6 Summary Comparisons of All ADS4 Flows

(a,b,c)

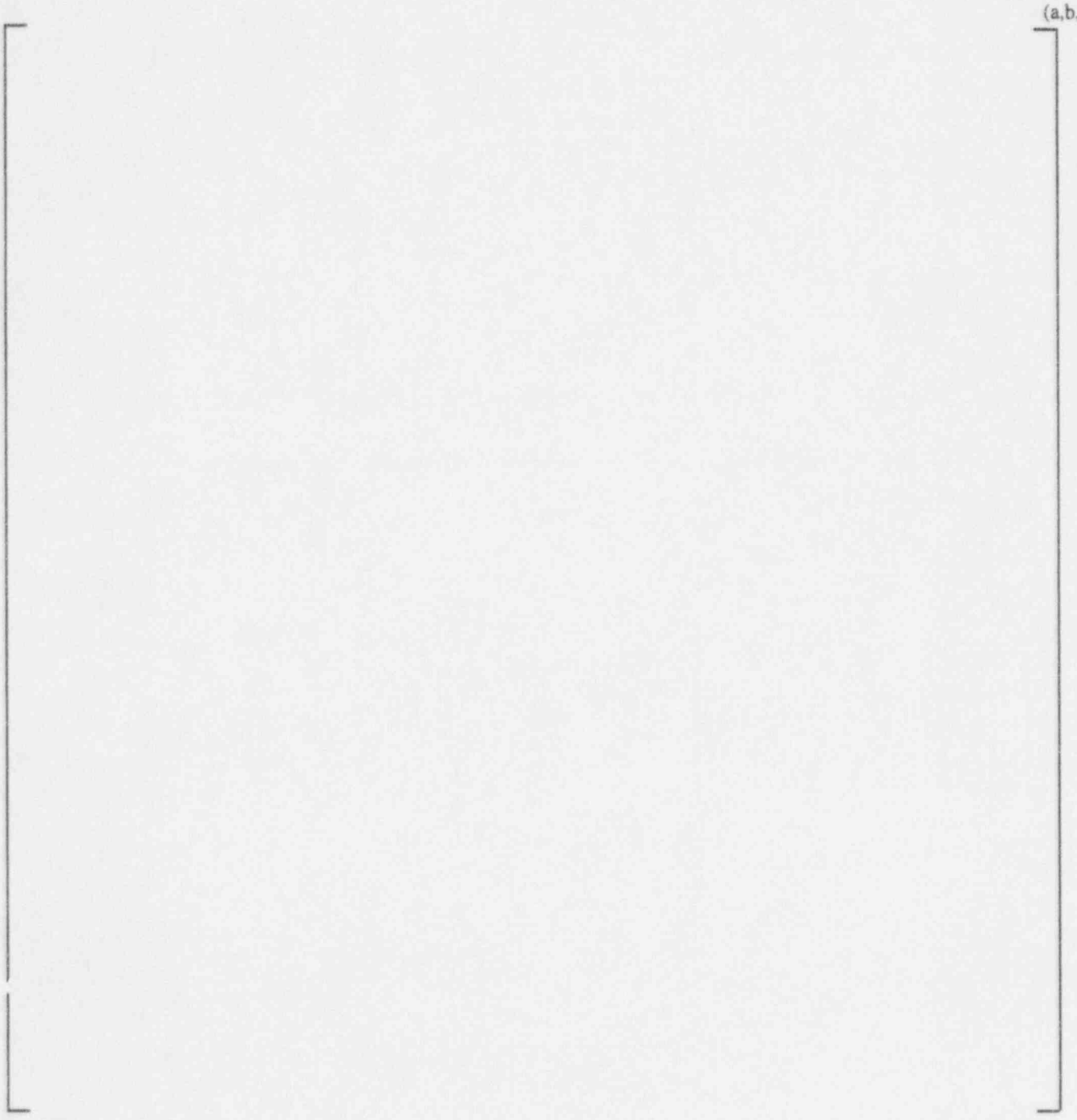

Figure 6-7 Summary Comparisons of All Flows

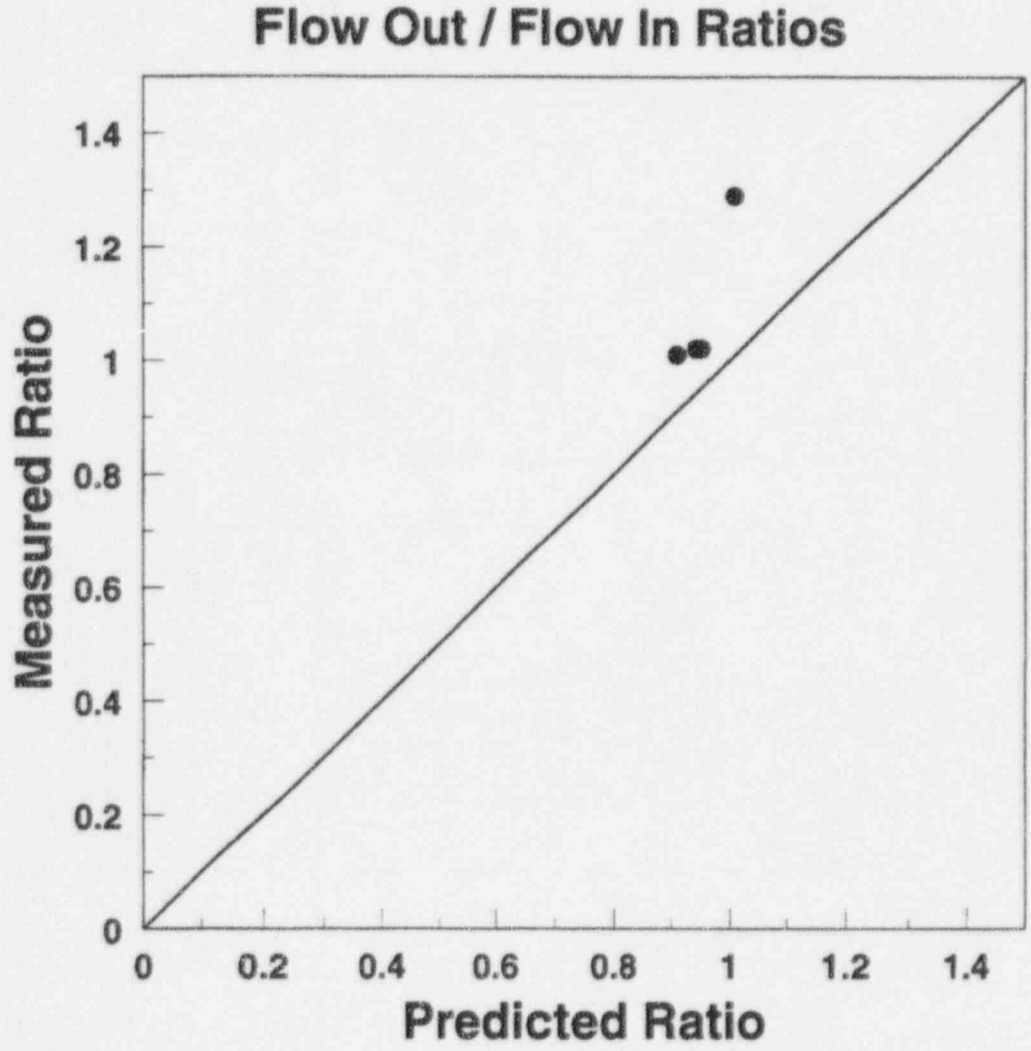

Figure 6-8 Comparison of Predicted-to-Measured OSU Inlet (DVI) and Outlet (ADS4) Flow Ratios

7.0 CONCLUSIONS

The WCOBRA/TRAC code was compared to selected Oregon State University (OSU) long-term cooling (LTC) tests, using a window-mode approach to represent selected time periods of the transient.

The key thermal-hydraulic phenomena identified in the Phenomena Identification Ranking Table (PIRT) (Table 1-1) were observed in the tests and were well predicted by WCOBRA/TRAC for the different window modes of the test transient.

The sensitivity studies performed for selected tests show that the LTC transient becomes independent of the assumed initial conditions and driven by the boundary conditions imposed on the system. Therefore, the calculations converge to the same end state when carried out for a sufficiently long period of time, approximately three time constants of the primary system.

The code comparisons to the LTC data indicate that WCOBRA/TRAC captures the highly ranked PIRT phenomena and is suitable for the LTC calculations for the AP600.

The WCOBRA/TRAC OSU comparisons show that the code adequately predicts the system behavior during the LTC phase of the transient and represents the system mass distribution and flows in the tests which indicates that ample core cooling margin is present.